5-11-2013

Paleoenvironmental Reconstruction by Identification of Glacial Cave Deposits, Helderberg Plateau, Schoharie County, New York

Jeremy M. Weremeichik

Paleoenvironmental reconstruction by identification of glacial cave deposits, Helderberg Plateau, Schoharie County, New York

By

Jeremy M. Weremeichik

A Thesis
Submitted to the Faculty of
Mississippi State University
in Partial Fulfillment of the Requirements
for the Degree of Master of Science
in Geoscience
in the Department of Geosciences

Mississippi State, Mississippi

May 2013

Paleoenvironmental reconstruction by identification of

glacial cave deposits, Helderberg Plateau,

Schoharie County, New York

By

Jeremy M. Weremeichik

Approved:

_____	_____
John E. Mylroie Professor of Geosciences (Director of Thesis)	Renee M. Clary Associate Professor of Geosciences (Committee Member)
_____	_____
Darrel W. Schimtz Professor of Geosciences (Committee Member)	Michael E. Brown Associate Professor of Geosciences (Graduate Coordinator)
_____	
R. Gregory Dunaway Professor and Interim Dean College of Arts & Sciences	

Name: Jeremy M. Weremeichik

Date of Degree: May 11, 2013

Institution: Mississippi State University

Major Field: Geoscience

Major Professor: John E. Mylroie

Title of Study: Paleoenvironmental reconstruction by identification ofglacial cave deposits, Helderberg Plateau, Schoharie County, New York

Pages in Study: 174

Candidate for Degree of Master of Science

Eight dissolution caves from the Helderberg Plateau in Schoharie County, New York were studied to investigate unusual sediment packages previously interpreted to be deposits laid down during stagnant ice-cover conditions of the Wisconsin glaciation. The sediment package, consisting of white finely laminated silts and clays are overlain by coarse gravels, in turn overlain by dark silts and clays. Analysis of 63 sediment samples was inconclusive in terms of organic content, but indicated a higher degree of fine-grained calcite material in the white clays than in the overlying units. The caves with the white clays exist only within the footprint of Glacial Lake Schoharie, with lower elevation caves containing a thicker white clay sequence, a measure of the duration of lake cover. The sediment sequence represents glacial rock flour formed under stagnant lake conditions, overlain by outwash deposits emplaced during lake termination, and more recent sediment from soil-loss deposition.

DEDICATION

I would like to dedicate this research to my love ones and amazing friends for being at my side in times of need.

ACKNOWLEDGEMENTS

I would like to thank Dr. John Mylroie for giving me the once in a life time opportunity of working with him. Kristen Stives, for always being there to encourage, support, assist, proofread, spell check, and feeding the bottomless pit. My Mom, Julianne, for traveling nearly a thousand miles to care for me when my health took a turn for the worse during my second semester at MSU. The management staff at Howe Caverns, Secret Caverns, the National Speleological Society, and the Northeastern Cave Conservancy for allowing access and sampling in their caves. Also thanks to Dr. Karen McNeal for use of her lab, and the assistance provided by Curry Templeton.

TABLE OF CONTENTS

LIST OF TABLES

LIST OF FIGURES

CHAPTER I

INTRODUCTION

The Helderberg Plateau is located in east-central New York State; it exists primarily in Schoharie and Albany counties (Figure 1.1). As glaciers advanced and retreated during the Pleistocene, sediment was stripped from the Helderberg Plateau and replaced by glacially transported sediment. The sediment was deposited in two places: a.) on the surface of the plateau, b.) in the caves that exist within the plateau. Sediment deposited within the caves is well preserved because it is protected from surficial weathering and erosion. Specific horizons of sediment found within the caves are thought to be associated with a glacial lake believed to have existed during the Late Wisconsinan glacial period approximately 23,000-12,000 years-before-present (ybp) in the Schoharie Valley (e.g. Dineen, 1986).

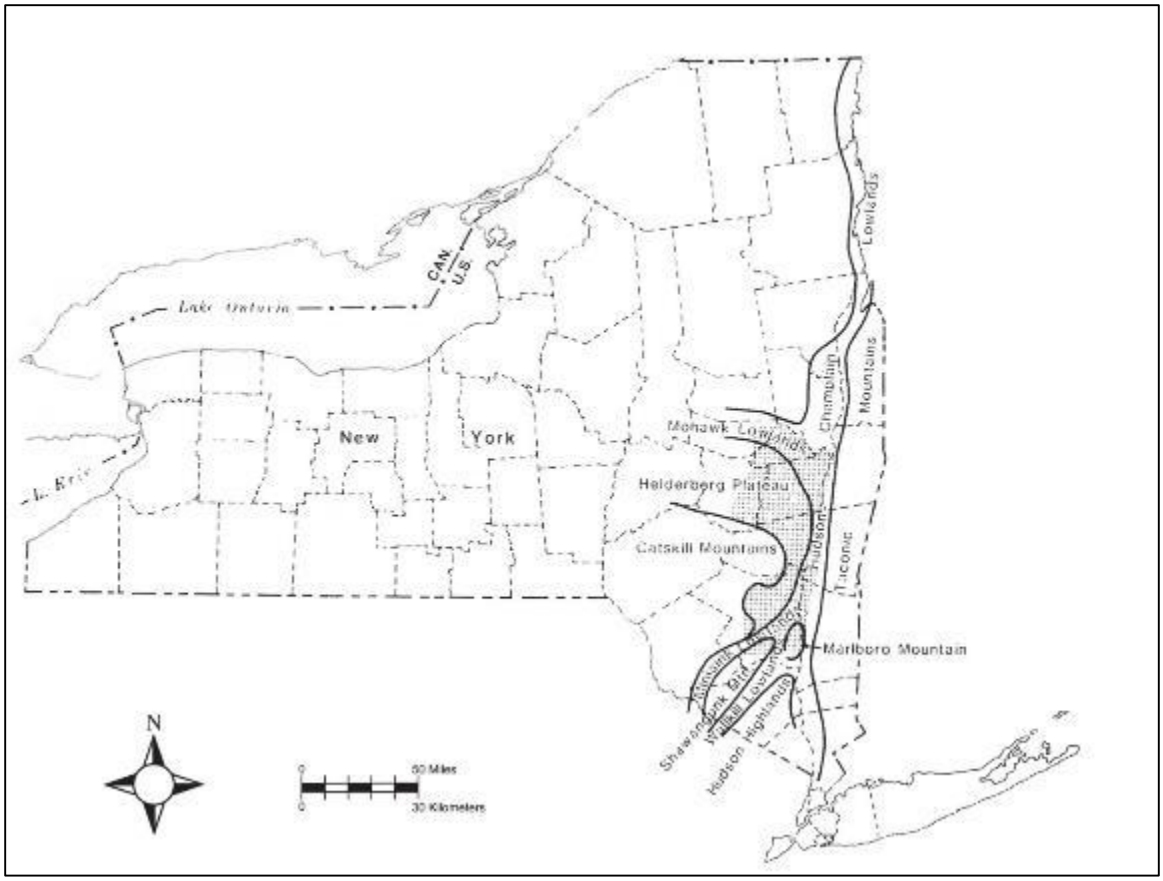

Figure 1.1 Map of the study area located in Helderberg Plateau of east-central New York State, primarily within the counties of Schoharie and Albany (modified from Dineen, 1986).

In July of 2012, multiple research trips were taken to selected caves located in the Helderberg Plateau. From west to east the caves in this study include: Barrack Zourie Cave, McFail's Cave, Howe Caverns, Secret-Benson Cave system, Gage Cavern, Westfall Spring Cave, Schoharie Caverns, Caboose Cave, and the control for the study, Knox Cave (Figure 1.2). The caves located in the plateau (with the exception of Westfall Spring Cave) predate the most recent glaciation, which took place during the Late Pleistocene. Caves in the Schoharie Valley Region of New York are known to predate the Wisconsinan glaciation. Age dating U/Th documented by Lauritzen and Mylroie,

(2000) show the age of speleothems in the caves exceed the onset of the most recent glaciation with the exception of Westfall Spring Cave, which was treated as an additional control for the study because of the cave's unique post-glacial geomorphological nature.

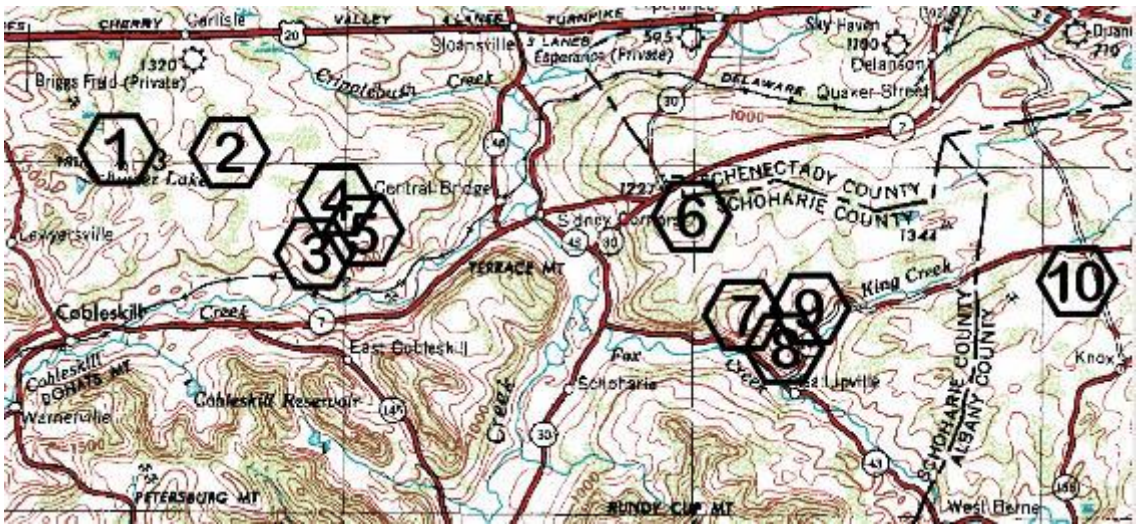

Figure 1.2 Locations of the caves included in this study.

1 = Barrack Zourie Cave, 2 = McFail's Cave, 3 = Howe Caverns, 4 = Secret Caverns, 5 = Benson's Cave,6 = Gage Caverns, 7 = Westfall Spring Cave, 8 = Schoharie Caverns, 9 = Caboose Cave, 10 = Knox Cave (background from USGS Digital Raster Graphic Binghamton Quadrangle (1:250,000 scale)).

Statement of Purpose

The purpose of this study is to reconstruct the paleoenvironment of a proglacial lake, Glacial Lake Schoharie, located within multiple counties of east-central, New York State. The glacial lake endured at least four readvances of the Mohawk and Hudson glacial lobes during Late Woodfordian time of the Late Wisconsinan glaciation; see Dineen (1986) for more detail on the nature of the readvances. The multiple readvances caused the shoreline of the lake to be modified multiple times throughout its existence. The caves selected to be investigated by this study were chosen because of the known or

suspected existence of what has been presumed to be glacially deposited clastic white clay (e.g. Mylroie, 1984; Dumont, 1995) (Figure 1.3 and Figure 1.4). It is also the purpose of this study to identify the composition of the white clay horizon. The clay is suspected to be associated with the existence of Glacial Lake Schoharie and/or be limestone rock flour scoured during the most recent glaciation from the limestone bedrock of the surrounding region. If the clay is found to contain organic material, this would help in determining the depositional environment of the white clay.

Figure 1.3 The presence of the 'white' clay recorded in various caves selected for this study.

Outcrop of 'white' clay found in Barrack Zourie Cave. The carabineer for scale is approximately 10 cm (Dumont, 1995); Outcrop found in Caboose Cave. Rock hammer for scale; Outcrop found in Howe Caverns. Rock hammer for scale; Outcrop found in McFail's Cave. Rock hammer for scale; Outcrop found in Gage Caverns. Rock hammer for scale; Outcrop found in Schoharie Caverns, note scale.

Figure 1.4 Image showing the distinct rhythmic pattern of an in-situ sediment outcrop found within Howe Caverns.

Swiss Army knife, 10 cm long, for scale

CHAPTER II

LITERATURE REVIEW

Geographic Location

The study area is located in northeastern Schoharie County and western Albany County, east-central New York State (Figure 2.1). Of the ten caves in this study, five are located in the Cobleskill Plateau, four are located within Barton Hill and one, Knox Cave, is located farther east in Albany County. The study area is located approximately 55 km (34 miles) west of the city of Albany, New York State. The western-most cave in the study is Barrack Zourie Cave located 5.6 km (3.5 miles) northwest of the town of Cobleskill, New York. Moving east, McFail's Cave is adjacent to Barrack Zourie Cave on the plateau. McFail's drainage basin is separated from Barrack Zourie's by a buried pre-glacial valley (Palmer et al., 2003) (Figure 2.2). In relation to the entrances of Barrack Zourie Cave, the 'old' main entrance to McFail's Cave, Ack's Shack, is 3 km (1.8 miles) to the immediate east of Barrack Zourie Cave and is 7.5 km (4.6 miles) north of the town of Cobleskill. Continuing east along the Cobleskill Plateau the next cave encountered is Howe Caverns which is 2.5 km (1.6 miles) northeast of the town Barnerville, and is 4.7 km (2.9 miles) southeast of the entrance to McFail's Cave. Secret-Benson Cave is located 1.5 km (1 mile) north of the entrance to Howe Caverns. The caves mentioned above are all located within what is referred to as the Cobleskill Plateau which is a specific region of the greater Helderberg Plateau. The Cobleskill Plateau is an

approximate area of 10 km (6 miles) E-W and 5 km (3 miles) N-S (Dumont, 1995). The plateau is bounded by the Cobleskill Creek to the south, the Helderberg escarpment to the north, the Schoharie Creek to the east and a gradational boundary to the west with clastic rocks. The elevation of the Cobleskill Plateau is between 300 m (1000 feet) and 600 m (2000 feet) above sea level.

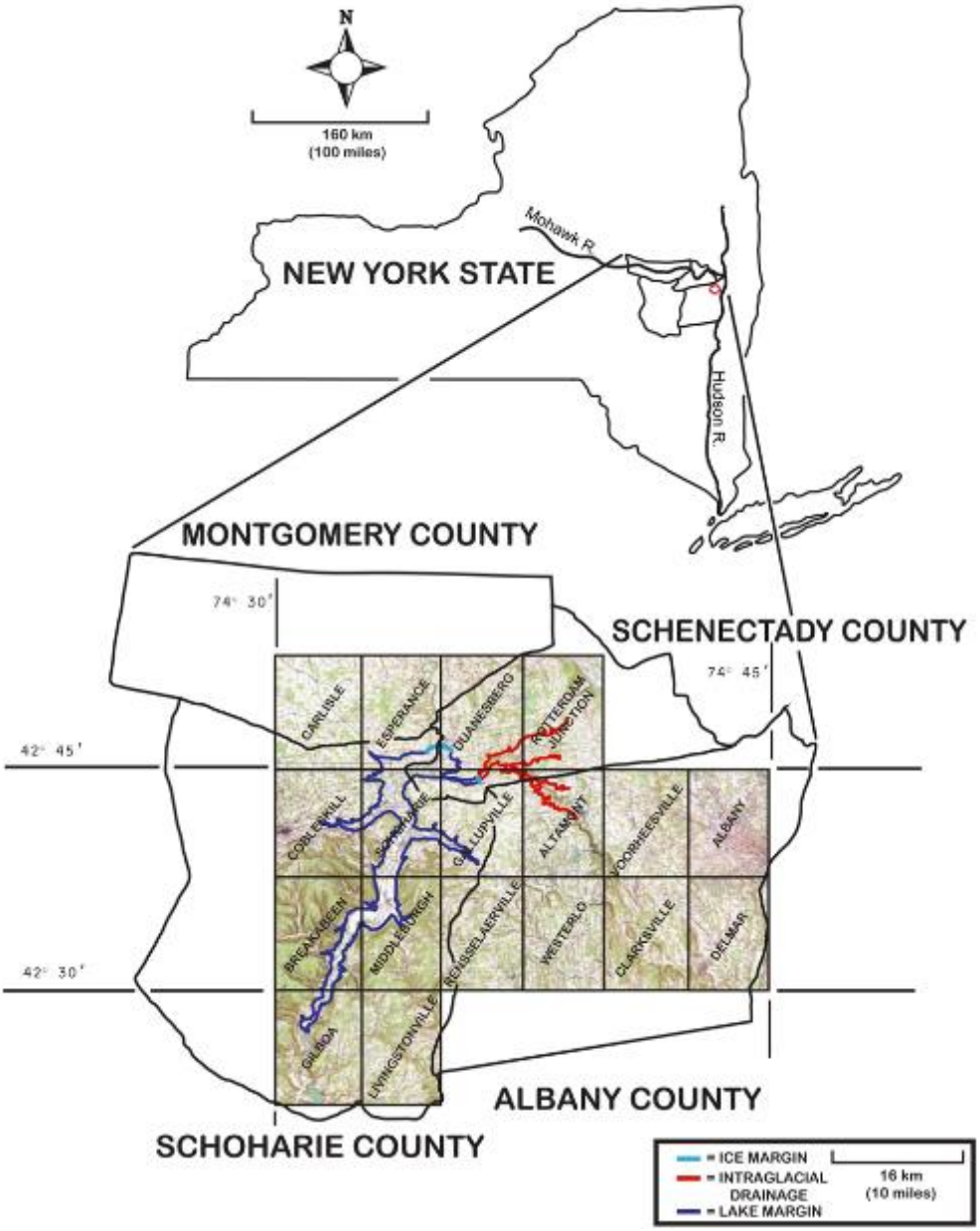

Figure 2.1 The location of the study area primarily exists in Schoharie and Albany County.

The location of a single stage of Glacial Lake Schoharie is shown above.

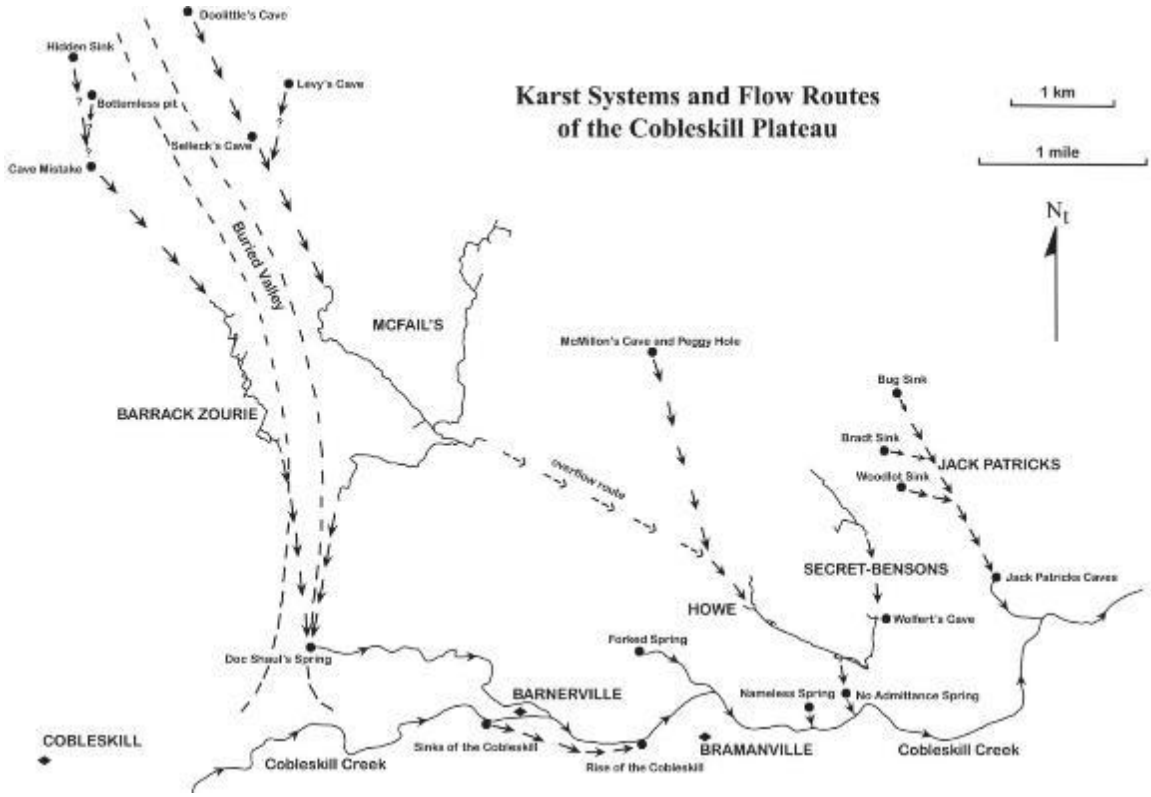

Figure 2.2 Map of the karst systems and flow routes of the Cobleskill Plateau. The buried valley is located between Barrack Zourie Cave and McFail's Cave (re-drawn from Dumont, 1995).

Gage Cavern, Schoharie Caverns, Westfall Spring Cave, and Caboose Cave are located east of the Cobleskill Plateau, across the Schoharie Valley, in what is known as Barton Hill. Gage Cavern is located 6.4 km (4 miles) northeast of the town of Schoharie (Figure 2.3). Westfall Spring Cave is about 0.6 km (0.4 miles) west of Schoharie Caverns. The entrance to Schoharie Caverns is found 1.6 km (1 mile) northwest from the town of Gallupville, and 5.6 km (3.5 miles) northeast from the town of Schoharie. Caboose Cave is located 1.2 km (0.76 miles) east of the entrance to Schoharie Caverns and approximately 1.6 km (1 mile) north of Gallupville. The elevation of Barton Hill is between 275 m (900 feet) and 400 m (1300 feet) above sea level.

Figure 2.3 Map of the karst systems and flow routes of Barton Hill (re-drawn from Mylroie, 1977).

Knox Cave is the control for the study, as it is outside the boundaries of Glacial Lake Schoharie. The plateau in which Knox Cave is found is considered part of the greater Helderberg Plateau, located immediately to the east in Albany County; therefore it exists within the same geologic units as the other caves in this study found in Schoharie County but its cave stream is fed by an entirely different drainage basin.

The boundary of Glacial Lake Schoharie was determined through the interpretation of the topography and morphology of the landscape (Figure 2.1). LaFleur (1965, 1969, 1976) and Dineen (1986) provide interpretations that suggest where the fluctuating shoreline of the glacial lake basin existed throughout the Late Wisconsian glaciation. LaFleur (1969) suggested that the size of the lake varied greatly throughout the waning years of the Late Wisconsian glaciation and this interpretation was confirmed by Dineen (1986).

Geologic Setting

The caves located in the Helderberg Plateau formed in the Upper Silurian and Lower Devonian limestones of the Helderberg Group. The major caves within the plateau primarily formed within the thick-bedded Coeymans Limestone and the thinly-bedded Manlius Limestone. It is important to note there has been some dissolution development that has occurred within the Becraft and Kalkberg Limestones. There has also been some cavern development within the Rondout Dolomite (e.g. Knox Cave and Barytes Cave (Mylroie, 1977; Palmer, 2009)); cavern development within this unit is normally limited to conduits with small cross-sectional areas.

Stratigraphy

Figure 2.4 shows the stratigraphy of the study area compiled from the work of Rickard (1962), Kastning (1975), Mylroie (1977), Palmer et al. (2003), Ebert et al. (2001, 2010), and Ver Straeten (2008, 2009). The Upper Ordovician Schenectady Formation is approximately 550-610 m (1800-2000 feet) thick and is the base unit outcropping in the Helderberg Plateau. The unit consists of alternating sandstones interbedded with black and grey shale (Mylroie, 1977).

Overlying the Schenectady Formation is the Upper Silurian Brayman Dolomite, also referred to as the Brayman Shale because of its extensive shale content within the dolomite. The unit is approximately 12 m (39 feet) thick and is an olive-green argillaceous dolostone containing pyrite nodules. The Brayman Dolomite is unconformably overlain by the Upper Silurian Cobleskill Limestone (Mylroie, 1977) (Figure 2.4).

The Cobleskill Limestone is about 3 m (10 feet) thick and is a very resistant unit that consists of two massive beds overlain by a thin-bedded section in the Cobleskill Plateau. Conduits are known to exist within the Cobleskill Limestone but no major cave systems have been found to exist within this unit. The Cobleskill Limestone thins to the east, pinching out just east of Knox Cave in Albany County (Figure 2.4).

The Upper Silurian Rondout Formation (Chrysler Dolomite Member) is roughly 11 m (36 feet) thick, argillaceous, shaly, limy, dolostone with high clay mineral content. As mentioned earlier, the Rondout is not usually a major cave passage forming unit. The unit is typically the floor of most major passages because of its relative resistance to

dissolution. The Rondout grades upward to the east, eventually into the overlying Manlius Formation (Dumont, 1995) (Figure 2.4).

The Silurian/Devonian boundary was not well defined within the units of the Helderberg Plateau prior to 2001. Many geologists previously believed the boundary existed within the Rondout Dolomite (e.g. Rickard 1962); the boundary was re-defined by Ebert et al. (2001) to exist unconformably between the Manlius and Coeymans Limestone and the actual boundary crosses both lithostratographic units (Figure 2.4).

The Upper Silurian Manlius Formation (Thatcher Limestone Member) is approximately 15 m (49 feet) thick in the study area and is a thin-bedded bluish-grey limestone with some dolostone beds and shaly interbeds. It is one of the two major cave forming units in the area. The unit's thin-bedded nature leads to a dense joint spacing, providing numerous potential flow paths to initiate speleogenesis (Figure 2.4).

The Lower Devonian Coeymans Formation is divided into two units the Dayville Member and the Ravena Limestone Member. (Please note that while the Dayville Member is officially a member of the Coeymans Formation Ebert et al., (2010) demonstrated that the member should be re-assigned to the Manlius Formation.) The Dayville Member has been correlated as far east as Thatcher Park (Ebert et al., 2010). The formation is about 18 m (59 feet) thick and is a relatively pure, massively bedded, cliff forming limestone. The unit acts as a protective cap rock for the underlying units. The Coeymans Limestone is the other major cave forming unit in the area (Figure 2.4).

The Lower Devonian Kalkberg Limestone is approximately 20 to 32 m (66 to 105 feet) thick, poorly soluble, cherty, fossiliferous limestone. The unit is not a major cave forming unit but is known to contain some sink holes and vertical shafts. The upper

contact is with the Becraft Limestone and it is conformable and gradational. The Kalkberg intertongues eastward with the New Scotland Limestone, eventually being replaced by the Devonian New Scotland Limestone, to the east of the Cobleskill Plateau. The New Scotland is an impure limestone that acts as an aquitard. Figure 2.3b shows the location of the caves in regards to one another as well as showing the units in which the caves formed in (Figure 2.4).

The Lower Devonian Becraft Limestone is approximately 2.5 to 6 m (8 to 20 feet) in the western extent of the study area but eventually grades to between 0.5 to 4 m (2 to 13 feet) thick in the eastern part of the study area, course-grained, massive, fossiliferous limestone, similar to the character of the Coeymans Limestone. Southeast of the study area the average thickness of the Becraft is significantly greater according to Ver Straeten (2009). The Becraft Limestone is overlain by the Alsen Limestone (Figure 2.4).

The Lower Devonian Alsen Limestone is approximately 1 m (3 feet) thick. The unit was first recognized by Grabau (1919), who noted that the unit contained modified Becraft fauna and is stratigraphically continuous with the Becraft Limestone. Ver Straeten (2009) agreed with Grabau (1919) by showing the unit is overlain by the Port Ewen and underlain by the Becraft in eastern New York. Ver Straeten (2009) further described the unit as being a limestone with minor clastic shale interbedded (Figure 2.4).

The Lower Devonian Port Ewen Limestone is approximately 1 m (3 feet) thick in the study area. Ver Staeten (2009) described the Port Ewan as being a limestone which contains some clastic shale interbedded and represents part of a carbonate shelf (Figure 2.4).

The Port Ewen Limestone is overlain by Wallbridge Unconformity which separates the Oriskany Formation from the Port Ewen. The Lower Devonian Oriskany Formation is 2 m (7 feet) thick and is a sandstone bed composed of pure white quartz sand cemented by calcium carbonate (Figure 2.4).

Overlying the Port Ewen and the Oriskany is the Lower Devonian Esopus Shale being approximately 15 m (49 feet) thick and the basal unit of the Tristates Group. The unit consists of mainly fine-grained, dark gray arenaceous shale (Mylroie, 1977) with well-developed slaty cleavage. In Schoharie County, the Alsen and Port Ewen limestones are missing, and the Oriskany Sandstone lies directly on the Becraft Limestone (Figure 2.4).

The Lower Devonian Carlisle Center Formation overlies the Esopus Shale and is approximately 12 m (40 feet) thick. The unit is composed of sandy shale commonly capped by greenish, glauconitic, argillaceous sandstone (Mylroie, 1977) (Figure 2.4).

The Lower Devonian Schoharie Limestone (Grit) is approximately 3 m (10 feet) thick and is the uppermost unit in the Tristates Group in the study area. The unit is an impure, siliceous, dark bluish-grey limestone which is argillaceous in parts (Mylroie, 1977) (Figure 2.4).

Above the Tristates Group is the Middle Devonian Onondaga Limestone, approximately 30 m (98 feet) thick, which is a major cave forming unit, especially to the east in Albany County (Figure 2.4).

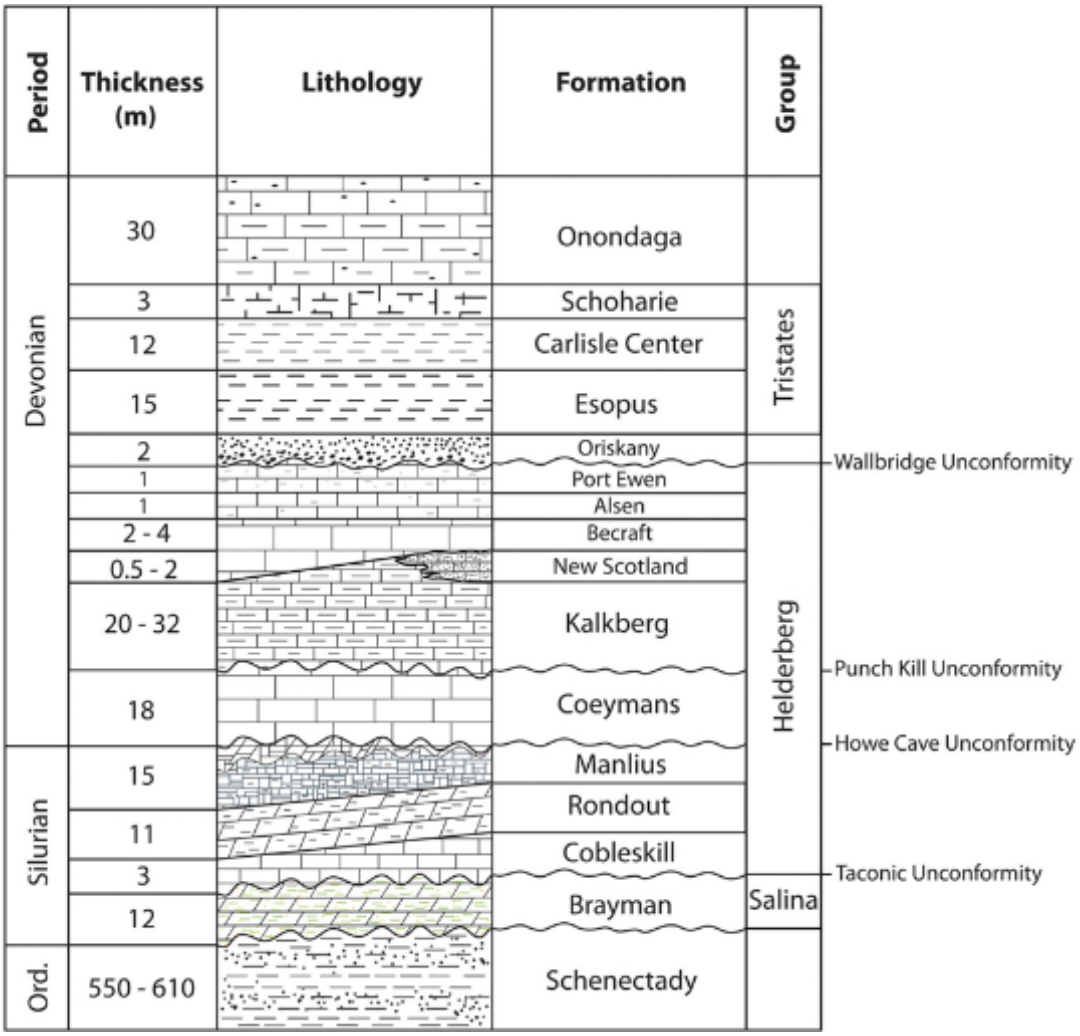

Figure 2.4 Stratigraphy of the Helderberg Plateau

(based on data from Rickard, 1962; Kastning, 1975; Mylroie, 1977; Palmer et al., 2003; Ebert et al., 2001, 2010; and Ver Straeten, 2008, 2009).

Structure

The geologic structure of the study area is on the whole, very simple and uniform. The bedrock of the area has only been subject to minor structural stresses caused by the Acadian orogenic event (~420 to 350 million ybp). The regional dip of the bedrock in this region varies slightly between approximately 1° and 2° to the south-southwest, with the strike of the bedrock varying from N70W and N80W. Minor thrust faults have been

observed both on the surface and within the subsurface of the study area. Table 2.1 lists the significant faults of the Cobleskill Plateau and Barton Hill.

Table 2.1 List of the significant faults of the Cobleskill Plateau and Barton Hill.

LOCATION	DESCRIPTION	SPELEOLOGICAL SIGNIFICANCE
McFail's Cave	Low angle (0 to 30 degrees) dipping NE, striking NW; some features dip SW and strike NW.	Major
	One vertical normal fault displaced 5 cm, striking NE.	None
Howe Caverns	Low angle reverse fault dipping 14 degreed S, striking N75W	Locally Major
Secret-Benson's Cave System	Vertical normal faults striking N18W with 2.5 cm displacement.	Minor
	Bedding plane fault striking NW with calcite and some barite and strontianite.	Undetermined
Gage Caverns	Low angle reverse fault dipping 13 degreed WSW, striking NW.	Locally Major

(modified from Mylroie, 1977)

The most notable structural feature in the area of study is the jointing of the bedrock. The jointing predominantly occurs within the Helderberg limestone units which cause preferential formation of passages along both strike and dip oriented joints. The joints of the region typically fall into two distinct orientations of N20E and N85W (Figure 2.5). The joints with the 'general' N20E orientation is the dominant joint set which is found to vary from N2E and N30E (Kastning, 1975). The second joint set at N85W is near-orthogonal to the first joint set and is less variable in its orientation; moreover it is less distinctly expressed in the bedrock (Mylroie, 1977).

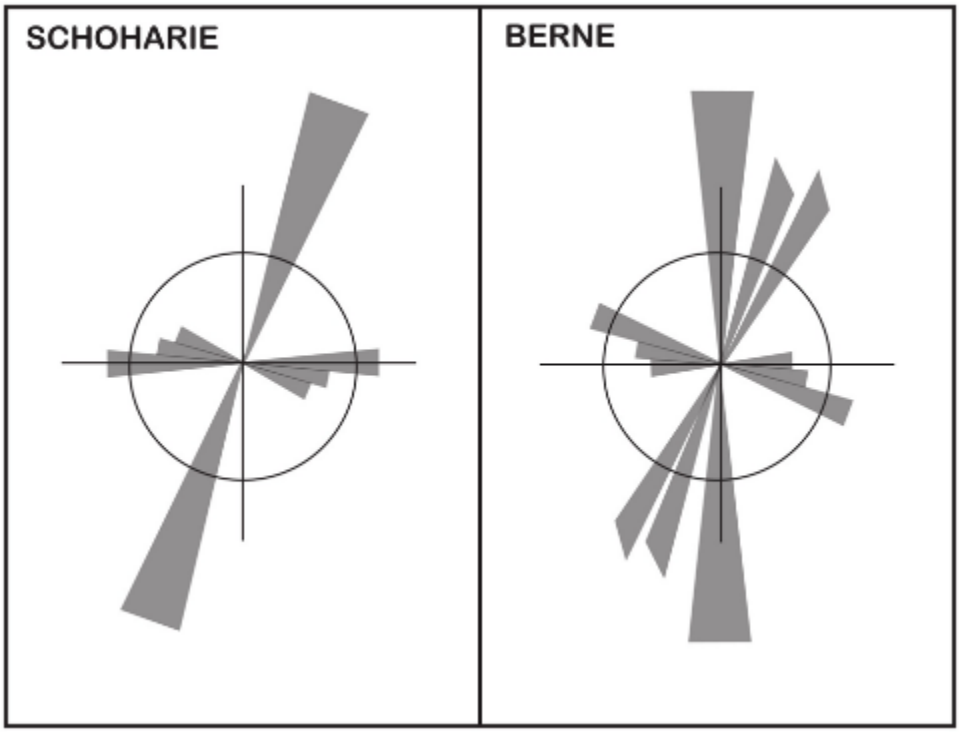

Figure 2.5 Major joint sets observed in the Schoharie and Berne areas (modified from Kastning, 1975). North is to the top of the diagram.

"Folding and folds are almost absent from the study area" (Mylroie, 1977, p. 23). For more detail on the minor folds and folding that exists in the region see Kastning (1975) and Mylroie (1977).

Climate

Based on the Köppen-Geiger climate classification (Kottek et al., 2006) the Helderberg Plateau region of Schoharie and Albany County, New York belongs to the classification **Dfb**, which is an abbreviation for Main climate: snow, Precipitation: fully humid, Temperature: warm summer. According to the National Oceanic and Atmospheric Administration, the mean annual temperature is 9.1 °C (48.3 °F), with freezing conditions lasting from late November/Early December through mid-March. The frost zone in the

region normally exists from late December/Early January through Early/mid-March. The average depth of penetration of the frost zone is between 1.2 to 1.8 m (four to six feet). The average annual rainfall is 99.85 cm (39.31 inches), and is relatively evenly distributed throughout the entirety of a year. Precipitation occurring in the winter months is typically delivered as snowfall and can accumulate on average 156.7 cm (61.7 inches) per year. The water stored in snowfall during the winter is typically released as seasonal flood events known as the spring or winter thaws. Summer thunderstorms, occasional hurricanes, tropical storms, and tropical depressions have been known to cause catastrophic flooding, both surface and subsurface in the Helderberg Plateau and Catskill Mountains region.

The Wisconsinan Glaciation in the Helderberg Plateau

The glacial history of the Helderberg Plateau has been described in great detail by many workers (e.g., LaFleur, 1969; Dineen and Hanson, 1985; Dineen, 1986; Muller and Calkin, 1993). The last major glaciation of the Pleistocene that occurred in New York State was the Late Wisconsinan glaciation (Figure 2.6 and Table 2.2).

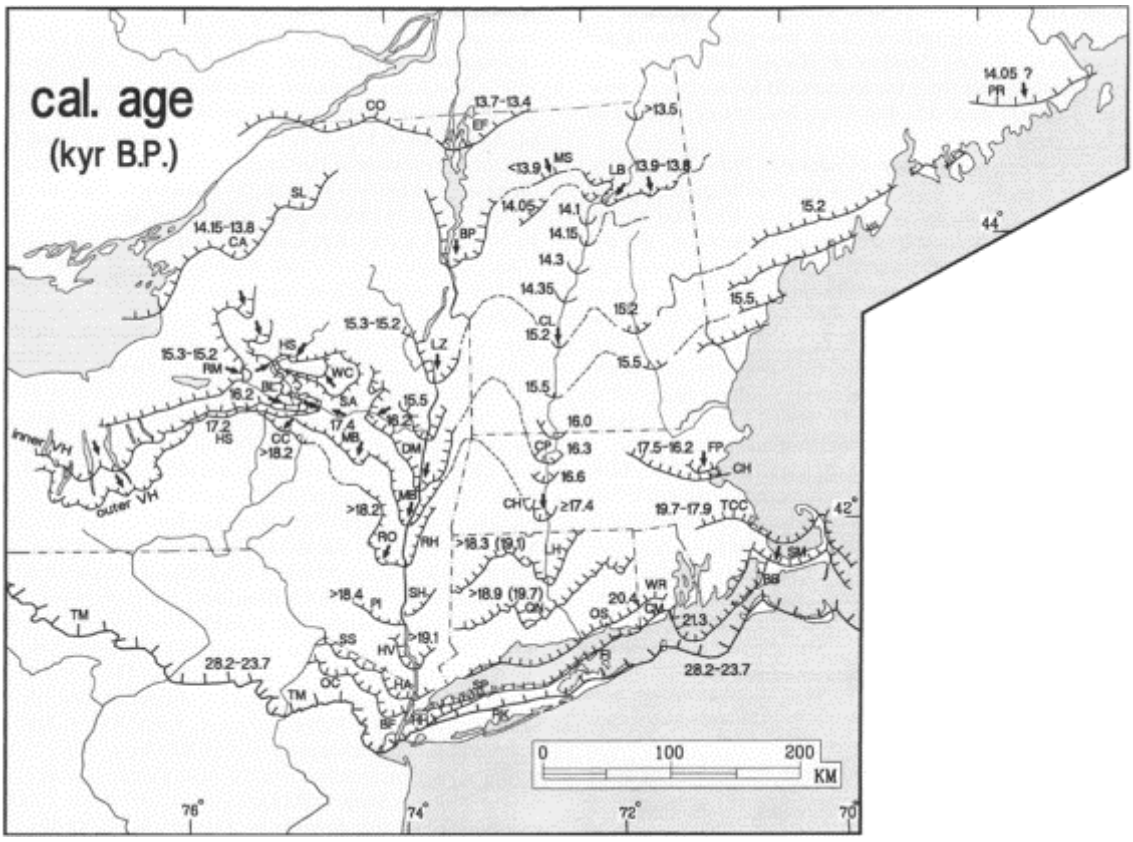

Figure 2.6 The chronology of the late Wisconsinan deglaciation of the northeastern United States in calibrated (U-Th) ka BP.

The arrows indicate ice front positions that are the limits of glacial readvances. The Late Wisconsinan maximum is marked TM which is the Late Wisconsinan Terminal Moraine. Abbreviations of end moraines, ice margins, and glacial readvances are given on Table 2.2 (from Ridge, 2004).

Table 2.2 Abbreviations of moraines, ice margins, and glacial readvances in Figure 2.6.

BB	Buzzards Bay Moraine
BF	Bloomfield ice margin
BL	Barneveld-Little Falls Readvance
BP	Bridport Readvance
CA	Carthage-Harrisonville ice margin
CC	Cassville-Cooperstown Moraine
CH	Chicopee Readvance
CL	Claremont moraines
CM	Charlestown Moraine
CO	Covey Hill ice margin
CP	Camp Meeting Cutting ice margin
DM	Delmar Readvance
EF	Enosburg Falls ice margin
FI	Fishers Island Moraine
FP	Fresh Pond Moraine
HA	Lake Hackensack ice margin
HH	Harbor Hill Moraine
HS	Hinckley-St. Johnsville Readvance
HV	Haverstraw ice margin
LB	Littleton-Bethlehem Readvance
LC	Lake Charles ice margin
LH	Lake Hitchcock dam ice margin
LZ	Luzerne Readvance
MB	Middleburg Readvance
MS	Middlesex Readvance
OC	Ogdensburg-Culvers Gap Moraines
OS	Old Saybrook Moraine
PI	Pellets Island Moraine
PR	Pineo Ridge Moraine
QN	Quinnipiac ice margin
RH	Red Hook Moraine
RK	Ronkonkama Moraine
RM	Rome Readvance
RO	Rosendale Readvance
SA	Salisbury Readvance
SH	Shenandoah Moraine
SL	Star lake Moraine
SM	Sandwich Moraine
SP	Sand Point Moraine
SS	Sussex Moraine
TCC	L. Taunton-Cape Cod ice margin
TM	Late Wisconsinan Terminal Moraine
VH	Valley Heads Moraines
WC	West Canada Readvance
WR	Wolf Rock Moraine

(modified from Ridge, 2004)

Woodworth (1905) was the first to postulate that active glacial retreat in the Mid-Hudson Valley was segmented by periodic glacial advances. Following Woodworth's (1905) publication, workers on the subject became divided amongst two factions with opposing models for explaining the origin of glacial deposits (Dineen, 1986). One group believed that stagnate ice contributed to glacial deposits while the opposing group believed that active glacial retreat is what created glacial deposits (Dineen, 1986). This argument persisted in the literature from approximately 1910 until the 1960s when LaFleur (1961, 1965) found deposits left behind by both active and stagnant glacial

retreat and was later supported by Connally and Sirkin (1970). The Helderberg Plateau was covered by three lobes of glacial ice during the onset of the Late Wisconsinan glaciation (Dineen, 1986). The three lobes were known as the Mohawk Lobe, Hudson Lobe, and the Schoharie sub-lobe (Dineen, 1986). The lobes which covered the plateau originally entered the region from the northeast. This is shown by drumlin orientations in the study area which indicate a clear NE-SW trend (Mylroie and Mylroie, 2004) (Figure 2.7).

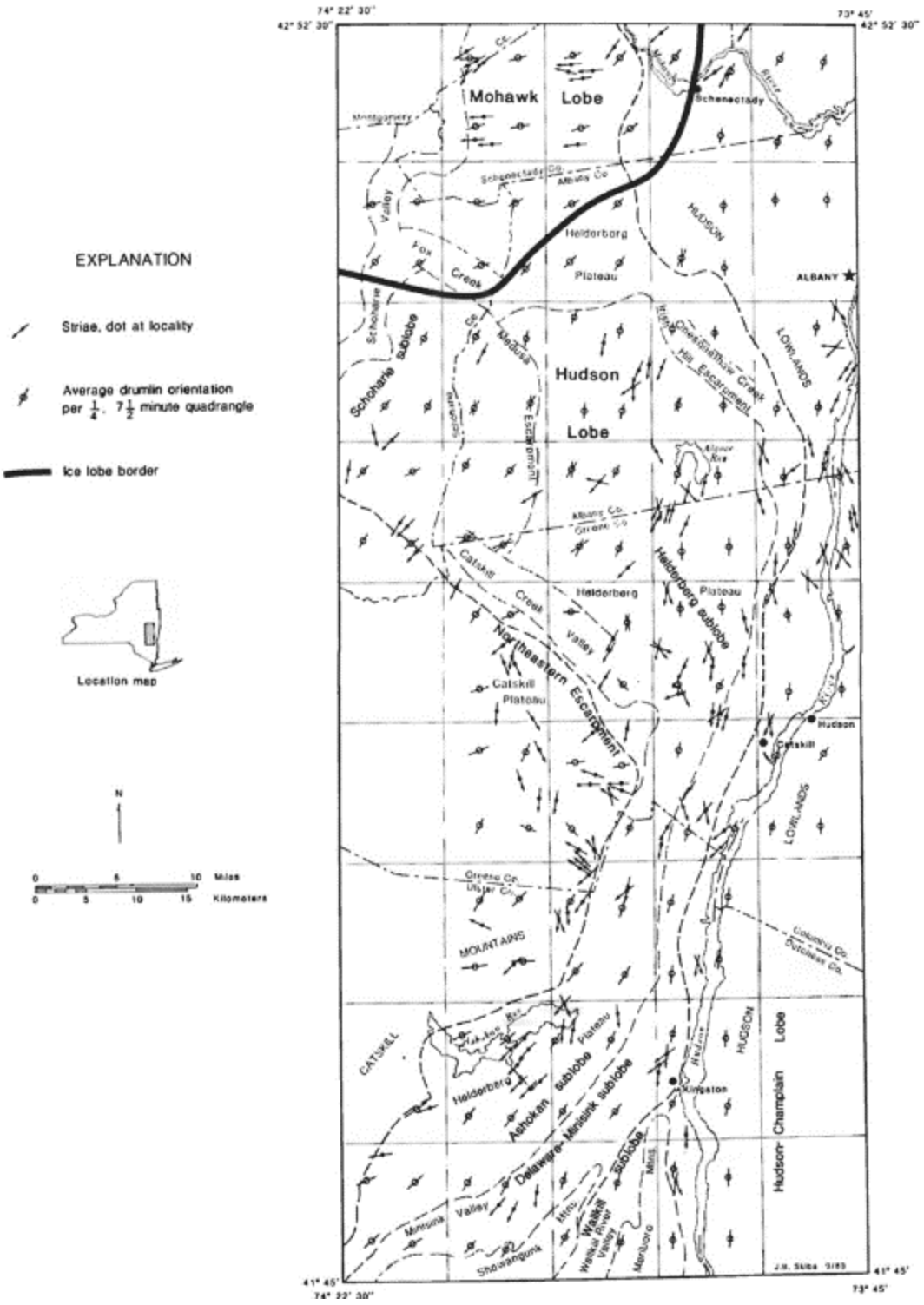

Figure 2.7 Map showing drumlin and striae orientations in addition to the location and names of particular lobes of the glacier

(from Dineen, 1986).

The glacial lobes deranged the landscape and altered it greatly to now be covered by drumlins, kames, glaciokarst, and glacial drainage basins as well as other paleoglacial landforms. Dineen and Hanson (1985) proposed the Late Wisconsinan glaciation ended in the region approximately 12,300 years ago. The exact end date of the Late Wisconsinan glaciation in the study area is still a highly debated topic to which there has been no exact answer. According to data compiled by Muller and Calkin (1993), the Wisconsinan is broken up into Early (~117,000-64,000 ybp), Middle (~64,000-23,000 ybp), and Late (~23,000-11,900 ybp) (Table 2.3).

Table 2.3 Timing of the Wisconsinan Glaciation.

Geologic Time					ka BP	Oxygen-isotope stage
PLEISTOCENE	Late	Wisconsinan	Late	Two Creeks Interstade	… 11.9	1
				Port Huron Stade	… 13.0	
				Mackinaw Interstade		
				Port Bruce Stade		2
					--- 15.5	
				Erie Interstade		
					--- 16.5	
				Nissouri Stade		
					--- 23.0	---
			Middle	Plum Point Interstade		3
				(Port Washington)	--- 35.0	
				Cherrytree Stade (Nassauan)		
					--- 40.0	
				Port Talbot Interstade		---
					--- 64.0	
			Early	Guildwood Stade		4

				St. Pierre Interstade	… 80.0	5a
				Nicolet Stade		5b
				[Eowisconsinan]		5d
	Middle	Sangamonian Interglacial			--- 117.0	--- 5e
					--- 130.0	…
		Illinoian				6, 7, 8
					--- 303.0	… 9
					--- 734.0	19

(modified from Muller and Calkin, 1993)

Glacial Deposits

Glacial deposits in which the source is carbonate rock, produce carbonate-rich glacial sediments, likewise, if the source rock is silica rich then the glacial sediments produced as the result of glaciation will also be silica rich (Stephenson et al., 1988). As described by Stephenson et al., (1988), deposits in glaciated regions are rarely uniform and isotropic with the exception of some glaciolacustrine and glaciofluvial deposits. Glacial lakes that formed during the Pleistocene contained an abundance of fine grained sediment, such as sand, silt, and clay (Stephenson et al., 1988). The damming of Schoharie Creek and subsequent influx of glacial melt water carrying large amounts of glacial sediment resulted in the deposition of glaciolacustrine clays at distinct elevations in the Schoharie Valley (Dumont, 1995). Clays of this type have been documented to exist in McFail's Cave, Barrack Zourie Cave, Howe Caverns and Caboose Cave (Mylroie, 1977, 1984; Dumont 1995) (Figure 2.8). Sediments such as that which are seen in Figure 1.3 are not only found in caves, they have also been found in outcrops on the surface as well. This sediment fits the description of a glaciolacustrine deposit given by Stephenson et al., (1988).

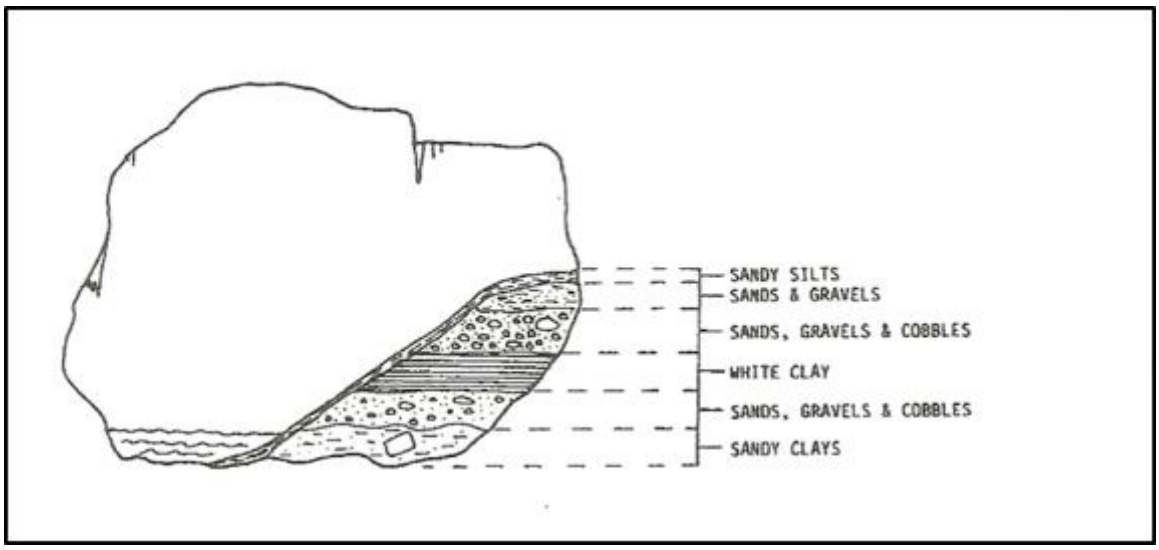

Figure 2.8 Model showing the various units which exists in the outcrops of interest within the examined caves

(modified from Mylroie, 1984).

The reason why the glaciolacustrine sediment can be found in the caves located in this area is because a glaciolacustrine environment existed during the most recent glacial period. The existence of the glaciolacustrine sediment implies that the water in the basin would have to be stagnant (no turbulent flow) therefore the sediment settling out of water could not have been mixed with other sediment previously deposited in the caves by flowing streams.

Formation of Karst

Karst features of the Helderberg Plateau were created by epigenic processes providing alternate flow routes through the bedrock allowing water to travel much quicker from hypothetical point 'A' to point 'B'. The karst features of the Helderberg Plateau have been described as being "one of the finest examples of glaciated karst in the country" (Palmer et al., 1991, p. 161).

Caves investigated within the Helderberg Plateau

Barrack Zourie Cave

Barrack Zourie Cave was discovered in 1992 and is located in western Schoharie County, (Lauritzen and Mylroie, 2000) (Figure 2.9). It is one of the larger cave systems in the Cobleskill Plateau whose main entrances to the cave are located in Brown's Depression (Dumont, 1995). Brown's Depression is not a dissolutional basin, but a former valley turned internal drainage basin, by drumlins blocking the southern end of the valley. The valley was likely created by flowing surface water during interglacials, and modified by later glacial scouring; the drumlins were then created later during glaciation. Subsurface drainage conduits such as Barrack Zourie Cave allow surface water to drain through or beneath them, bypassing the drumlin blockage. Barrack Zourie Cave prevented the depression from becoming a lake similar to those to the west, such as the Finger Lakes of New York State. Located at the bottom of the depression is clay which may have been clastic sediment deposited by Glacial Lake Schoharie (Mylroie, 1977). This cave is rich in calcite-rich and fine-grained rhythmites that contribute to further evidence of Glacial Lake Schoharie (Palmer et al., 2003). Dumont (1995) described the cave system, noting that the sediment in the cave varies in size from fine grains to immense stones and contains what was interpreted to be glacial rock flour. Dye tests were performed in order to accurately determine the flow of water through the cave system, the largest contributor is located near Brown's Depression as water winds its way through Barrack Zourie in a north to south pattern (Figure 2.2) (Dumont, 1995).

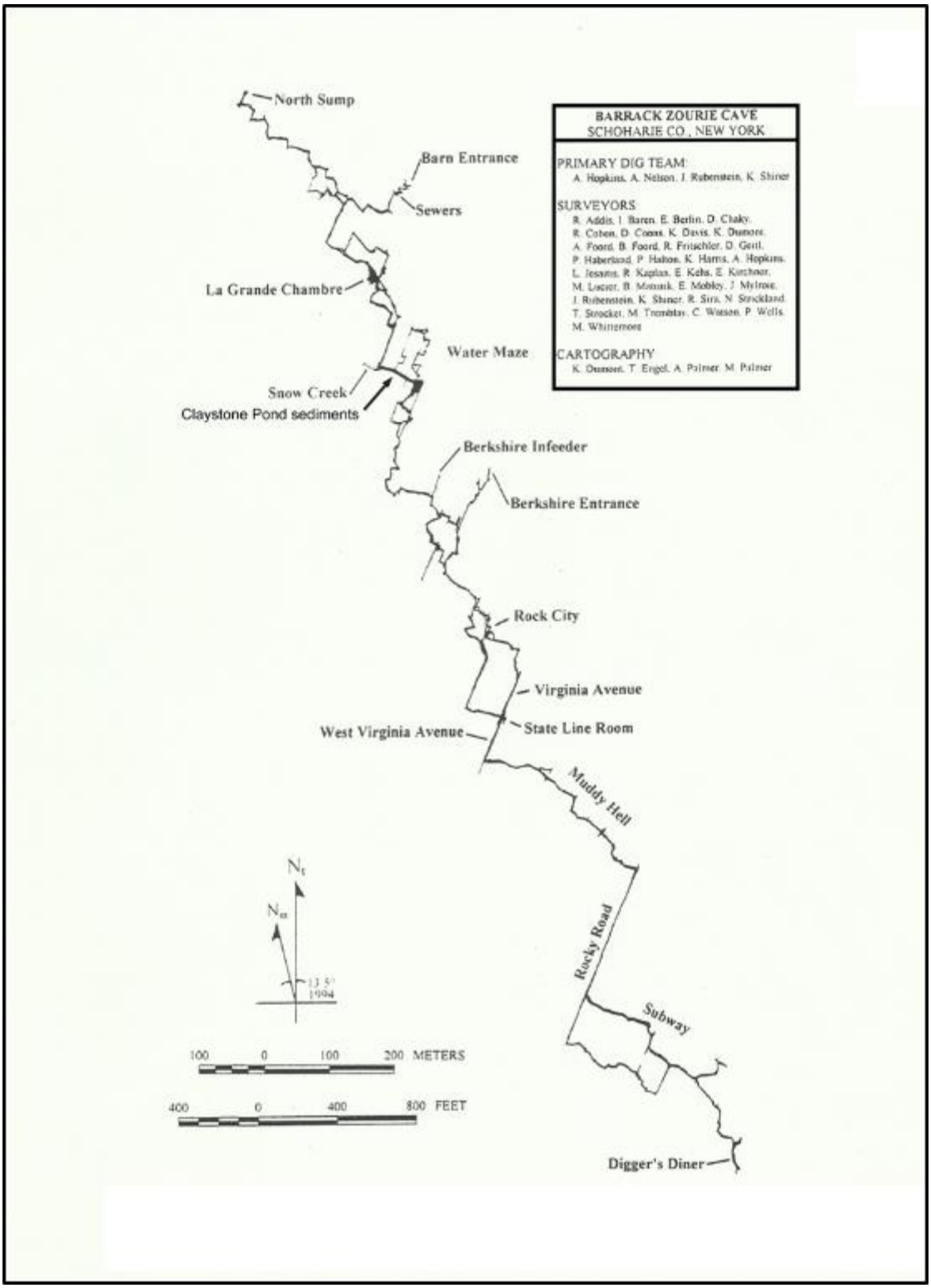

Figure 2.9 Map of Barrack Zourie Cave showing the location of sediment collection (modified from Dumont, 1995).

McFail's Cave

McFail's Cave is named after Professor Thomas Alfred McFail who entered the site in 1854 (Stone, 2005). It is located to the northeast of Cobleskill, New York and owned by the National Speleological Society (Figure 2.10). The entrance to the cave is a vertical descent which requires cavers to proceed with caution (Stone, 2005). This cave is the longest and deepest in the Helderberg Plateau; its length is 10.7 km (6.6 miles) (Palmer et al., 2003). As mentioned by Lauritzen and Mylroie (2000), rock flour deposits were found to exist in both McFail's Cave and Howe Caverns. Prior to the Wisconsinan glaciation, many caves in the Helderberg Escarpment may have been a part of a larger interconnected system (Palmer et al., 2003).

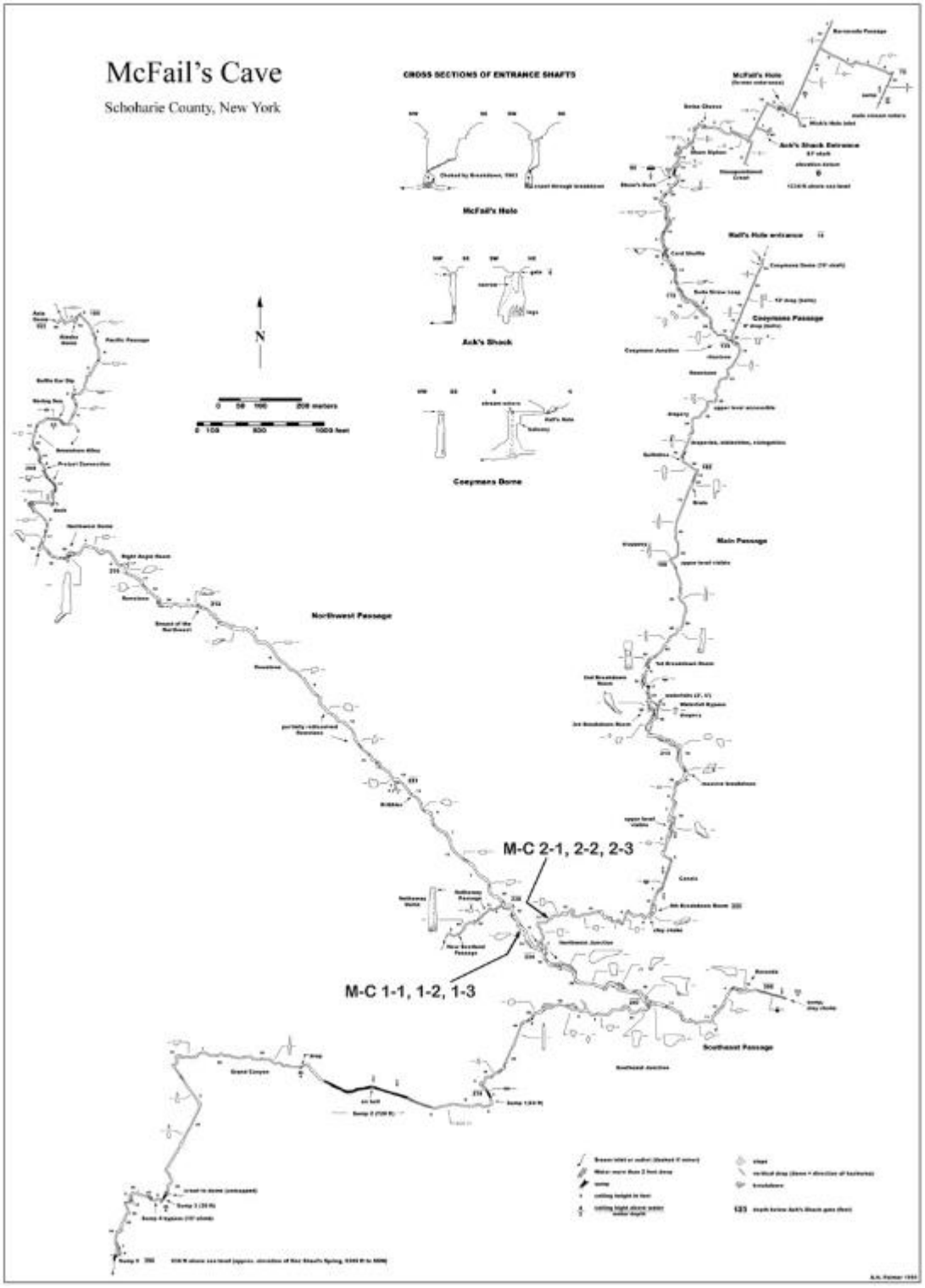

Figure 2.10 Map of McFail's Cave.

The sample numbers which correspond to collection sites within the cave are shown above (from Palmer, 1991).

Howe Caverns

Howe Caverns is one of two caves that are open to the public in the Helderberg Plateau (Figure 2.11). The layout of this cave has continued to change since the site's early discovery and some portions have been removed by quarrying activities away which are still active today (Palmer et. al., 2003). Palmer (2007) noted that the cave system has formed a semi-dendritic pattern in which small passages snake towards the main passageway. Evidence of the last glaciation can be observed in this cave as well as the history of the climate spanning multiple glaciations (Lauritzen and Mylroie, 2000). This cave exhibits many of the features that are to be expected of areas affected by advance and retreat phases of glaciation. These features include glaciolacustrine deposits such as rhythmite deposits as well as stratified sediment deposits. According to Palmer (2007), the lacustrine deposits found in this area are the result of Glacial Lake Schoharie.

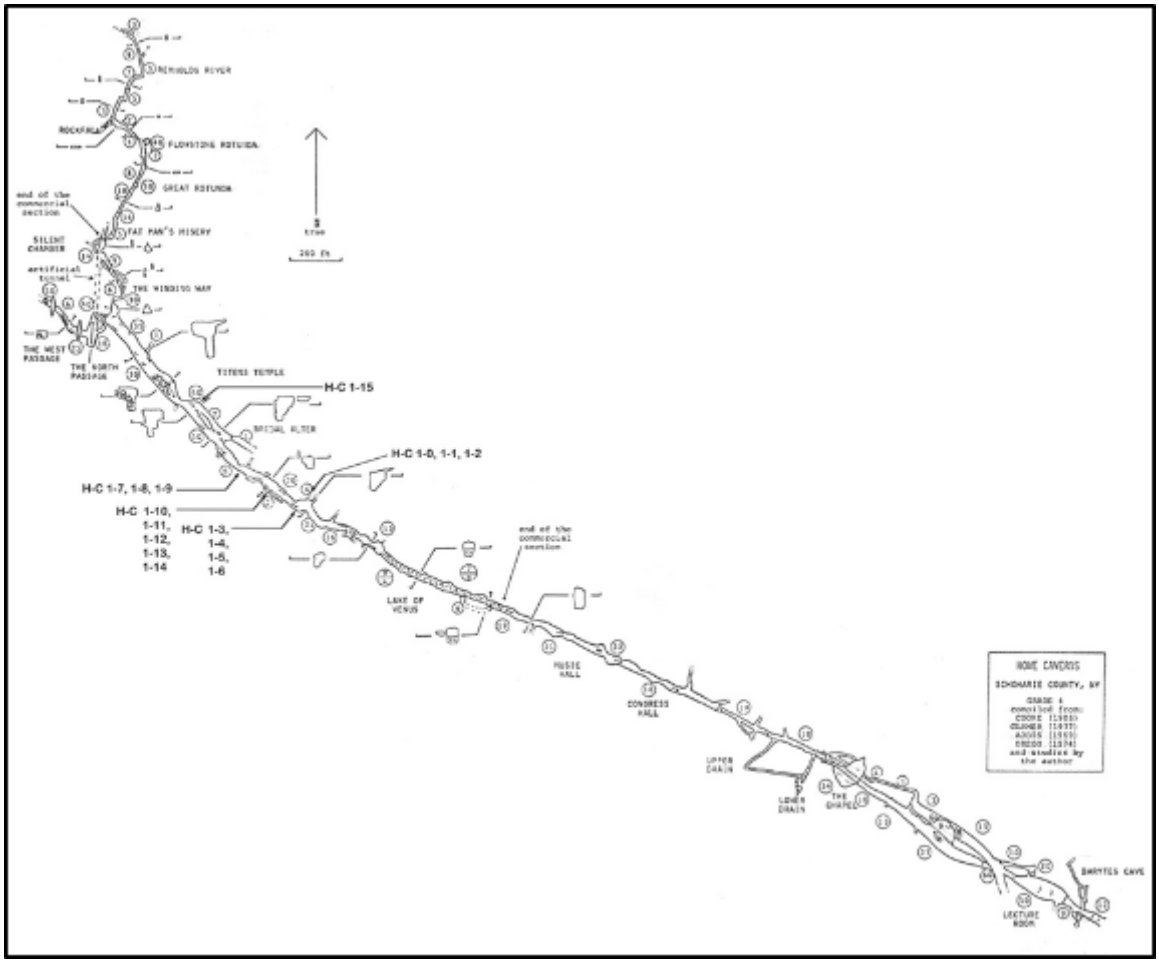

Figure 2.11 Map of Howe Caverns showing the locations of sample collection sites (modified from Mylroie, 1977).

Secret-Benson Caverns

In addition to Howe Caverns, Secret Caverns is the only other cave open to the public. Mylroie (1977) described this cavern in detail. The cave has been historically divided into two separate caves: Secret Caverns located in the upstream portion of the system and Bensons Cave (not open to the public) located downstream (Figure 2.12). The cave developed in the Chrysler Dolomite, the Thatcher Limestone and the Ravena Dolomite. The cave stream in the Benson part flows northeast against the regional dip

(Mylroie, 1977). Secret-Benson Caverns may have once been a part of larger more integrated system, but has been divided into separate areas (Palmer, 2007). Though beginning at separate junctures, the water from Secret Caverns and Bensons Cave converges and continue south toward the Cobleskill Creek (Mylroie, 1977).

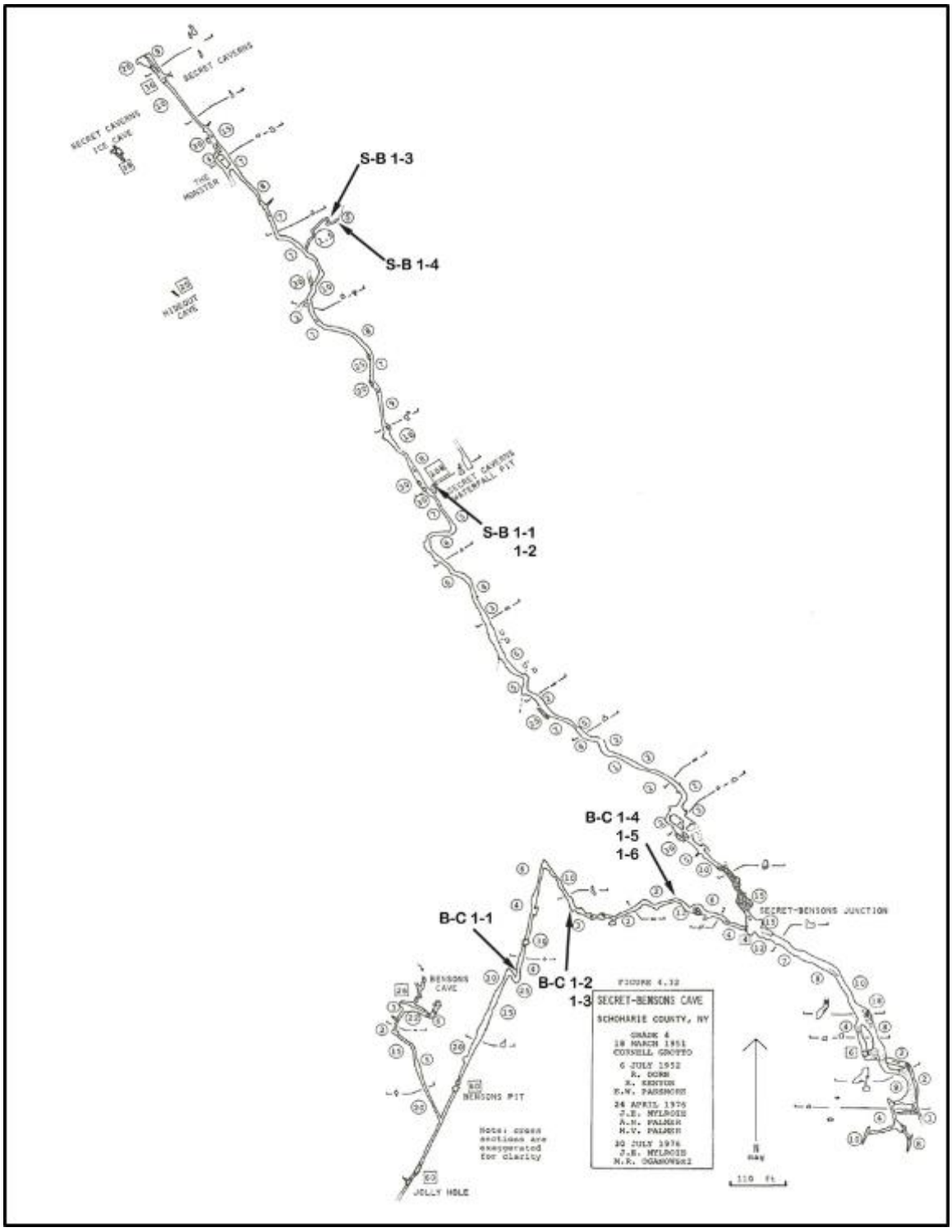

Figure 2.12 Map of Secret-Benson's Cave showing the location of sample sites (modified from Mylroie, 1977).

Gage Caverns

Gage Caverns was originally named Balls Cave after its discovery by Peter Ball in 1831 (Sheppard, 1853) (Figure 2.13). Mylroie (1977) divided the cave into three levels, the Coeymans/Manlius Limestone, Middle Manlius Limestone and the Manlius Limestone/Rondout Dolomite. The water flow in these areas differs as the middle Manlius limestone is occupied upstream and the Manlius Limestone/Rondout Dolomite is active downstream (Mylroie, 1977). The cave is essentially a single passage carrying a stream from north to south. The cave contains a large main passage way that branches off upstream into tributary passages; with many sediment-blocked passages downstream (Mylroie, 1977).

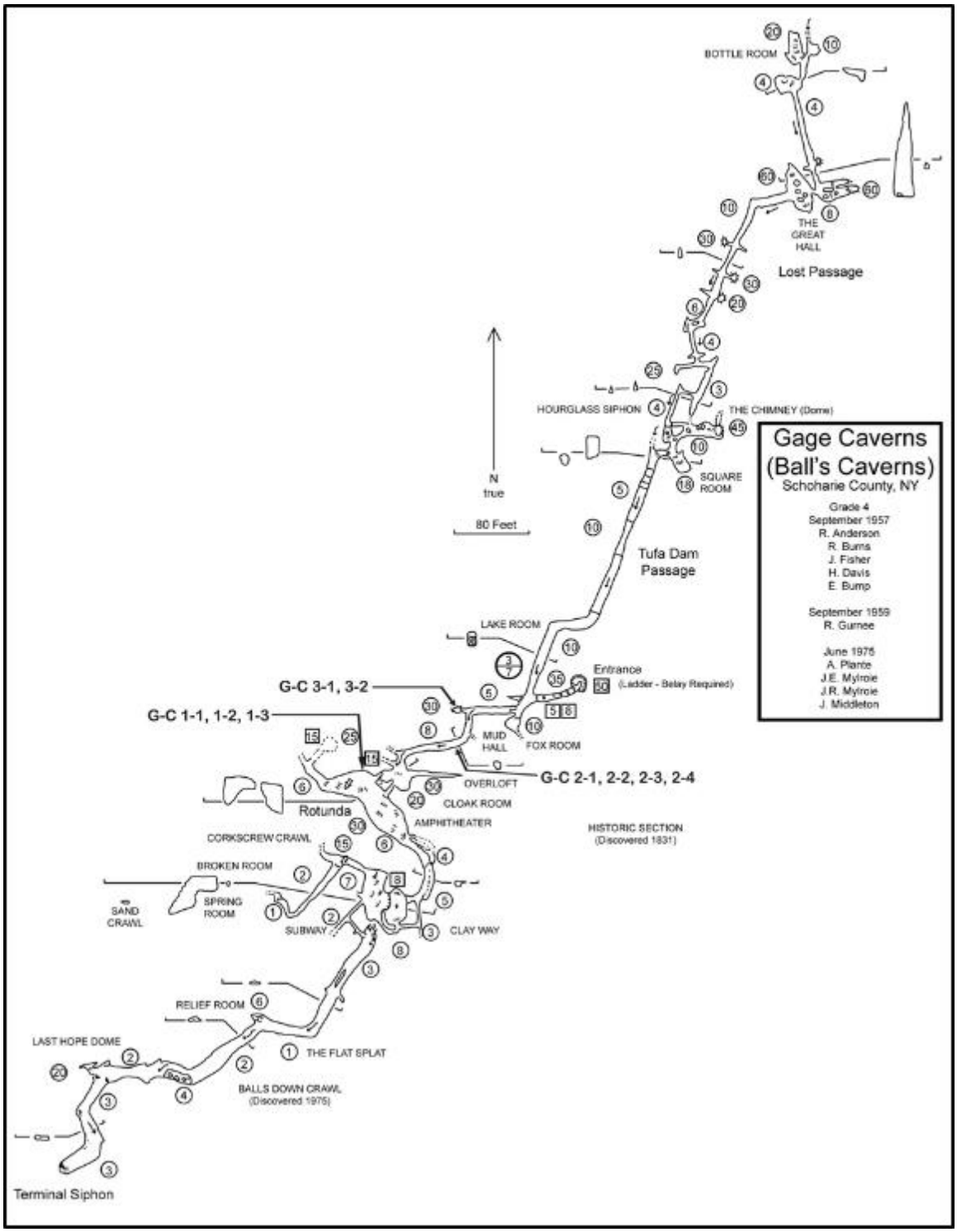

Figure 2.13 Map of Gage Caverns showing the locations from which samples were collected

(modified from Mylroie, 1977).

Westfall Spring Cave

Westfall Spring Cave was originally an occluded bluff spring which was excavated in 1975 (Mylroie, 1977). The entire cave exists within the Cobleskill Limestone in contact with the overlying Rondout Formation. The cave is presumed to be a tapoff passage for a master cave system located in the vicinity (Mylroie, 1977). Reasons why the cave is thought to be a tapoff passage is because its total mapped length is less than 152 m, (500 feet) also the passage is a low oval tube which is only 0.5 m (1.5 feet) high and 1.5 m (5 feet) wide inferring it is post-glacial in origin, meaning it formed after the major cave systems had already been established (Figure 2.14).

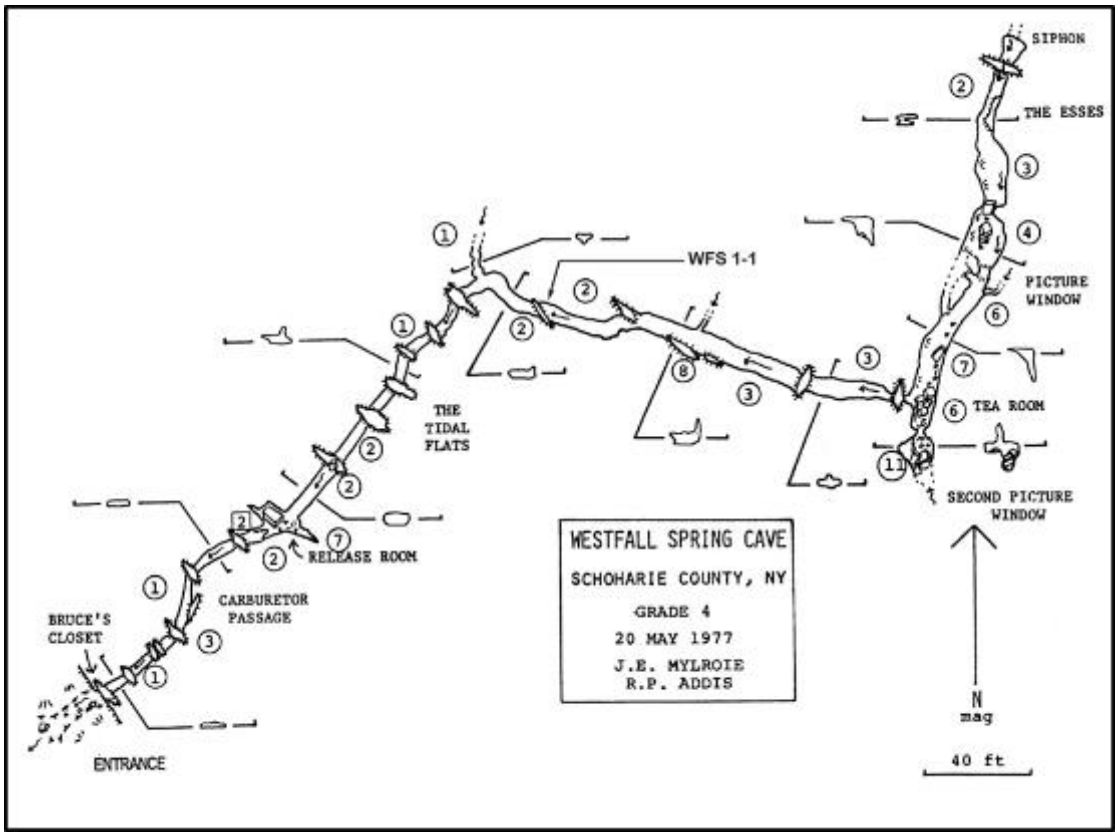

Figure 2.14 Map of Westfall Spring Cave showing the location of the collection site (modified from Mylroie, 1977).

Schoharie Caverns

Schoharie Caverns, Gage Caverns and McFail's Cave are owned by the National Speleological Society and visitors must sign a waiver before entering (Palmer et al., 2003) (Figure 2.15). The entrance is a high but narrow passage. The cavern consists almost entirely of just one large passage (Palmer et al., 2003). Radiometric dating by U/Th methods of speleothems found in the cave predates the Wisconsin glaciation as proven by Lauritzen and Mylroie (2000). The entrance to the cave is especially large and contains evidence of glaciation (Mylroie and Mylroie, 2004). As noted by Mylroie and Mylroie (2004), there are striations on the outcrop surrounding the entrance to the cave. The striations would have been created by glaciers that once covered the area during the last glaciation.

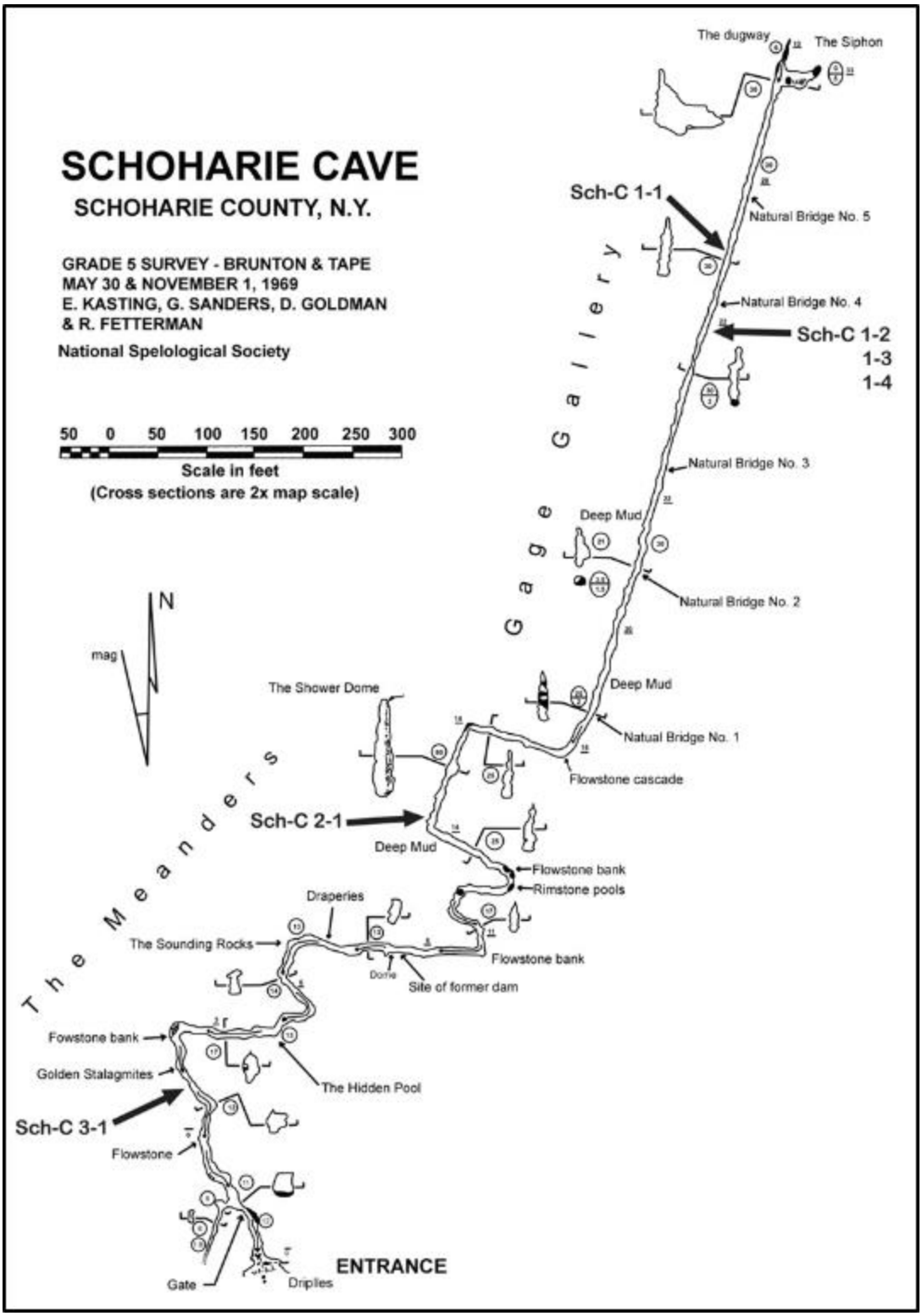

Figure 2.15 Map of Schoharie Caverns showing the locations of sample sites (modified from Kastning, 1975).

Caboose Cave

Caboose Cave is located in eastern Schoharie County (Figure 2.16). As noted by Mylroie (1977), the entire Caboose cave system is comprised of Caboose Cave, an overflow spring, Caboose spring, and surface dolines. The layer of white clay in this cave was deposited during the Pleistocene when glaciers covered the area (Mylroie, 1984), or near the end of the glacial period when Glacial Lake Schoharie covered the cave making the clay a glaciolacustrine deposit. This sediment was deposited by glacial ice and mobilized by melt water (Palmer, 2007).

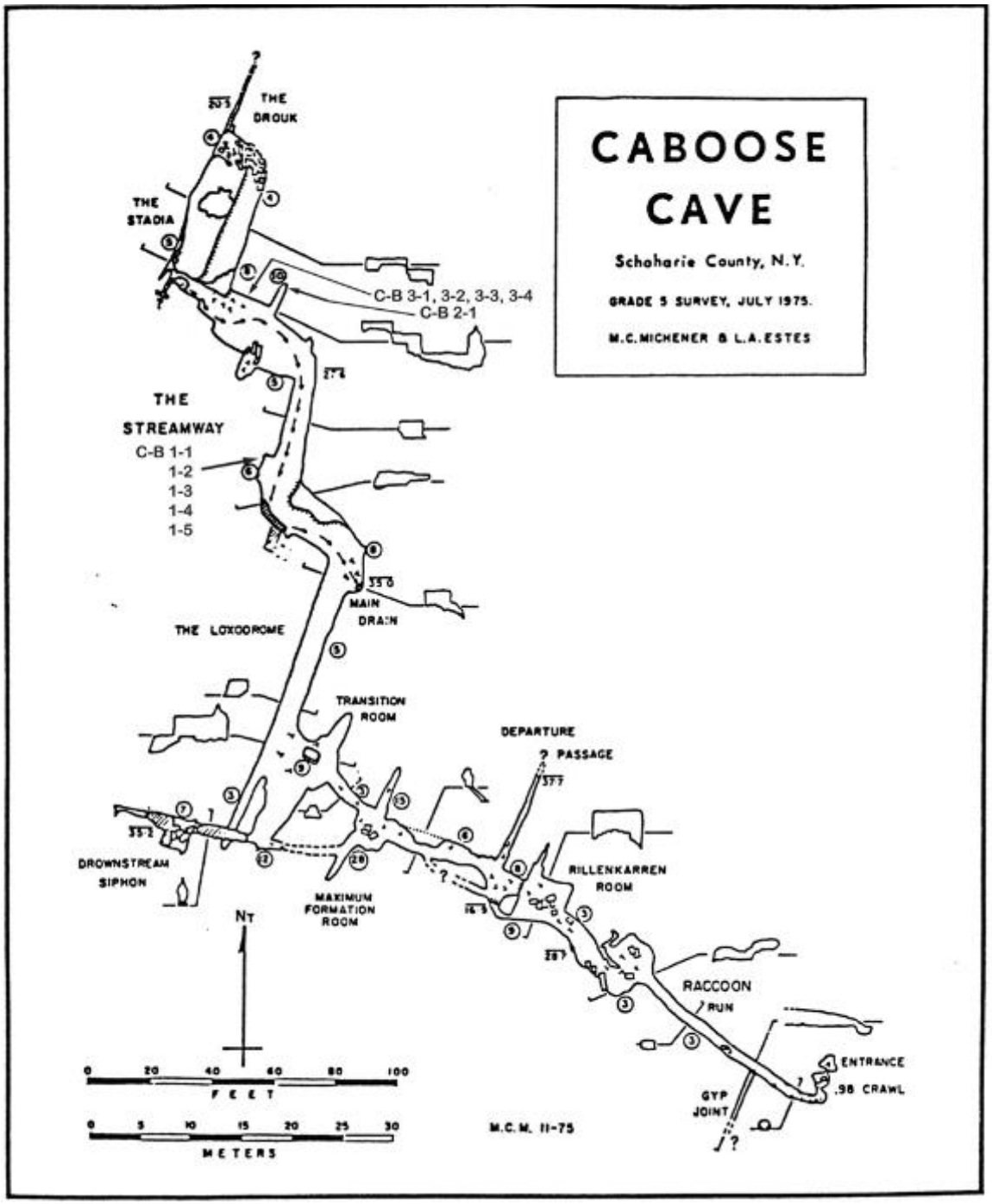

Figure 2.16 Map of Caboose Cave showing the location of sample sites (modified from Mylroie, 1977).

Knox Cave

Knox Cave is located in Albany County, New York and owned by the Northeastern Cave Conservancy (Figure 2.17). Palmer (2003) highlighted that the cave is located at a 2.5 degree gradient which is double the degree of slope for most other cave sites in the area. Evidence of severe flooding is present, as the springs that the cave water drains to are partially blocked by glacial till and other sediment (Palmer, 2003). The location of Knox Cave has been known for many decades now and few discoveries had been made since the 1950s; however in the 1990s, new areas of the cave were uncovered (Palmer, 2009). As Palmer (2009) mentioned, the known passages in the cave are located near the bottom of the Silurian-Devonian but the newly discovered areas are beneath those. This newest area has been termed the Brayman Formation; it is located on a thrust fault that allowed the passage of water through poorly soluble rock (Palmer, 2009).

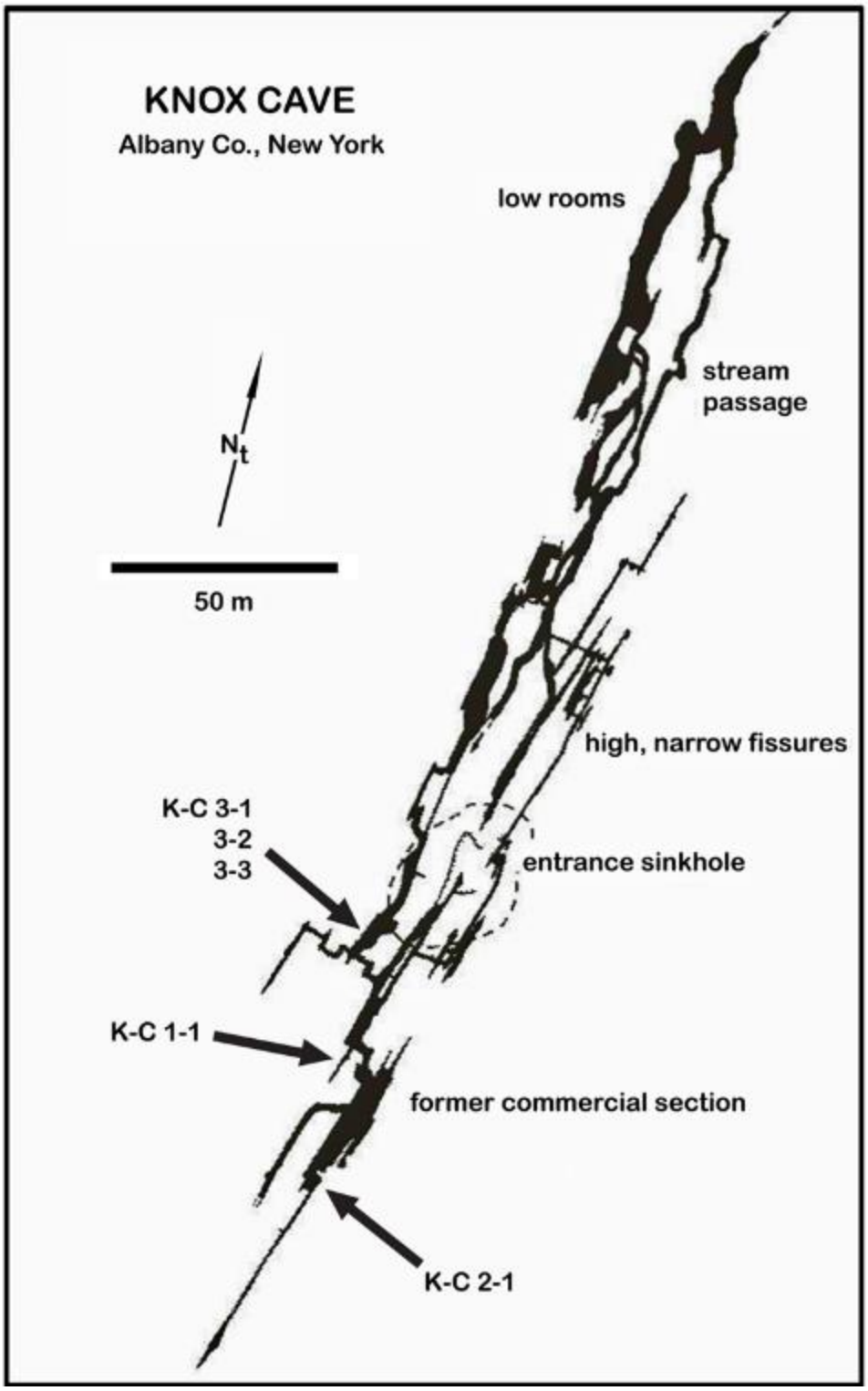

Figure 2.17 Map of Knox Cave showing the locations of sample collection (modified from Palmer et al., 2003).

Cave Elevations

Figure 2.18 shows the elevations occupied by each cave in order from the northwest to the southeast. These elevations include only known passages, not connections demonstrated by dye tracing. The elevations of three different levels of Glacial Lake Schoharie are also shown. Note that Knox Cave is almost entirely out of the lake's highest footprint. The passages in Knox Cave which are barely within the footprint are small passages at the base of the cave thought to be post-glacial in age (Palmer 2009). These youthful passages were not sampled.

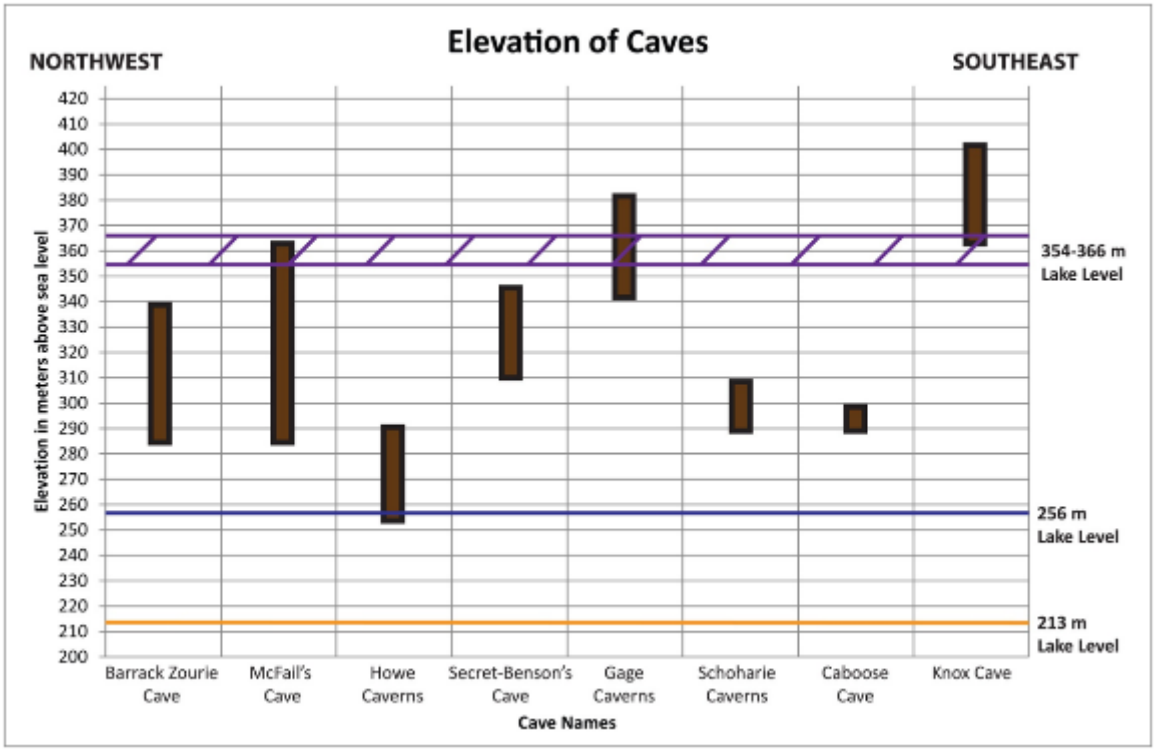

Figure 2.18 The elevations occupied by each cave in order from Northwest to Southeast is shown above as well as the proposed shore line elevations of Glacial Lake Schoharie.

CHAPTER III

PREPARATION & FIELD WORK

Though there has been extensive documentation and work conducted regarding the caves located in Cobleskill Plateau and adjoining areas (e.g. Dumont, 1995; Mylroie, 1977; Mylroie, 1984; Palmer et al., 2003), analysis of possible glacial deposits within the caves and their link to a postulated glacial lake which existed in the study area has not been thoroughly investigated. Speleological investigations required multiple caving trips to sites within the Helderberg/Cobleskill Plateau. The purpose of the trips was to acquire white clay samples, and adjacent sediment samples, that were suspected to have been deposited during the most recent glaciation. To obtain these samples, teams of no less than three cavers participated in the caving trips. For some of the cave trips, vertical descent methods were required; extra caution was taken. Clay samples were collected and stored in 35 mm plastic film canisters. Prior to collecting any samples, the film canisters were sterilized using a mixture of 3.25 L (3.43 qt) of tap water mixed with 60 ml (2.03 fl. oz.) of Chlorox Bleach® heated to 82.22 °C (180 °F) in a 3.79 L (4 qt) pot on a conventional stove. The canisters were fully submerged in the solution for one minute, then air dried for four hours.

During in-cave sample collection, the location, time, and date was recorded as well as the sample number. Photo documentation and cataloging accompanied each sample. The distance between each sample and the number of samples per cave was

determined based on the size of the existing outcrop(s) of sediment found within each cave.

A total of 63 samples were collected for this study (excluding the three samples collected from Barrack Zourie Cave) (Table 3.1). The minimum number of samples collected from a cave in this study was one from Westfall Spring Cave. The reason why only one sample was recovered from this cave was because the cave was believed to be post-glacial in origin making the one sample collected from this cave a control sample (Figure 2.13). The maximum number of samples collected from on cave was fifteen from Howe Caverns. The reason why such a large number of samples were collected from this cave was because of the abundance of available sampling locations encountered in the cave. The labeling of each sample was done in such a manner that: a.) the cave which the sample was collected from could be determined, b.) which outcrop from within the cave the sample was collected from and, c.) which unit had been collected from the outcrop (e.g. C-B 1-4 means that the sample was collected from Caboose Cave and was the fourth sample collected from outcrop number one).

Table 3.1 The above table shows the number of samples collected from each cave, the classification assigned to each sample, and the symbology used in table seven.

Cave	Number of Samples Collected	Sample Number	Unit Classification	Symbol	Color of symbol
Secret Caverns	Four	S-B 1-0	Dark Brown/Dark Grey Clay	Square	Blue
		S-B 1-1	Dark Brown/Dark Grey Clay	Square	Blue
		S-B 1-2	Tan 'White' Clay	Diamond	Red
		S-B 1-3	Dark Brown/Dark Grey Clay	Square	Blue
Benson's Cave	Six	B-C 1-1	Dark Brown/Dark Grey Clay	Square	Blue
		B-C 1-2	Dark Brown/Dark Grey Clay	Square	Blue
		B-C 1-3	Dark Brown/Dark Grey Clay	Square	Blue
		B-C 1-4	Dark Brown/Dark Grey Clay	Square	Blue
		B-C 1-5	Dark Brown/Dark Grey Clay	Square	Blue
		B-C 1-6	Dark Brown/Dark Grey Clay	Square	Blue
Howe Caverns	Fifteen	H-C 1-0	Tan 'White' Clay	Diamond	Red
		H-C 1-1	Light Grey Clay	Circle	Green
		H-C 1-2	Dark Brown/Dark Grey Clay	Square	Blue
		H-C 1-3	Tan 'White' Clay	Diamond	Red
		H-C 1-4	Light Grey Clay	Circle	Green
		H-C 1-5	Dark Brown/Dark Grey Clay	Square	Blue
		H-C 1-6	Dark Brown/Dark Grey Clay	Square	Blue
		H-C 1-7	Dark Brown/Dark Grey Clay	Square	Blue
		H-C 1-8	Dark Brown/Dark Grey Clay	Square	Blue
		H-C 1-9	Dark Brown/Dark Grey Clay	Square	Blue
		H-C 1-10	Tan 'White' Clay	Diamond	Red
		H-C 1-11	Tan 'White' Clay	Diamond	Red
		H-C 1-12	Light Grey Clay	Circle	Green
		H-C 1-13	Dark Brown/Dark Grey Clay	Square	Blue
		H-C 1-14	Allogenic Glacial Outwash	Triangle	Yellow
		H-C 1-15	Dark Brown/Dark Grey Clay	Square	Blue
Barrack Zourie Cave	Three	BZ-C FL	Light Grey Clay	Circle	Green
		BZ-C CS	Tan 'White' Clay	Diamond	Red
		BZ-C SL	Tan 'White' Clay	Diamond	Red
McFail's Cave	Six	M-C 1-1	Tan 'White' Clay	Diamond	Red
		M-C 1-2	Allogenic Glacial Outwash	Triangle	Yellow
		M-C 1-3	Dark Brown/Dark Grey Clay	Square	Blue
		M-C 2-1	Tan 'White' Clay	Diamond	Red
		M-C 2-2	Allogenic Glacial Outwash	Triangle	Yellow
		M-C 2-3	Allogenic Glacial Outwash	Triangle	Yellow

Table 3.1 (Continued)

Cave	Number of Samples Collected	Sample Number	Classification	Symbol	Color of symbol
Caboose Cave	Ten	C-B 1-1	Tan 'White' Clay	Diamond	Red
		C-B 1-2	Tan 'White' Clay	Diamond	Red
		C-B 1-3	Allogenic Glacial Outwash	Triangle	Yellow
		C-B 1-4	Allogenic Glacial Outwash	Triangle	Yellow
		C-B 1-5	Dark Brown/Dark Grey Clay	Square	Blue
		C-B 2-1	Allogenic Glacial Outwash	Triangle	Yellow
		C-B 3-1	Allogenic Glacial Outwash	Triangle	Yellow
		C-B 3-2	Allogenic Glacial Outwash	Triangle	Yellow
		C-B 3-3	Tan 'White' Clay	Diamond	Red
		C-B 3-4	Tan 'White' Clay	Diamond	Red
Gage Caverns	Nine	G-C 1-1	Dark Brown/Dark Grey Clay	Square	Blue
		G-C 1-2	Dark Brown/Dark Grey Clay	Square	Blue
		G-C 1-3	Dark Brown/Dark Grey Clay	Square	Blue
		G-C 2-1	Dark Brown/Dark Grey Clay	Square	Blue
		G-C 2-2	Allogenic Glacial Outwash	Triangle	Yellow
		G-C 2-3	Tan 'White' Clay	Diamond	Red
		G-C 2-4	Tan 'White' Clay	Diamond	Red
		G-C 3-1	Dark Brown/Dark Grey Clay	Square	Blue
		G-C 3-2	Dark Brown/Dark Grey Clay	Square	Blue
Schoharie Caverns	Six	Sch-C 1-1	Light Grey Clay	Circle	Green
		Sch-C 1-2	Dark Brown/Dark Grey Clay	Square	Blue
		Sch-C 1-3	Tan 'White' Clay	Diamond	Red
		Sch-C 1-4	Tan 'White' Clay	Diamond	Red
		Sch-C 2-1	Tan 'White' Clay	Diamond	Red
		Sch-C 3-1	Light Grey Clay	Circle	Green
Westfall Spring Cave	One	WFS 1-1	Control Sample	Square	Green
Knox Cave	Five	K-C 1-1	Control Sample	Square	Purple
		K-C 2-1	Control Sample	Square	Purple
		K-C 3-1	Control Sample	Square	Purple
		K-C 3-2	Control Sample	Square	Purple
		K-C 3-3	Control Sample	Square	Purple

CHAPTER IV

LABORATORY METHODS

Introduction

Mylroie (1984) examined these glacial sediments solely from Caboose Cave. The samples collected for this study come from a wider suite of caves and more sophisticated analysis were conducted to determine: 1.) Were the Mylroie (1984) results reliable and 2.) How did other cave sample data compare to the Caboose Cave data. These sample analyses were not intended to be diagnostic, but to provide a reconnaissance baseline to guide further work. These analyses determined moisture content, organic content, and calcium carbonate content by changes in mass of the sample after each experimental treatment. Mass was determined by weighing the samples; in the following discussion use of the term weighing and weight is used to describe mass changes.

Weight Loss by Ashing

Sample Preparation

The sediments obtained during fieldwork were tested in a laboratory to determine the percentage of calcium carbonate and organics present in the sediment. There were several stages to this process beginning with the sterilization of all laboratory material/equipment and the elimination of any moisture within the sample by drying. In the lab located in Buchner Lane Building A (MSU campus), a five gallon tub filled with

13.21 L (3 gallons) of tap water, mixed with 236 ml (8 fl oz) of Clorox Bleach® and 29.57 ml (1 fl oz) of Dawn Dishwashing Detergent® was used to sterilize 64, 15 ml sized, stout crucibles. The crucibles were allowed to soak in the bath for 24 hours. The crucibles were then removed from the tub and were dried, then placed on a Gyratherm II hot plate for approximately 5 minutes. The crucibles were allowed to cool for approximately 20 minutes then all 64 crucibles were placed in a Cascade TEK Microprocessor Controlled Forced Air Oven Model: TF 0-1, TF 0-3, TF 0-5, TF 0-10, TF 0-28; with a Watlow Microprocessor Ramping Controller (WMRC) Series 982 for 12 hours, set to 100 °C.

Wet Weight and Moisture Removal Procedure

To obtain the total hydrated weight of each sample, prior to being heated to remove moisture, a Mettler AE 160 balance was used. The samples were individually removed from the film canisters using a metal scoopula and placed in square plastic weighing boat. Prior to weighing each sample an empty weighing boat was used to zero/tare the balance. The empty weighing boat weighed 2.54 grams. The samples were then separated into two parts and weighed. The first part or 'samples to be archived' were weighed using the same procedure mentioned above. The 'samples to be archived' remained hydrated in labeled plastic bags, the other part or 'wet sample' was hydrated as well but after weighing the samples were then placed in the crucibles. Prior to placing the 'wet samples' in the crucibles, each crucible weight was recorded without the lid. The 'wet samples' in the crucibles, with lids placed on top of the crucibles, were then placed in the Controlled Forced Air Oven for 24 hours with the Watlow Microprocessor Ramping Controller WMRC set to 105 °C. After 24 hours the oven was shut off and the

crucibles were allowed to cool in the oven for twelve hours. After cooling, the crucibles containing the samples were removed from the oven and weighed again without the crucible lids. Once being weighed the crucible lids were replaced and the sample was set aside to await packing for transport. Once all the crucibles had been weighed they were placed on sheets of cardboard then wrapped tightly in cellophane. The cellophane was used to minimize the possibility of sample loss from the crucibles while in transit from Buckner Lane Building A Lab to the Biogeochemistry and Geoscience Education Research Group (BGERG) Laboratory in Hilbun Hall.

Powdering Samples and Splitting of Samples

At the BGERG Laboratory, the crucibles were removed from the cellophane wrap and placed on a shelf exposed to the environment of the lab. The samples were individually ground into a fine powder using an agate mortar and pestle. Between grinding each sample, the mortar, pestle, and scoopula was cleaned using acetone and wiped clean of any residue left behind using Kimwipes®. A fraction of the powdered sample was placed on a 100 mm by 100 mm Fisherbrand® Weighing Paper to be weighed using a metal scoopula. Prior to weighing a fractionated sample the weighing paper was placed on a Denver Instrument Model: SI-234 balance and zeroed. After the fractionated sample had been weighed it was transferred into a 20 ml vial, with color coded labeling tape, using a piece of weighing paper folded into a conical shape. The above process was repeated three times per sample, resulting in a total of 189 individual vials filled with powdered sample. One third of the samples in the vials would be used for X-ray Diffraction (XRD) analysis (vials color coded with red tape). A second third would be ashed to determine weight loss on ignition (vials color coded with blue tape).

The final third would be used to determine weight loss by dissolution (vials color coded with yellow tape).

Calibration/Correction of Balances

Prior to any further analysis of the samples in the labeled vials, it was discovered that the three fractionated samples did not add up to the weight of the pre-separated dry sample. It was first suspected that the Mettler AE 160 balance used in the lab of Buckner Lane Building A was not calibrated the same as the Denver Instrument Model: SI-234 balance used in the BERG Lab. The hypothesis was tested using five pennies, four nickels, six dimes, nine quarters, and a 100 g brass weight. The test was preformed first on the Mettler balance. The balance was turned on and zeroed. Five pennies were placed on the balance, stacked vertically, and the weight was recorded. The pennies were removed from the balance and the balance was zeroed again. This process was repeated for the nickels, dimes, quarters, and the 100 g brass weight; with the balance being zeroed in between each weighing. The test was preformed five times to ensure accuracy. The coins and brass weight were placed in a Ziploc bag and taken to the BERG lab to test the Denver Instrument balance using the same method which was used to test the Mettler balance. After the test had been conducted on both balances it was found that they were similarly calibrated within a reasonable margin of error. The results of the test can be seen in Table 4.1.

Table 4.1 Shows the results of the test preformed on a Mettler balance and a Denver Instrument balance to confirm that they were calibrated the same

	Buckner Lane Mettler Balance All weights recorded are in grams						
	Run 1	Run 2	Run 3	Run 4	Run 5	Average	Average Deviation
Five Pennies	12.4684	12.4683	12.4683	12.4682	12.4684	12.46832	0.0001
Four Nickels	19.8000	19.8000	19.8001	19.8000	19.8002	19.80006	0.0001
Six Dimes	15.8486	15.8487	15.8486	15.8488	15.8486	15.84866	0.0001
Nine Quarters	50.7412	50.7415	50.7415	50.7414	50.7414	50.7414	0.0001
100 gram brass weight	100.0043	100.0044	100.0042	100.0041	100.0041	100.0042	0.0001

	BERG Lab Denver Insrument Balance All weights recorded are in grams						
	Run 1	Run 2	Run 3	Run 4	Run 5	Average	Average Deviation
Five Pennies	12.4676	12.4684	12.4685	12.4682	12.4684	12.46822	0.0003
Four Nickels	19.8002	19.8000	19.8001	19.8001	19.8001	19.8001	0.0000
Six Dimes	15.8487	15.8486	15.8486	15.8486	15.8485	15.8486	0.0000
Nine Quarters	50.7414	50.7414	50.7413	50.7412	50.7414	50.74134	0.0001
100 gram brass weight	100.0044	100.0049	100.0044	100.0045	100.0045	100.0045	0.0001

Moisture Removal II and Re-weighing

It was then speculated the samples had gained moisture resulting in weight increase. This was thought to be the source of error because after the samples had been initially dried in the crucibles in the forced air oven they were not placed in a desiccator to eliminate the chance of introducing moisture to the samples. The then dried again at 105 °C to remove any moisture re-introduced to the samples then the samples were place in desiccators to cool prior to any further analysis.

A combination of stout and tall 20 ml vials had been used to store the fractionated samples, the 'ashing samples' that had been stored in tall 20 ml vials were then transferred into stout 20 ml vials to assure that all samples were heated evenly when placed in the Fisher Scientific Thermo Scientific Oven Model: 664 (drying oven). The

63 ‘ashing samples’ were placed in the oven set to 105 °C for 24 hours to remove all moisture. The ‘ashing samples’ were then placed in a desiccator to cool for approximately 12-24 hrs.

The stout 20 ml vials that had been used to store the ‘ashing samples’ were now sterilized so they could be used to replace the tall 20 ml vials. Once the stout 20 ml vials were clean and dried, the contents from the tall 20 ml vials were transferred into the stout 20 ml vials. The XRD and the dissolution sample vials were then placed in the oven for 24 hours at 105 °C then were placed in a desiccator to cool. Once the vials had cooled they were removed from the desiccator, weighed, and then capped until needed for further analysis.

Weight Loss by Ashing

Since the crucibles were empty they needed to be cleaned and dried to be reused for further weight loss analysis. Once the crucibles were sterilized they were individually weighed without their lids and the weight was recorded. The ‘ashing samples’ were then transferred from the stout 20ml vials into the labeled crucibles. The weight of the crucible was subtracted from the total weight (total weight – crucible weight = ‘ashing sample’ weight) to determine the weight of the ‘ashing sample’. Then the crucible lids were replaced and the crucibles were placed in a desiccator for 24 hours to remove any residual moisture. The procedure followed to determine weight loss due to the ignition of organics and carbonates was Heiri et al. (2001). The crucibles were then placed in a W.H. Curtin and CO. Type 2000 Thermolyne Furnace Model: F-A2025P with a Temperature Dubque II Controller (muffle furnace) set to 550 °C in batches of six for two hours. After two hours, the crucibles were removed from the muffle furnace and

placed in a desiccator to allow the crucibles to cool to room temperature. Once all 63 crucibles had been heated to 550 °C and were allowed to cool in the desiccator, the lids of the crucibles were removed and the crucibles with the samples were weighed. Again, to find the weight the total weight post 550 °C heating was found by subtracting the crucible weight from the total weight to find the 'ashing weight' post-heat treatment. With the data recorded, crucibles were then placed in the muffle furnace set to 950 °C for two hours, three crucibles at a time. In order to remove the samples from the muffle furnace a drop forged steel adjustable wrench was used since conventional crucible tongs would have melted due to the extreme temperatures. The samples were again placed in desiccators to allow the crucibles to be handled.

Weight Loss by Dissolution

Modification of Procedure

The procedure used for weight loss by dissolution was modified from the method set forth in Kunze and Dixon (1986). This modification included allowing the samples to dry between the removal of carbonates by dissolution and the removal of organics by dissolution prior to recording weight loss. Thirty grams of sodium acetate was weighed out and added into 1000 mL flask until a concentration of 136 g/L with Nano-pure water was achieved. Once the sodium acetate had dissolved completely in the Nano-pure water the pH of the solution was tested using a Denver Instrument pH/mV Meter UB-10 Ultra Basic. The mixture was then poured into a 1000 mL beaker and placed on a Sybron Thermolyne Nuova II stir plate. Acetic acid diluted with Nano-pure water was added to the sodium acetate solution using a glass dropper till a pH of five was reached. The solution was then transferred back into a 1000 mL flask and covered using parafilm.

Removal of Carbonates by Dissolution

Following the procedure set forth by Soukup et al., (2008) the 63 samples in the 20 mL stout vials labeled 'dissolution' were transferred into 100 mL centrifuge tubes. Prior to transferring the samples into the centrifuge tubes, the tubes were placed in an empty 400 mL beaker to determine the weight of each individual tube. The next step added 50 mL of one molar sodium acetate, pH of five, to the centrifuge tubes. The centrifuge tubes were then placed in 400 mL beakers filled approximately halfway with Nano-pure water. The 400 mL beakers were then placed in an 80 °C hot water bath to activate the reaction between the sodium acetate and the calcium carbonate to release CO2 and create a weight change. Once the reaction between the sodium acetate and carbonates had been completed the centrifuge tubes were removed from the hot water bath and placed into the centrifuge holders and weighed. The centrifuge being utilized for the study could run four samples at a time, so the centrifuge holders which were adjacent from one another when placed in the centrifuge must be the equivalent weight in order for the centrifuge to operate properly. To solve this issue, since no two samples in the centrifuge tubes weighed the same, Nano-pure water was used to compensate for the difference in weight. The Nano-pure water was pipetted into the centrifuge holders till the weight of the two adjacent holders were approximately (± .50 g) equal in weight. The samples were then centrifuged for three cycles lasting five minutes each at 1500 rpms. After the samples were centrifuged the supernatant fluid was decanted and discarded.

To be sure that all of the sodium acetate was removed from the sample, 50 mL of Nano-pure water was added to the centrifuge tubes. The samples in the tubes were then agitated using a Barnstead Thermolyne MAXI MIX Plus to assure complete mixture of

the sample and the Nano-pure water in the centrifuge tubes. The centrifuge tubes were again uncapped and placed in the hot water bath for approximately twelve hours then the tubes were centrifuged for three cycles lasting five minutes each at 1500 rpm's. The supernatant water was decanted from the centrifuge tubes and the tubes were then placed in the drying oven set to 105 °C for approximately 6-12 hours to remove all moisture from the samples. Once the samples had been dried they were placed in a desiccator to cool to room temperature. The change in weight due to the dissolution of carbonate material was recorded using the Mettler balance. When this step was completed it became time to introduce hydrogen peroxide to the samples to attempt to remove any and all organics from the sample.

Removal of Organics by Dissolution

To remove the organics from the sample, the procedure set forth by Kunze and Dixon (1986) was used this process results in a weight reduction as the organics are consumed. Kunze and Dixon (1986) called for the use of 30% hydrogen peroxide (H_2O_2) to remove the organics and 102 g/L, 0.5M magnesium chloride ($MgCl_2 \cdot 6H_2O$) to act as a flocculent agent if needed. The only modification made to Kunze and Dixon (1986) was to allow the sample to completely dry for approximately 12 hours at the end of the procedure in the drying oven set to 105 °C. The centrifuge tubes were then transferred to the desiccator and allowed to cool for 12 hours. The weight change due to the removal of organics by dissolution was then recorded and the samples were then stored until needed. Approximately only a dozen samples were subject to the dissolution of organics. It was found that the amount of organics being removed as result of the introduction of the H_2O_2 was negligible. This led to the conclusion that the use of this method to remove organics

was neither cost effective, due to the copious amount of H_2O_2 required to carry out the procedure, nor time effective, because of the tedious nature of the procedural method.

X-Ray Diffraction

To determine a general mineralogical content of the samples collected, x-ray diffraction (XRD) was utilized because of its ability to provide reliable results which are cost-effective and time-efficient. All XRD analyses of powdered samples were conducted using the Rigaku Ultima III X-ray diffractometer. All data were interpreted using MDI Jade 8 program, at Mississippi State University Institute for Imaging and Analytical Technology (I2AT). Each powdered sample was placed in a standard slotted glass mount and inserted into the diffractometer. The XRD pattern for each sample was obtained using a CuKα radiation with a wavelength of 1.541867 Å (at the recommendation of the I2AT staff). Scan speed was set for 2.000 degrees a minute with a scan step of 0.0200 degrees, a scan axis of 2-theta/theta, and an effective scan range of 3.0000 – 70.0000 degrees.

Thin-Sections

In order to determine the grain size, shape, and sorting of the samples collected two samples of each unit (i.e. light grey clay unit) were selected at random to study. Samples composed of finer grained material such as the light grey, dark brown, and tan 'white' clays were placed on a glass slide with a few drops of water added then a slip cover was placed on top of the fine grained material. The slide was then placed under a microscope and viewed using 10x and 40x objective lenses. Samples composed of the allogenic glacial outwash unit were examined using 10x and 20x coddington hand lenses.

CHAPTER V

RESULTS

Tables 5.1 through 6.1 and Appendices A through C contain all data from the sediment analysis. Table 3.1 shows the classification assigned to each sample, the number of samples collected from each cave, and the symbology used in table 5.2 through 5.5. Appendix B contains tables showing the numerical results of each treatment for each cave sample. Tables 5.1 through 5.6 are derived from the data in Appendix B. Table 5.1 is a box plot diagram which shows one technique (water weight loss) used to analyze and interpret the data collected including whisker plots shown in Appendix 3.

Table 5.1 A box plot diagram comparing the amount of water as a weight percent lost by samples, containing the dark grey-dark brown clay unit, resulting from being heated to 105 °C

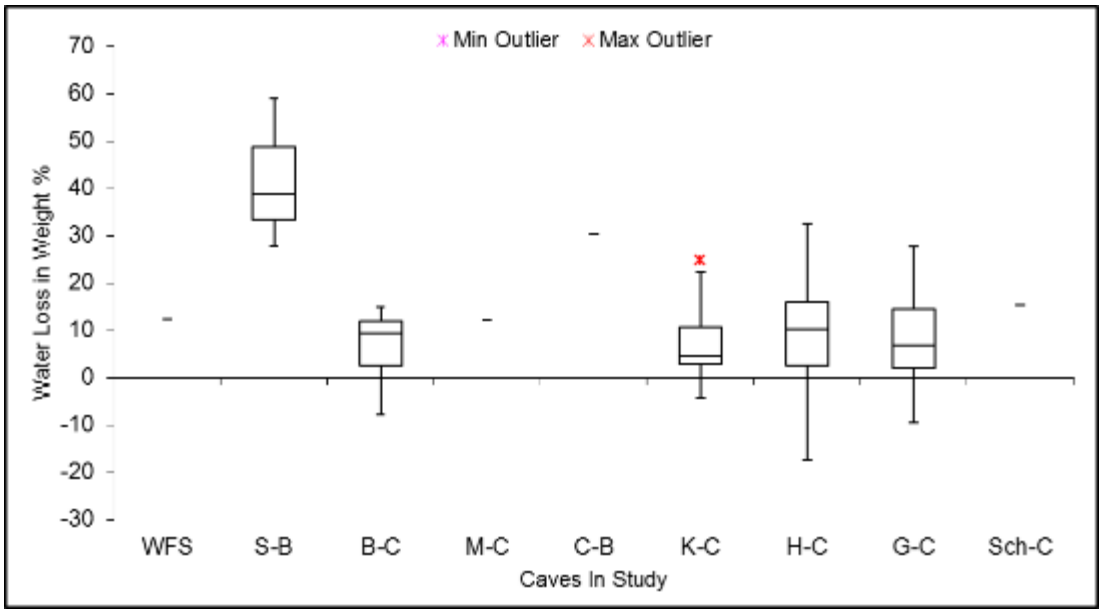

WFS=Westfall Spring Cave; S-B=Secret Caverns; B-C=Benson's Cave; M-C=McFail's Cave; C-B=Caboose Cave; K-C=Knox Cave; H-C=Howe Caverns; G-C=Gage Caverns; Sch-C=Schoharie Caverns. The dashed lines indicate that only one sample was available to be plotted. To see more charts like the one above see Appendix Three.
Scatter plots were produced so the sediment types could be presented for each cave.

Sample Percent Water Lost

The average weight percent of water content removed by the initial heating, of samples from all caves containing the dark grey-dark brown clay unit, to 105 °C was 13.47%. In terms of an average weight in grams it was found that 2.36 grams of the raw hydrated sample in the crucible was lost. The average weight percent of water content removed by the initial heating, of samples from all caves containing the light grey clay unit, to 105 °C was 13.68%. In terms of an average weight in grams it was found that 2.11 grams of the raw hydrated sample in the crucible was lost. The average weight percent of water content removed by the initial heating, of samples from all caves containing the allogenic glacial outwash unit, to 105 °C was 0.72%. In terms of an

average weight in grams it was found that 0.75 grams of the raw hydrated sample in the crucible was lost. The average weight percent of water content removed by the initial heating, of samples from all caves containing the tan 'white' clay unit, to 105 °C was 14.27%. In terms of an average weight in grams it was found that 2.74 grams of the raw hydrated sample in the crucible was lost. The average weight percent of water content removed by the initial heating, of samples from all caves containing the control sediments, to 105 °C was 8.46%. In terms of an average weight in grams it was found that 1.67 grams of the raw hydrated sample in the crucible was lost. Scatter plots were produced so the sediment types could be presented for each cave. Table 5.2 is a scatter plot which shows the distributions of weight percent of H2O lost per sample, by the heating the samples to 105 °C, type (i.e. tan 'white' clay unit) by cave. The various sediments found in the cave are referred to as units as they have no formal status. Table 5.1 demonstrates how the data were organized using Microsoft Excel, including specific values for each sample (as opposed to the general averages described above).

Table 5.2 A scatter plot which shows the distributions of weight percent of H_2O lost per sample, by the heating the samples to 105 °C, type (i.e. tan 'white' clay unit) by cave.

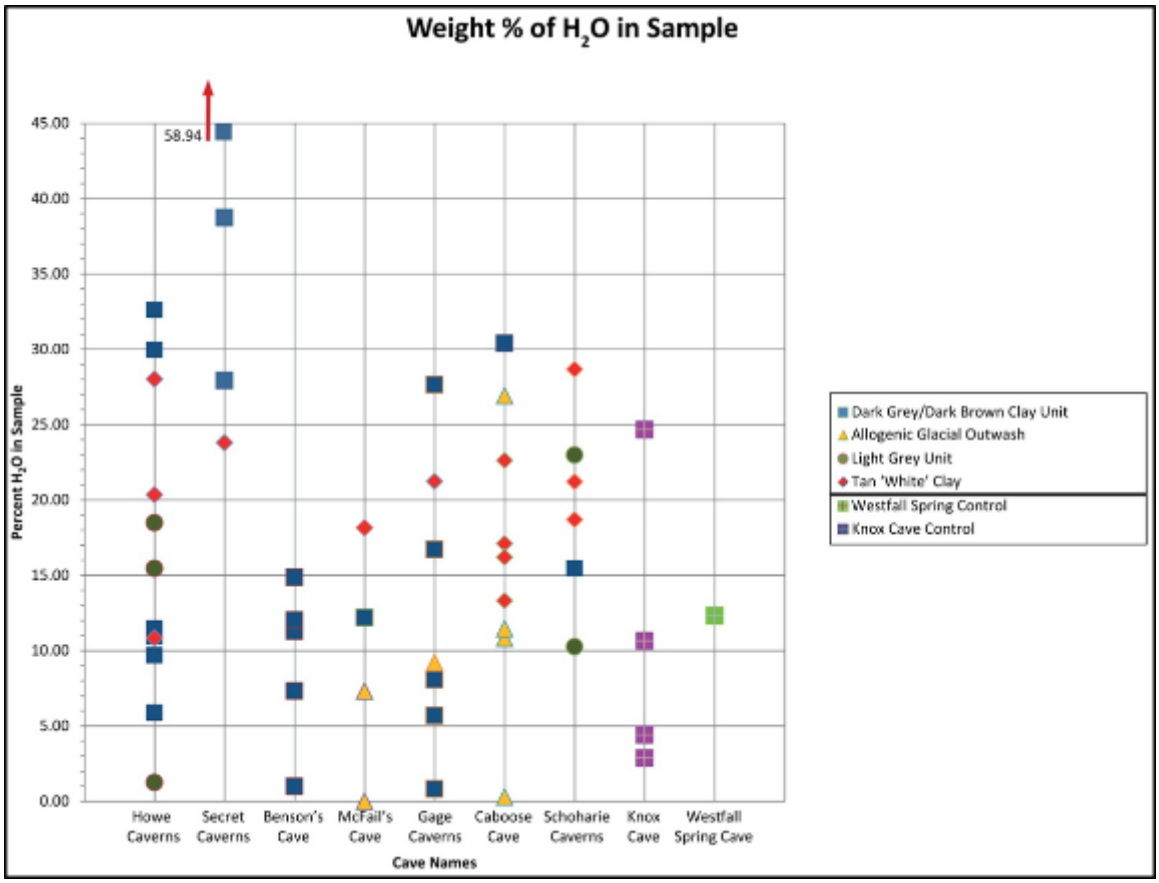

Weight Loss on Ignition at 550 °C

Refer to Table 3.1 for specific data, and Appendices B and C. The average weight lost by ignition of samples from all caves containing dark grey/dark brown clay unit at 550 °C was found to be 0.81 grams. In terms of an average weight percent it was found that 2.47% of the sample used for the ashing process was lost during ignition at 550 °C. The average weight lost by ignition of samples from all caves containing light grey clay unit at 550 °C was found to be 0.19 grams. In terms of an average weight percent it was found that 2.92% of the sample used for the ashing process was lost during

ignition at 550 °C. The average weight lost by ignition of samples from all caves containing the allogenic glacial outwash unit at 550 °C was found to be 0.16 grams. In terms of an average weight percent it was found that 2.15% of the sample used for the ashing process was lost during ignition at 550 °C. The average weight lost by ignition of samples from all caves containing the tan 'white' clay unit at 550 °C was found to be 0.26 grams. In terms of an average weight percent it was found that 3.68% of the sample used for the ashing process was lost during ignition at 550 °C. The average weight lost by ignition of samples from all caves containing the control sediments at 550 °C was found to be 0.16 grams. In terms of an average weight percent it was found that 1.87% of the sample used for the ashing process was lost during ignition at 550 °C. See Appendices B and C for specific tables and whisker plots of the data. Table 5.3 is a scatter plot which shows the distributions of the weight percent $LOI_{550\,°C}$ per sample type (i.e. tan 'white' clay unit) by cave.

Table 5.3 A scatter plot which shows the distributions of the weight percent Loss On Ignition at 550 °C ($LOI_{550\,°C}$) per sample type (i.e. tan 'white' clay unit) by cave.

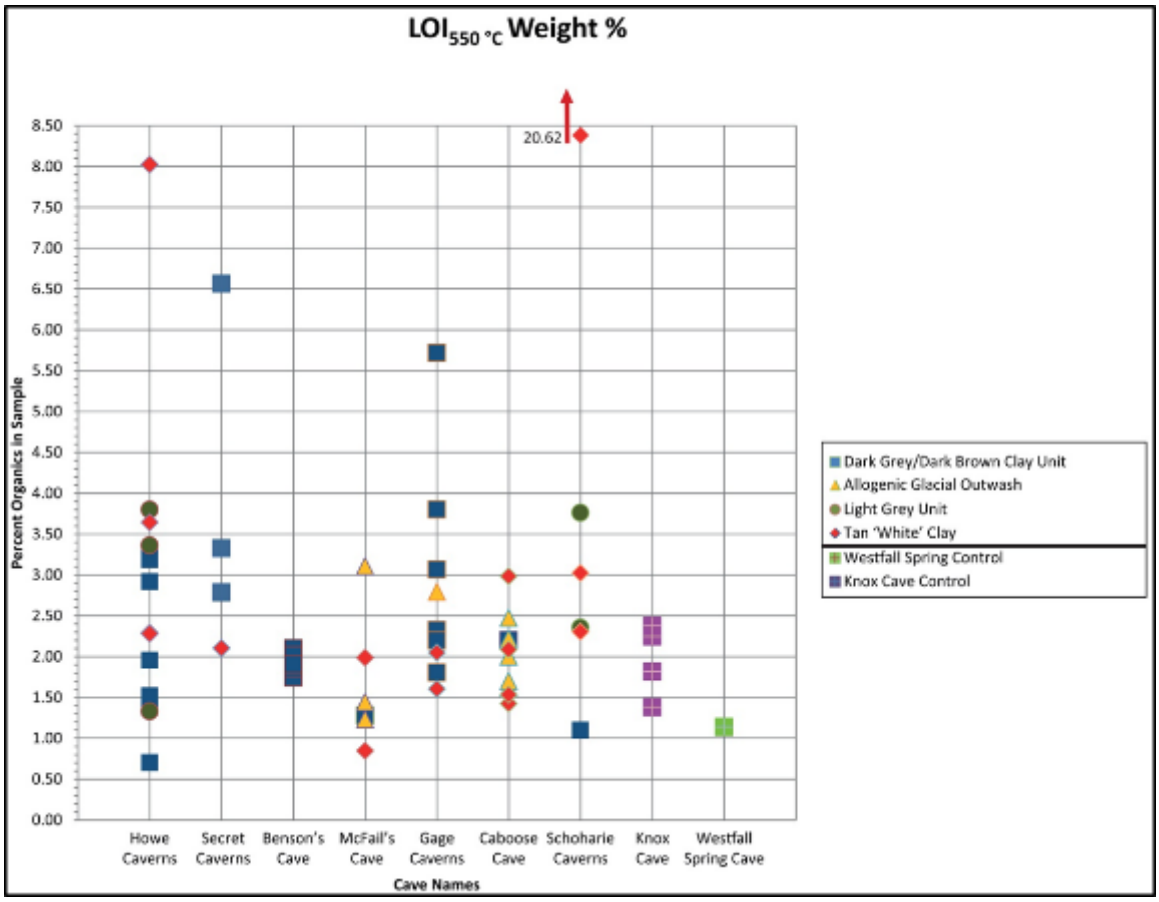

Weight Loss on Ignition at 950 °C

Refer to Table 3.1 for specific data, and Appendices B and C for tables and whisker plots. The average weight lost by ignition of samples from all caves containing the dark grey/dark brown clay unit at 950 °C was found to be 0.23 grams. In terms of an average weight percent it was found that 3.10% of the sample used for the ashing process was lost during ignition at 950 °C. The average weight lost by ignition of samples from all caves containing the light grey clay unit at 950 °C was found to be 0.27 grams. In terms of an average weight percent it was found that 3.63% of the sample used for the

ashing process was lost during ignition at 950 °C. The average weight lost by ignition of samples from all caves containing the allogenic glacial outwash unit at 950 °C was found to be 0.20 grams. In terms of an average weight percent it was found that 2.62% of the sample used for the ashing process was lost during ignition at 950 °C. The average weight lost by ignition of samples from all caves containing the tan 'white' clay unit at 950 °C was found to be 0.43 grams. In terms of an average weight percent it was found that 5.57% of the sample used for the ashing process was lost during ignition at 950 °C. The average weight lost by ignition of samples from all caves containing the control sediments at 950 °C was found to be 0.29 grams. In terms of an average weight percent it was found that 3.31% of the sample used for the ashing process was lost during ignition at 950 °C. Table 5.4 is a scatter plot which shows the distributions of the weight percent $LOI_{950\ °C}$ per sample type (i.e. tan 'white' clay unit) by cave.

Table 5.4 A scatter plot which shows the distributions of the weight percent loss on ignition at 950 °C ($LOI_{950\,°C}$) per sample type (i.e. tan 'white' clay unit) by cave.

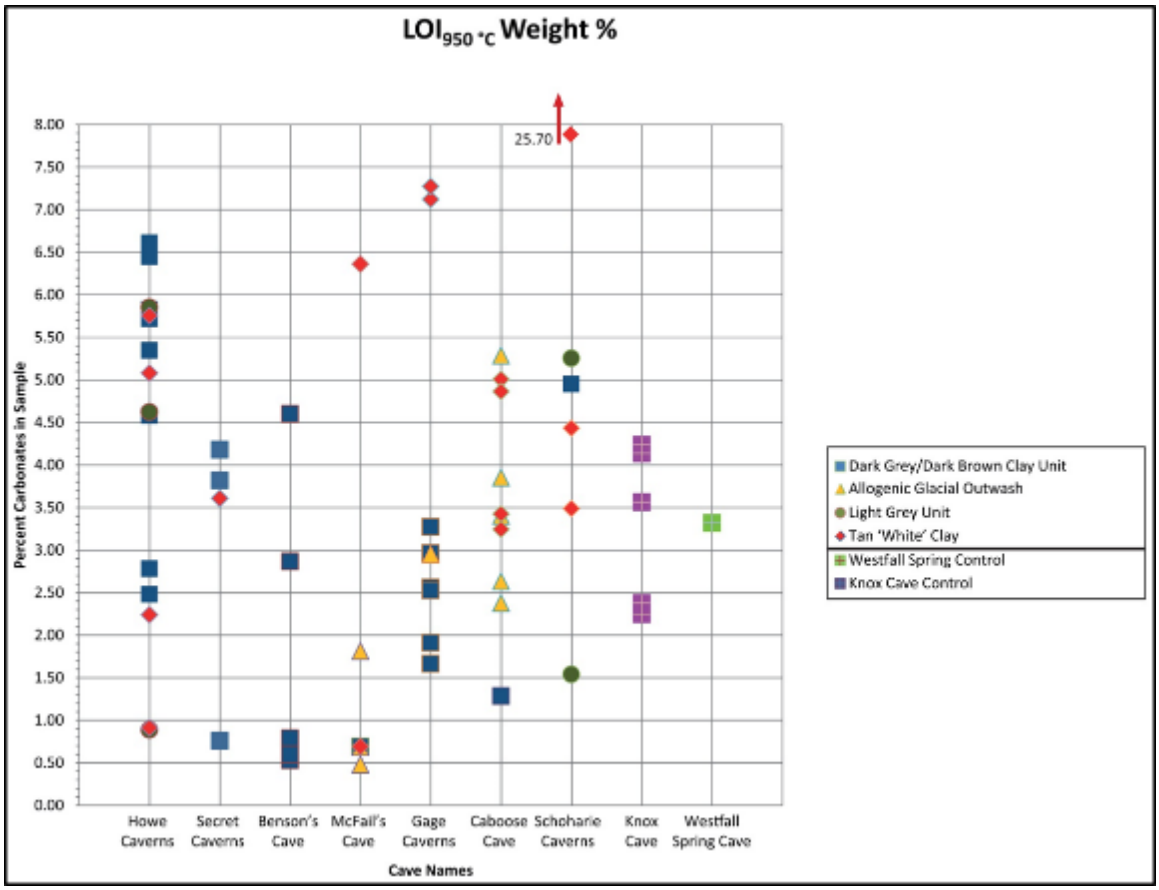

Weight Loss by Dissolution of Carbonates

The actual data are presented in Appendices B and C. The average weight lost by dissolution of the samples from all caves, containing the dark grey/dark brown clay unit, using sodium acetate was found to be 0.32 grams. In terms of an average weight percent it was found the samples lost 7.59% of their weight during solution. The average weight lost by dissolution of the samples from all caves, containing the light grey clay unit, using sodium acetate was found to be 0.38 grams. In terms of an average weight percent it was found the samples lost 9.07% of their weight during solution. The average weight lost by

dissolution of the samples from all caves, containing the allogenic glacial outwash unit, using sodium acetate was found to be 0.20 grams. In terms of an average weight percent it was found the samples lost 5.14% of their weight during solution. The average weight lost by dissolution of the samples from all caves, containing the tan 'white' clay unit, using sodium acetate was found to be 0.37 grams. In terms of an average weight percent it was found the samples lost 7.97% of their weight during solution. The average weight lost by dissolution of the samples from all caves, containing the control sediments, using sodium acetate was found to be 0.25 grams. In terms of an average weight percent it was found the samples lost 5.12% of their weight during solution. Table 5.5 is a scatter plot which shows the distributions of the weight percent LOD_{NaA} (loss on dissolution using sodium acetate) per sample type (i.e. tan 'white' clay unit) by cave.

Table 5.5 A scatter plot which shows the distributions of the weight percent loss on dissolution using sodium acetate (LOD_{NaA}) per sample type (i.e. tan 'white' clay unit) by cave.

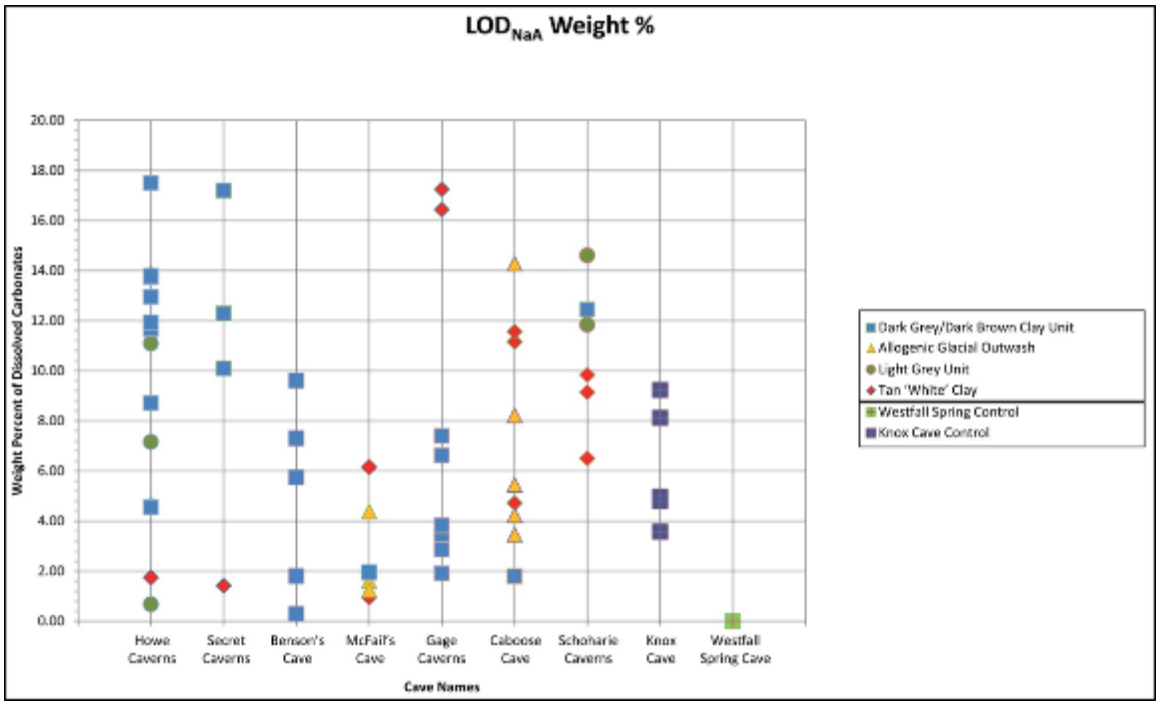

Mineral Composition

X-ray diffraction (XRD) of the 63 samples collected yielded graphs which plotted the 2theta angle vs. the intensity counts; these graphs can be found in Appendix 1. The mineralogical content of each sample was determined through the use of MDI Jade 8 program. The Jade 8 program allowed for the comparison of the position and intensity of peaks found in the graphs with those found in mineralogical databases. Table 8 shows the mineralogical content found to exist in each sample. The XRD data were not used to determine actual amounts of materials in a given sample; it was an assay of presence or absence. For example, the dark grey/dark brown clay unit had calcite in 62% of the samples, and the allogenic outwash unit had calcite in 40% of the samples. Together,

these post-glacial lake sediments had 56% calcite occurrence. The light grey clay unit had calcite in 100% of the samples, and the tan "white" clay unit had calcite in 75% of the samples. Together, the glacial lake sediments had calcite in 81% of the samples. The Knox Cave and Westfall Cave sediments, as controls, had calcite in only 32% of the samples. Brushite shows a different trend, being more common in the post-glacial sediments (Table 5.6).

Table 5.6 X-ray Diffraction Results

	Post Glacial Sediment			Glacial Lake Sediment			
Mineral	Dark Brown Clay	Allogenic Glacial Outwash	Total	Light Grey Clay	Tan 'White' Clay	Total	Control Samples
	Percentage of Mineral found in Unit	Percentage of Mineral found in Unit	Percentage of Mineral found in Post-Glacial Units	Percentage of Mineral found in Unit	Percentage of Mineral found in Unit	Percentage of Mineral found in Glacial Units	Percentage of Mineral found in Unit
Calcite	62%	40%	56%	100%	75%	81%	33%
Dolomite ?	4%	0%	3%	0%	0%	0%	0%
Quartz	100%	100%	100%	100%	100%	100%	100%
Muscovite	73%	80%	75%	60%	69%	67%	83%
Phlogopite	31%	40%	33%	40%	19%	24%	67%
Chlorite	0%	0%	0%	0%	0%	0%	0%
Montmorillonite	0%	0%	0%	0%	0%	0%	0%
Albite (low temp)	58%	50%	56%	20%	44%	38%	67%
Enstatite ?	0%	0%	0%	0%	6%	5%	0%
Brushite	65%	40%	58%	40%	31%	33%	83%
Nacrite	15%	0%	11%	20%	0%	5%	17%
Carbon	8%	30%	14%	0%	25%	19%	67%

Thin-Section analysis of grain size

Particle size analysis based on USCS (United Soils Classification System) particle sizes of the sediments collected revealed that the samples which were comprised of the light grey clay or the tan 'white' clay have sub-angular to sub-rounded, light gray/tan-

white in color, very fine sand to silt/clay size particles, sub-0.08 to 0.43 mm in diameter. Similarly the samples comprised of the dark grey/dark brown clay have the same characteristics as listed above except that they are dark grey to dark brown in color. The samples comprised of the allogenic glacial outwash have sub-rounded, light brown to dark brown, medium sand to coarse gravel size particles, 0.43 to 75 mm in diameter.

CHAPTER VI

DISCUSSION

Explanation of Controls

The explanation behind utilizing samples collected from control sites (Knox Cave and Westfall Spring) was to collect samples from caves which had not been inundated by Glacial Lake Schoharie. Knox Cave for example, is outside the proposed maximum footprint of Glacial Lake Schoharie; therefore no sediment being carried by the glacial lake water could have been deposited in the cave. Westfall Spring Cave was used as a control because it is thought to be post-glacial in origin; therefore it did not exist at the same time as Glacial Lake Schoharie and could not contain any glacially deposited sediment even though it is within the maximum footprint of the glacial lake. Westfall Spring Cave is within the lake footprint, however, and therefore could have gained glacial lake sediment that washed in from surface deposits (whereas Knox Cave could not).

Glacial Lake Schoharie

A glacial lake is a body of fresh water which is confined or partially contained by a glacier or geomorphic feature produced by a glacier (LaFleur, 1976). As mentioned earlier there were a number of advance, retreat, and readvance phases of glacial ice associated with the Late Wisconsinan glaciation in New York. Resulting from instability

of the glacial ice, Glacial Lake Schoharie had a number of shorelines at varying elevations throughout the course of the Late Wisconsinan glaciation. Sometime after the Woodstock ice margin was established by the halt of retreating stagnant ice (<18,200 ybp based on Ridge, 2004); glacial meltwater began to flood the Schoharie Valley. As the stagnated glacial ice continued to melt and retreat toward the northeast, water levels continued to rise until a glacial lake was established with a shoreline at an elevation of 213.4 m (700 feet) above sea level (Dineen, 1986) (Figure 6.1).

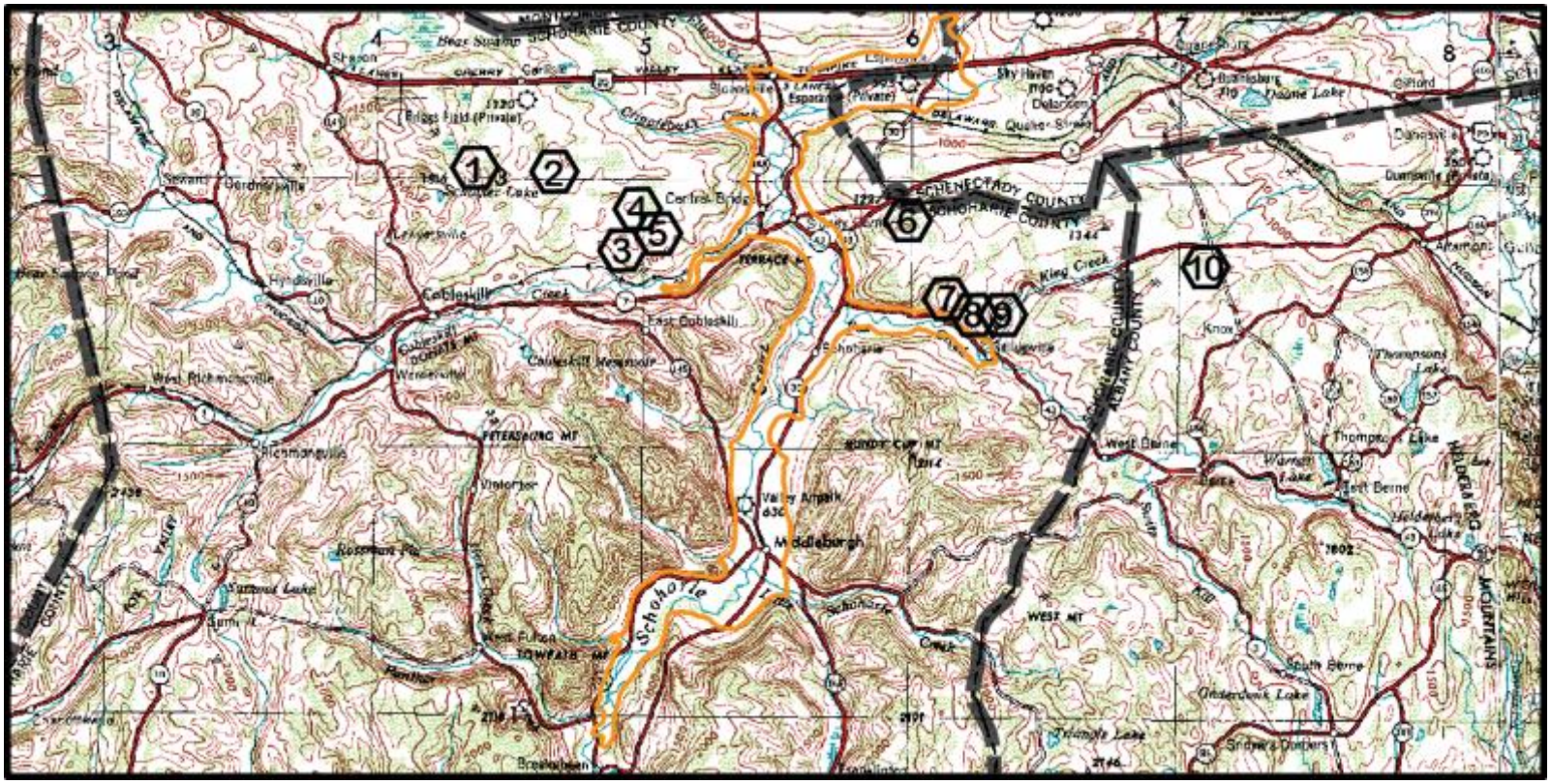

Figure 6.1 Topographic map showing the location of the caves in relation to the 213.4 m (700 foot) shoreline of Glacial Lake Schoharie outlined in orange

(created using information provided by Dineen, 1986). Refer to Figure 1.2 for identification of caves.

During this stage of Glacial Lake Schoharie's development there would have not been any outlet for the water to escape from the Schoharie basin. It would have been possible, given present topography, for the water in Glacial Lake Schoharie to drain north towards what would be known today as the Mohawk Valley. There is a problem with this idea since at the time the Mohawk Valley was filled with the active Mohawk glacial lobe (Figure 6.2).

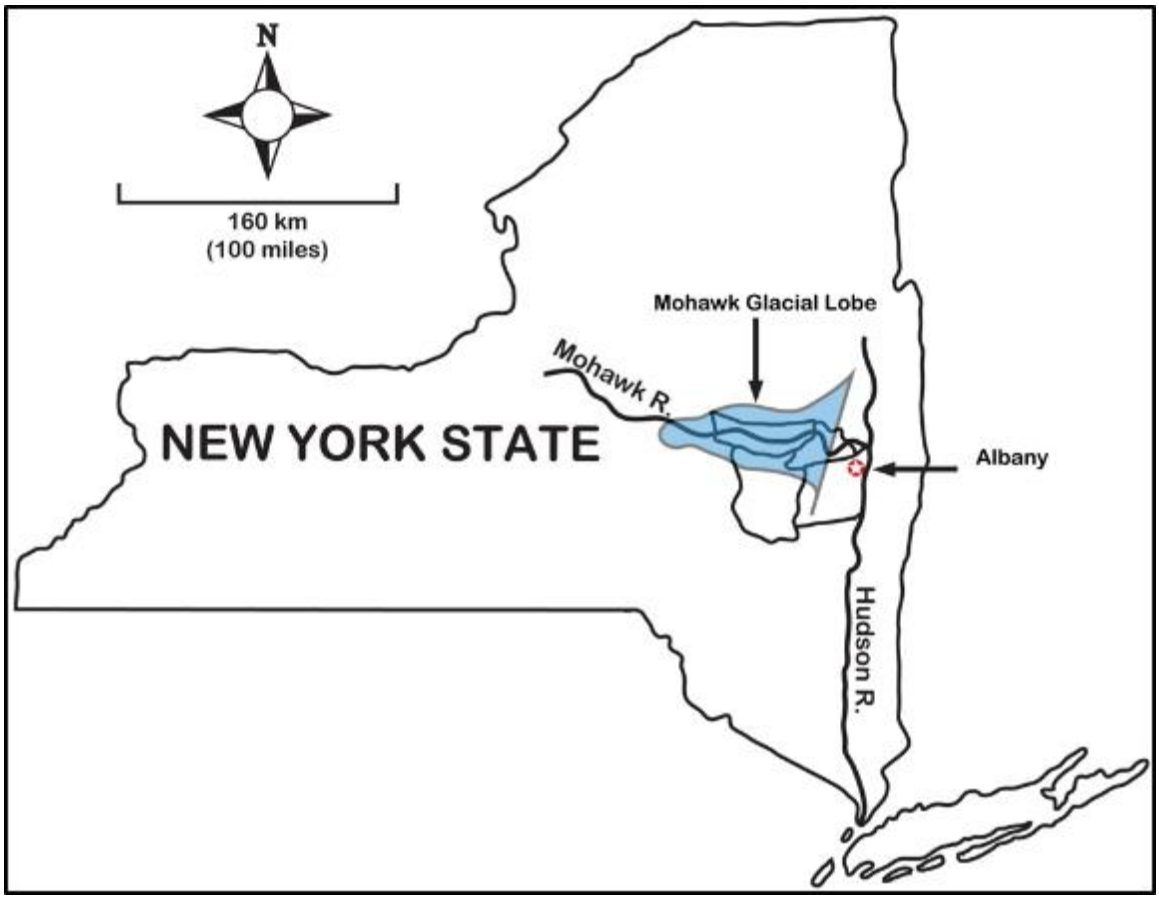

Figure 6.2 Overview of New York State showing the general location and extent of the Mohawk glacial lobe

(modified from Brigham, 1929).

The Mohawk glacial lobe, also known as the Mohawk Ice Block, filled the area between neighboring Cobleskill and Barton Hill plateaus of the Schoharie Valley and acted as a plug to trap glacial melt water (LaFleur, 1969). At this point, near the end of the Wisconsinan glaciation, greater than or equal to 50% of Glacial Lake Schoharie would have been covered by active glacial ice from the Schoharie sub-lobe (Dineen, 1986). Figure 6.3 illustrates the difference between stagnant glacial ice and active glacial ice. For more information on the stagnation of glacial ice can be found in Mulholland (1982). Stagnation and retreat of the local glacial lobes halted and began to reverse with the onset of the Middleburg readvancement.

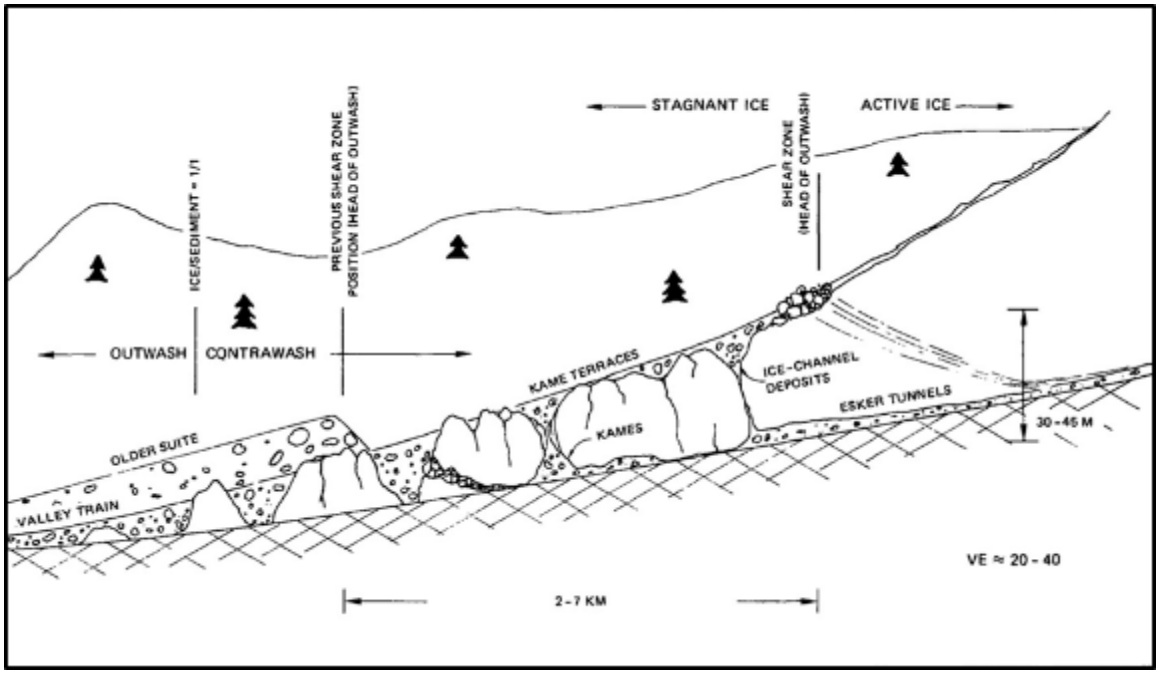

Figure 6.3 Illustration depicting the difference between stagnant glacial ice and active glacial ice

(from Mulholland, 1982).

Based on the interpretation of Figure 6.1 and Figure 2.18 there would have been an insufficient amount of water in Glacial Lake Schoharie to even partially inundate the caves of the Cobleskill Plateau and Barton Hill included in this study.

With the onset of the Middleburg readvancement (17,400 ybp, estimate based on Ridge, 2004) active glacial ice re-entered the Schoharie Valley. The active glacial ice overrode the stagnated glacial ice, left behind by the Rosendale readvance, located in the valley and continued until it reached the Catskill Front. Upon reaching the Catskill Front the glacier stagnated and once again began to retreat north. While retreating, the glacier produced a vast amount of water resulting in the enlargement or creation of several proglacial lakes (Dineen, 1986). In the case of Glacial Lake Schoharie, it enlarged considerably and established a shoreline between 354-366 m (1,160-1,200 feet) above sea level (Figure 6.4).

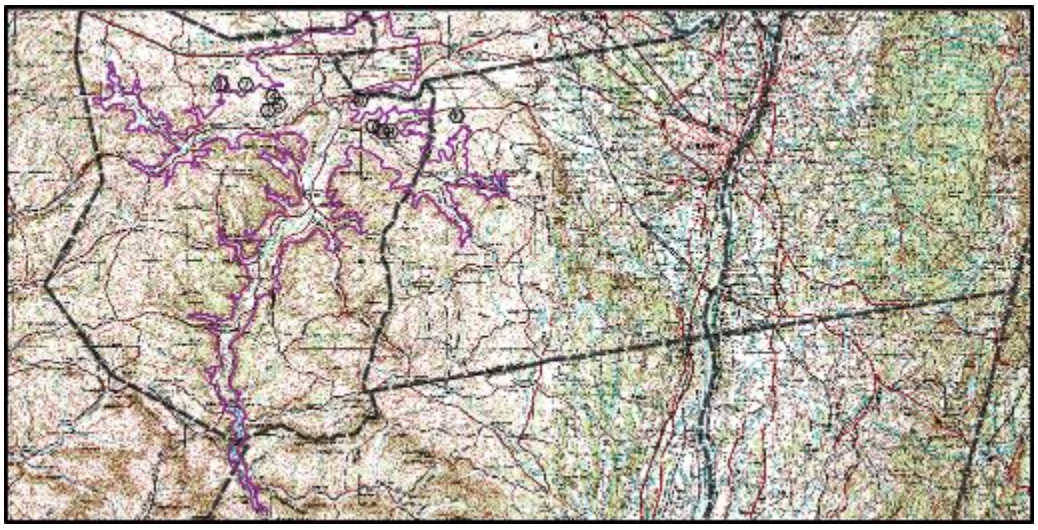

Figure 6.4 Glacial Lake Schoharie with an established shoreline at 354-366 m (1,160-1,200 feet) above sea level.

The area inside the purple line indicates the size and location of the glacial lake. Refer to Figure 1.2 for identification of caves.

Through interpretation of Figures 2.18 and 6.4 it can be seen that nearly all of the caves in the Cobleskill Plateau and Barton Hill are completely inundated by water from Glacial lake Schoharie. Note that although the entrances to both McFail's Cave and Gage Caverns are not inundated, the majority of the master cave passages are over 30 m below the surface and would have been inundated based on their elevation relative to sea level. This would include inundation of locations within the caves where samples were collected for the study. It is also important to note that the upper passages where samples were collected in Knox Cave would not have been inundated by glacial lake water due to their elevation above sea level (Figure 2.18), and so these samples acted as a control.

During the time period between what is known as post-Alcove ice margin and pre-Delmar ice margin (>16,200 ybp, estimate based on Ridge, 2004), water from Glacial Lake Schoharie drained to the north, through what is known as the Delanson spillway, in close proximity to the ice plug (LaFleur, 1969). The spillway which drained Lake Schoharie was located just southwest of the ice block and fed the Delanson River which eventual drained into Glacial Lake Albany (LaFleur 1976). LaFleur, (1969), provides an estimate for the depth of Glacial Lake Schoharie as being approximately 73 m (240 feet), with a shoreline elevation of 256m (840 feet) above sea level (Figure 6.5).

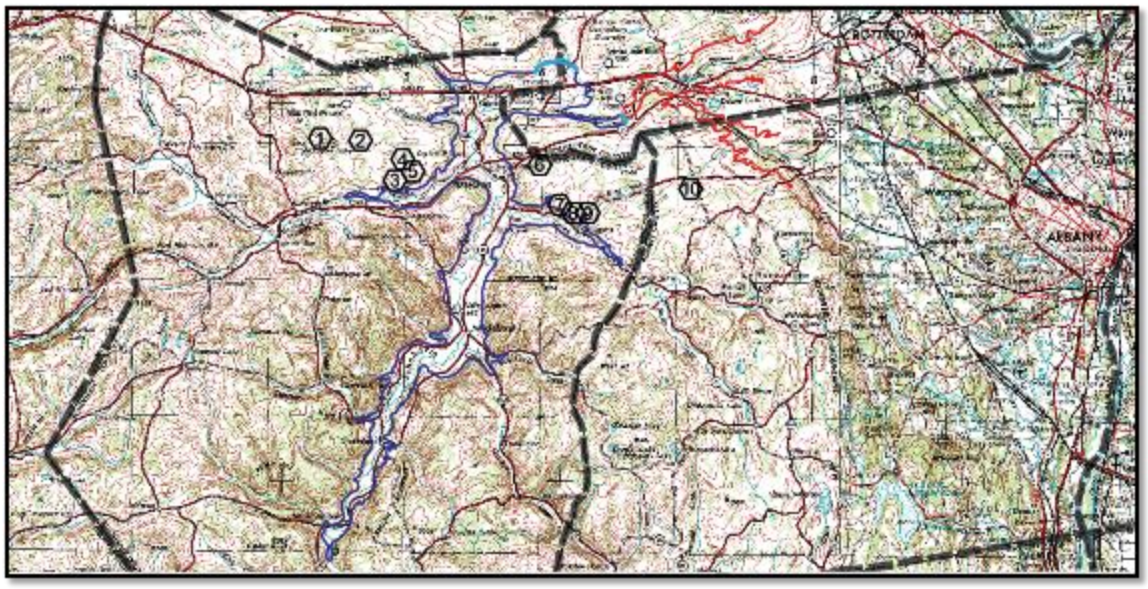

Figure 6.5 Glacial Lake Schoharie (outlined blue) with a shore line at 256 m (840 feet) above sea level

(created using information provided by LaFleur, 1969 and Dineen and Hanson, 1985). Area between red lines indicate spillway and lite blue lines indicate boundary between glacial lake water and active glacial ice. Refer to Figure 1.2 for identification of caves.

The estimate given for the Lake Schoharie by Dineen and Hanson (1985) of an established shoreline at 256-213 m (840-700 feet) above sea level compliments the estimate given by LaFleur, (1969). At this lake elevation, only the lowest stream passages in Howe Caverns would have been inundated by lake water (Figure 2.18).

Glacial Sediment in Caves

The glacially deposited sediments found within the caves have particular characteristics which make them unique both when they are studied from afar or up close. The presumption was that the tan 'white' clay is derived of limestone rock-flower and this hypothesis was supported by the findings of the mineralogical content presented in Table 8. This study also described how the sediments were glacially derived and that

they were in fact glaciolacustrine deposits. Photographic evidence shows that the clays are layered and rhythmic in character and are not simply one continuous outcrop of sediment; refer to Figures 1.3, 1.4, and 6.6.

Figure 6.6 Image showing the distinct varve layering of the tan 'white' clay unit found in Caboose Cave.

Rock hammer for scale.

The sediments encountered fit the description of a varved sequence. Varves are usually couplets of fine and coarse grained material (Neuendorf et al., 2011). These sediments do not show the alternating coarse fine sequencing, they appear to only contain the fine sediments. A possible reason to explain why the sediments which comprise the

units are so uniform is because the insurgences and resurgences of the caves were most likely choked with glacially transported material so only the smallest of sediments would be able to pass through the debris. These deposits are consistent with a laminar flow regime expected with deposition deep in cave passage at the bottom of a glacial lake.

The Howe Caverns sediment section is especially instructive. It is the thickest of all such sequences. While most caves have less than or equal to 1 m of the light grey and tan 'white' clay, Howe Caverns has over 2 m of section. This greater thickness is the result of Howe Caverns' main stream passage being the lowest in elevation of all the cave passages studied, by a significant amount (approximately 30 meters Figure 2.18). Therefore, while lake surface elevations shifted vertically, Howe Caverns spent more time under Glacial Lake Schoharie than any other cave in the study. In addition, Figure 1.3b shows an interesting transition from a very amorphous white clay deposit at the base (next to the knife), to a progressively better layered light grey clay in which the individual layers get thicker upwards to the contact with more traditional cave sediments. This transition can be interpreted to indicate initial clay deposition under the 354-366 m lake elevation stage, when the Howe Caverns stream passage would have been ~100 m below the lake surface. Sediment transport by laminar flow into the cave would have been slow, and quite isolated from seasonal changes, indicated by the lack of rhythmical layering in the 'white' clay deposit. As lake level lowered to the 256 m level, the Howe Caverns main stream passage would have been merely meters below the lake surface, and more likely to record the seasonal changes in water and sediment addition to the lake, as demonstrated by the light grey clay. The upward thickening may record the final transition of Howe Caverns out of the lake footprint as the lake drained away.

The XRD analyses show the minerals present in a fine silt and clay deposit generated by glacial erosion on the surface (Table 6.1). This material is likely a glacial rock flour. Quartz is ubiquitous, as is to be expected. There is a difference in calcite concentrations between the glacial lake sediments and the post-glacial sediments, with higher calcite occurrences in the glacial lake sediments. The fine-grained calcite particles produced by glacial erosion have a very high surface to volume ratio, and much like granulated sugar versus sugar cubes, dissolve rapidly in dissolutionally aggressive water. Given the stagnant conditions which would have existed inside cave passages under a glacial lake, which would have created water with little dissolutional capability, the survival of these calcite particles is understandable, and present further evidence of glacial lake conditions.

Table 6.1 Minerals identified from caves in this study located in the Helderberg Plateau and percentage of each mineral found in each identified unit.

Mineral	Chemical Formula	Dark Grey/Dark Brown Clay Unit																										Allogenic Glacial Outwash Unit											Total
		S-B 1-0	S-B 1-1	S-B 1-3	B-C 1-1	B-C 1-2	B-C 1-3	B-C 1-4	B-C 1-5	B-C 1-6	M-C 1-3	C-B 1-5	H-C 1-2	H-C 1-5	H-C 1-6	H-C 1-7	H-C 1-8	H-C 1-9	H-C 1-13	H-C 1-15	G-C 1-1	G-C 1-2	G-C 1-3	G-C 2-1	G-C 3-1	G-C 3-2	Sch-C 1-2	Percentage of Mineral found in Unit	M-C 1-2	M-C 2-2	M-C 2-3	C-B 1-3	C-B 1-4	C-B 2-1	C-B 3-1	C-B 3-2	H-C 1-14	G-C 2-2	Percentage of Mineral found in Unit	Percentage of Mineral found in Post-Glacial Units
Calcite	$CaCO_3$		†	†		†	†	†			†			†	†		†		†	†		†	†	†	†		†	62%			†	†				†		†	40%	56%
Dolomite ?	$CaMg(CO_3)_2$										†																	4%											0%	3%
Quartz	SiO_2	†	†	†	†	†	†	†	†	†	†	†	†	†	†	†	†	†	†	†	†	†	†	†	†	†	†	100%	†	†	†	†	†	†	†	†	†	†	100%	100%
Muscovite	$KAl_2(AlSi_3O_{10})(OH)_2$		†	†	†	†	†	†	†	†	†	†			†				†		†	†	†	†	†	†	†	73%		†	†	†	†	†	†	†		†	80%	75%
Phlogopite	$KMg_3(AlSi_3O_{10})(OH,F)_2$			†	†					†			†								†	†	†	†				31%					†	†	†	†			40%	33%
Chlorite	$(R_{2+}, R_{3+})_{4\text{-}6}(Si, Al)_4O_{10}(OH,O)_2$																											0%											0%	0%
Montmorillonite	$(Na, Ca)_{0.33}(Al, Mg)_2(Si_4O_{10})(OH)_2 \cdot nH_2O$																											0%											0%	0%
Albite (low temp)	$NaAlSi_3O_8$				†	†	†	†	†	†	†	†		†					†		†	†	†			†	†	58%	†			†		†	†	†			50%	56%
Enstatite ?	$MgSiO_3$																											0%											0%	0%
Brushite	$Ca(HPO_4) \cdot 2H_2O$		†	†	†	†	†	†	†		†		†	†				†		†	†	†	†	†		†		65%			†		†	†				†	40%	58%
Nacrite	$Al_2(Si_2O_5)(OH)_4$																				†	†		†		†		15%											0%	11%
Carbon	C										†				†													8%			†		†			†			30%	14%

Mineral	Chemical Formula	Light Grey Clay Unit							Tan 'White' Clay Unit																			Total	Control Samples						
		H-C 1-1	H-C 1-4	H-C 1-12	Sch-C 1-1	Sch-C 3-1	BZ-C FL	Percentage of Mineral found in Unit	S-B 1-2	M-C 1-1	M-C 2-1	C-B 1-1	C-B 1-2	C-B 3-3	C-B 3-4	H-C 1-0	H-C 1-3	H-C 1-10	H-C 1-11	G-C 2-3	G-C 2-4	Sch-C 1-3	Sch-C 1-4	Sch-C 2-1	BZ-C CS	BZ-C SL	Percentage of Mineral found in Unit	Percentage of Mineral found in Glacial Units	WFS 1-1	K-C 1-1	K-C 2-1	K-C 3-1	K-C 3-2	K-C 3-3	Percentage of Mineral found in Unit
Calcite	$CaCO_3$	†	†	†	†	†	?	100%		†		†	†	†	†		†		†	†	†	†	†	†	?	?	75%	81%	†				†		33%
Dolomite ?	$CaMg(CO_3)_2$							0%																			0%	0%							0%
Quartz	SiO_2	†	†	†	†	†	?	100%	†	†	†	†	†	†	†	†	†	†	†	†	†	†	†	†	?	?	100%	100%	†	†	†	†	†	†	100%
Muscovite	$KAl_2(AlSi_3O_{10})(OH)_2$			†	†	†	†	60%	†		†	†	†	†	†		†		†	†	†			†	†	†	69%	67%	†	†	†	†		†	83%
Phlogopite	$KMg_3(AlSi_3O_{10})(OH,F)_2$				†	†		40%				†		†	†												19%	24%		†	†	†	†		67%
Chlorite	$(R_{2+}, R_{3+})_{4\text{-}6}(Si, Al)_4O_{10}(OH,O)_2$						†	0%																	†	†	0%	0%							0%
Montmorillonite	$(Na, Ca)_{0.33}(Al, Mg)_2(Si_4O_{10})(OH)_2 \cdot nH_2O$							0%																	†		0%	0%							0%
Albite (low temp)	$NaAlSi_3O_8$		†					20%		†		†	†		†		†				†	†					44%	38%	†	†		†		†	67%
Enstatite ?	$MgSiO_3$							0%															†				6%	5%							0%
Brushite	$Ca(HPO_4) \cdot 2H_2O$			†		†		40%	†			†	†		†		†								?		31%	33%	†	†	†	†		†	83%
Nacrite	$Al_2(Si_2O_5)(OH)_4$				†			20%																			0%	5%						†	17%
Carbon	C							0%	†	†			†		†										?		25%	19%	†		†	†		†	67%

†=Mineral identified by XRD scans, **?**=Mineral not identified by XRD scans but mineral may be present. S-B=Secret Caverns, B-C=Benson's Cave, M-C=McFail's Cave, BZ-C=Barrack Zourie Cave, C-B=Caboose Cave, H-C=Howe Caverns, G-C=Gage Caverns, Sch-C=Schoharie Caverns, WFS=Westfall Spring Cave, K-C=Knox Cave.

Recommendations for Further Study

It would be possible to compare the sediment found within the caves of the region associated with Glacial Lake Schoharie with the sediment on the surface to achieve a better understanding of the multiple shorelines associated with the glacial lake. Since organics were found in the samples collected in the caves it could be possible to determine the age of the organics within in the samples to see if that age correlates to the age provided in this paper.

CHAPTER VII

CONCLUSION

The purpose of this study was to reconstruct the paleoenvironment of a proglacial lake, Glacial Lake Schoharie, located within multiple counties of east-central, New York State.

Caves suspected to have been inundated by glacial lake water do not show any statistical correlation between samples collected, but as seen in Figure 1.3, it is apparent that physical similarities between the samples collected exist. These physical similarities can be identified in the mineral color, and grain size. It was originally hypothesized in the infancy of the study that the sediment in the caves may have been deposited during a retreat phase of glaciation resulting from stagnant lake conditions. This hypothesis was found to be true because it explained how the fine grained sediment was deposited in the caves. This could not be accomplished if there was turbid or even transitional laminar flow through the caves. The stagnation of the glacial lake partially occurred during a retreat phase during the Wisconsinan glaciation; however, the glacial lake was present during readvance, standstill, and retreat phases of glaciation. Through the interpretation of previous literature on the subject it was found that Glacial Lake Schoharie endured multiple retreats and readvances of glacial ice by being insulated and protected by a layer of stagnated glacial ice. During retreat phases of glacial activity new glacial meltwater carrying glacial-derived sediment must have been delivered to the lake and the through to

these cave by directly percolating down through the stagnant ice and by subglacially through active ice as well. During advance phases of glacial activity it would have only been possible to deliver new meltwater to the lake and caves by subglacial means and since during the advance phases the glacial lake water did not inundate the caves by flooding; if there was any waterflow through the caves it would have been turbid. Again, to deposit very fine-grained sediments like the observed white clay requires near stagnant conditions within the caves.

The location of glacial lake sediments in the caves of the Helderberg Plateau indicate the elevation of the lake surface, and coupled with topography, demonstrate the footprint of the lake. The footprint so derived agrees with work on lake elevations and spillway positions when the ice dam was in place. The caves acted as a unique preservational site for glacial lake sediments, which are commonly stripped or hidden by Holocene weathering activities on the land surface.

The analyses of the sediments themselves are consistent with the glacial lake hypothesis. They are extremely fine-grained, very low in organics, and with a measurable soluble content. They are visually striking when observed in the field, and are easily recognized. They are, to date, known only from the footprint of Glacial Lake Schoharie. This final aspect is important, as the deposits were originally considered by other earlier workers (e.g. Mylroie, 1984) to be sub-ice deposits. The failure to find such deposits elsewhere in the Helderberg Plateau, or in other glaciated karst regions, was very problematic. Everyone who saw the deposits in situ agreed with the glacial rock flour hypothesis (e.g. Palmer et al., 2003). The use of the Glacial Lake Schoharie footprint to

explain these deposits as not sub-ice, but sub-glacial lake deposits, answers the final question about the failure to find such deposits in other glaciated karst locales.

REFERENCES

Baker, V.R., 1976, Hydrology of a Cavernous Limestone Terrane and the Hydrological Mechanisms of its Formation, Mohawk River Basin, New York: Empire State Geogram, v. 12, p. 2-65.

Brigham, A.P., 1929, Glacial geology and geographic conditions of the Lower Mohawk Valley: A survey of the Amsterdam, Fonda, Gloversville and Broadalbin Quadrangles: The University of the State of New York, no. 280.

Brodzikowski, K., van Loon, A.J., 1991, Glacigenic Sediments, Developments in Sedimentology 49, New York, Elsevier Science Publishing Company INC.

Chisholm, T., Hart, P., 1980, Preliminary Methods for the Analysis of Cave Sediments: Western Kentucky Speleological Survey Annual Report, p. 39-43.

Connally, G.G., Sirkin, L.A., 1970, Late glacial history of the upper Wallkill Valley, New York: Geological Society of America Bulletin, vol. 81, no. 11, p. 3297-3306.

Dineen, R.J., 1986, Deglaciation of the Hudson Valley Between Hyde Park and Albany, New York, in D.H. Cadwell, ed., The Wisconsinan Stage of the First Geological District, Eastern New York p. 89-108.

Dineen, R.J., Hanson, E.L., 1985, Deglaciation of the Middle Mohawk and Sacandaga Valleys, or a tale of two tongues, in R.H. Lindemann, ed., Field trip guidebook of the New York State Geological Association 57th meeting, p. 250-256.

Dumont, K.A., 1995, Karst Hydrology and Geomorphology of the Barrack Zourie Cave System, Schoharie County, New York [M.S. thesis]: Mississippi State, Mississippi, Mississippi State University, reprinted as New York Cave Survey, Bulletin 5.

Ebert, J.R., Matteson, D.K., Natel, E.M., 2001, Parting the Helderberg Sea: cryptic unconformities and the Silurian-Devonian boundary in the classic epeiric sea sequence of New York: Geologic Society of America, Abstracts and Programs, (Annual Meeting, Boston), v. 33, p. 321-322.

Ebert, J.R., Matteson, D.K., Wilson, R., 2010, Sedimentologic Observation and Stratigraphic Interpretation of the Lower Devonian (Lochkovian) Manlius Formation along the Mohawk River Valley in Upstate New York: A Discussion: Chicago Journals, v. 118, p. 333-337.

Grabau, A.W., 1919, Significance of the Sherburne sandstone in upper Devonic stratigraphy: Geological Society of America Bulletin, v. 30, no. 4, p. 423-470.

Heiri, O., Lotter, A.F., Lemcke, G., 2001, Loss on Ignition as a Method for Estimating Organic and Carbonate Content in Sediments: reproducibility and comparability of results: Journal of Paleolimnology, v. 25, p. 101-110.

Kastning, E.H., 1975, Cavern Development in the Helderberg Plateau, East-Central New York: Bulletin 1 New York Cave Survey.

Kottek, M., Grieser, J., Beck, C., Rudolf, B., Rubel, F., 2006, World map of the Koppen-Geiger climate classification updated, v. 15, no. 3, p. 259-263.

Kunze, G.W., and Dixon, J.B., 1986, Pretreatment for mineralogical analysis in Methods of Soil Analysis: Part 1—Physical and Mineralogical Methods, p. 91-100.

Lauritzen, S-E., Mylroie, J.E., 2000, Results of a Speleothem U/Th Dating Reconnaissance from the Helderberg Plateau, New York: Journal of Cave and Karst Studies, v. 62, p. 20-26.

LaFleur, R.G., 1961, Glacial features in the vicinity of Troy, New York: in LaFleur, R.G., ed., Guidebook to Field Trips: New York State Geological Association 33rd Annual Meeting, Troy, New York, p. (A1)-(A21).

LaFleur, R.G., 1965, Glacial lake sequence in the eastern Mohawk-northern Hudson Region: in Hewitt, P.C. and Hall, L.M., ed., Guidebook to Field Trips: New York State Geological Association Meeting, Schenectady, New York, p. (C1)-(C23).

LaFleur, R.G., 1969, Glacial Geology of the Schoharie Valley: in 61st Annual Meeting of the New England Intercollegiate Geological Conference Guidebook for Field Trips New York, Massachusetts, and Vermont, p. (5-1)-(5-20).

LaFleur, R.G., 1976, Glacial Lake Albany, in Rittner, Donald ed., The Pine Bush Albany's Last Frontier: Albany, N.Y., Pine Bush Historic Preservation Project, p. 1-10.

Mulholland, J.W., 1982, Glacial stagnation-zone retreat in New England: Bedrock Control: Geological Society of America, Geology, v. 10, p. 567-571.

Muller, E.H., Calkin, P.E., 1993, Timing of Pleistocene glacial events in New York State: Canadian Journal of Earth Sciences, v. 30, p. 1829-1845.

Mylroie, J.E., 1977, Speleogenesis and Karst Geomorphology of the Helderberg Plateau, Schoharie County, New York [Ph.D. dissertation]: Troy, N.Y., Rensselaer Polytechnic Institute reprinted as Bulletin 2 of the New York Cave Survey.

Mylroie, J.E., 1984, Pleistocene Climatic Variation and Cave Development: Norsk Geogr. Tidsskr, v. 38, p. 151-156.

Mylroie, J.E., Mylroie, J.R., 2004, Glaciated Karst: How the Helderberg Plateau Revised the Geologic Perception: Northeast Geology & Environmental Sciences, v. 26, no. 1&2, p. 82-92.

Neuendorf, K.K.E., Mehl Jr., J.P., Jackson, J.A., 2011, ed., Glossary of Geology, 5th revised ed., Alexandria, Virginia, American Geosciences Institute.

Palmer, A.N., 2007, Cave Geology: Dayton Ohio, Cave Books.

Palmer, A.N., 2009, Cave Exploration as a Guide to Geologic Research in the Appalachians: Journal of Cave and Karst Studies, v. 71, no. 3, p. 180-192.

Palmer, A.N., Rubin, P.A., Palmer, M.V., 1991, Interaction between karst and glaciation in the Helderberg Plateau, Schoharie and Albany Counties, New York: New York State Geological Association, Field-trip guidebook for annual meeting, Oneonta, NY, p. 161-190.

Palmer, A.N., Rubin, P.A., Palmer, M.V., Engel, T.D., Morgan, B., 2003, Karst of the Schoharie Valley and land use analysis, Schoharie County, New York State, in New York State Geological Association Field Trip Guidebook (75th Annual), p. 141-165.

Rickard, L.V., 1962, Lake Cayugan (Upper Silurian) and Helderbergian (Lower Devonian) stratigraphy in New York: New York State Museum and Science Service Bulletin 386, p.157.

Ridge, J.C., 2004, The Quaternary glaciation of western New England with correlations to surrounding areas: Developments in Quaternary Sciences, v. 2, p. 169-199.

Sheppard, C.U., 1853, On the strontianite of Schoharie (N.Y.), with a notice of the limestone cavern in the same place: American Journal of Science and Arts, v. 27, p. 363-370.

Soukup, D.A., Buck, B.J., Harris, W., 2008, Preparing soils for mineralogical analyses in Methods of Soil Analysis Part 5—Mineralogical Methods, p. 13-31.

Stephenson, D.A., Fleming, A.H., Mickelson, D.M., 1988, Glacial Deposits: The Geological Society of America, The Geology of North America, v. 0-2, Hydrology, p. 301-314.

Stone, F.D., 2005, McFails Cave, The Beginnings of NSS Cave Ownership and Development of a Model for Interactive Cave Management: 2005 National Cave and Karst Management Symposium, p. 221-231.

Ver Straeten, C.A., 2008, Volcanic Tephra Bed Formation and Condensation Processes: A Review and Examination from Devonian Stratigraphic Sequences: The Journal of Geology, v. 116, p. 545-557.

Ver Straeten, C.A., 2009, The Classic Devonian of the Catskill Front: A Foreland Basin Record of Acadian Orogenesis in New York State Geological Association Field Trip Guidebook (81st Annual), p. 7-1 to 7-54.

Woodworth, J.B., 1905, Ancient water levels of the Hudson and Champlain Valleys: New York State Museum Bulletin 84, p. 65-265.

APPENDIX A

XRD APPENDIX

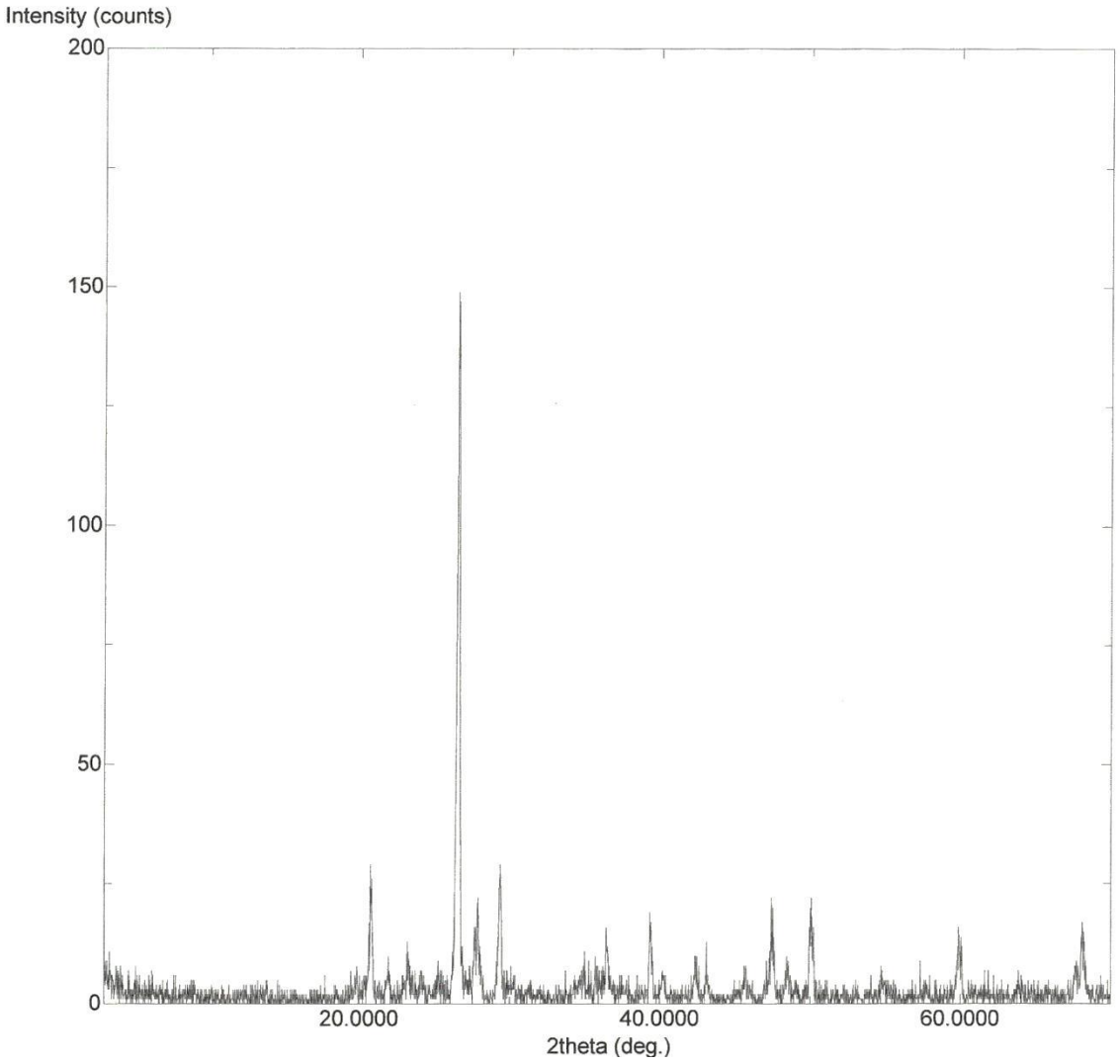

Figure A.1 M-C 1-1

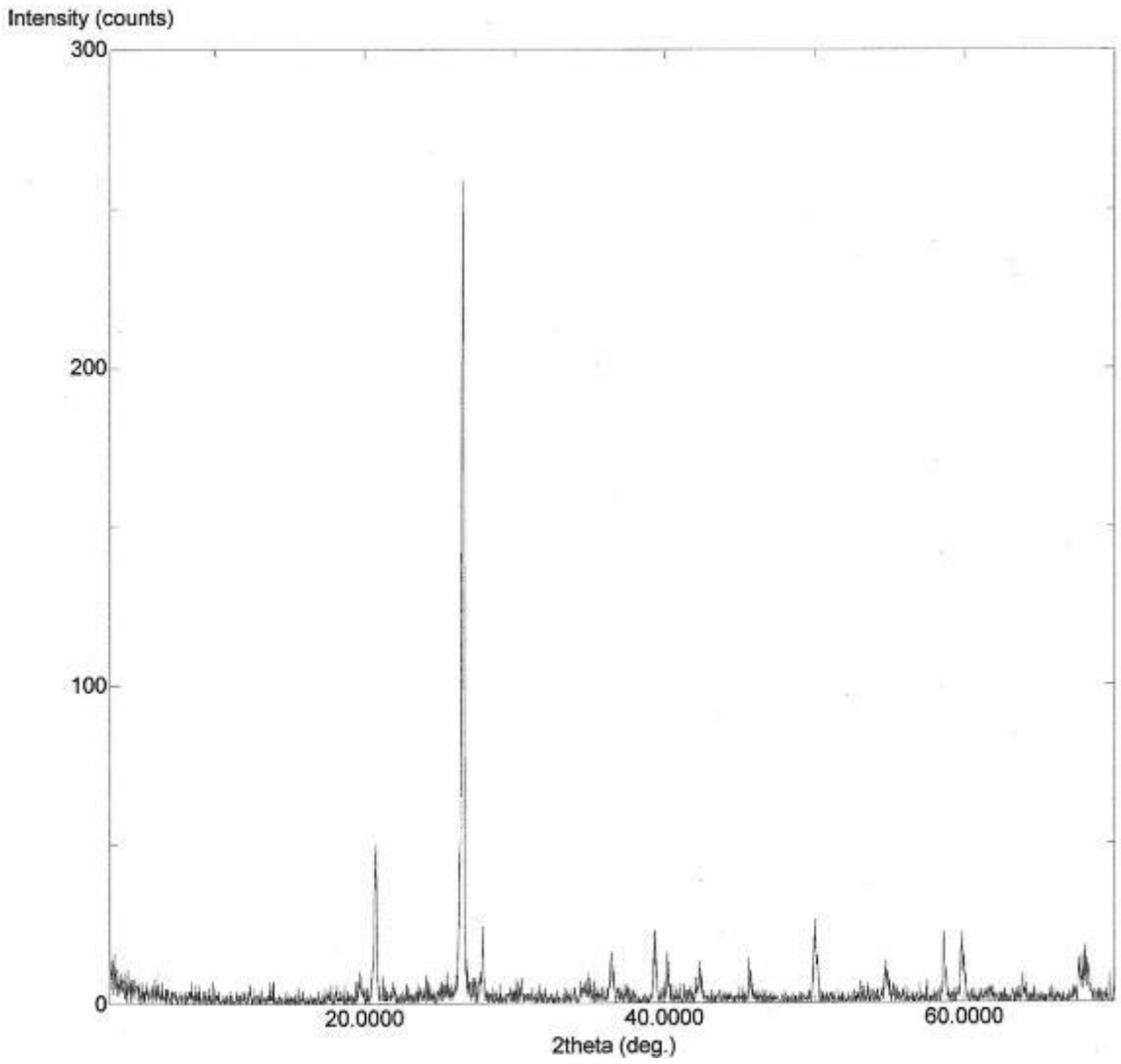

Figure A.2 M-C 1-2

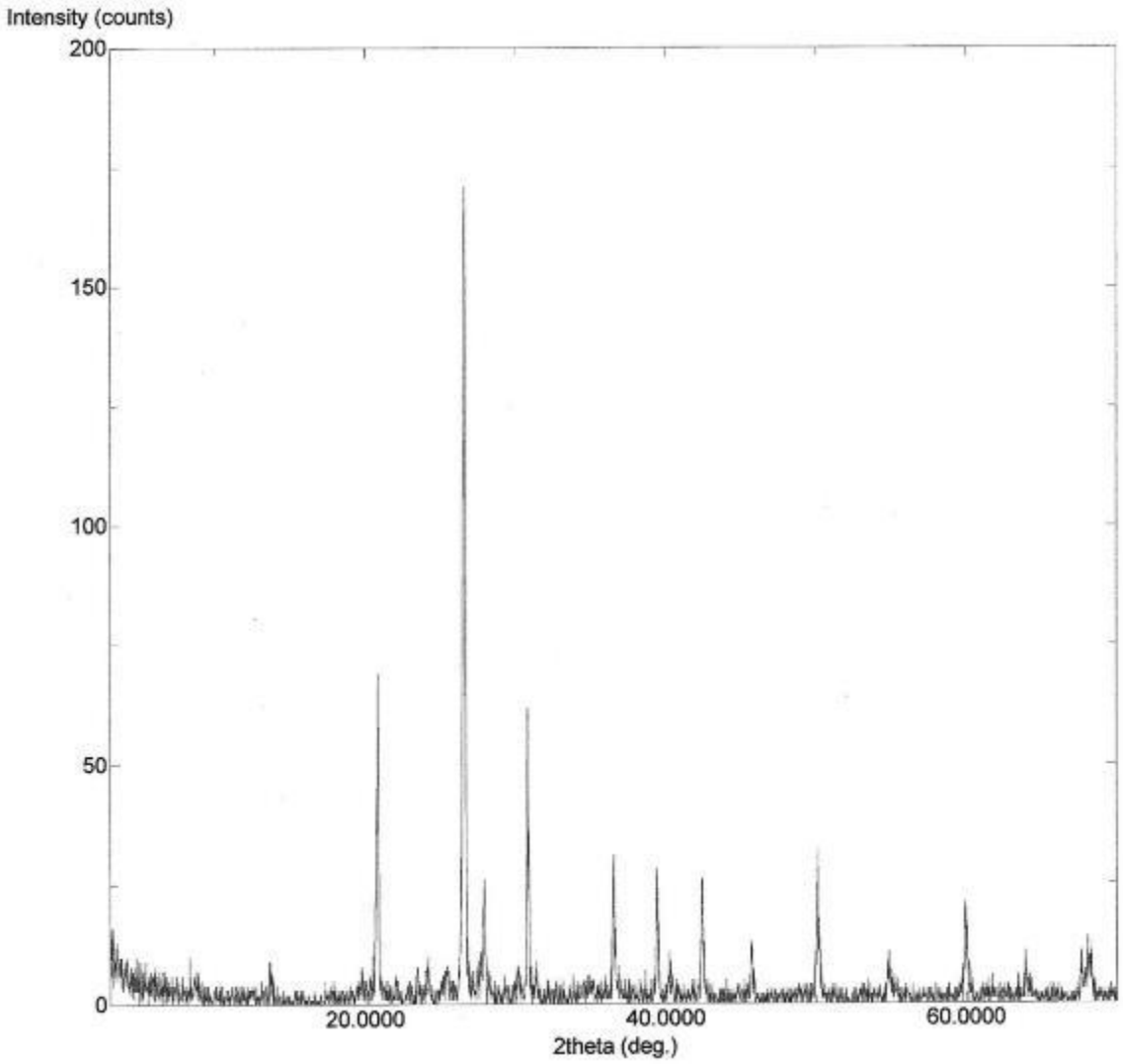

Figure A.3 M-C 1-3

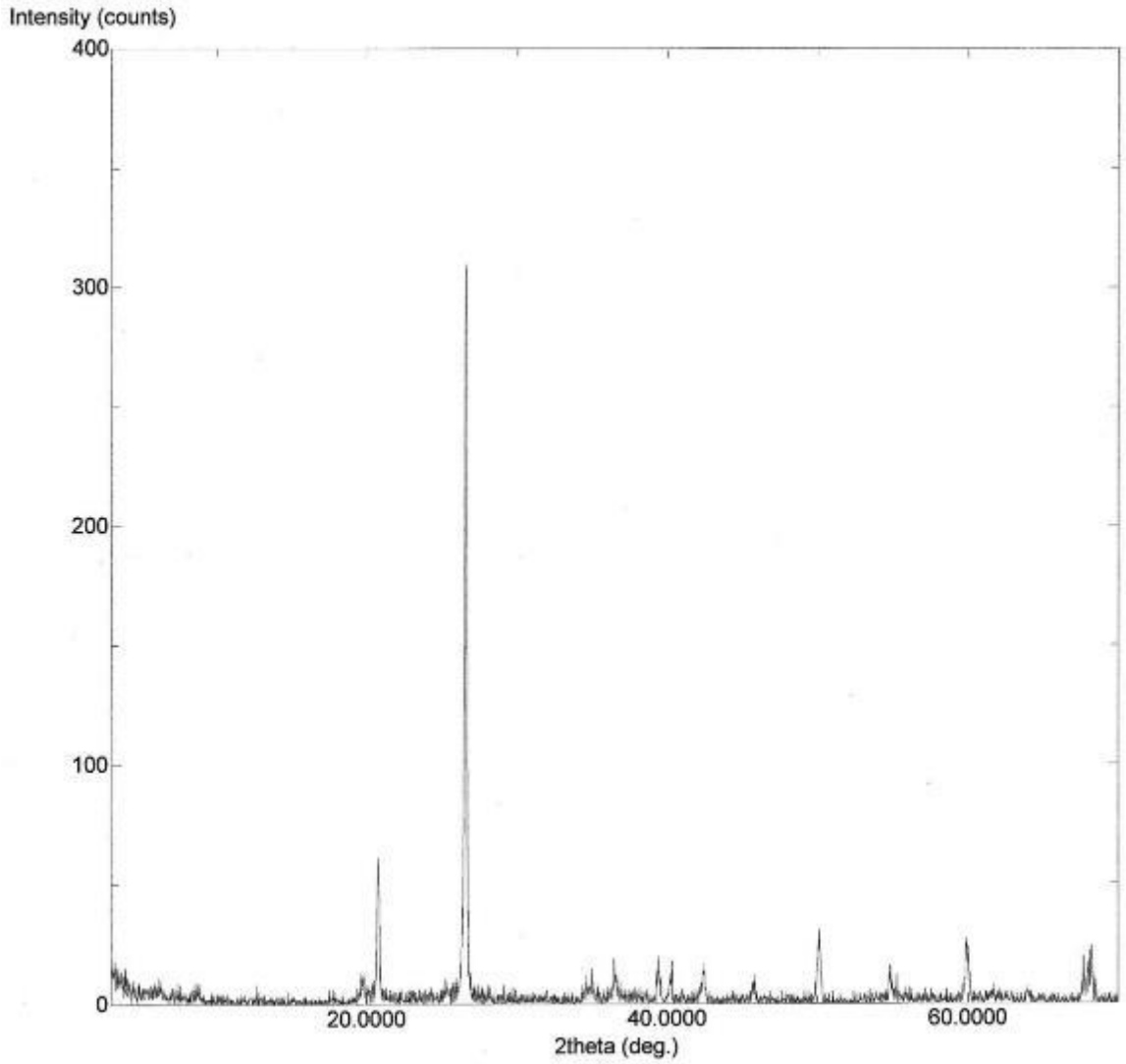

Figure A.4 M-C 2-1

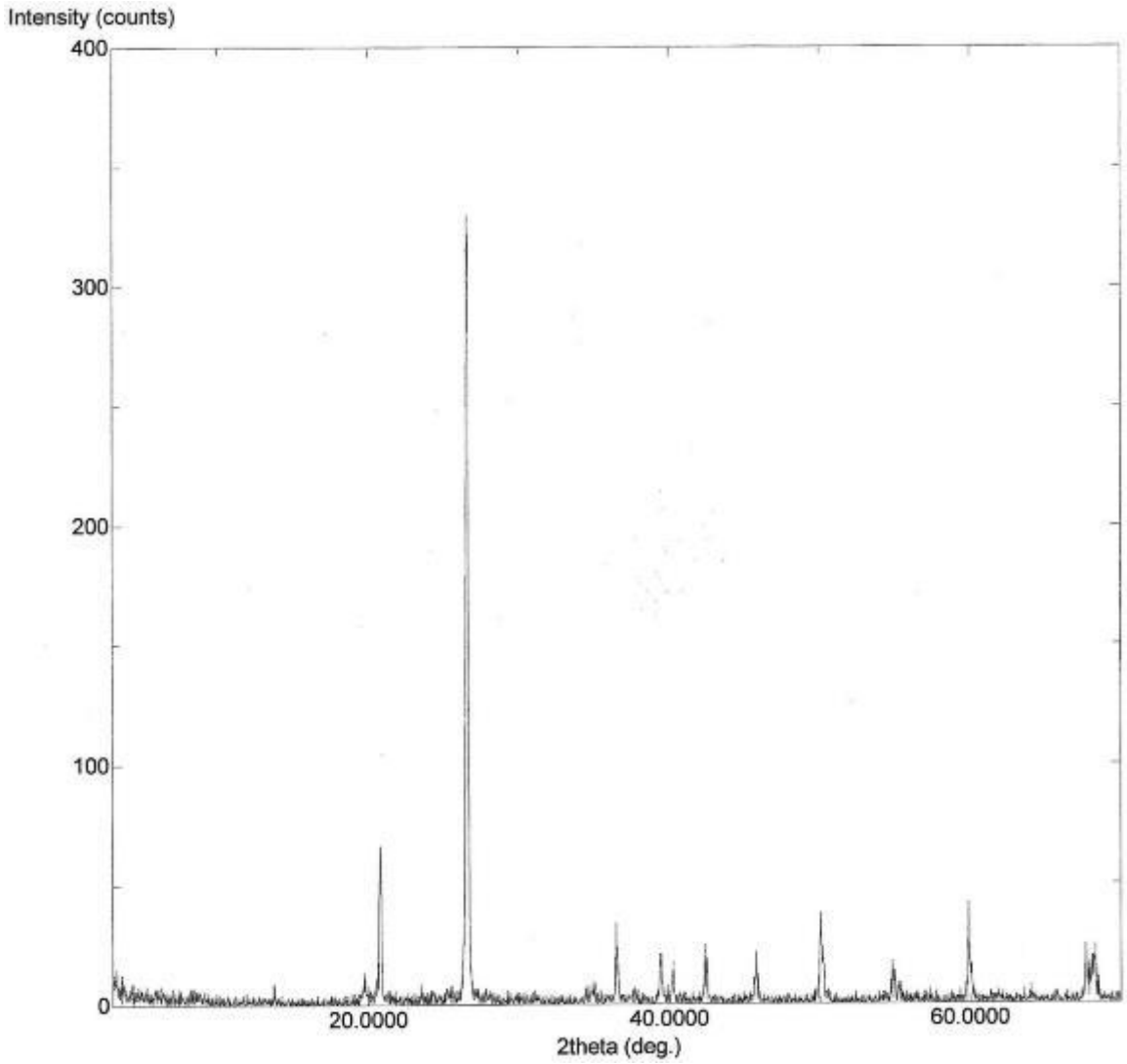

Figure A.5 M-C 2-2

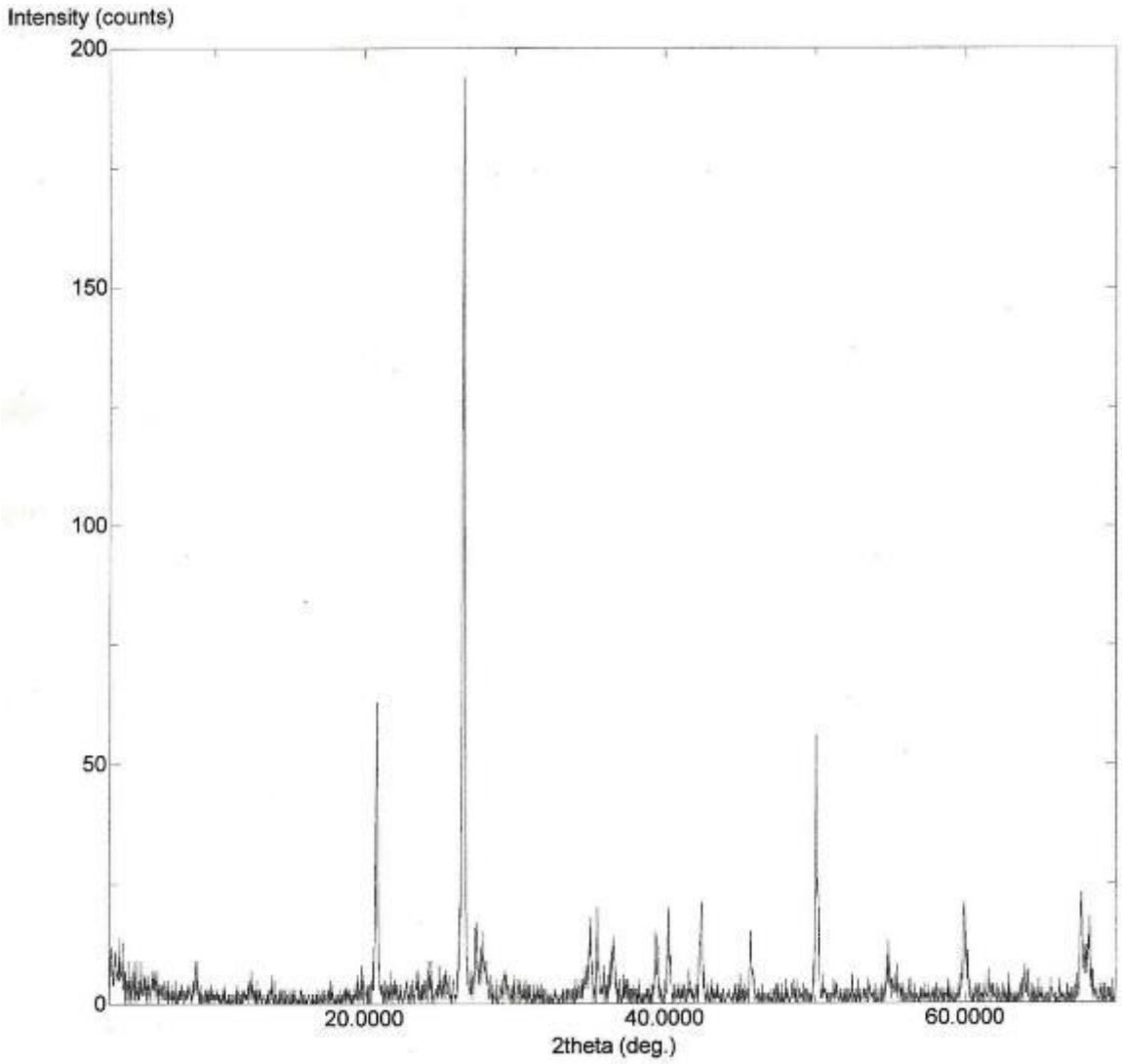

Figure A.6 M-C 2-3

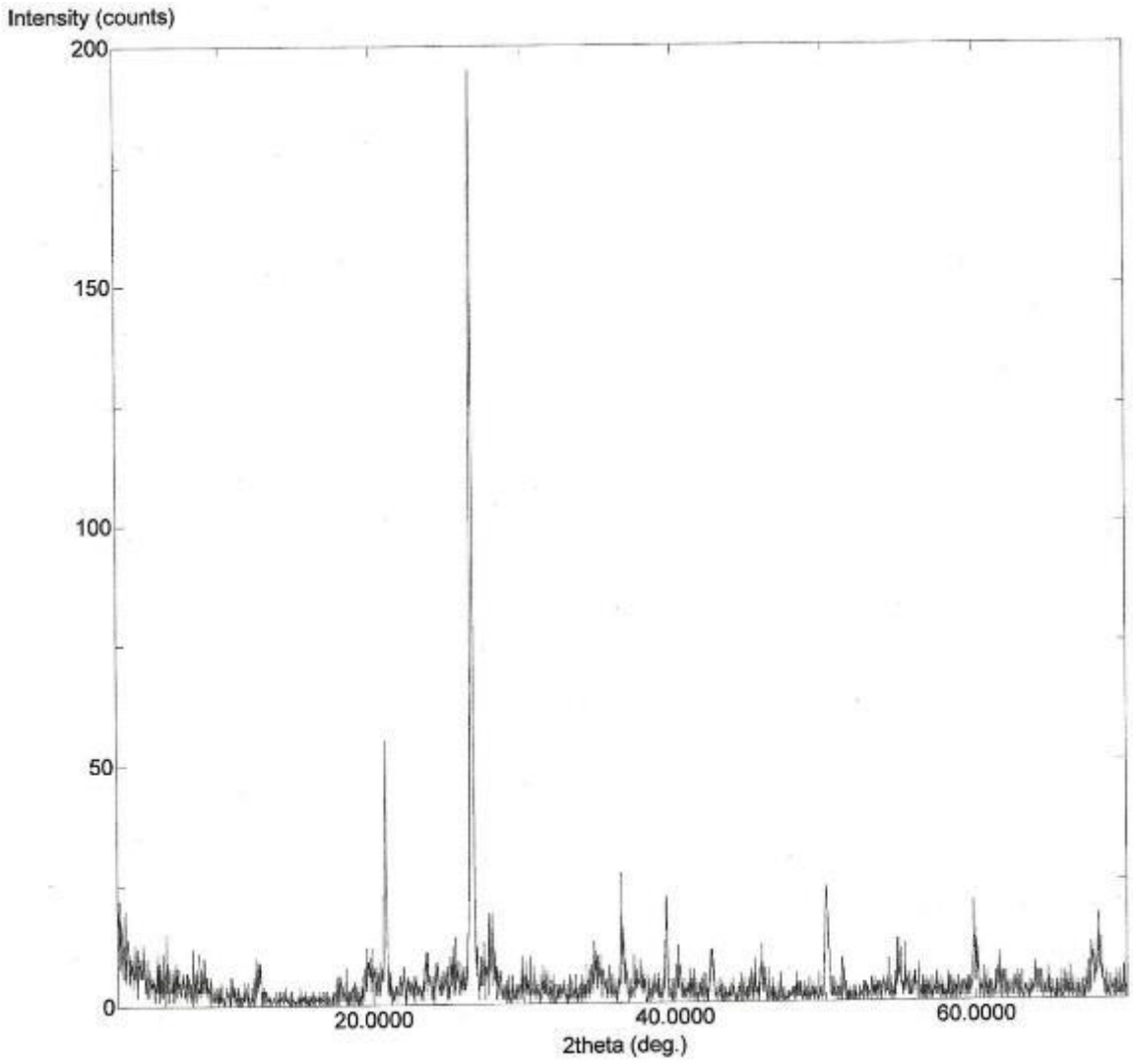

Figure A.7 H-C 1-0

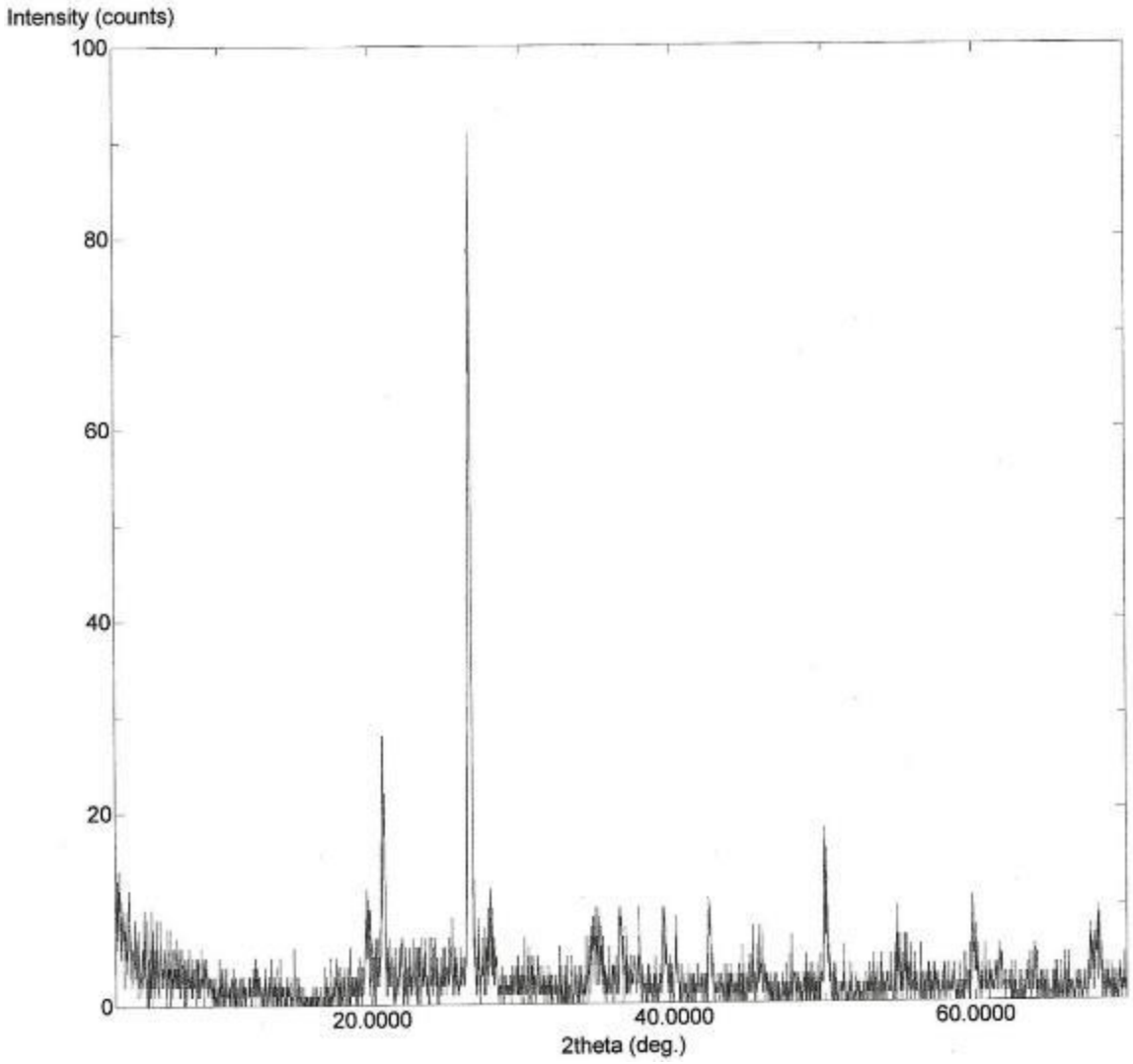

Figure A.8 H-C 1-1

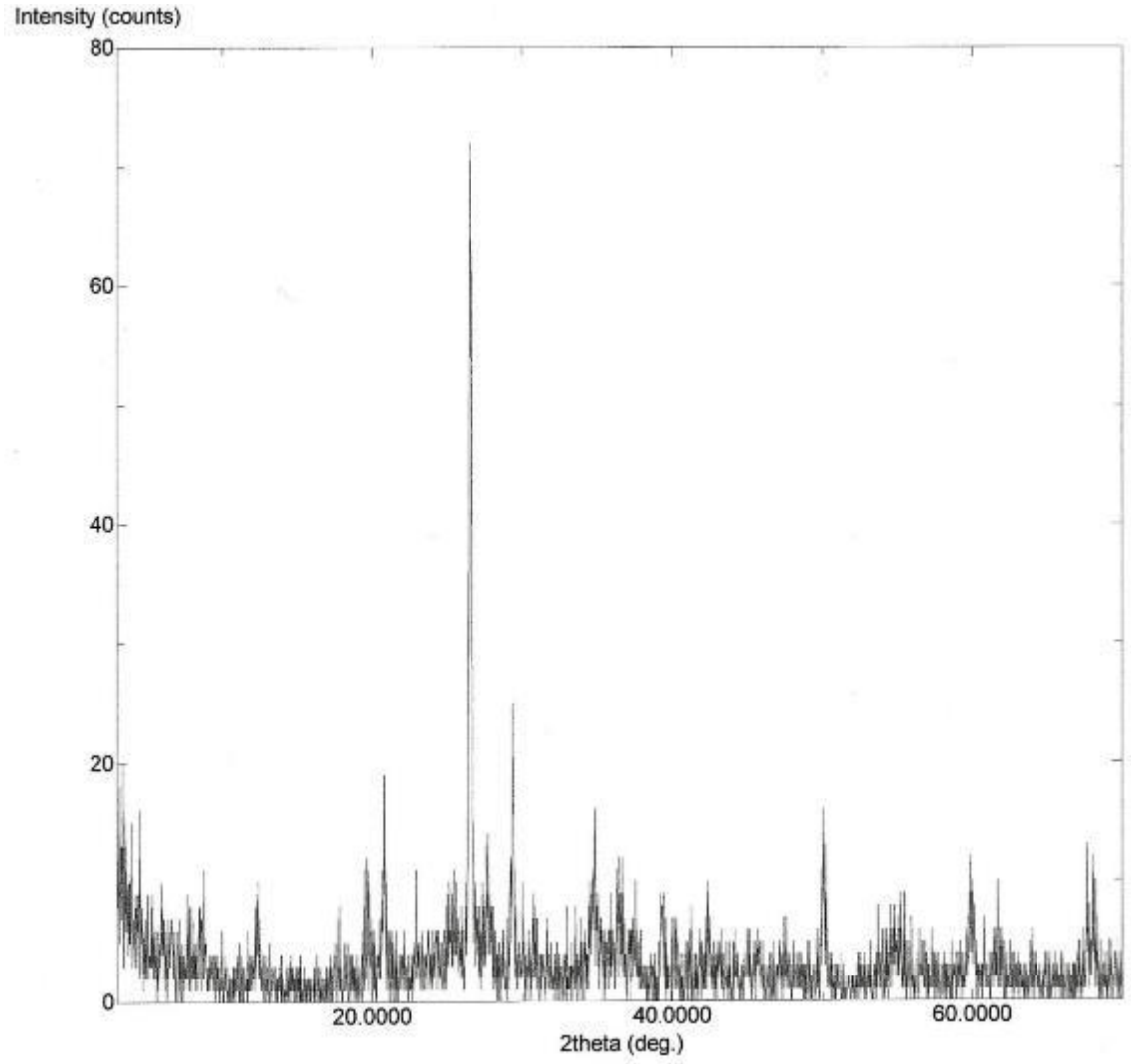

Figure A.9 H-C 1-2

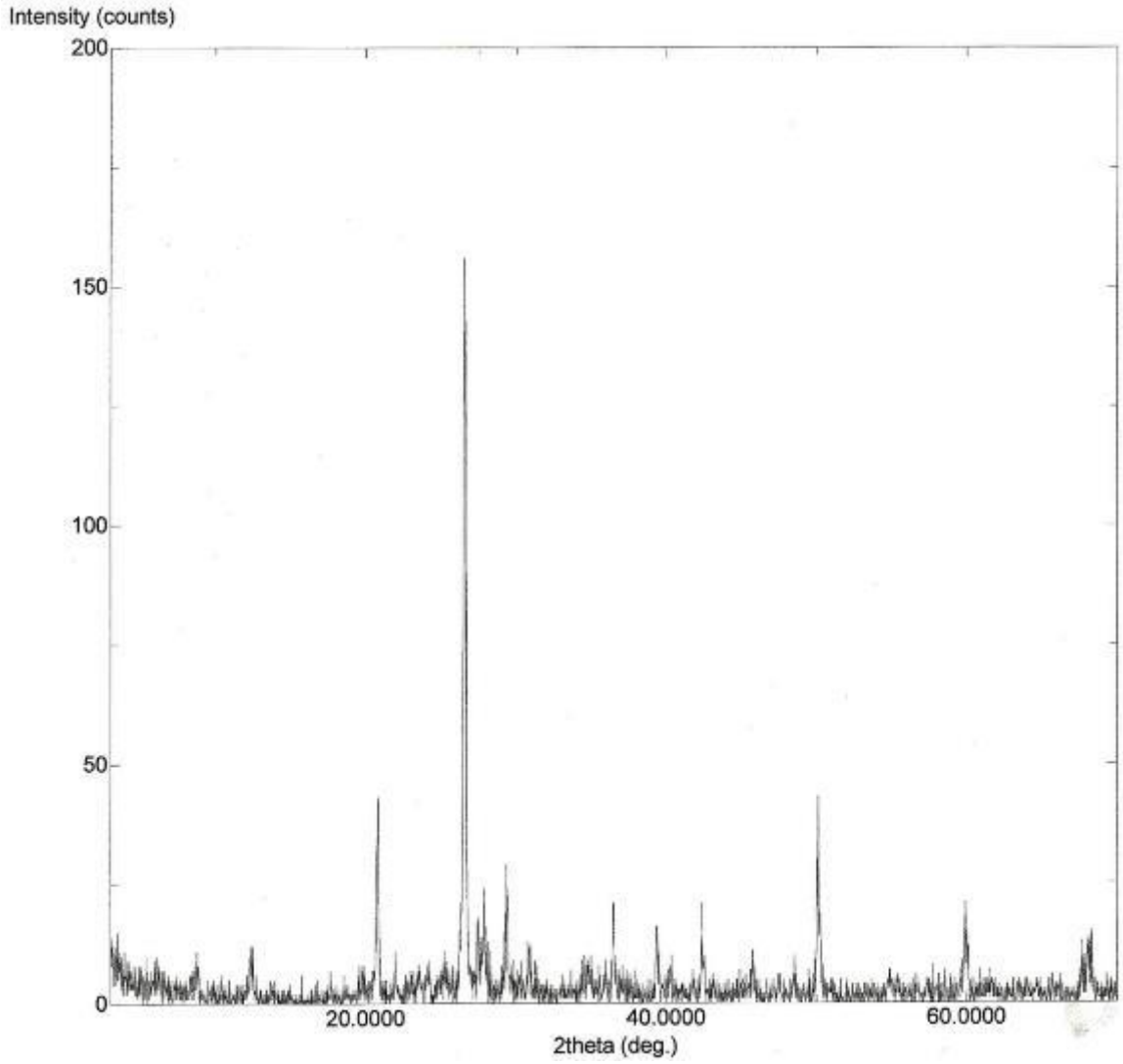

Figure A.10 H-C 1-3

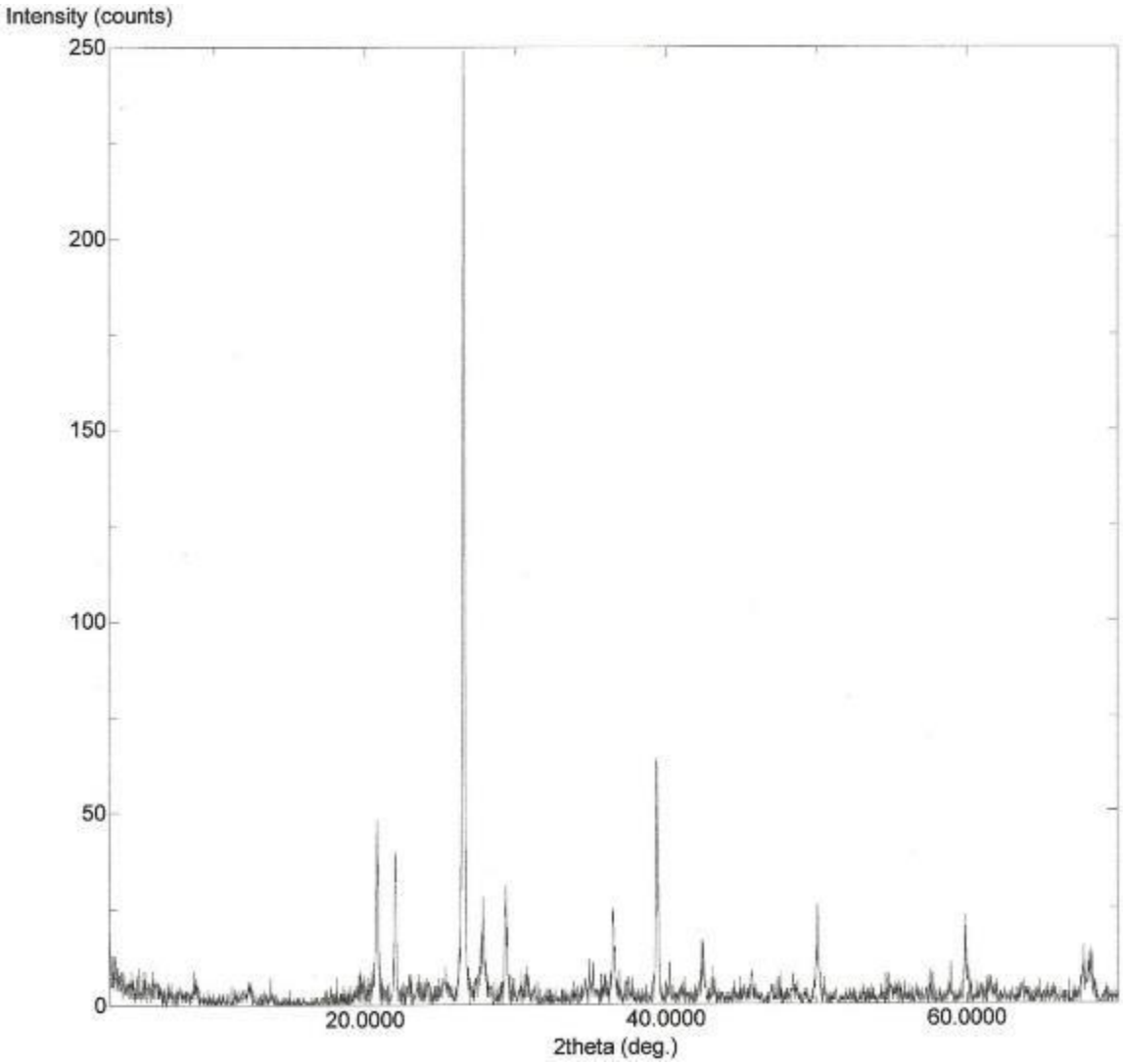

Figure A.11 H-C 1-4

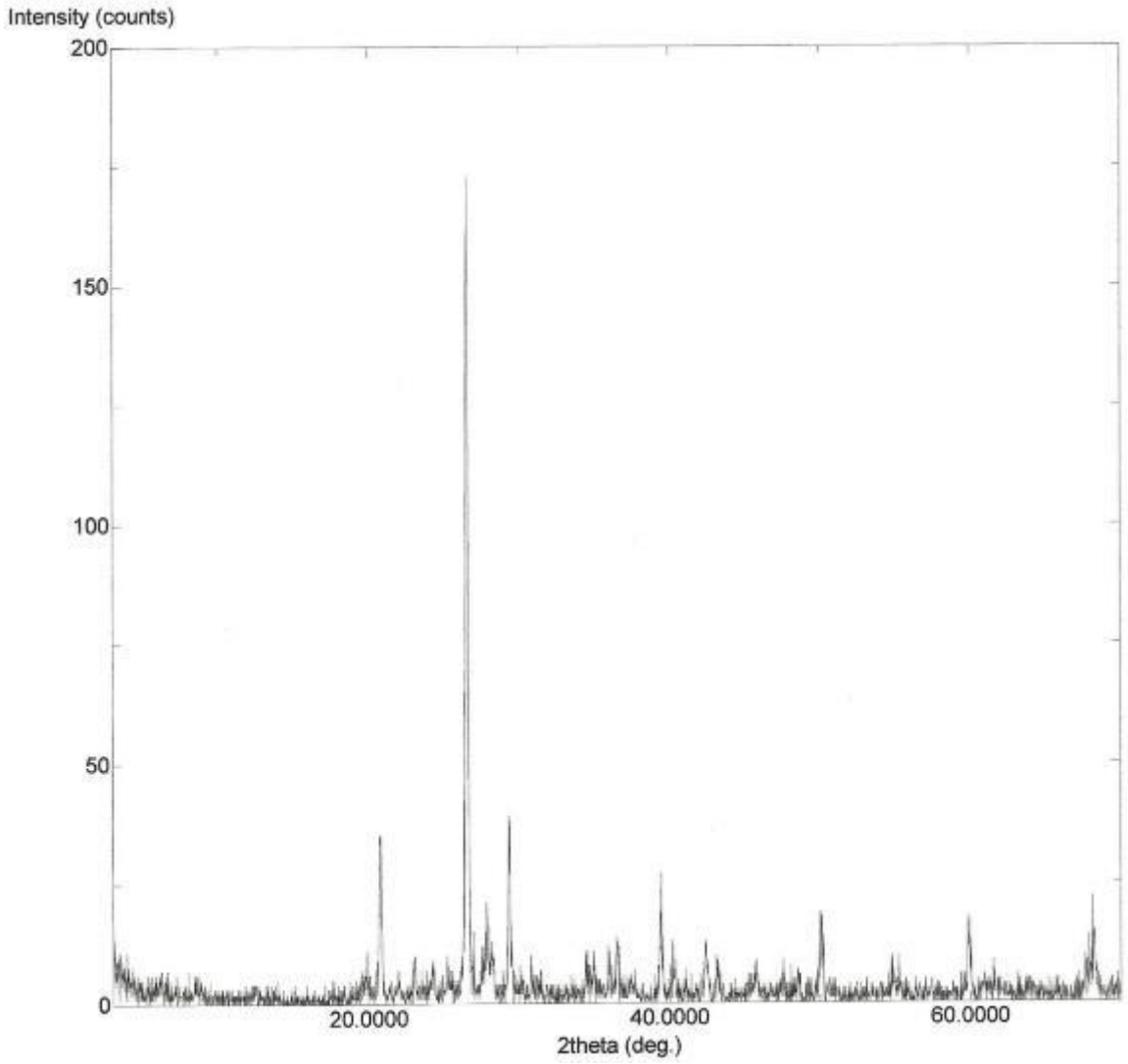

Figure A.12 H-C 1-5

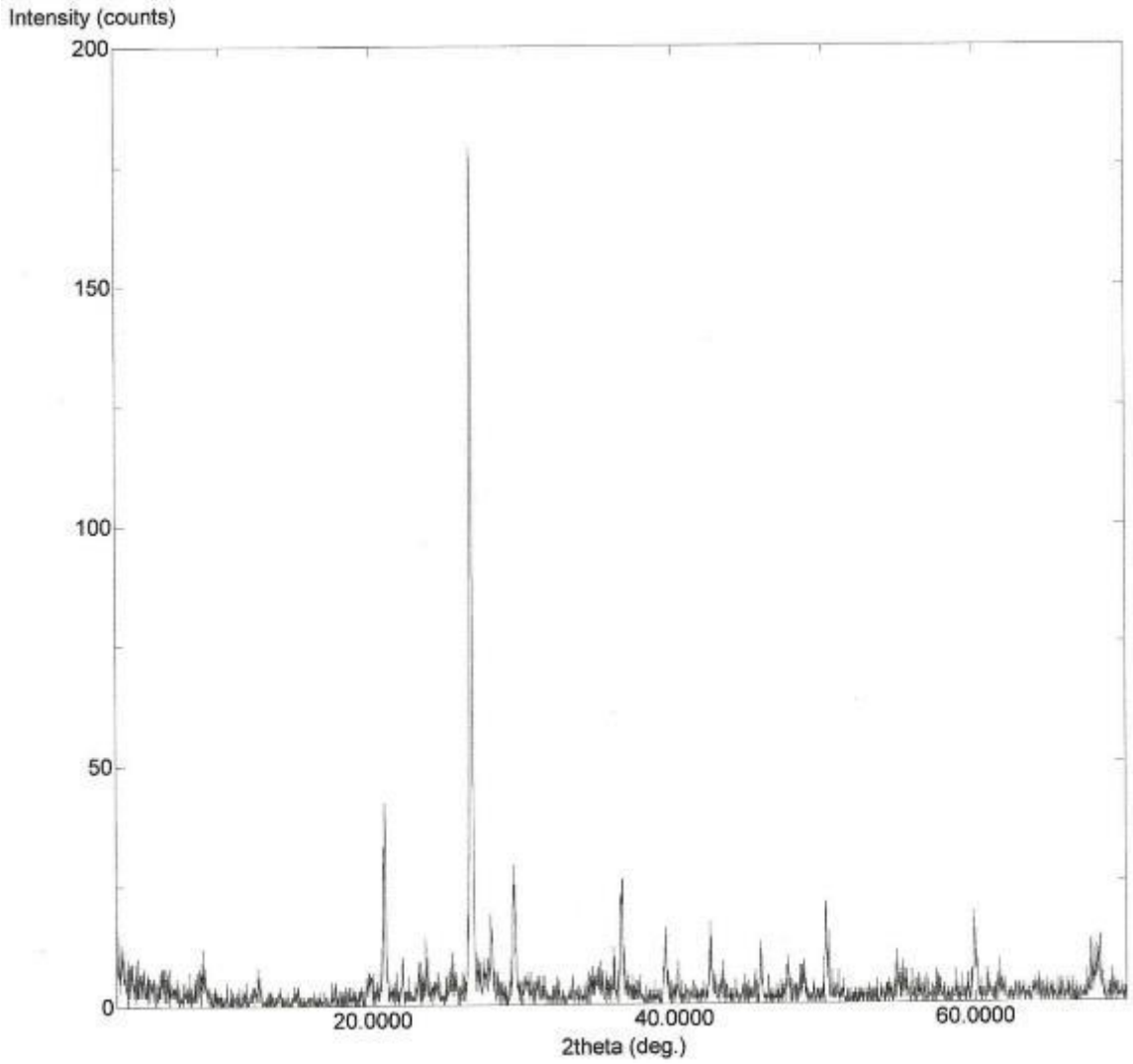

Figure A.13 H-C 1-6

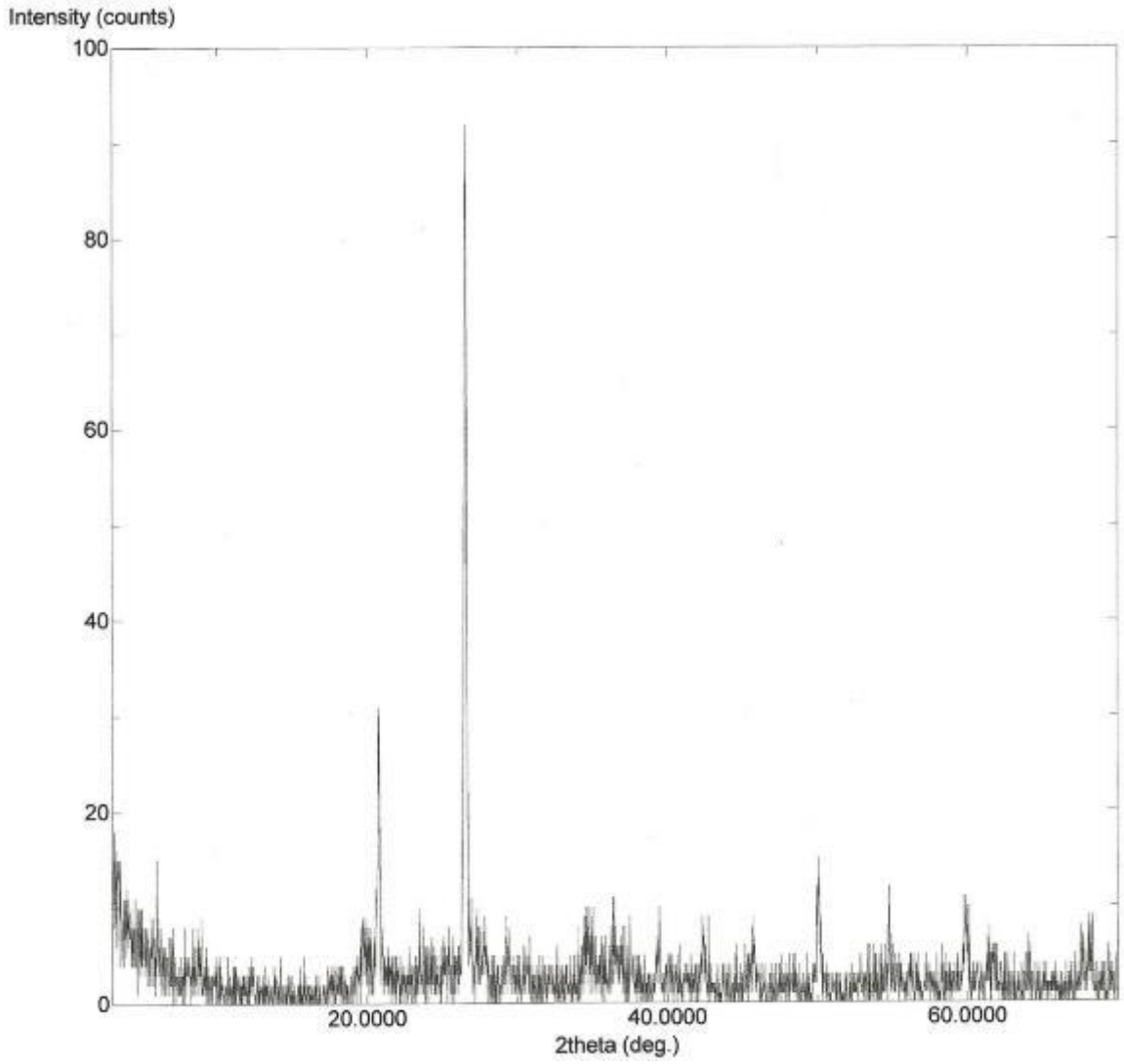

Figure A.14 H-C 1-7

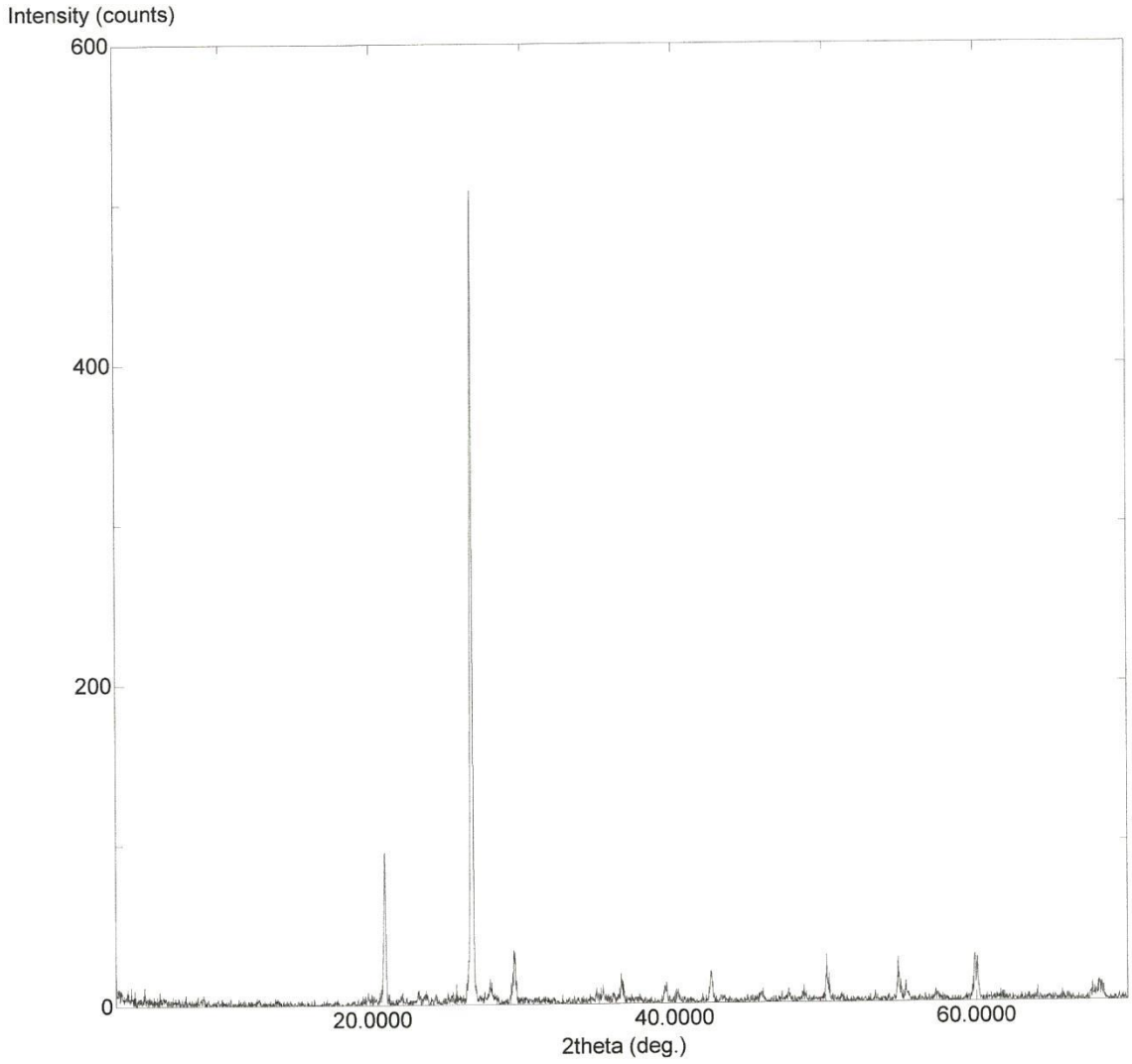

Figure A.15 H-C 1-8

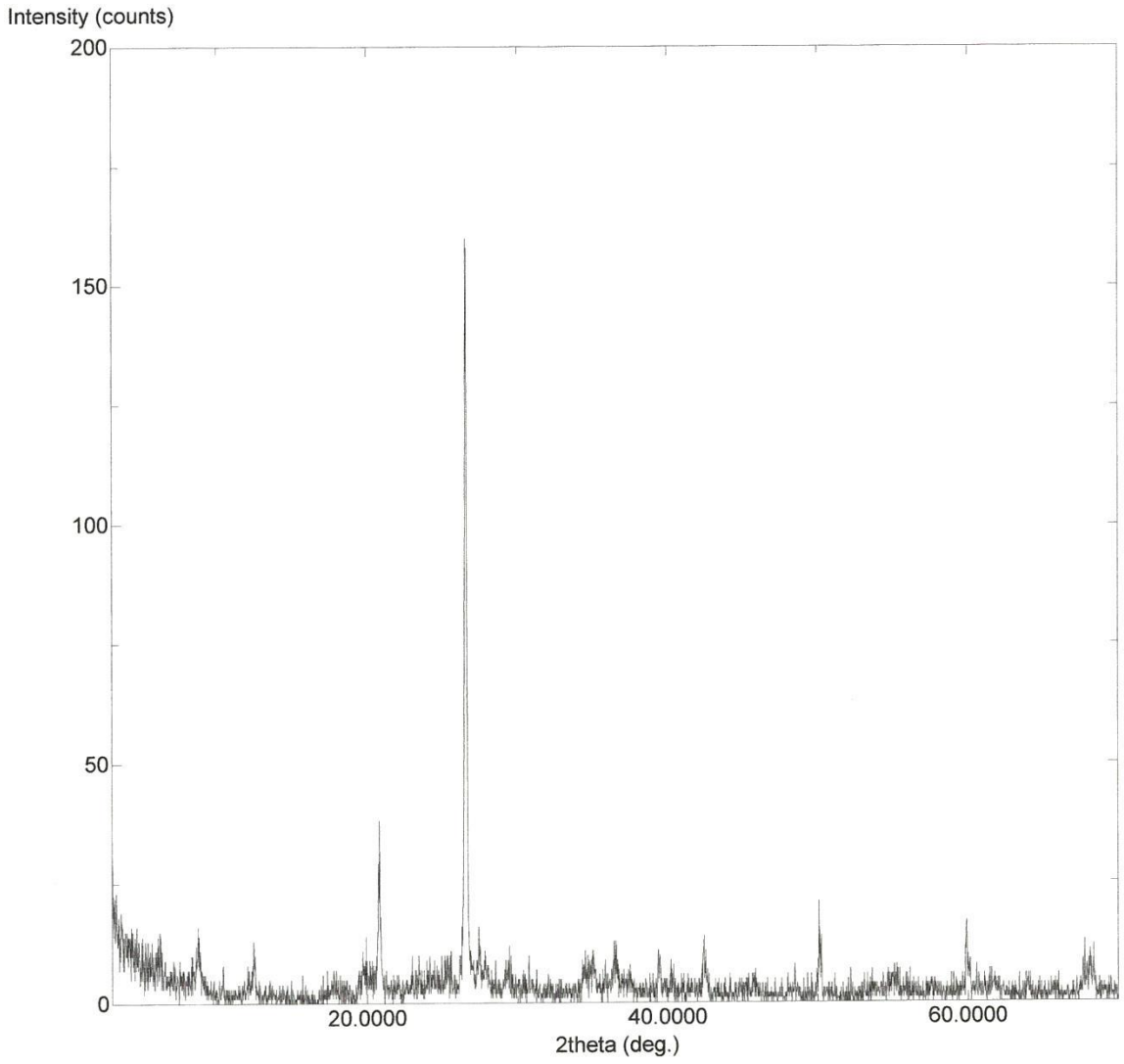

Figure A.16 H-C 1-9

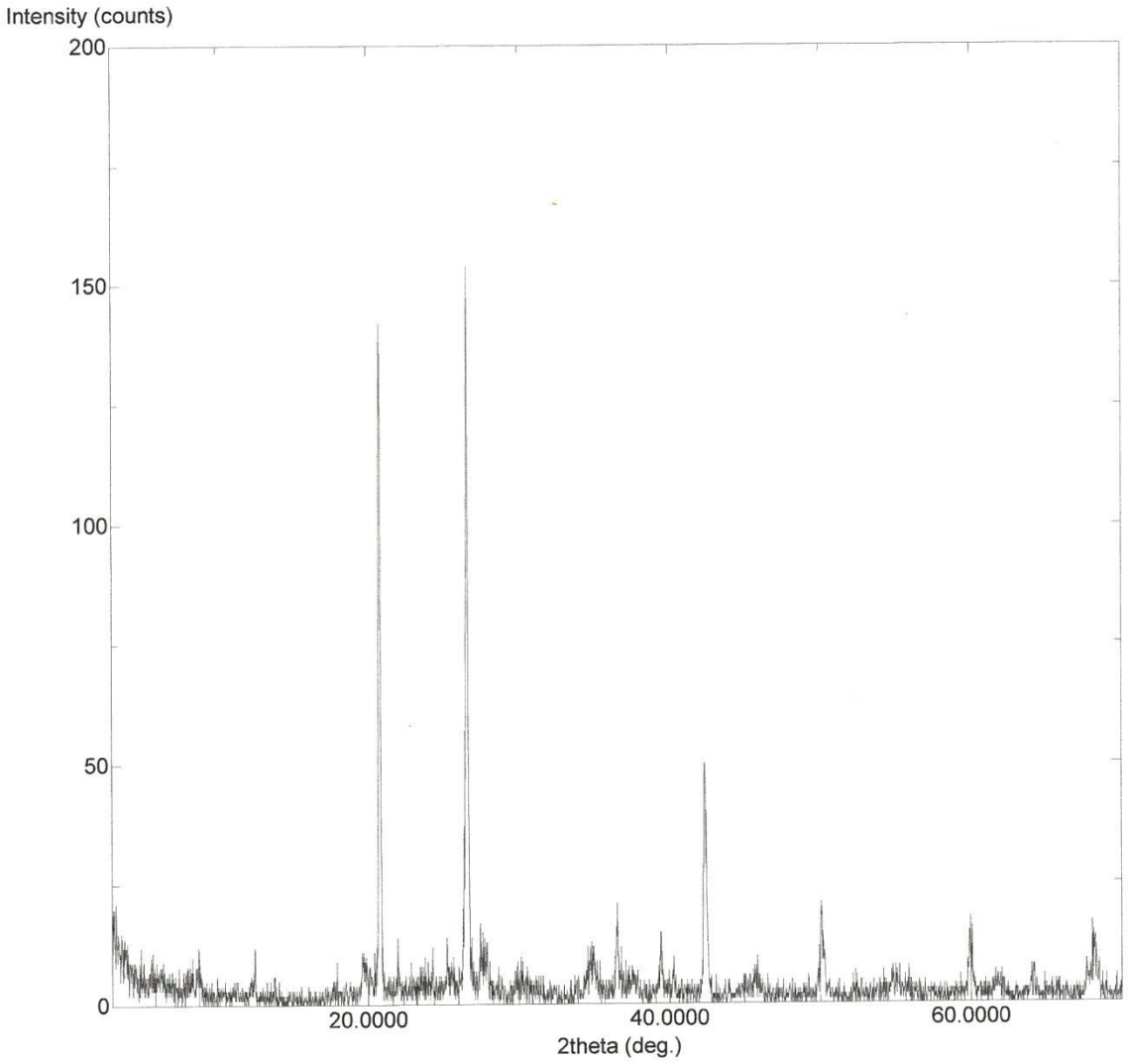

Figure A.17 H-C 1-10

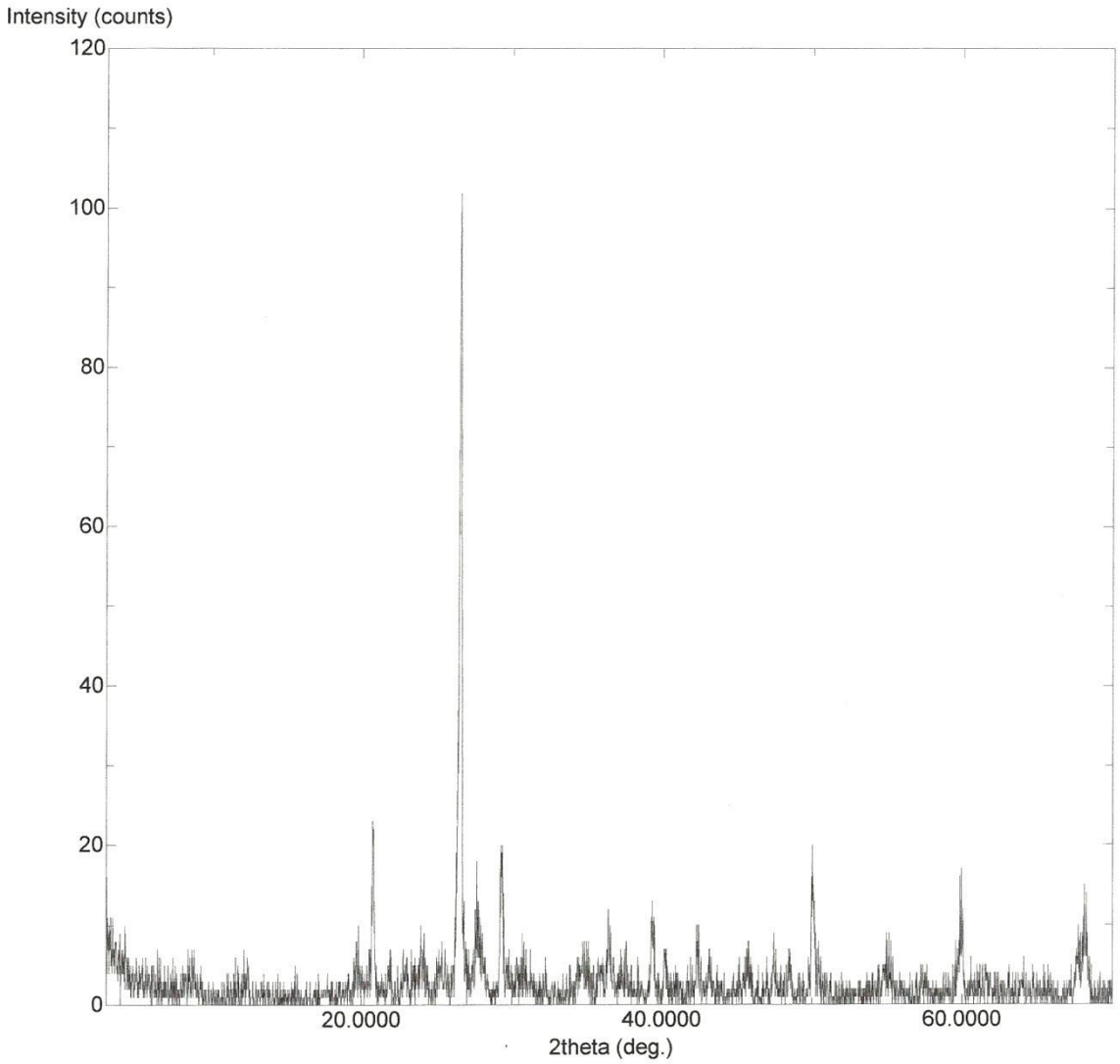

Figure A.18 H-C 1-11

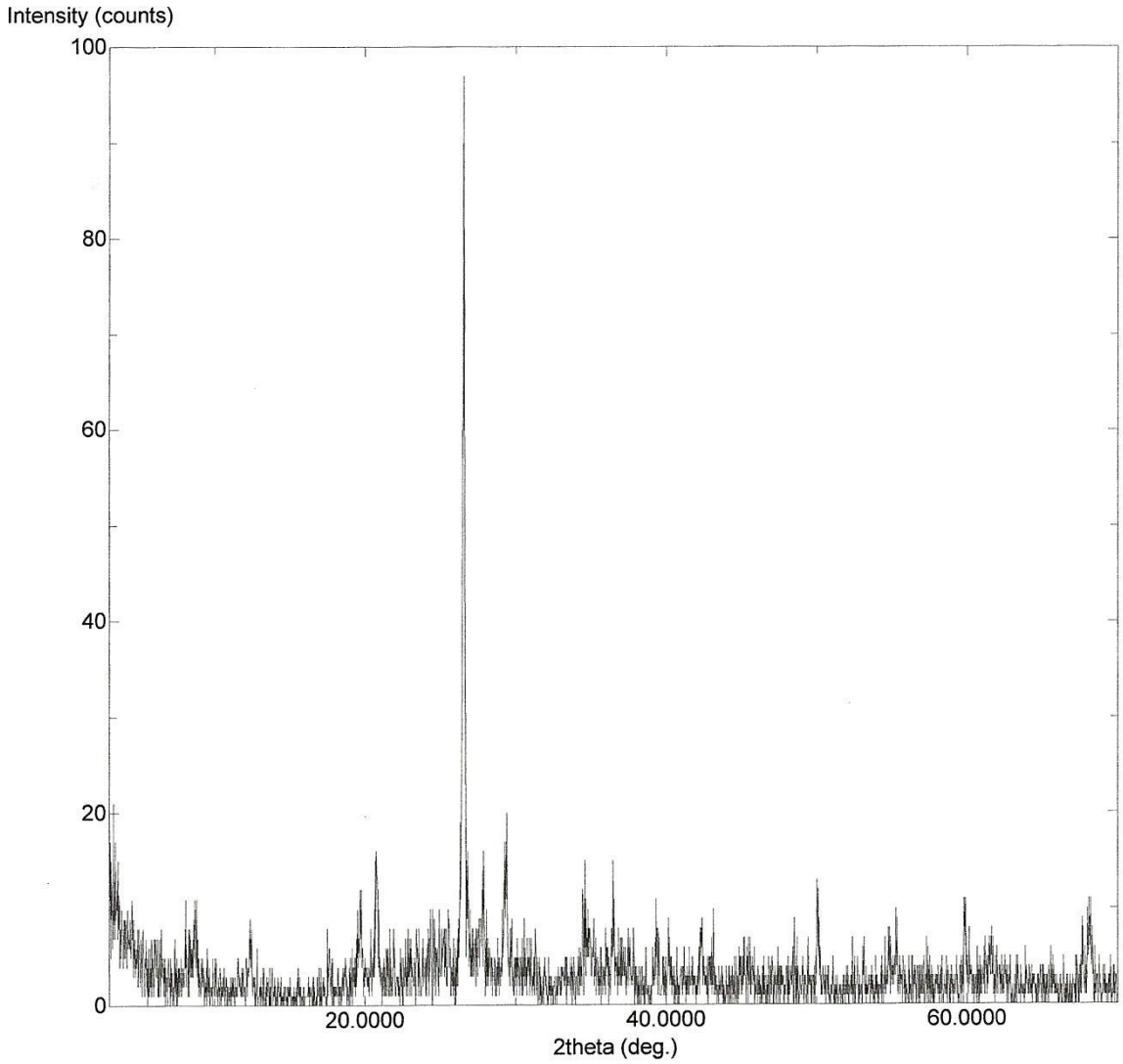

Figure A.19 H-C 1-12

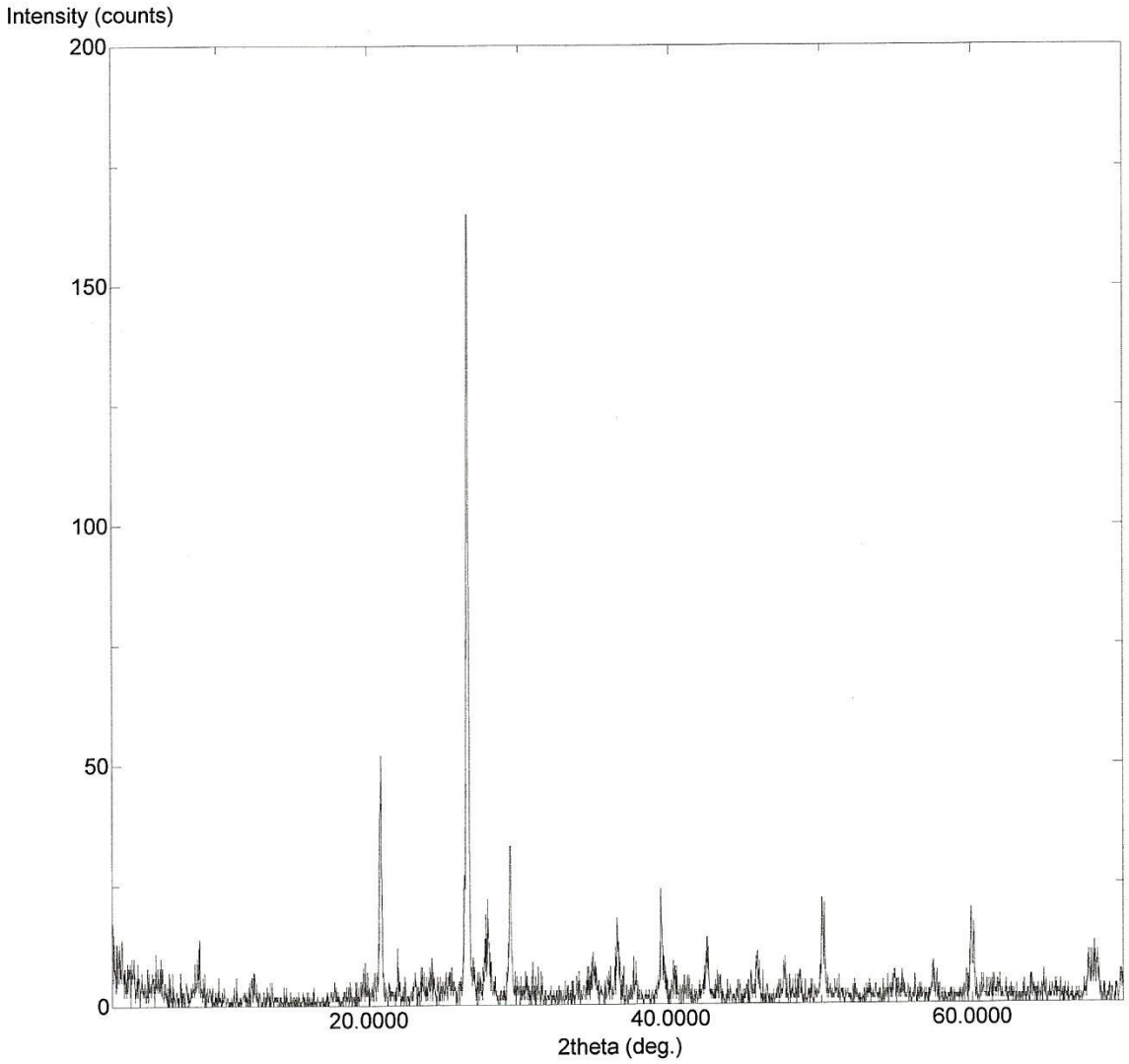

Figure A.20 H-C 1-13

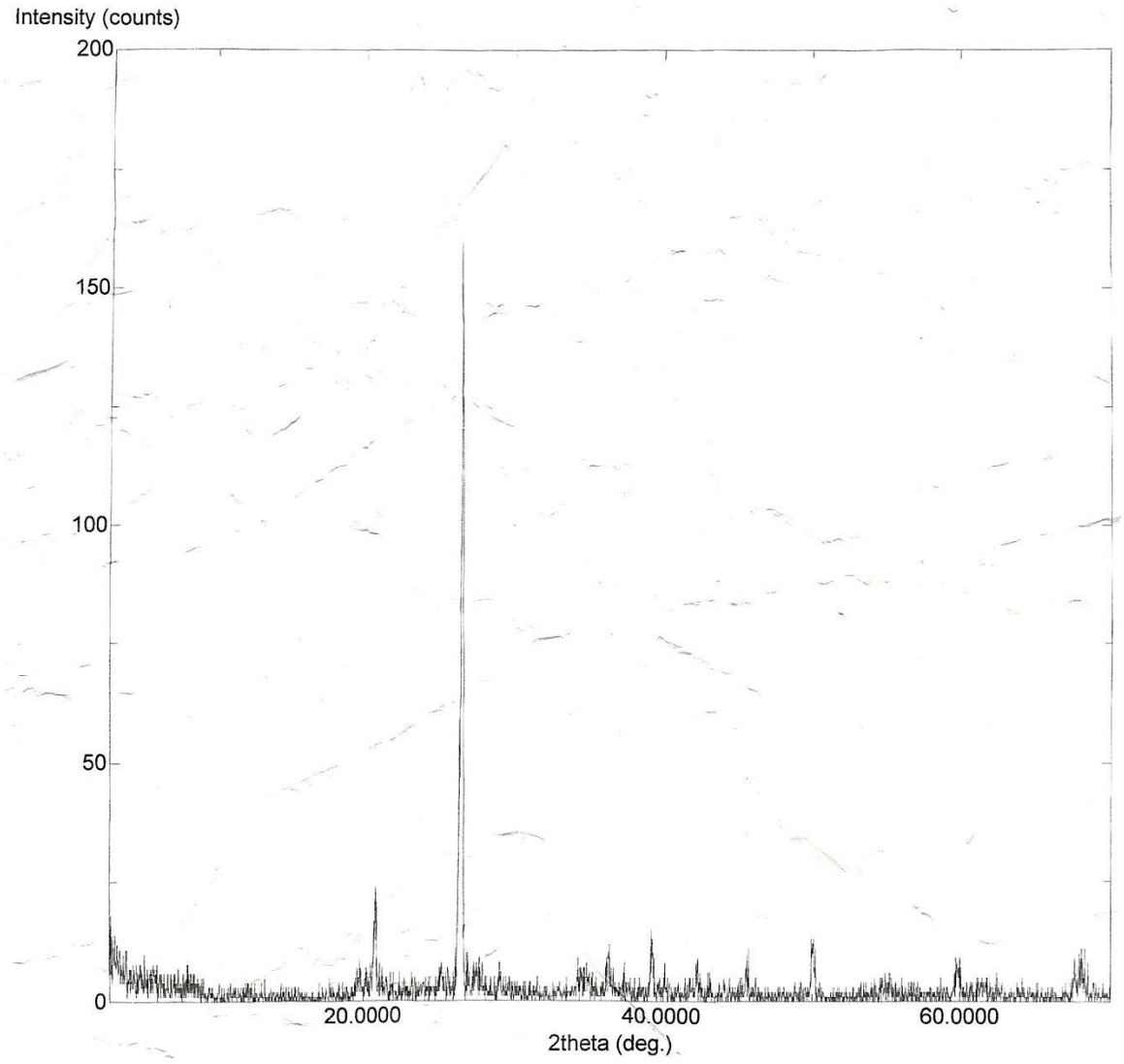

Figure A.21 H-C 1-14

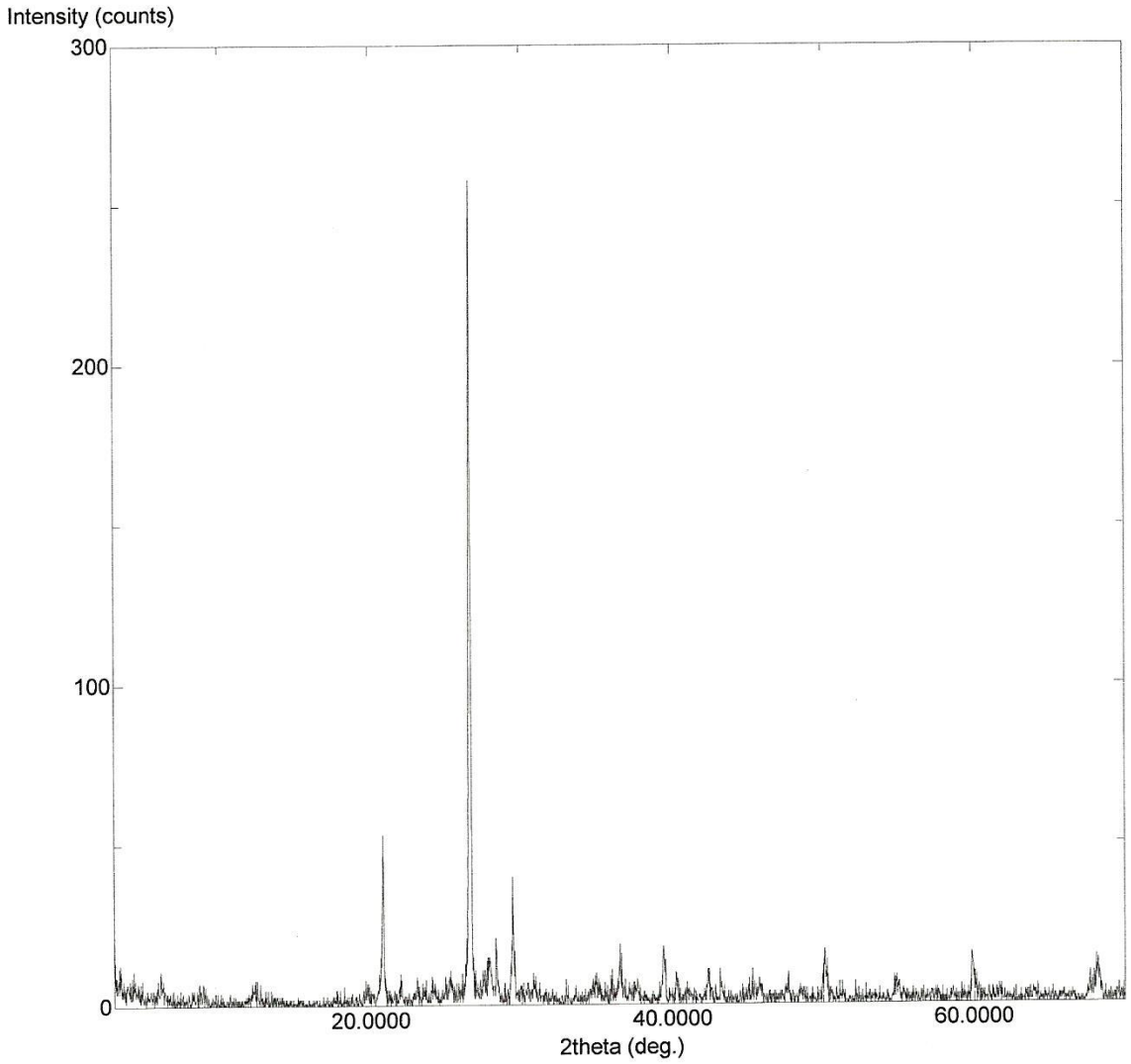

Figure A.22 H-C 1-15

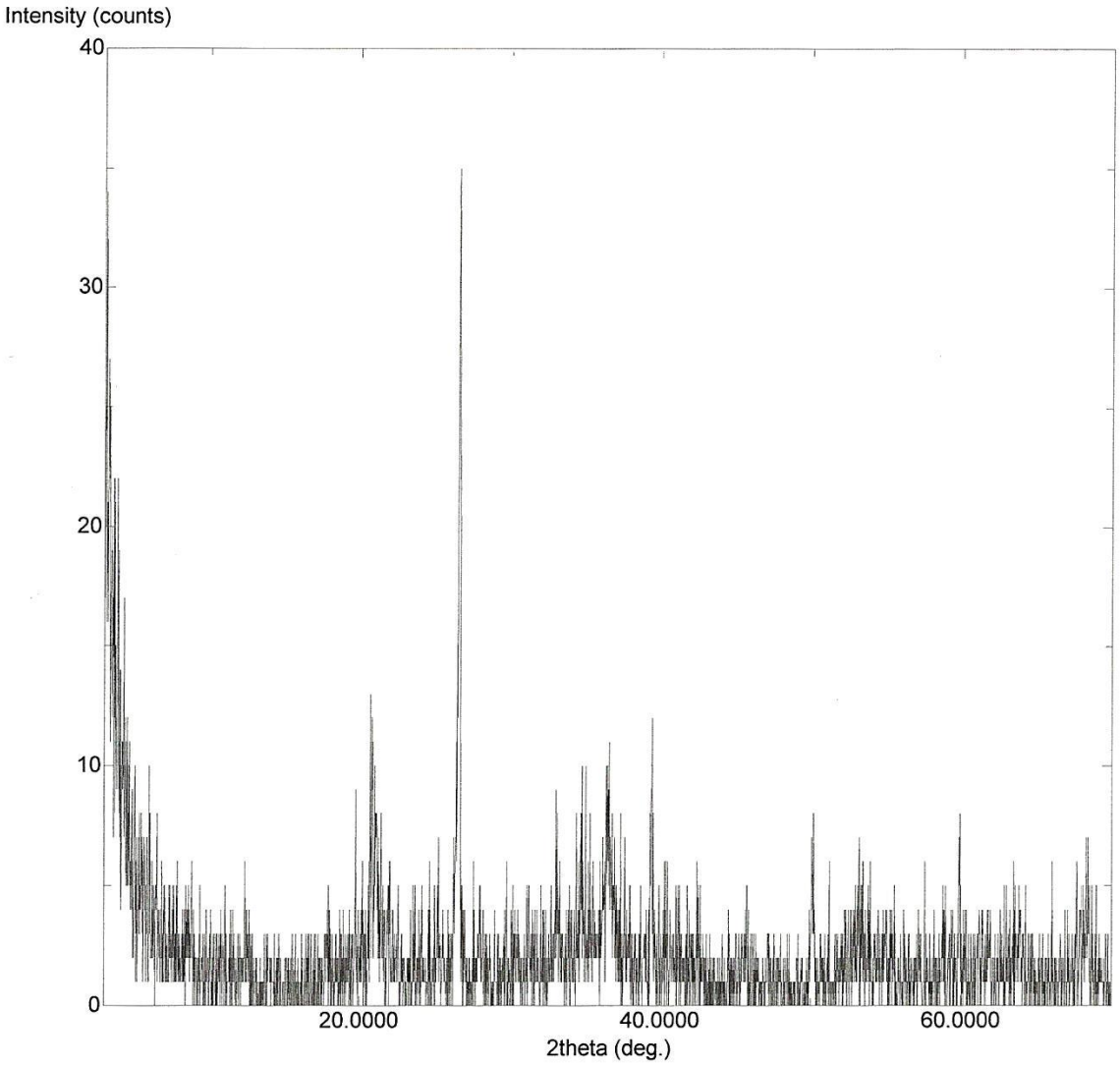

Figure A.23 S-B 1-0

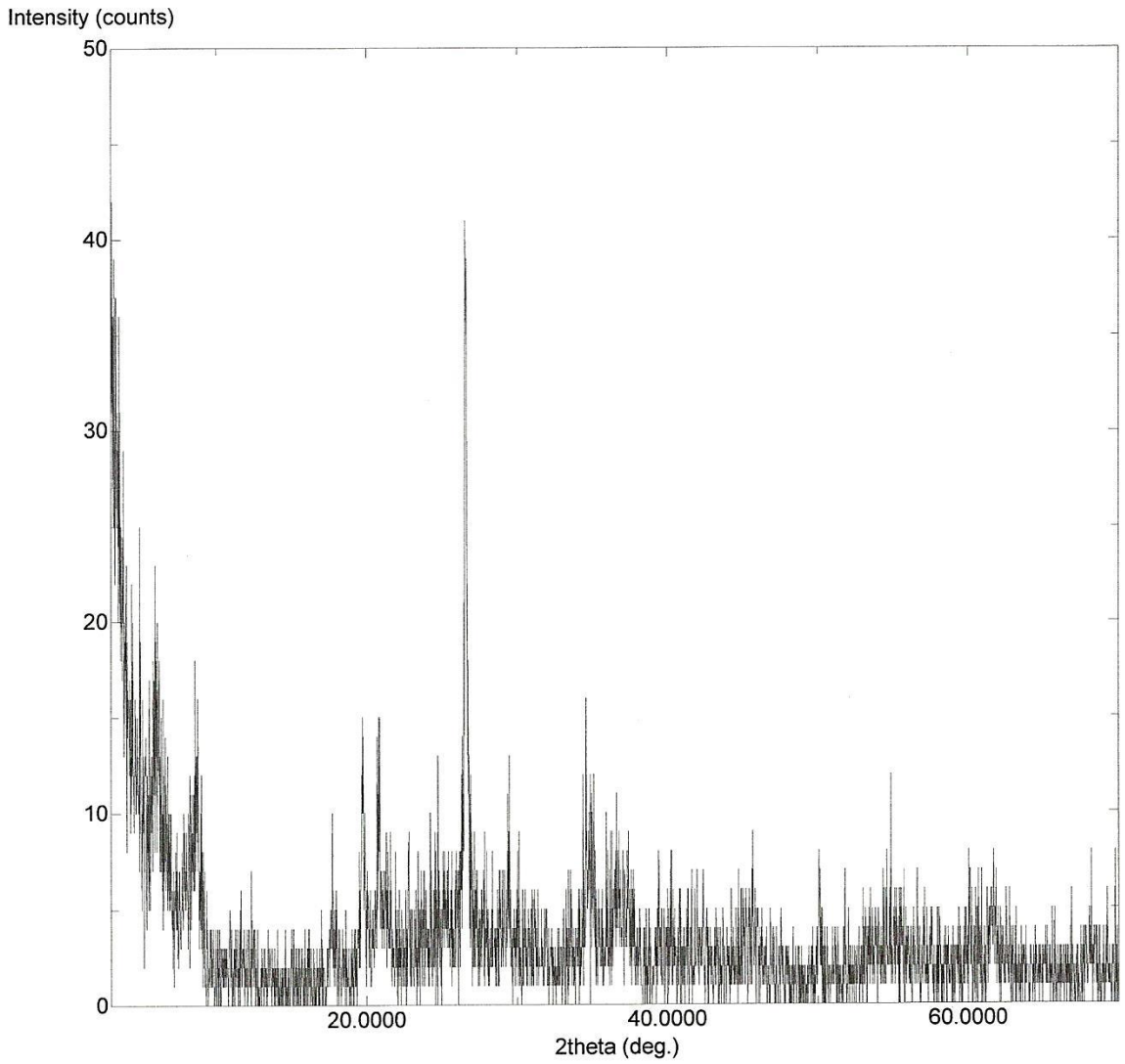

Figure A.24 S-B 1-1

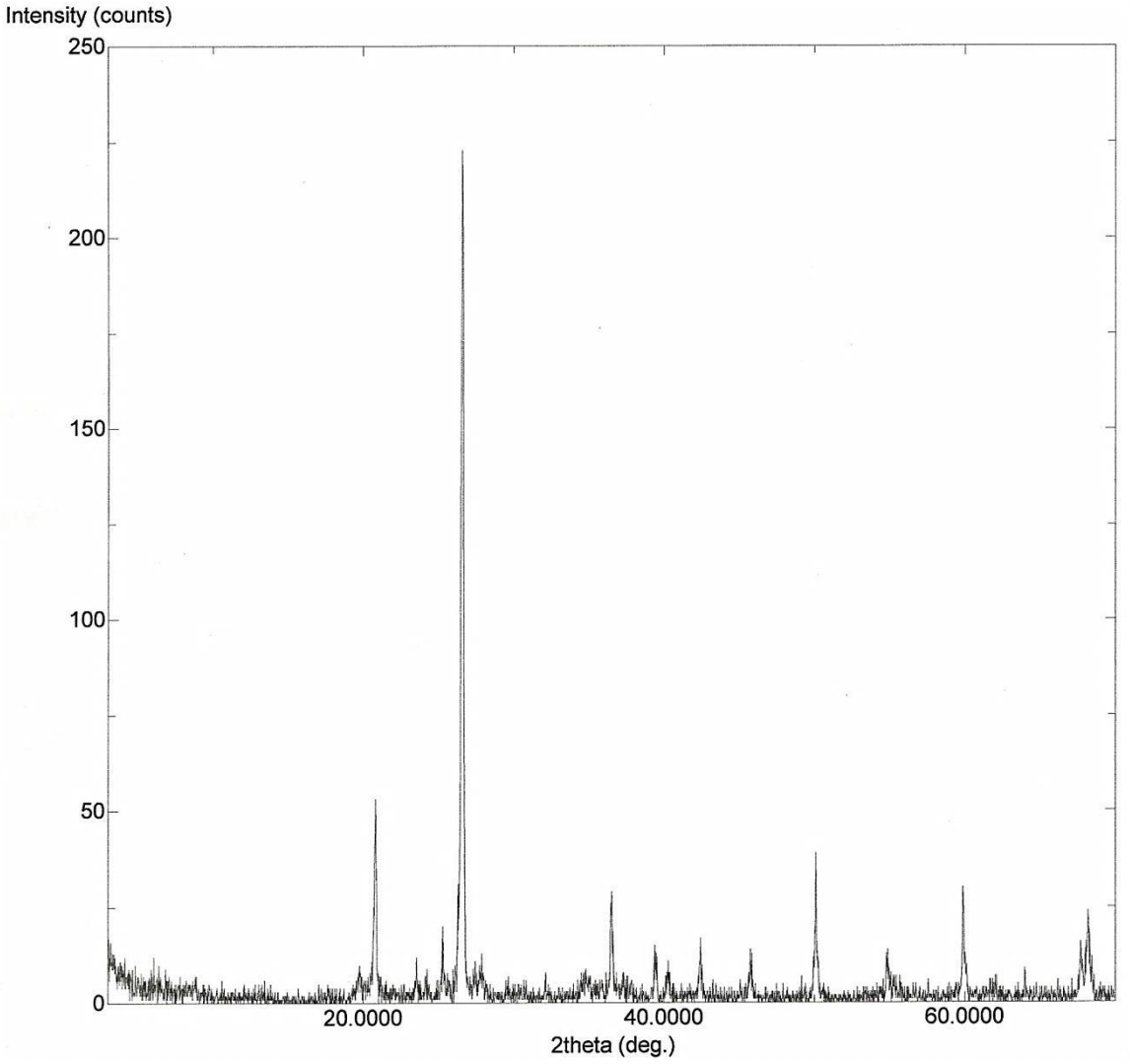

Figure A.25 S-B 1-2

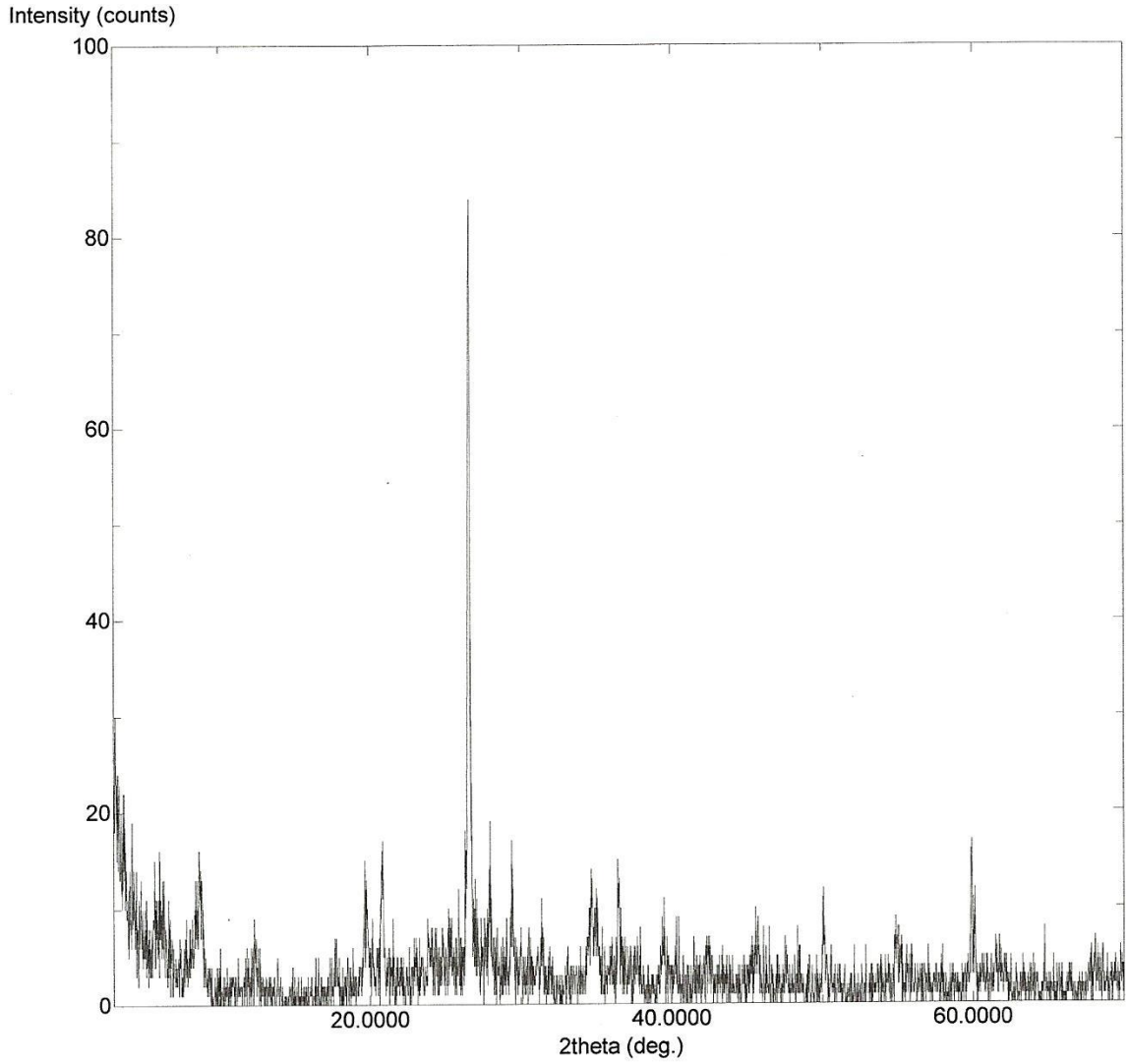

Figure A.26 S-B 1-3

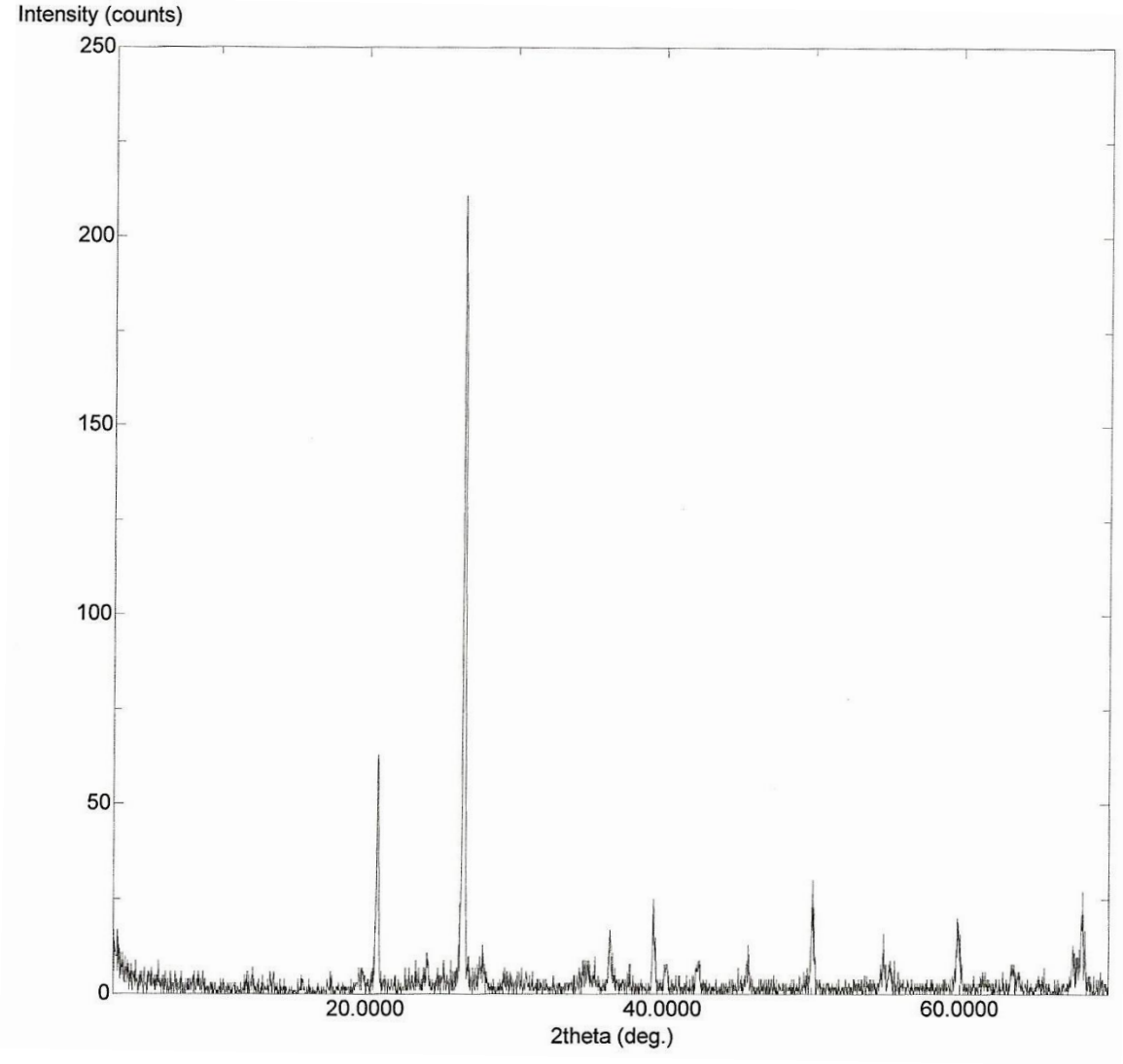

Figure A.27 B-C 1-1

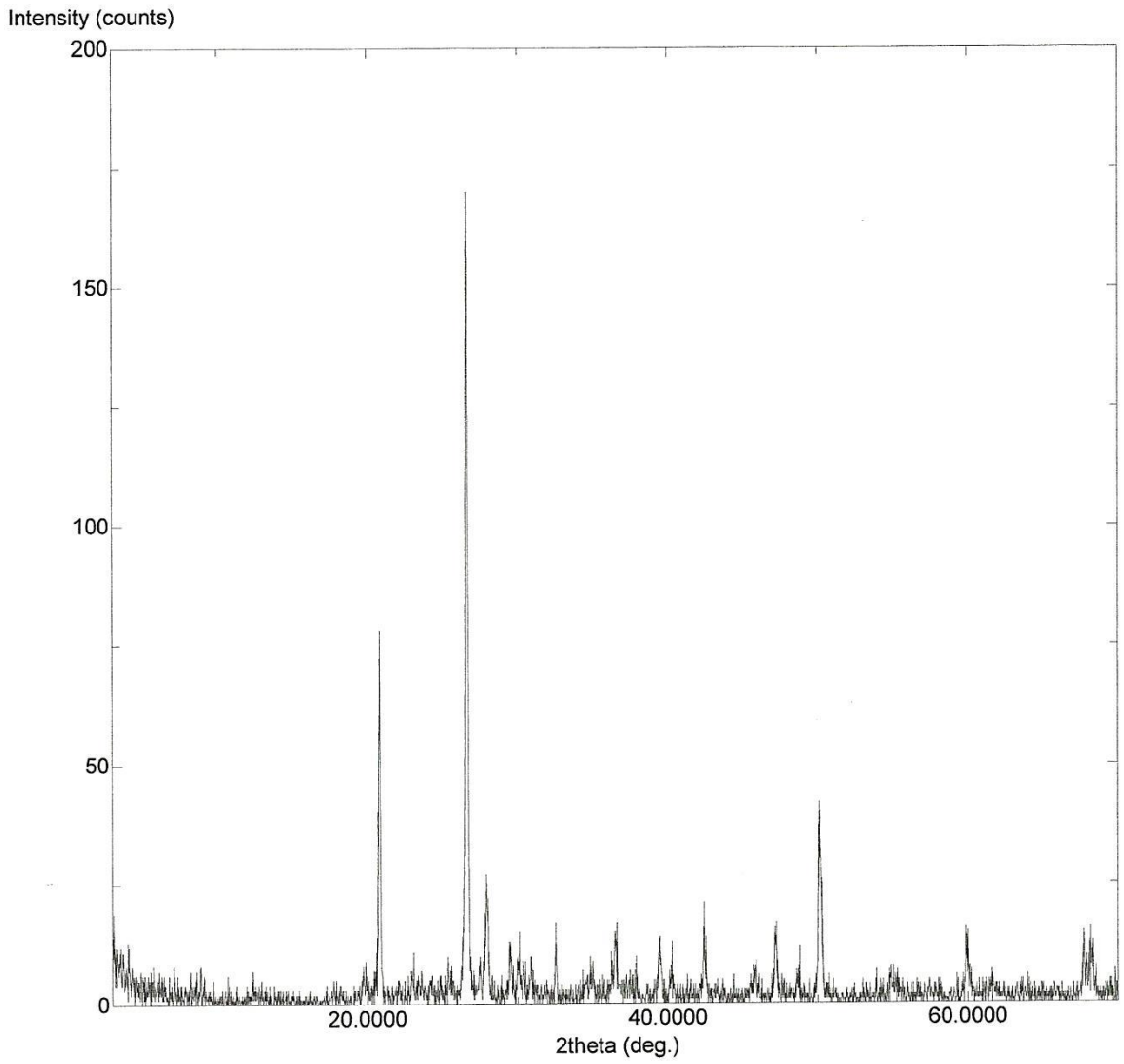

Figure A.28 B-C 1-2

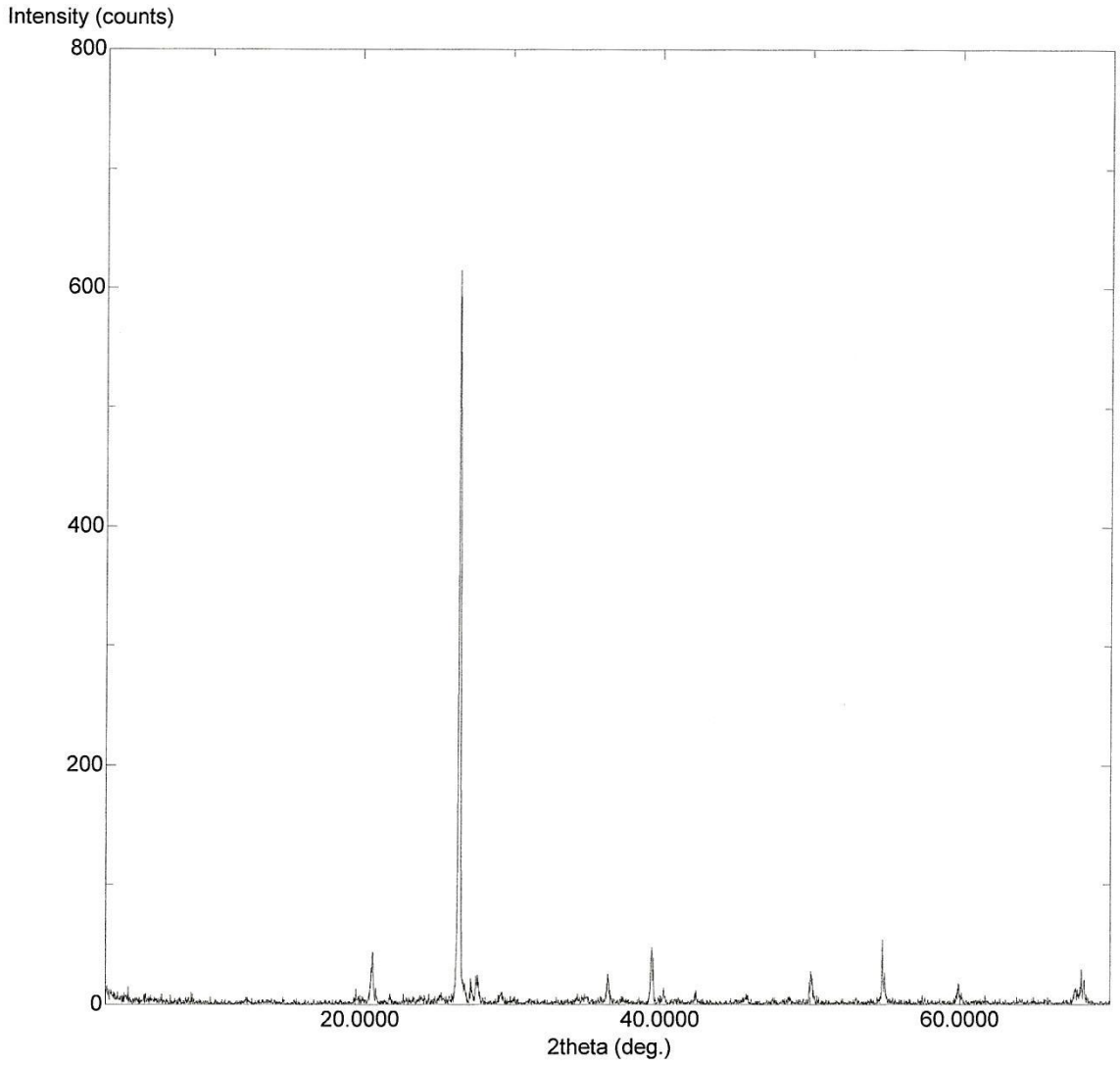

Figure A.29 B-C 1-3

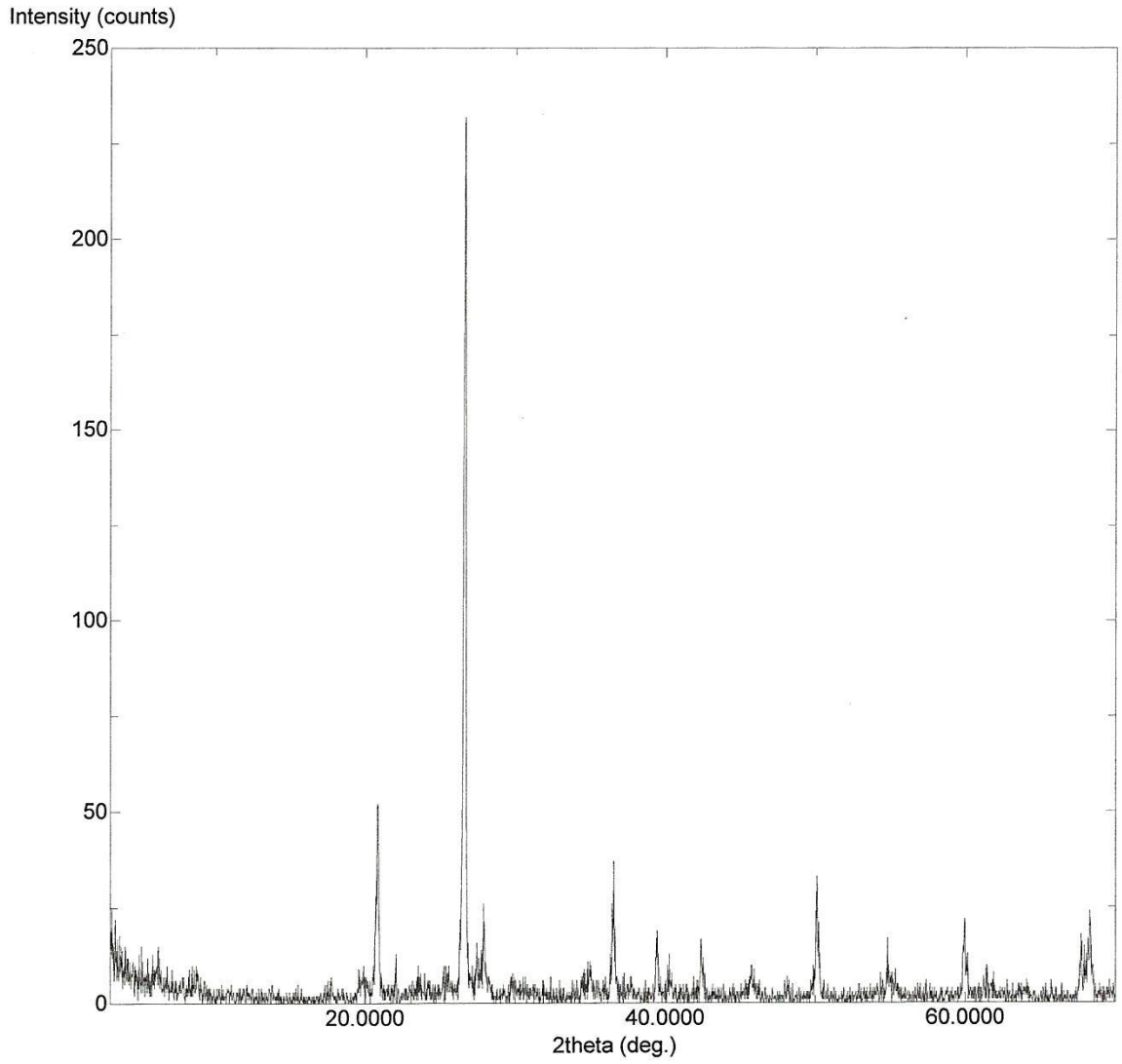

Figure A.30 B-C 1-4

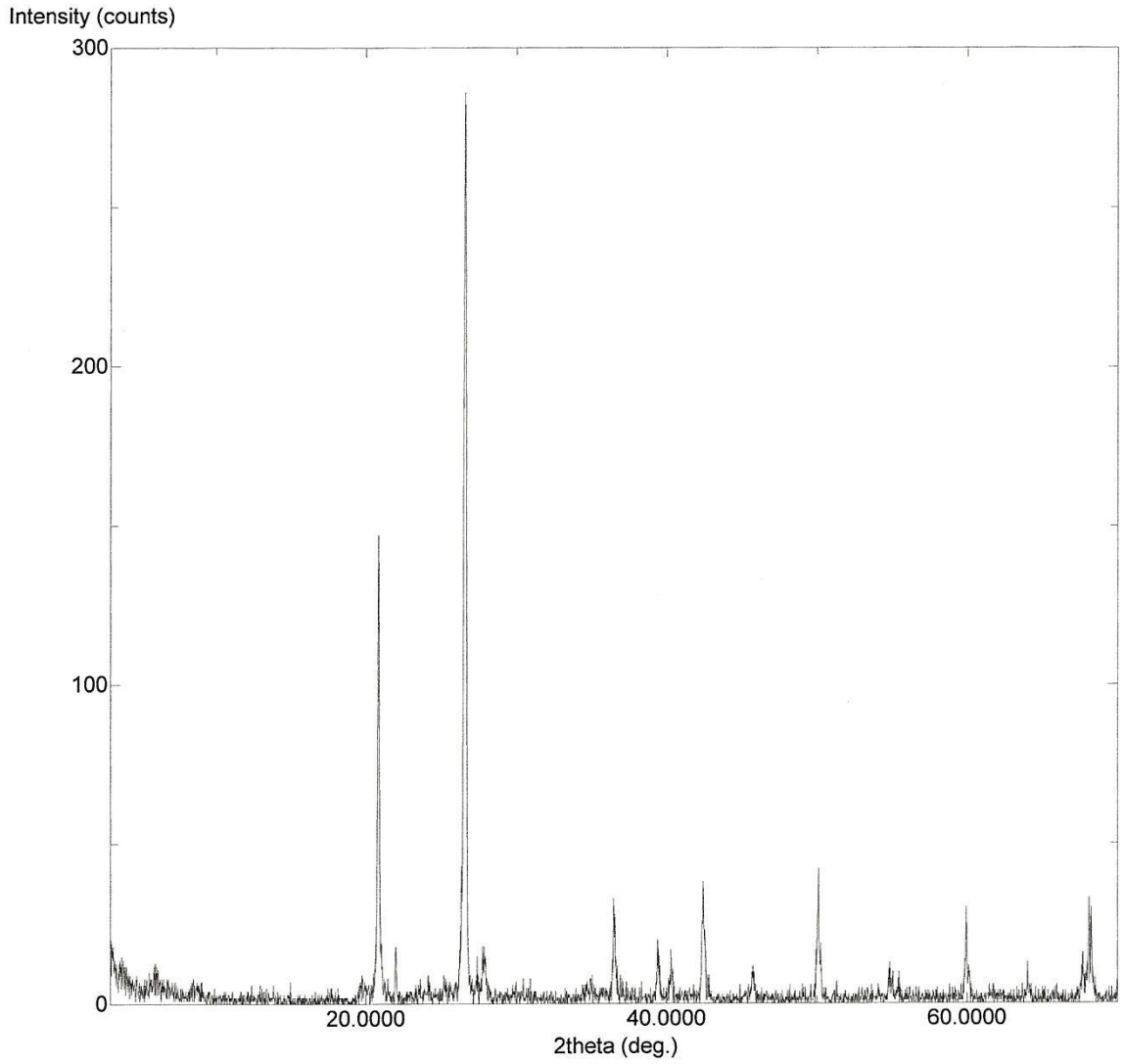

Figure A.31 B-C 1-5

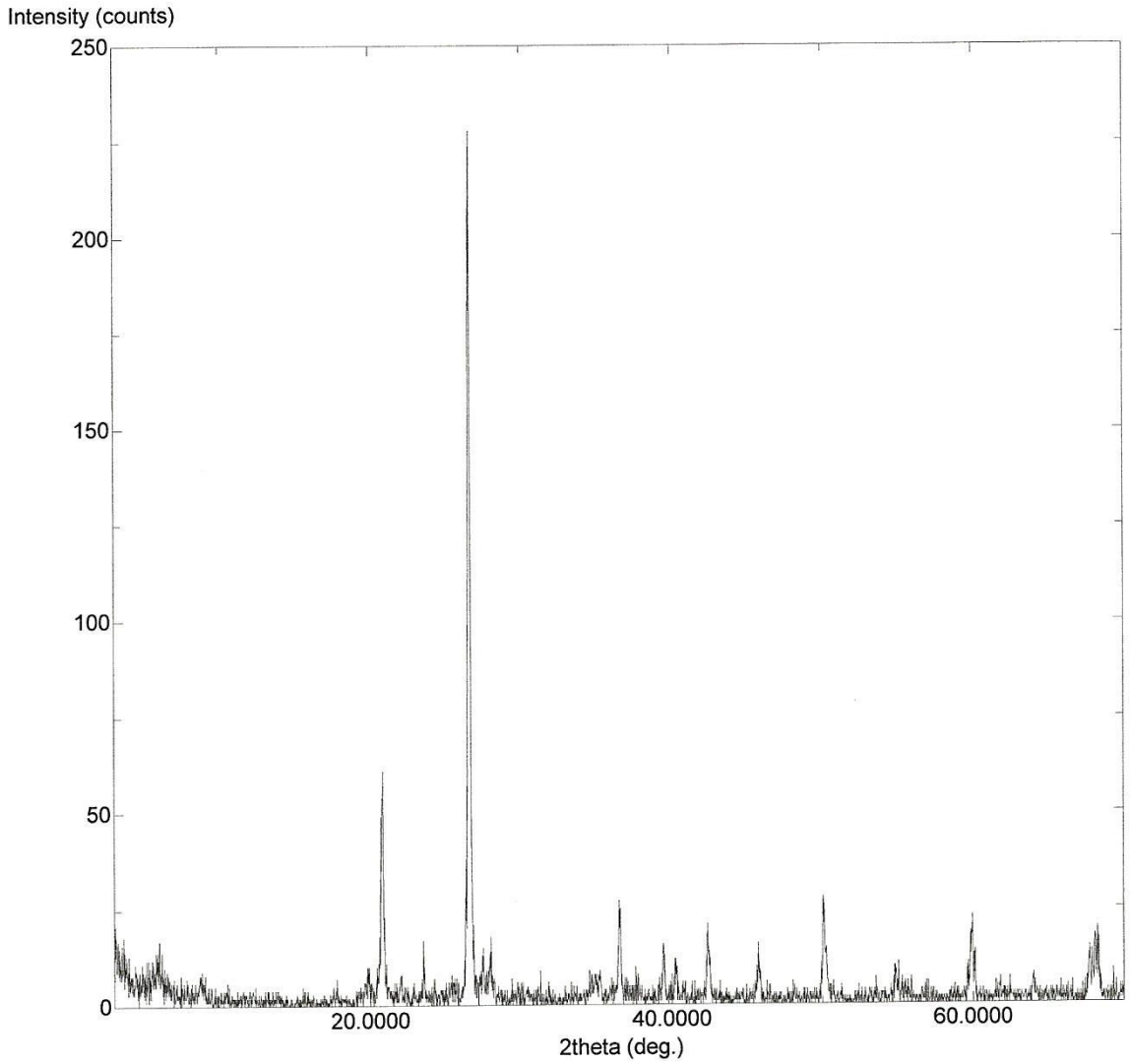

Figure A.32 B-C 1-6

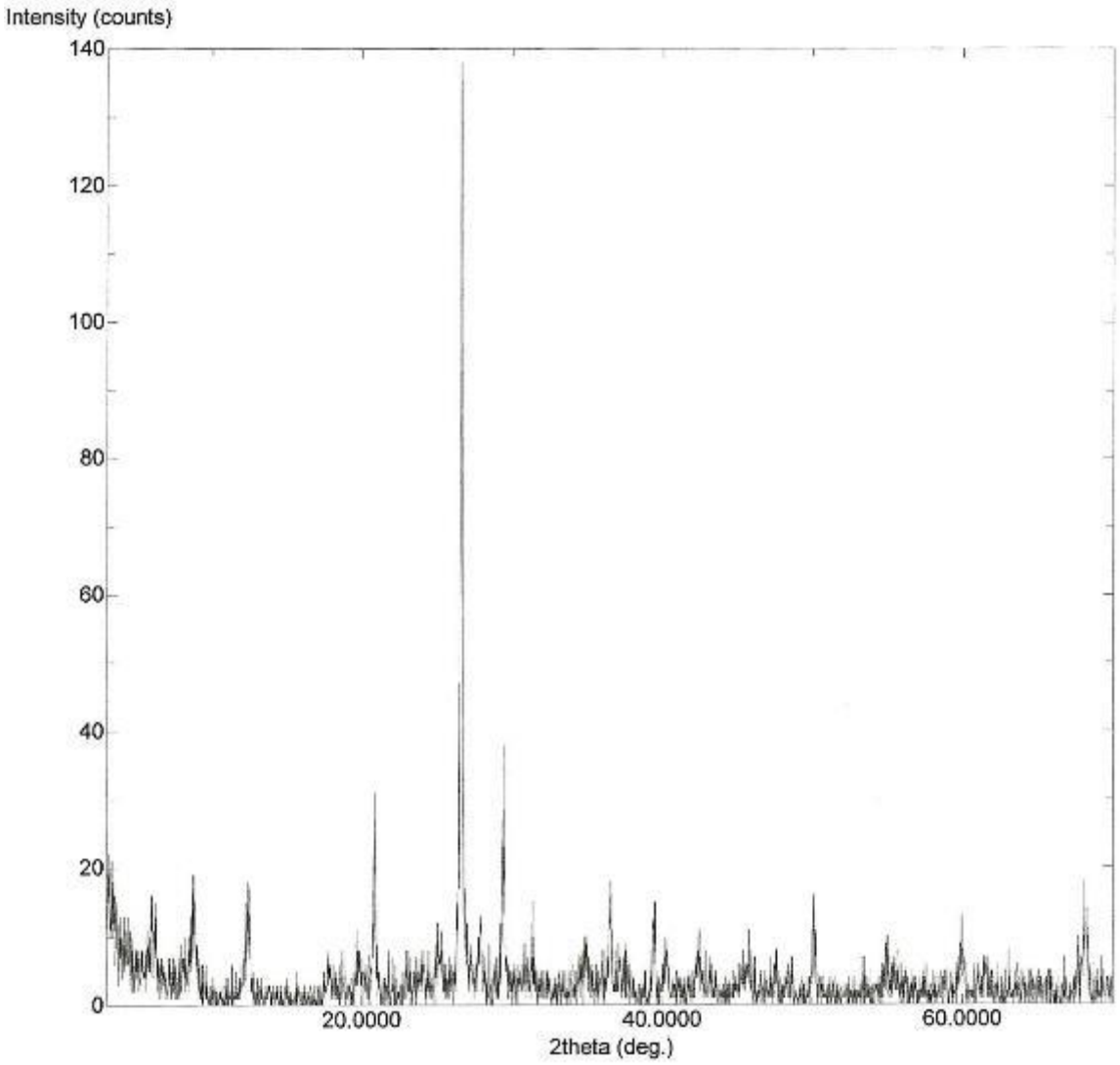

Figure A.33 Sch-C 1-1

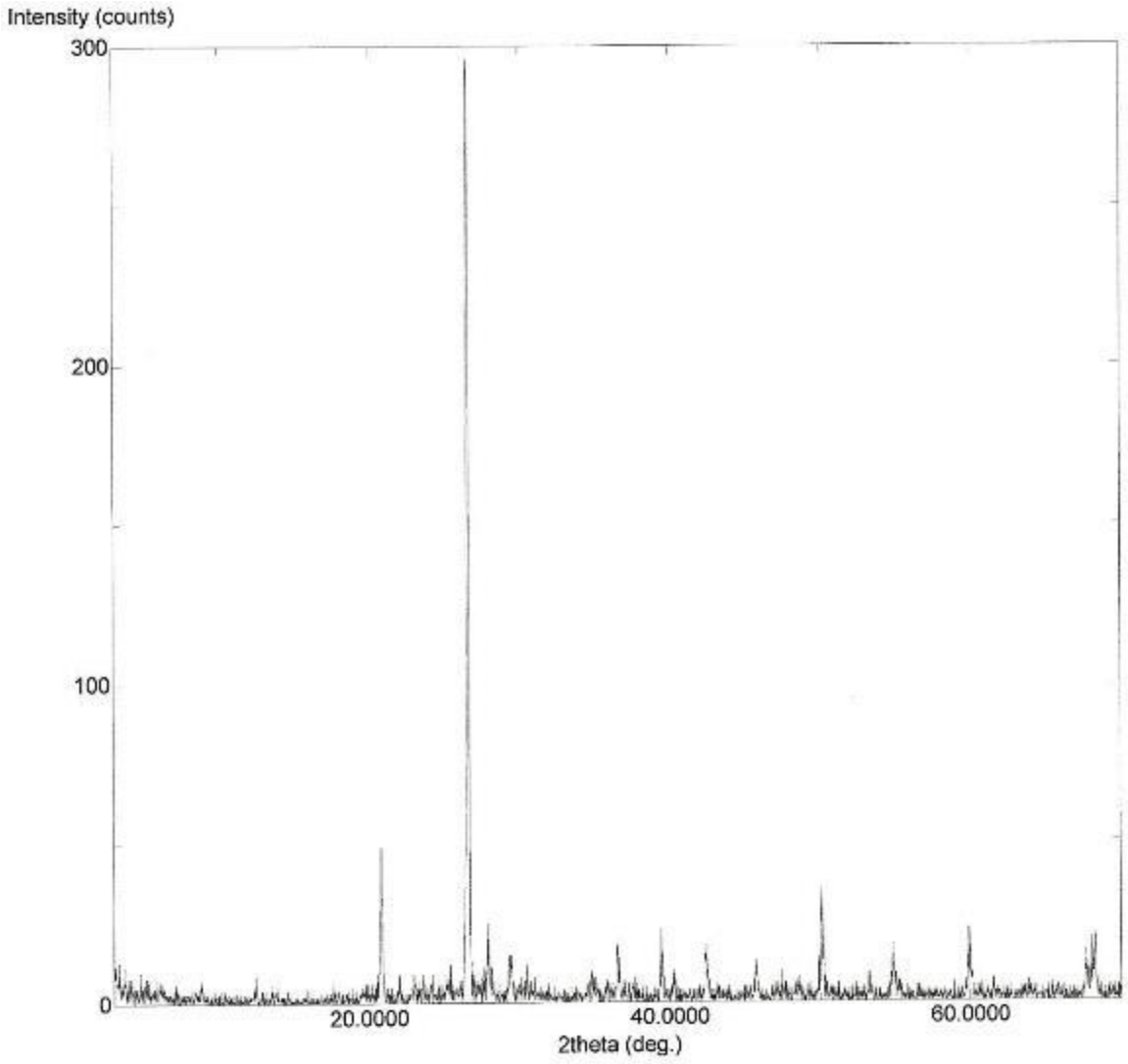

Figure A.34 Sch-C 1-2

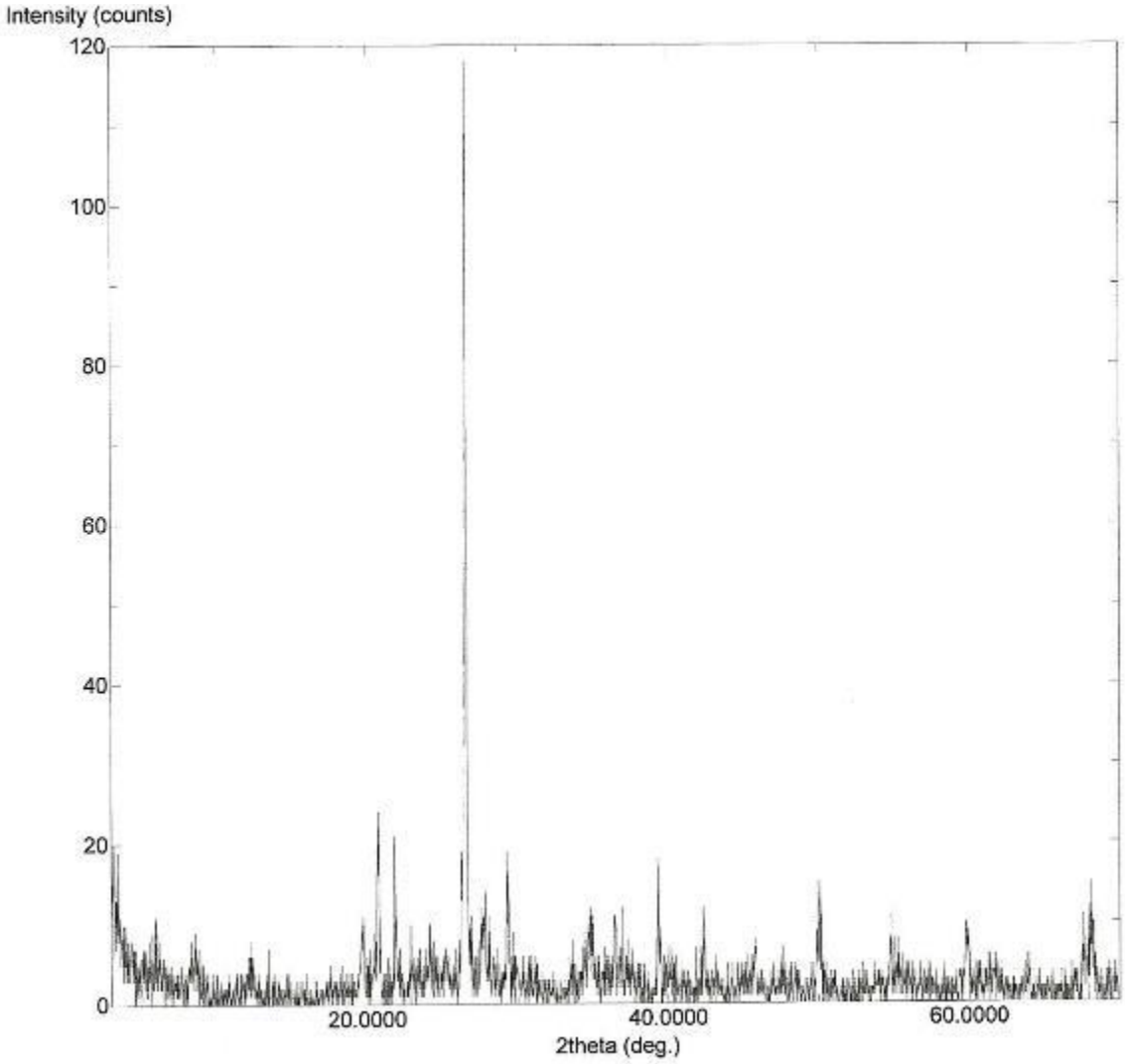

Figure A.35 Sch-C 1-3

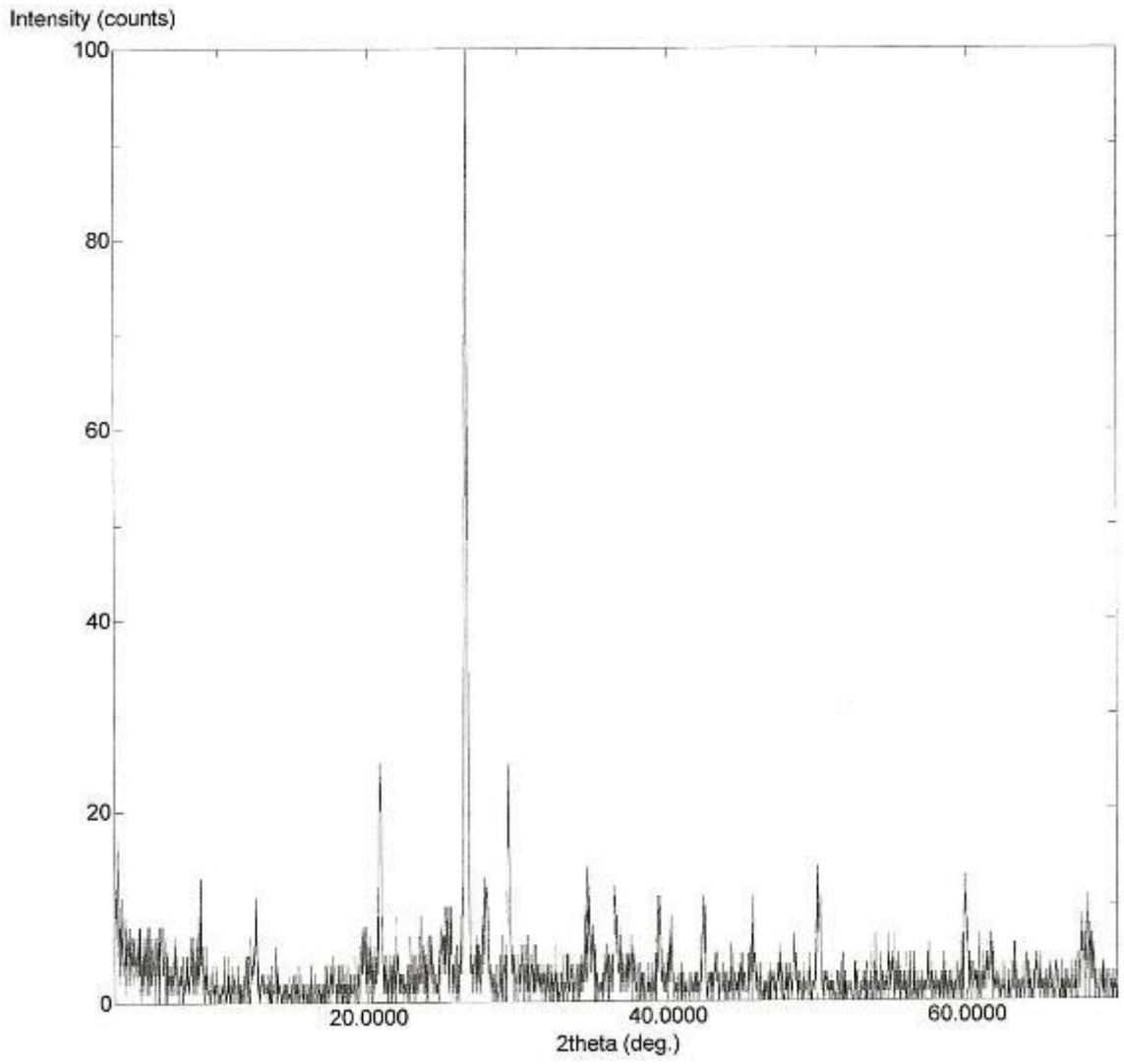

Figure A.36 Sch-C 1-4

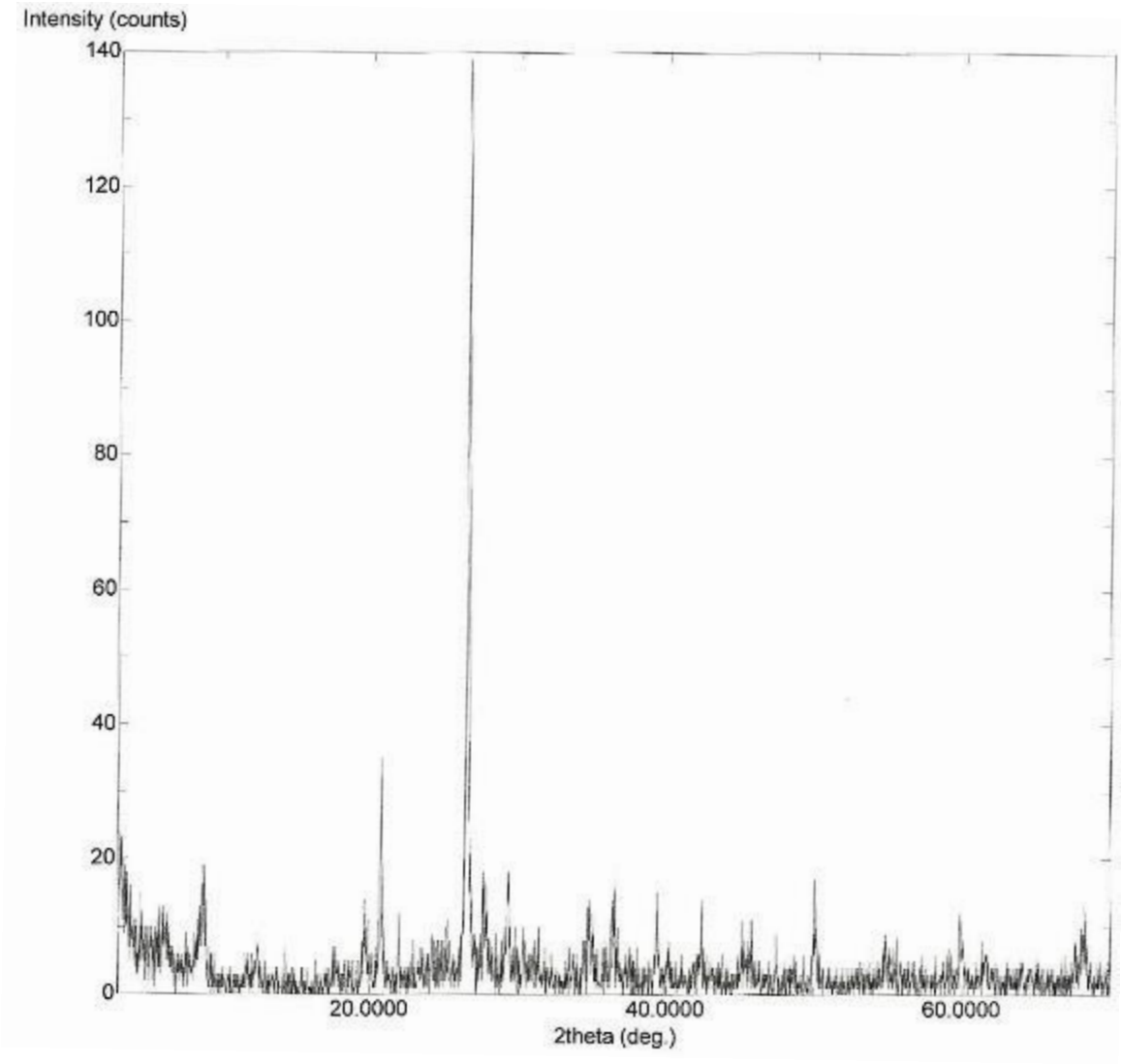

Figure A.37 Sch-C 2-1

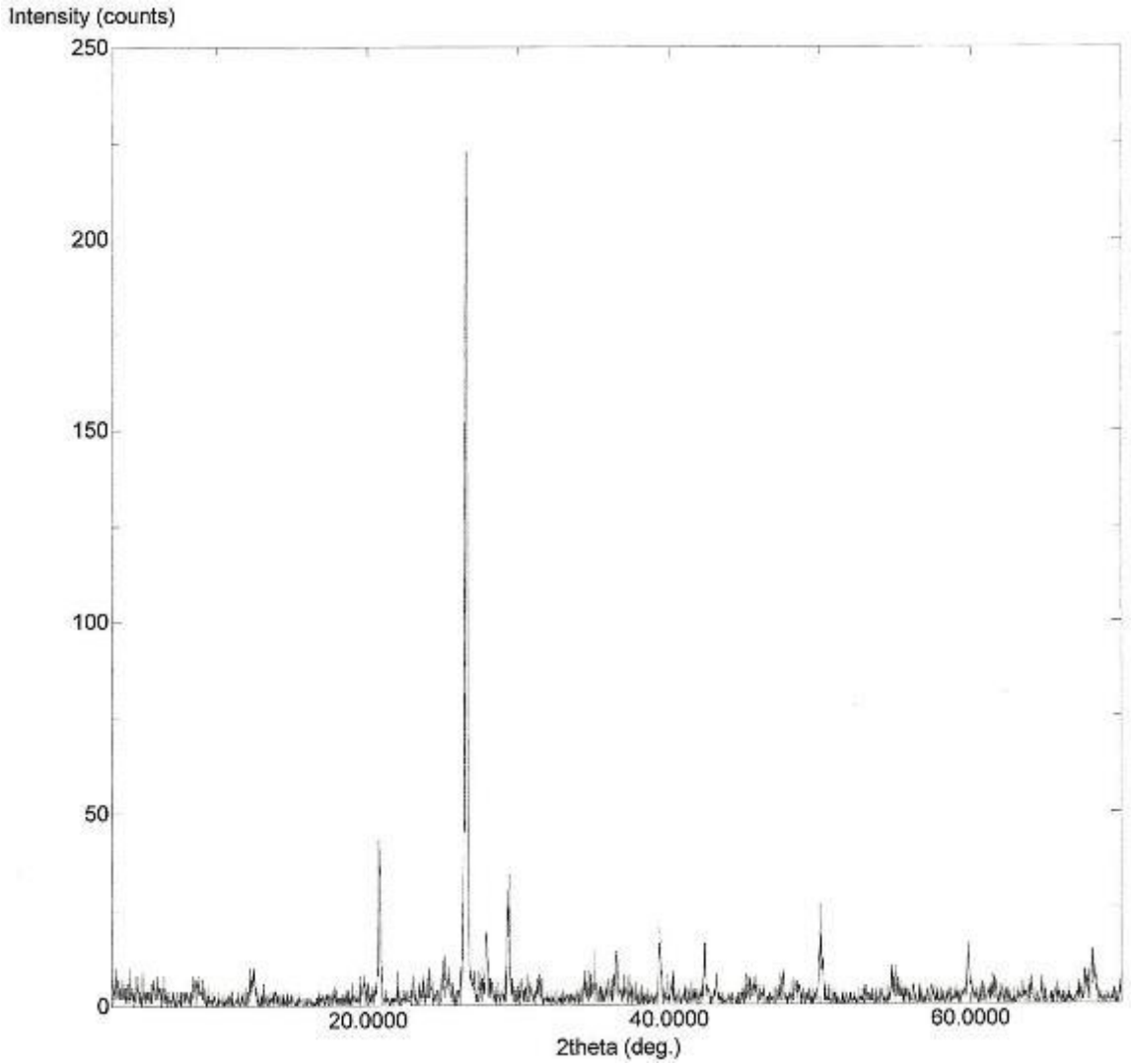

Figure A.38 Sch-C 3-1

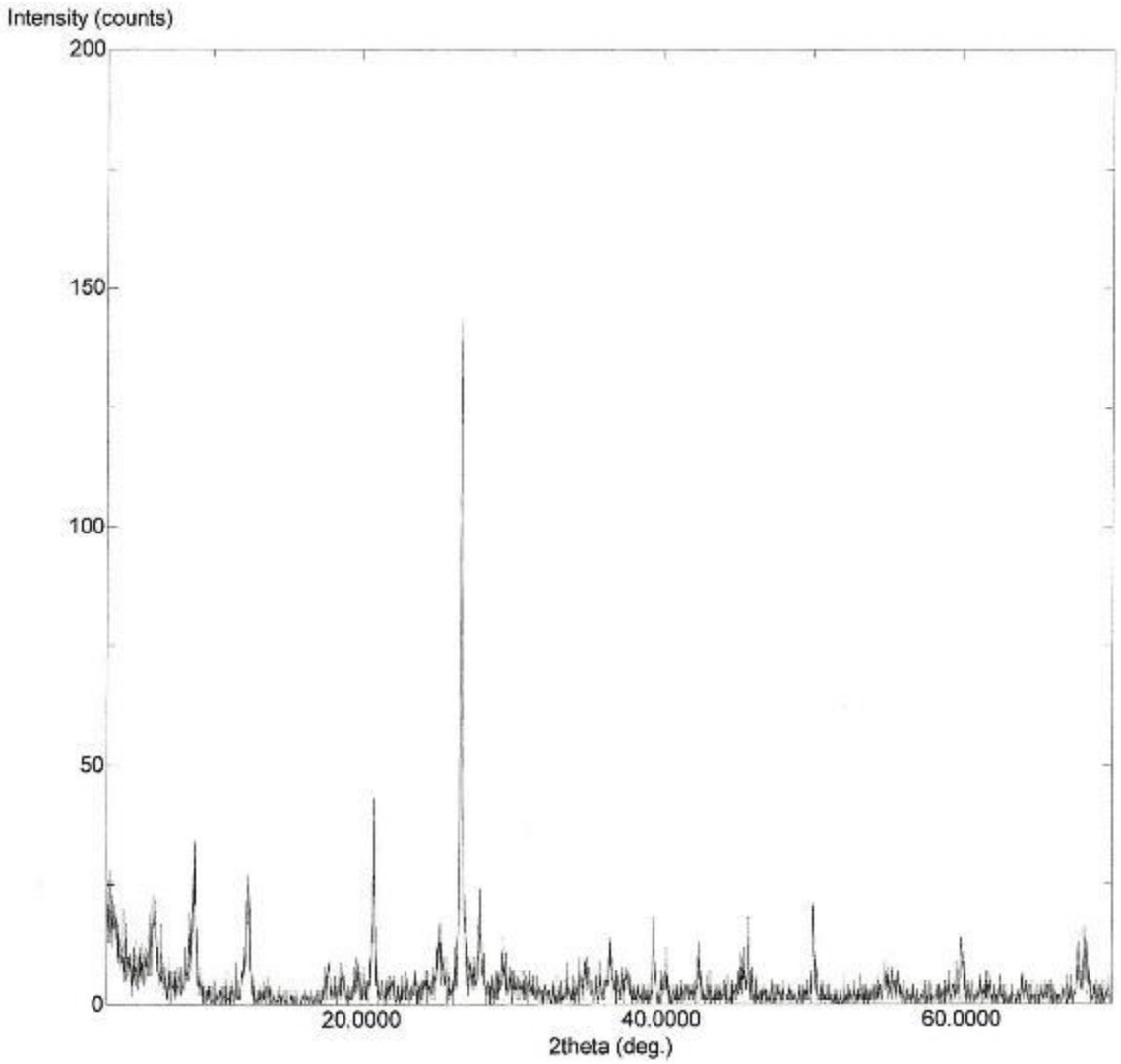

Figure A.39 G-C 1-1

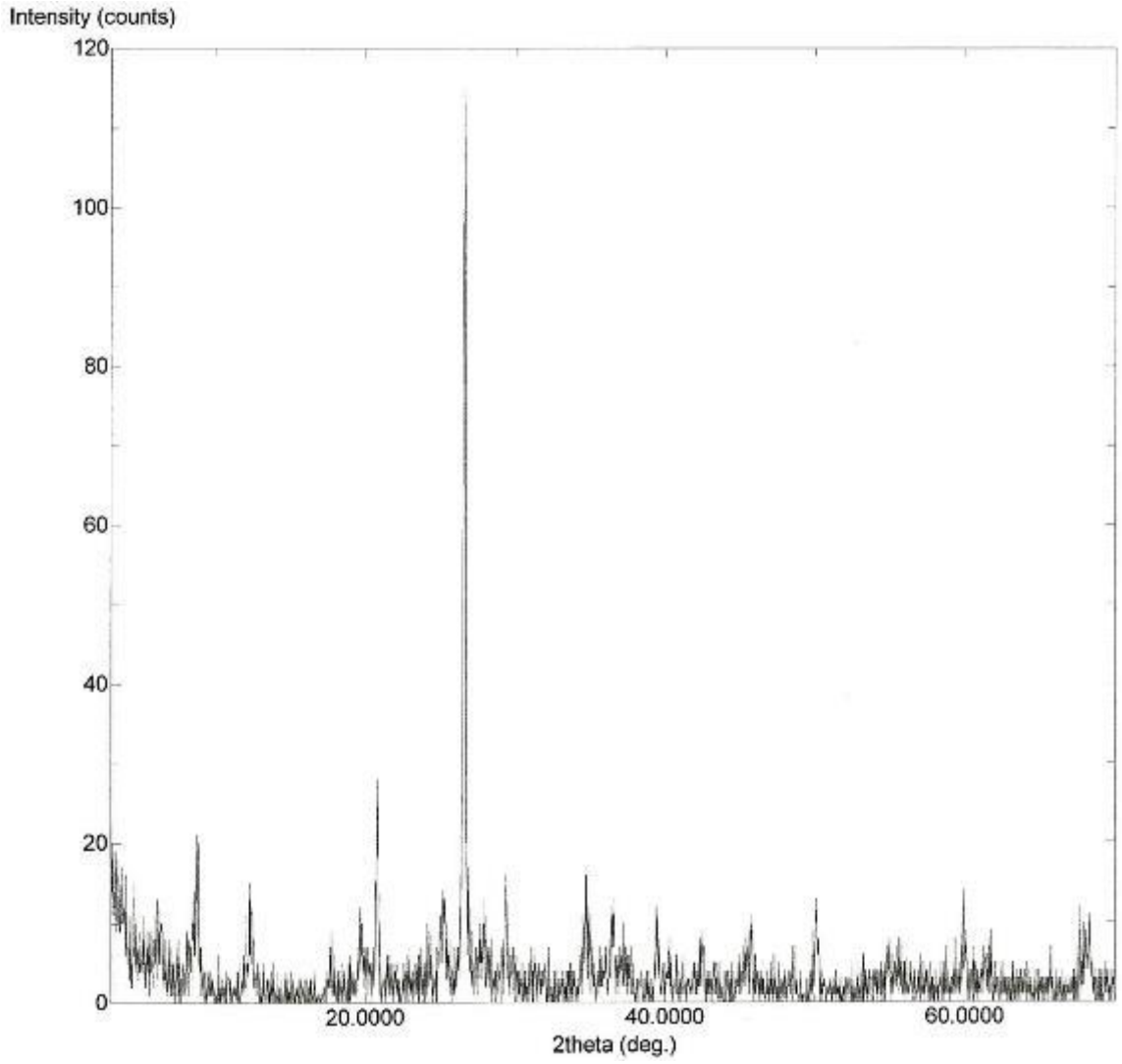

Figure A.40 G-C 1-2

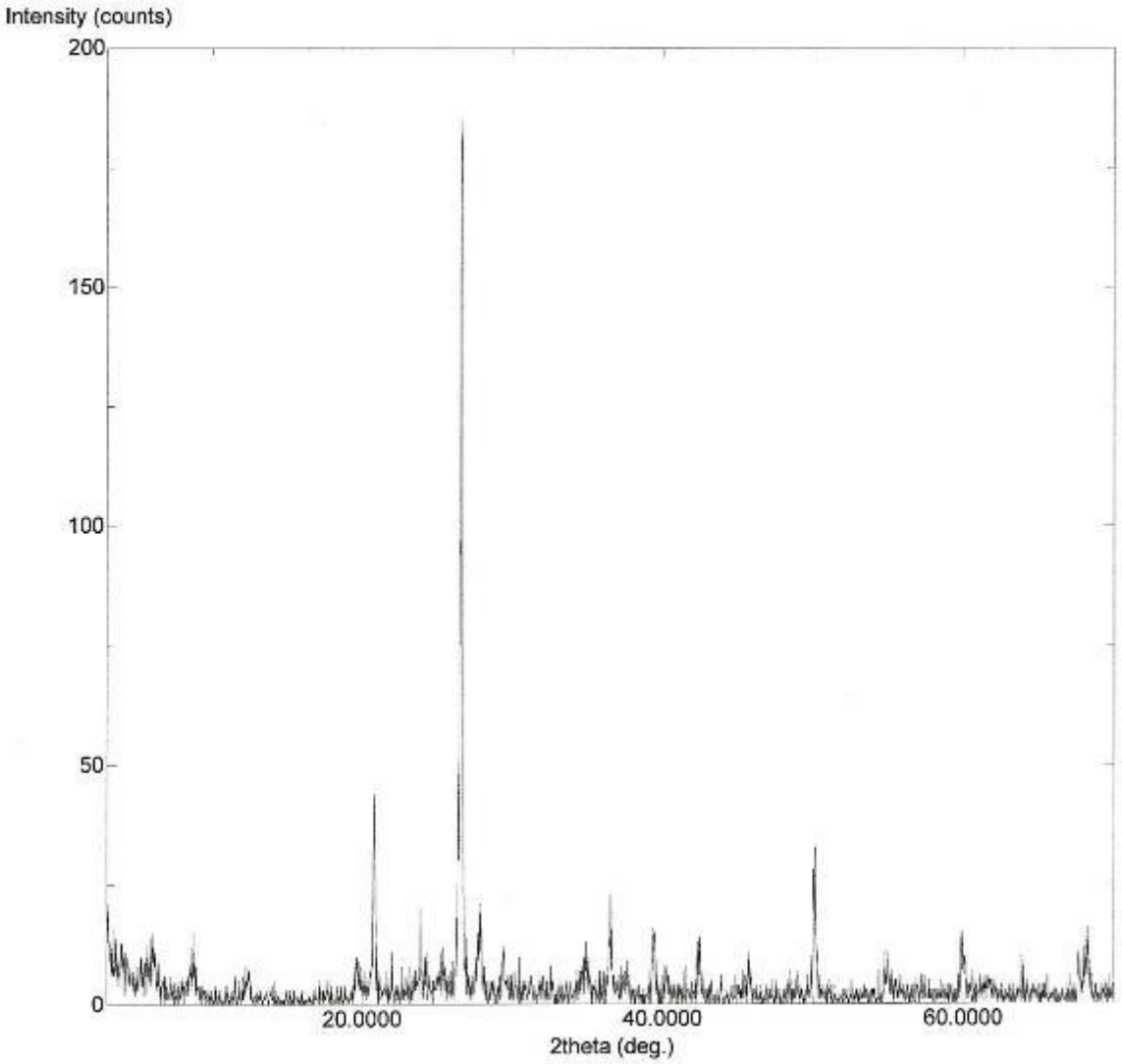

Figure A.41 G-C 1-3

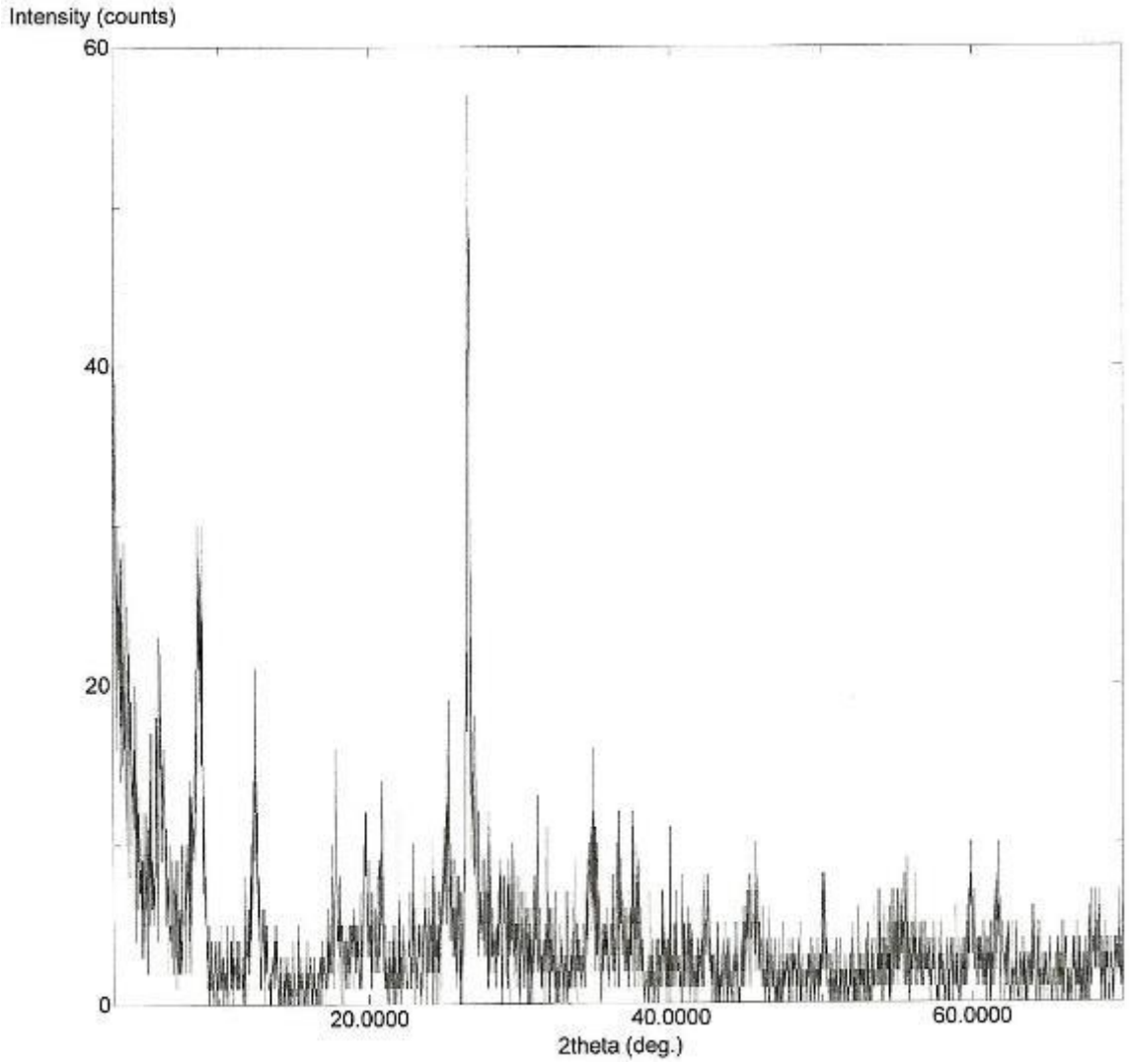

Figure A.42 G-C 2-1

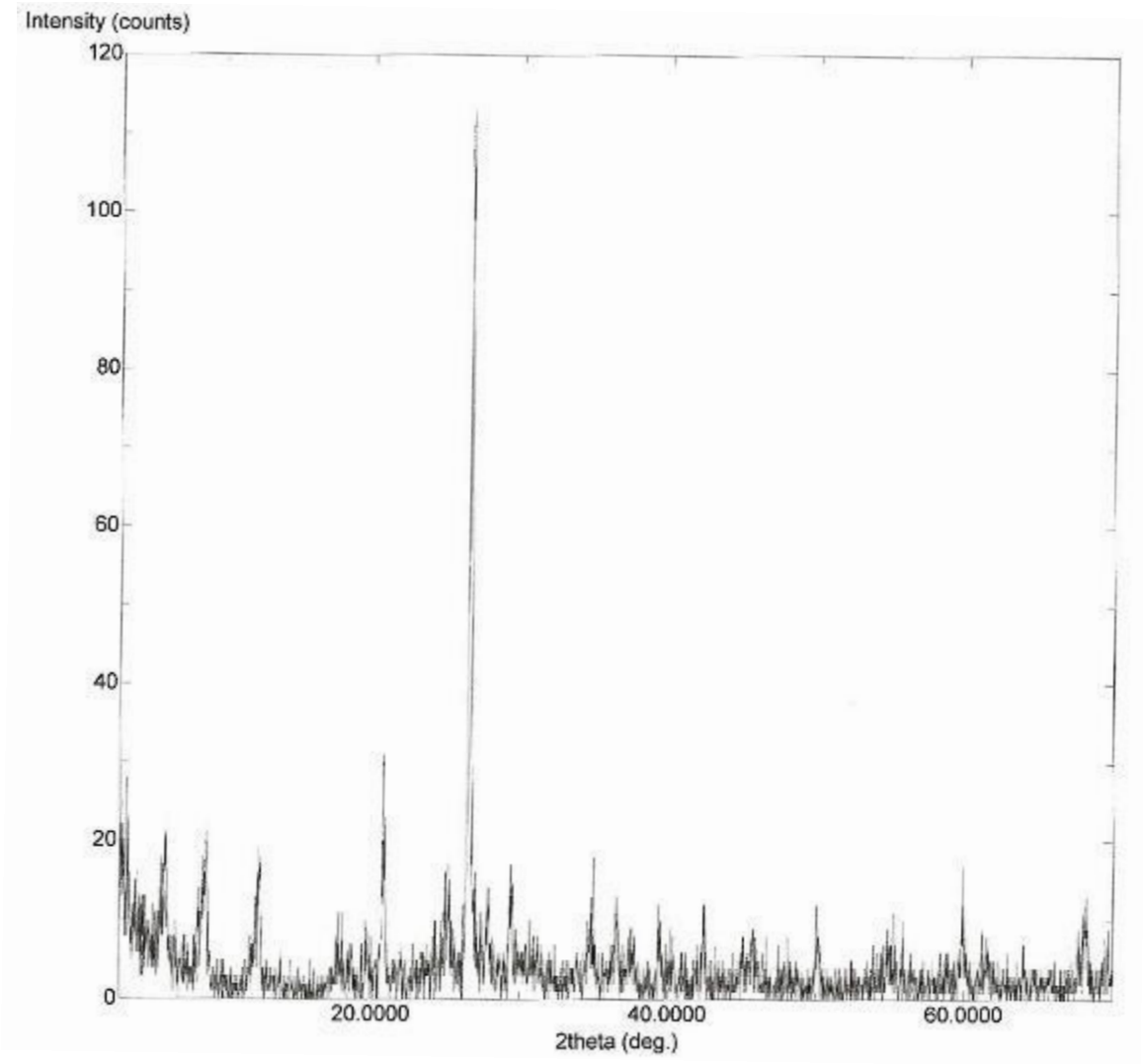

Figure A.43 G-C 2-2

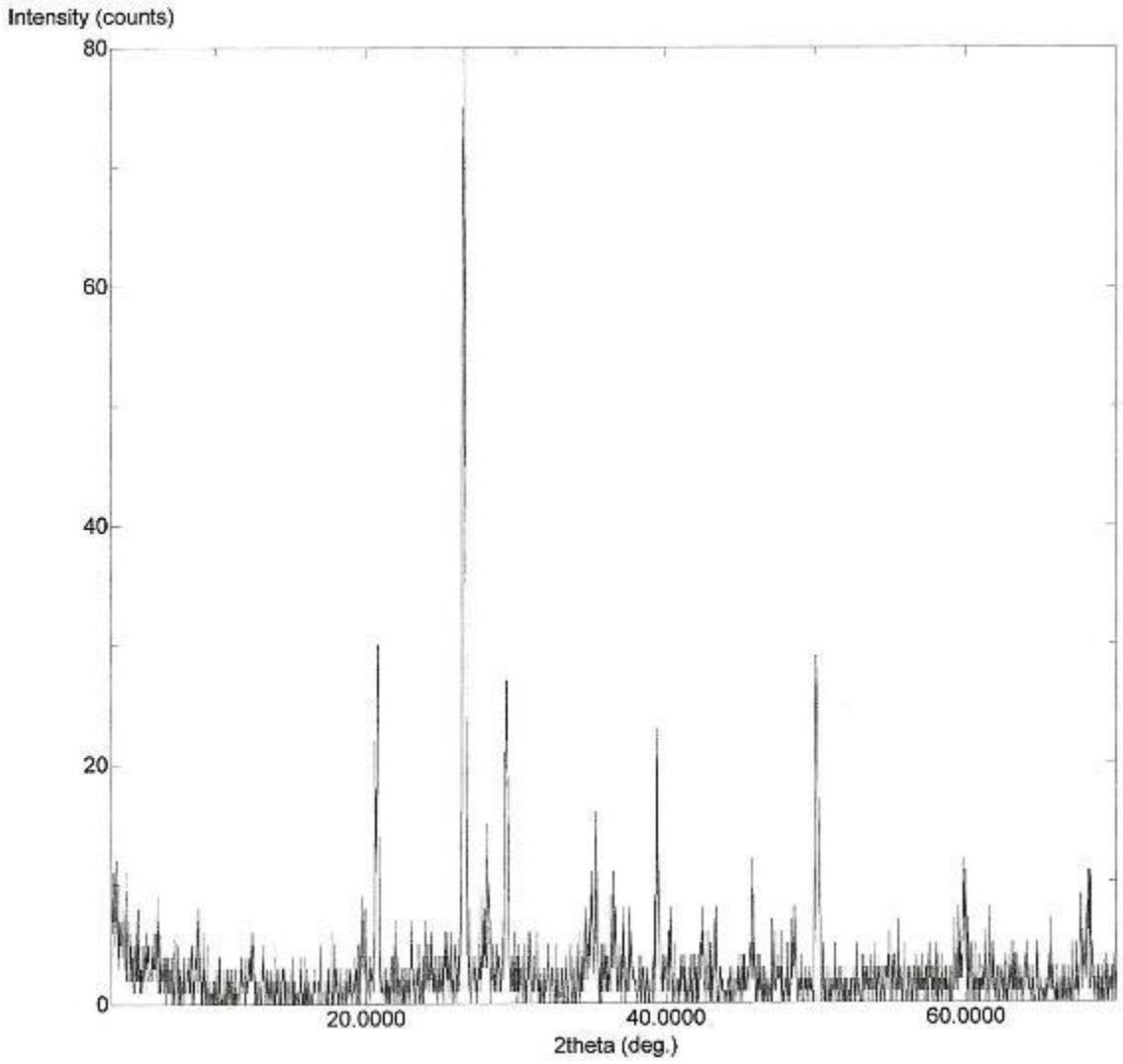

Figure A.44 G-C 2-3

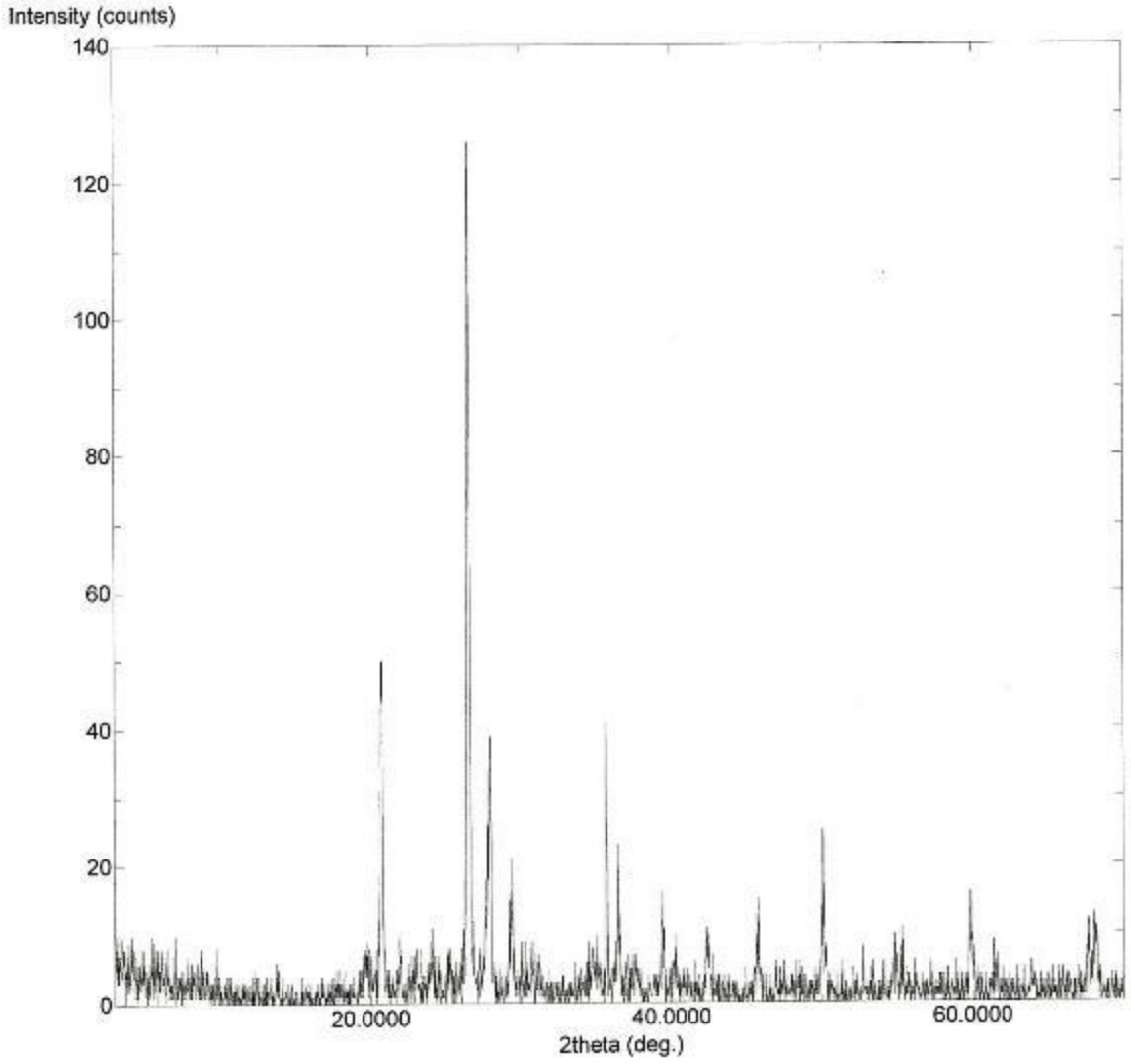

Figure A.45 G-C 2-4

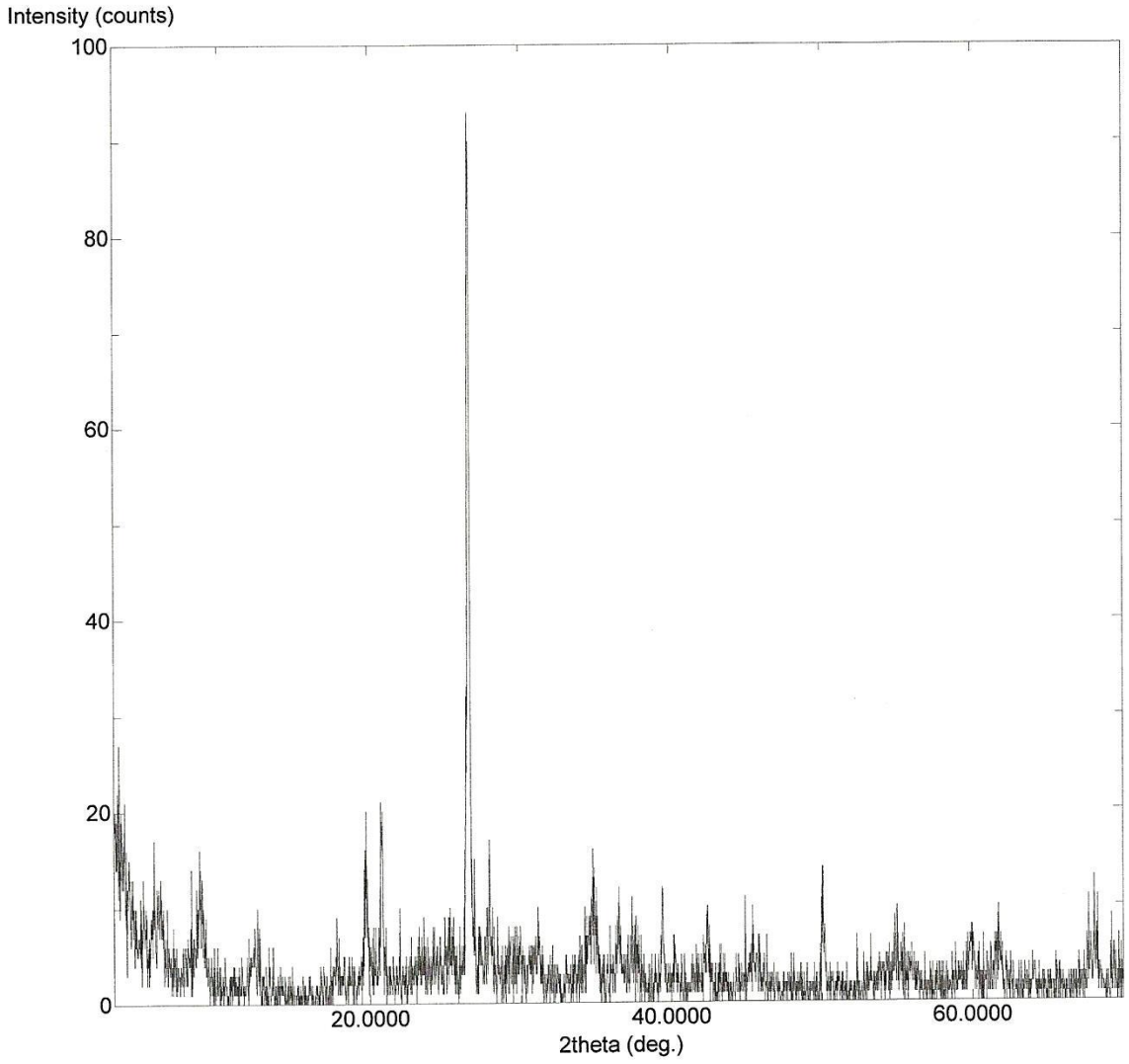

Figure A.46 G-C 3-1

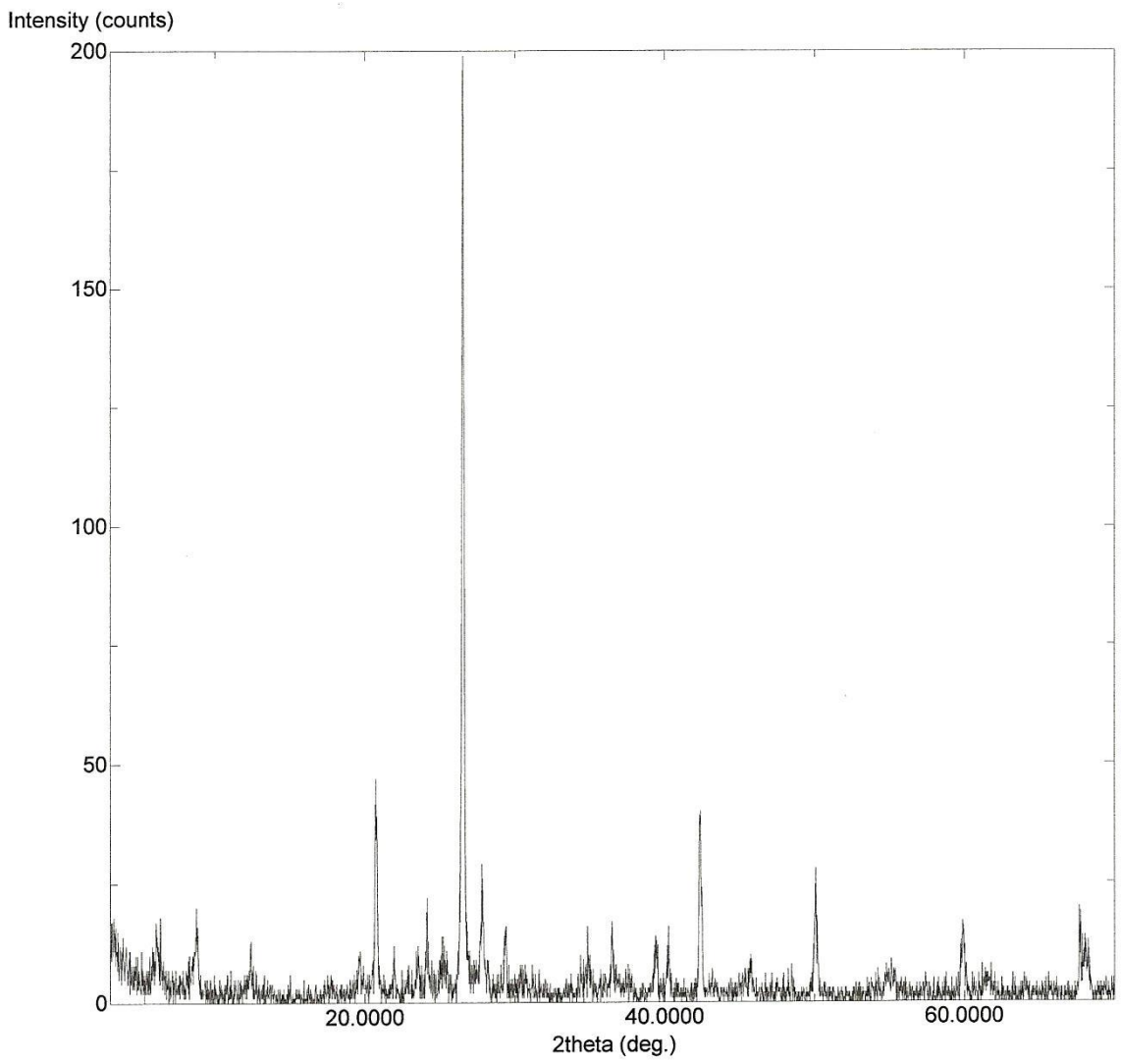

Figure A.47 G-C 3-2

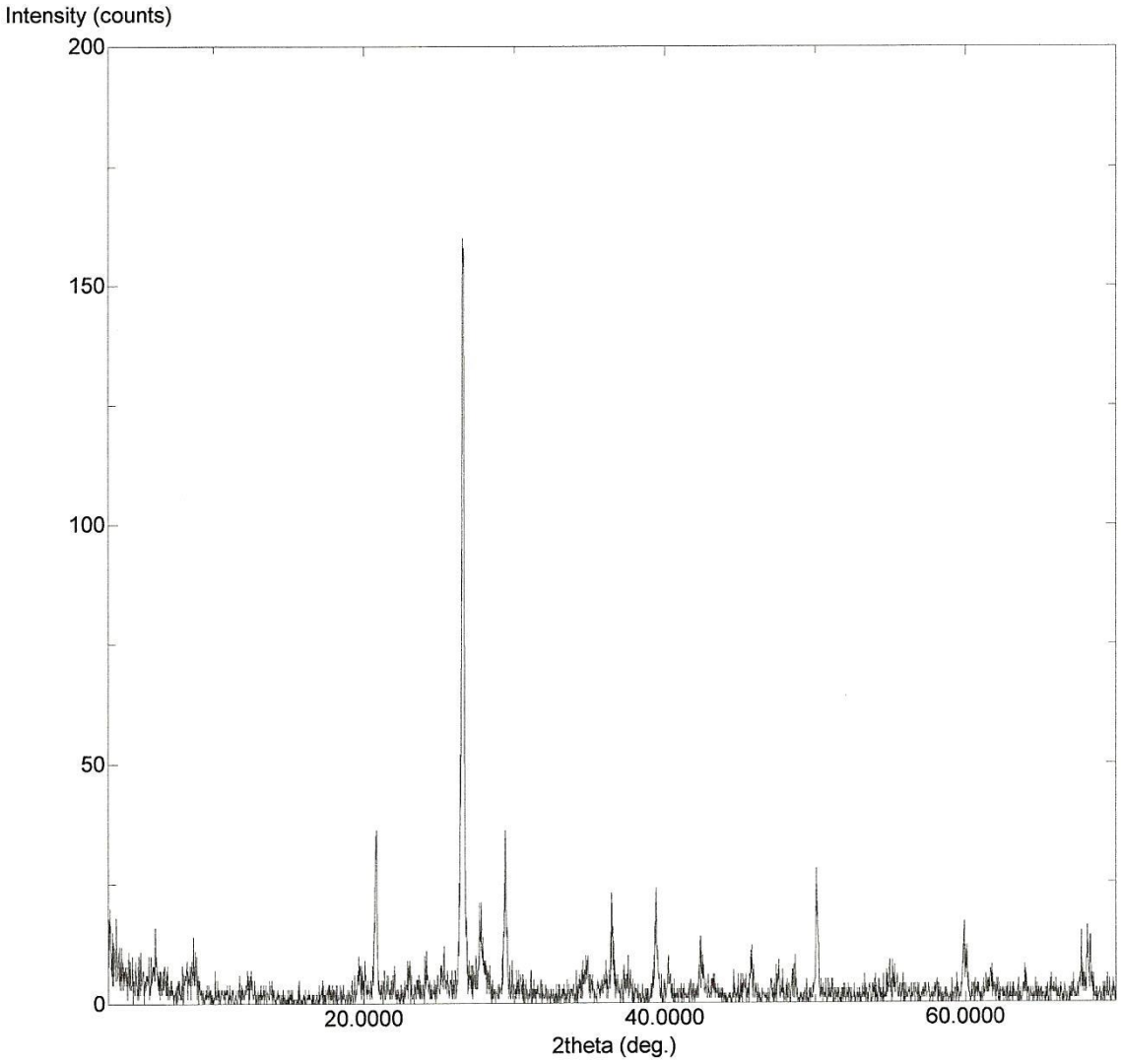

Figure A.48 C-B 1-1

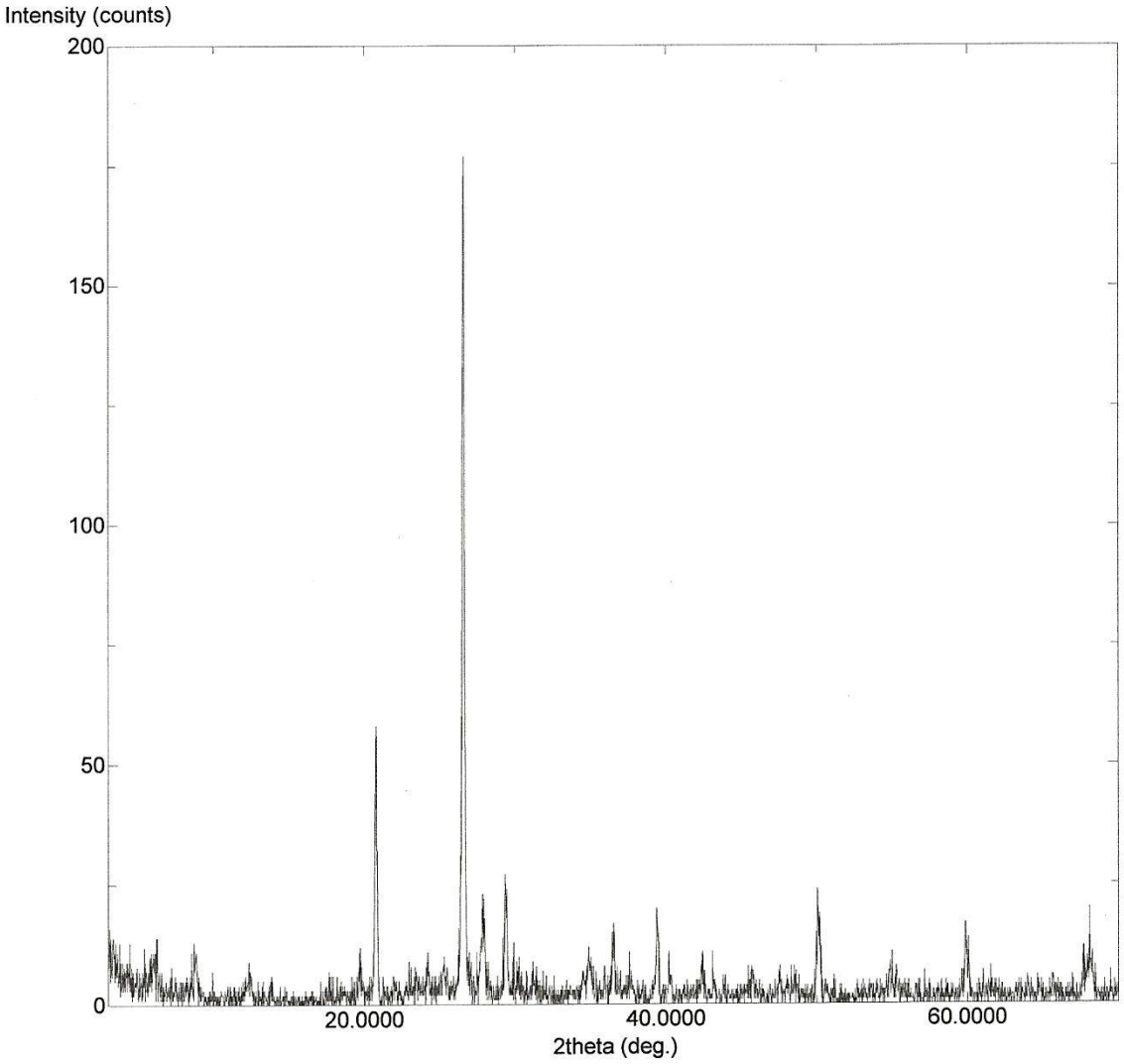

Figure A.49 C-B 1-2

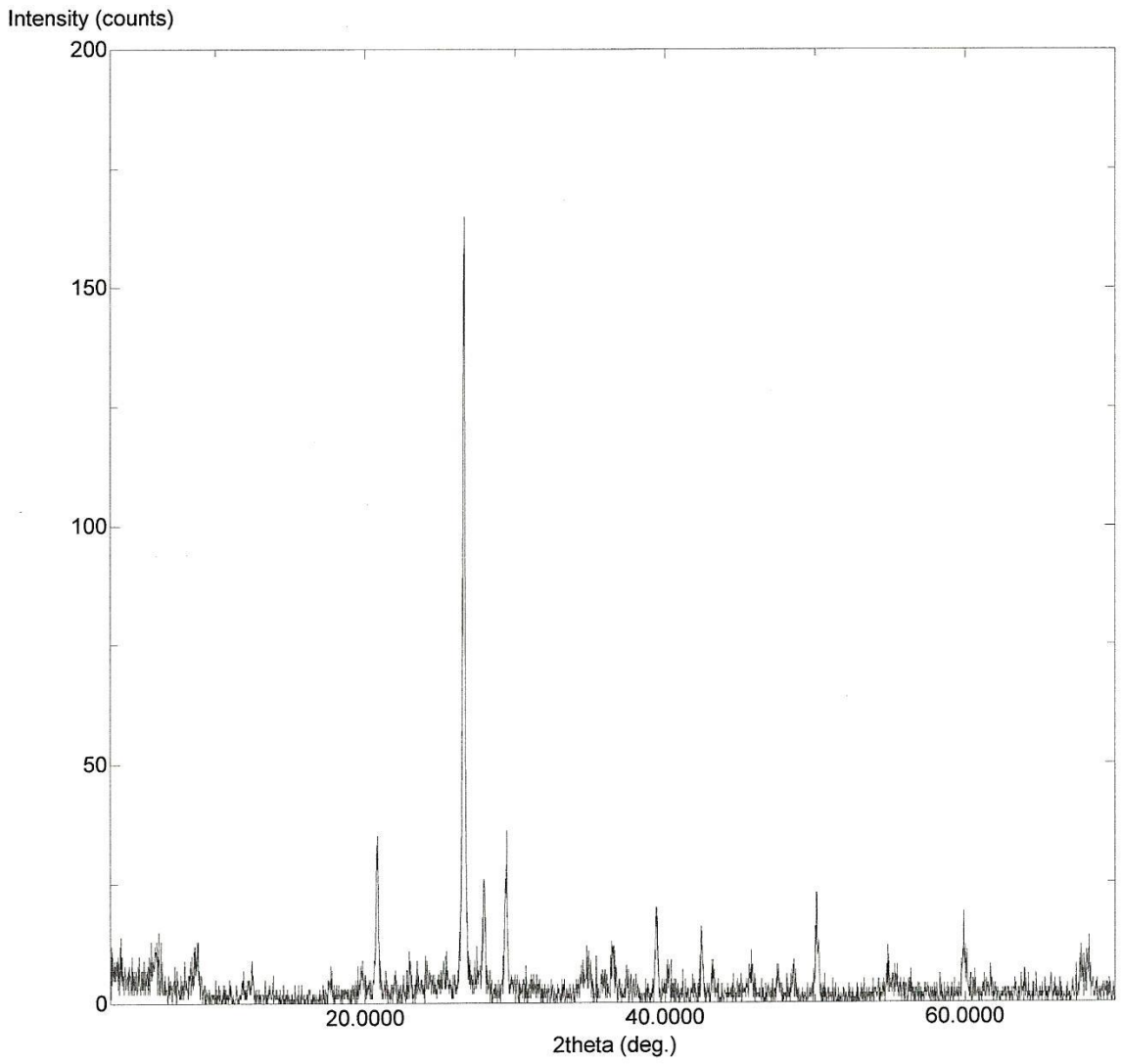

Figure A.50 C-B 1-3

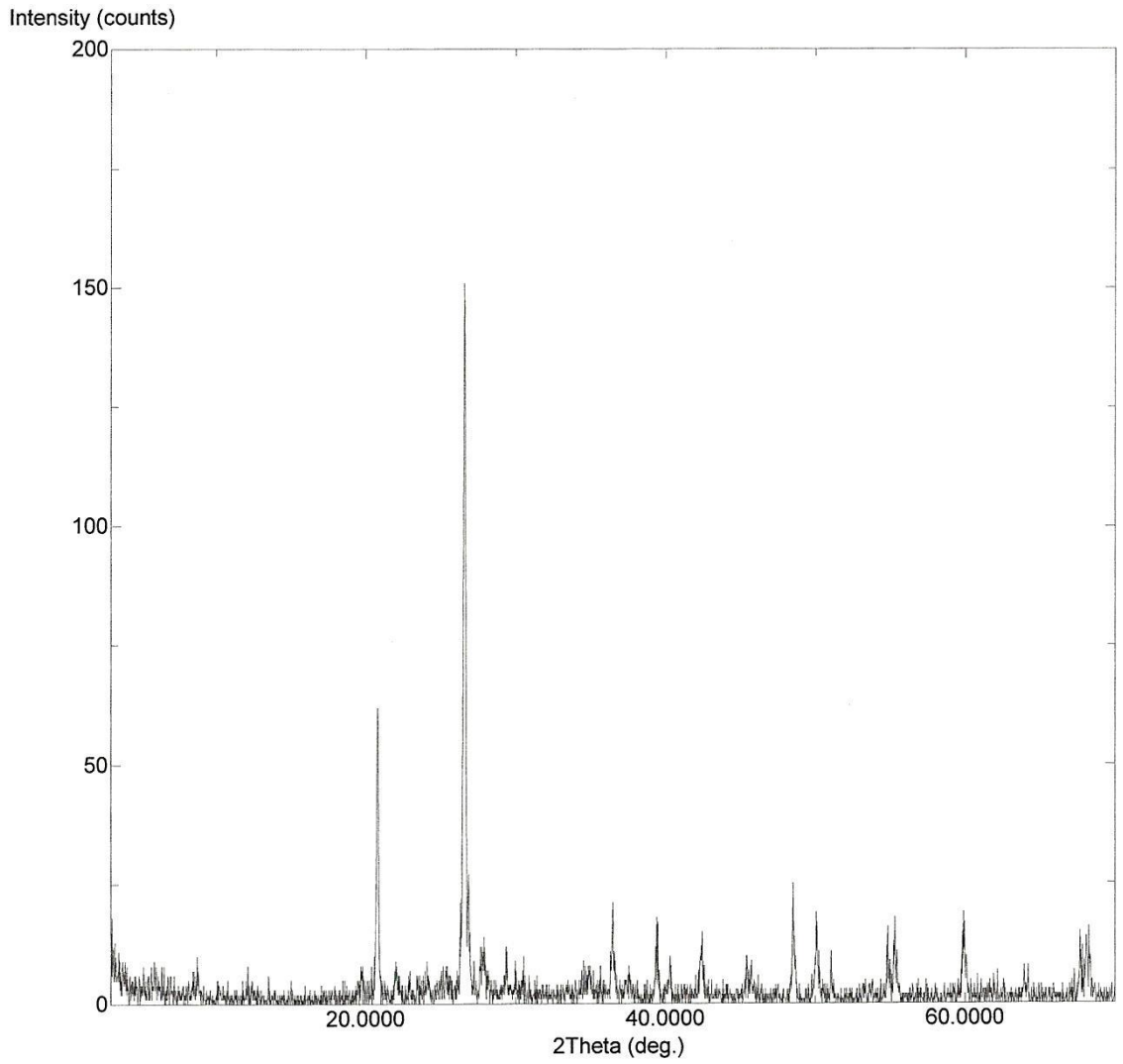

Figure A.51 C-B 1-4

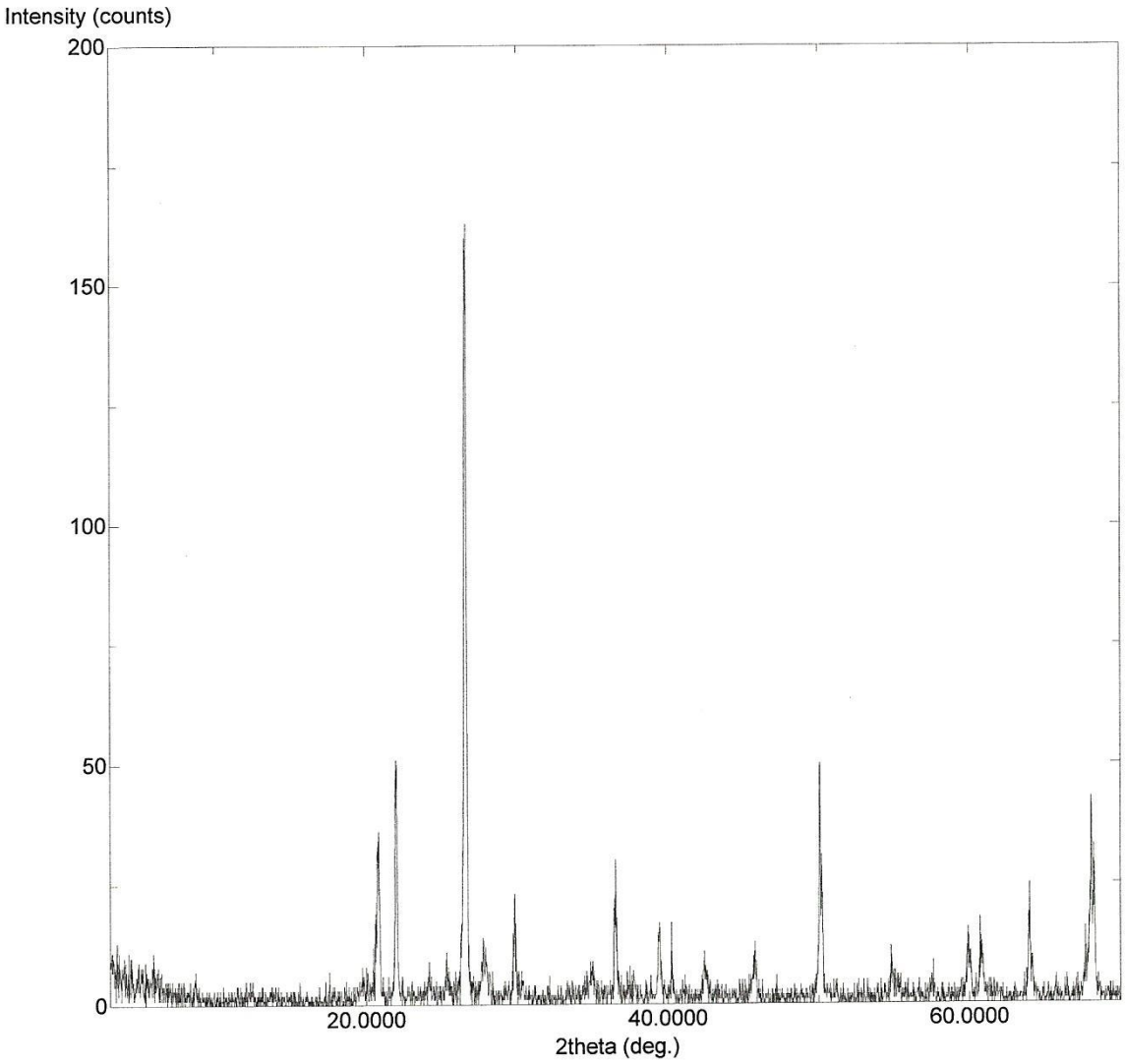

Figure A.52 C-B 1-5

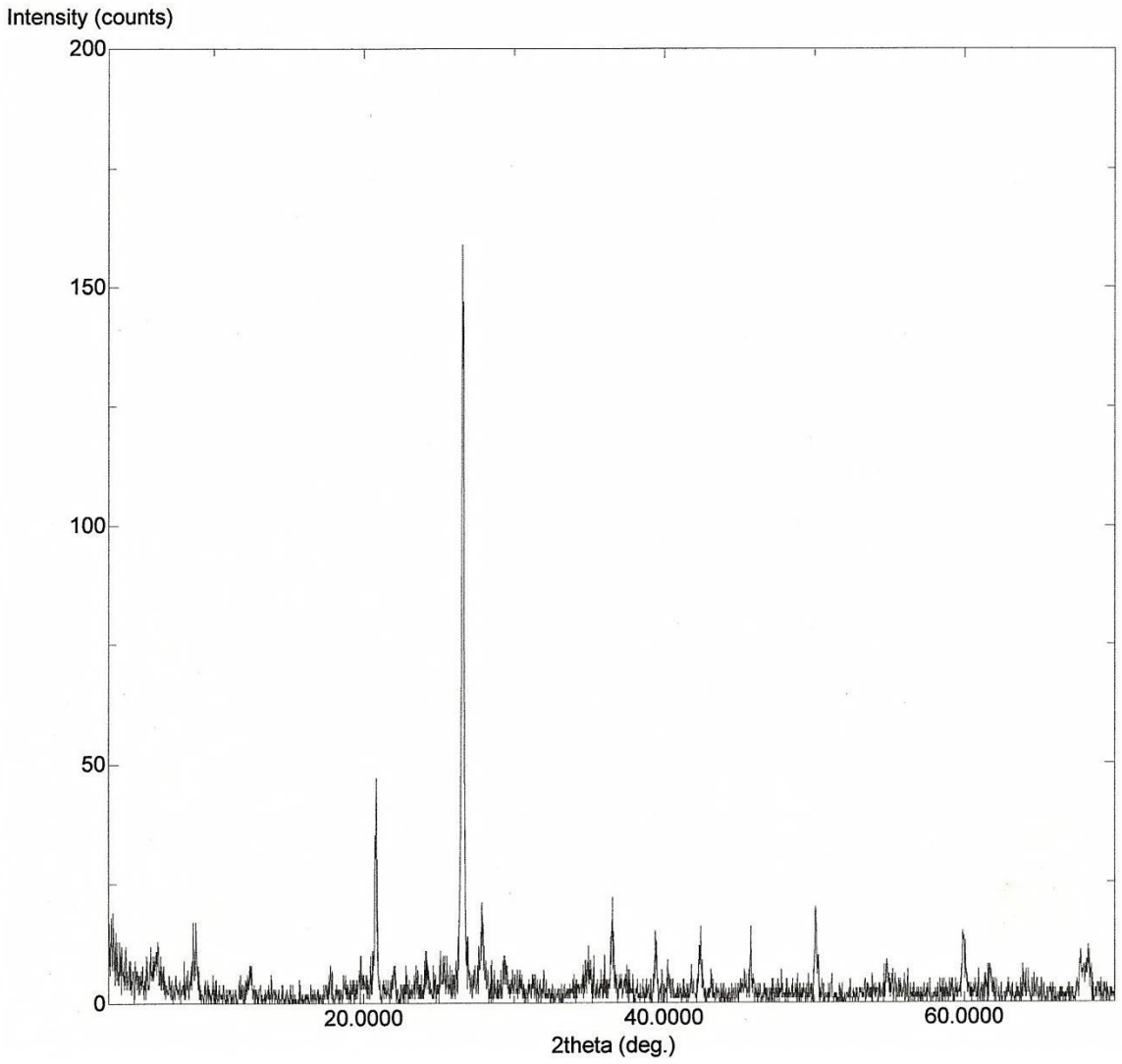

Figure A.53 C-B 2-1

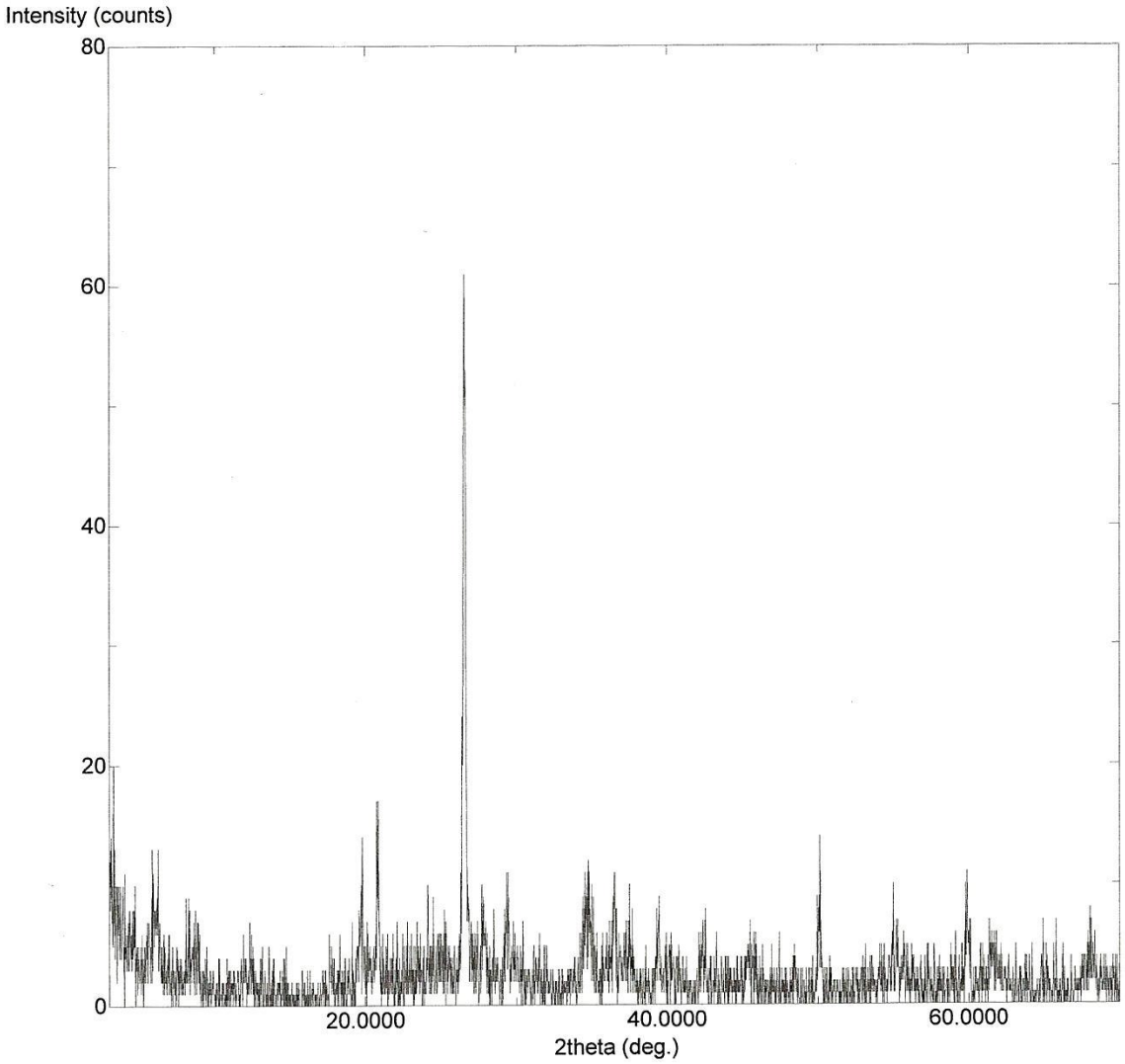

Figure A.54 C-B 2-2

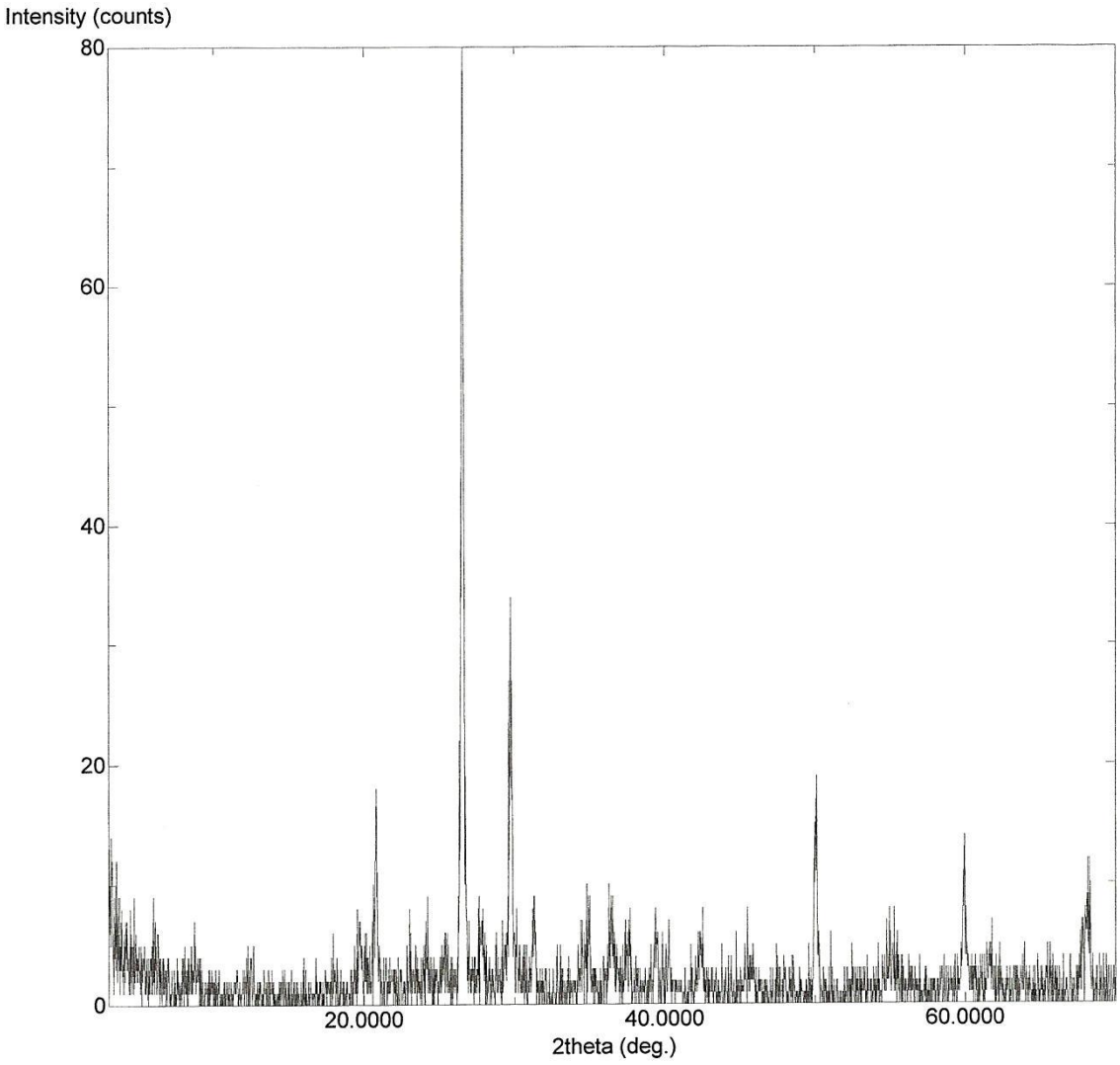

Figure A.55 C-B 3-1

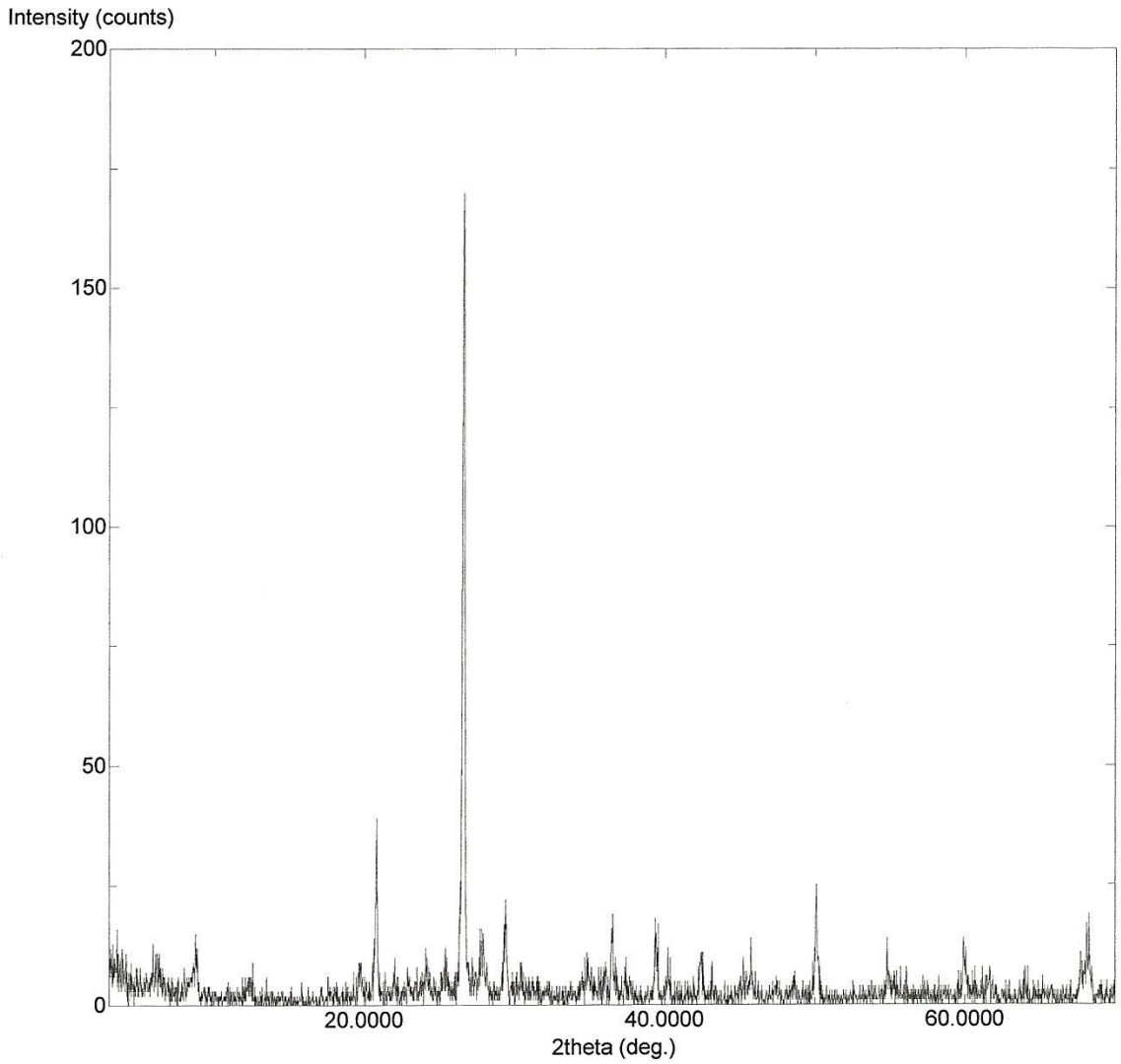

Figure A.56 C-B 3-2

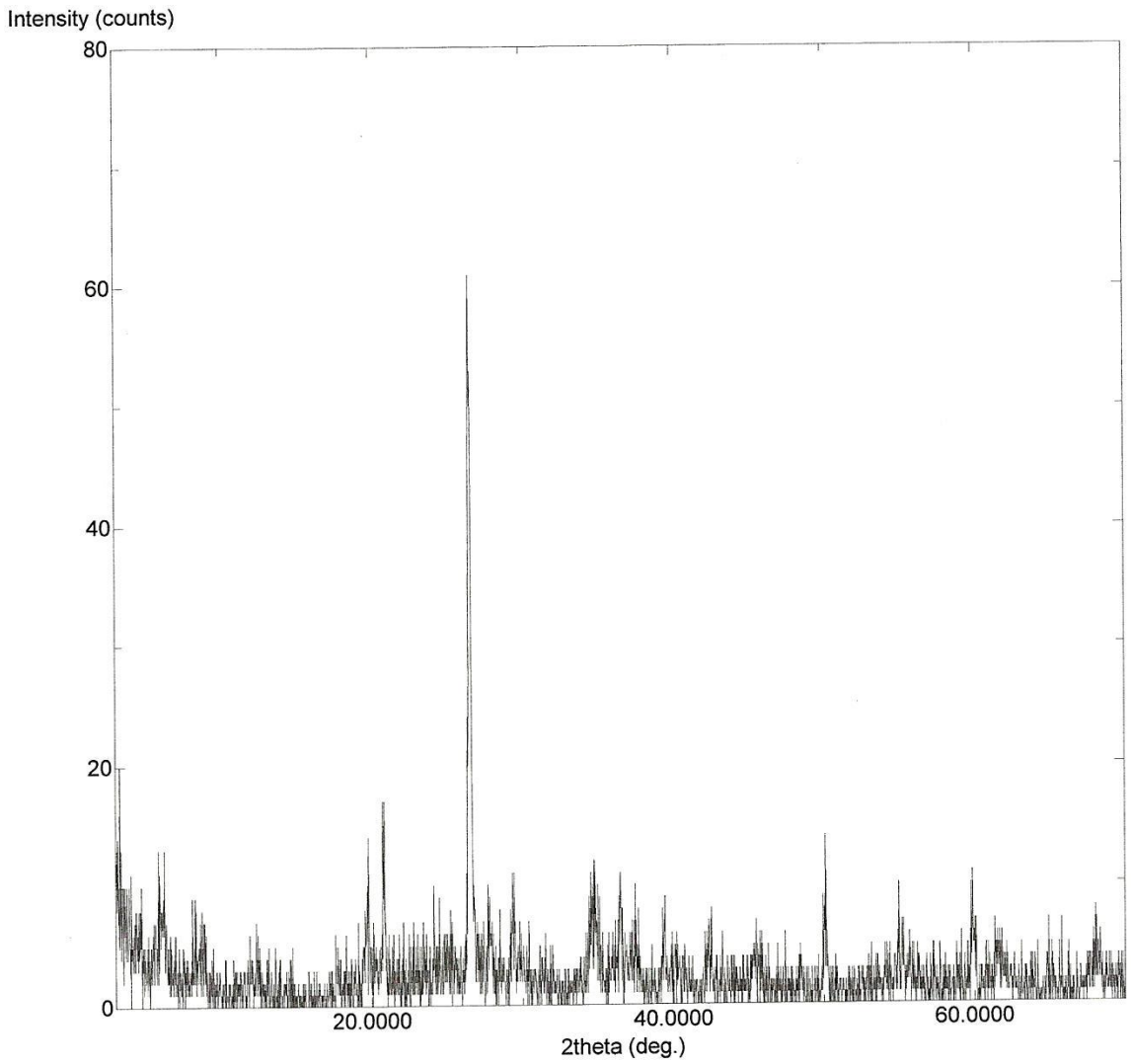

Figure A.57 C-B 3-3

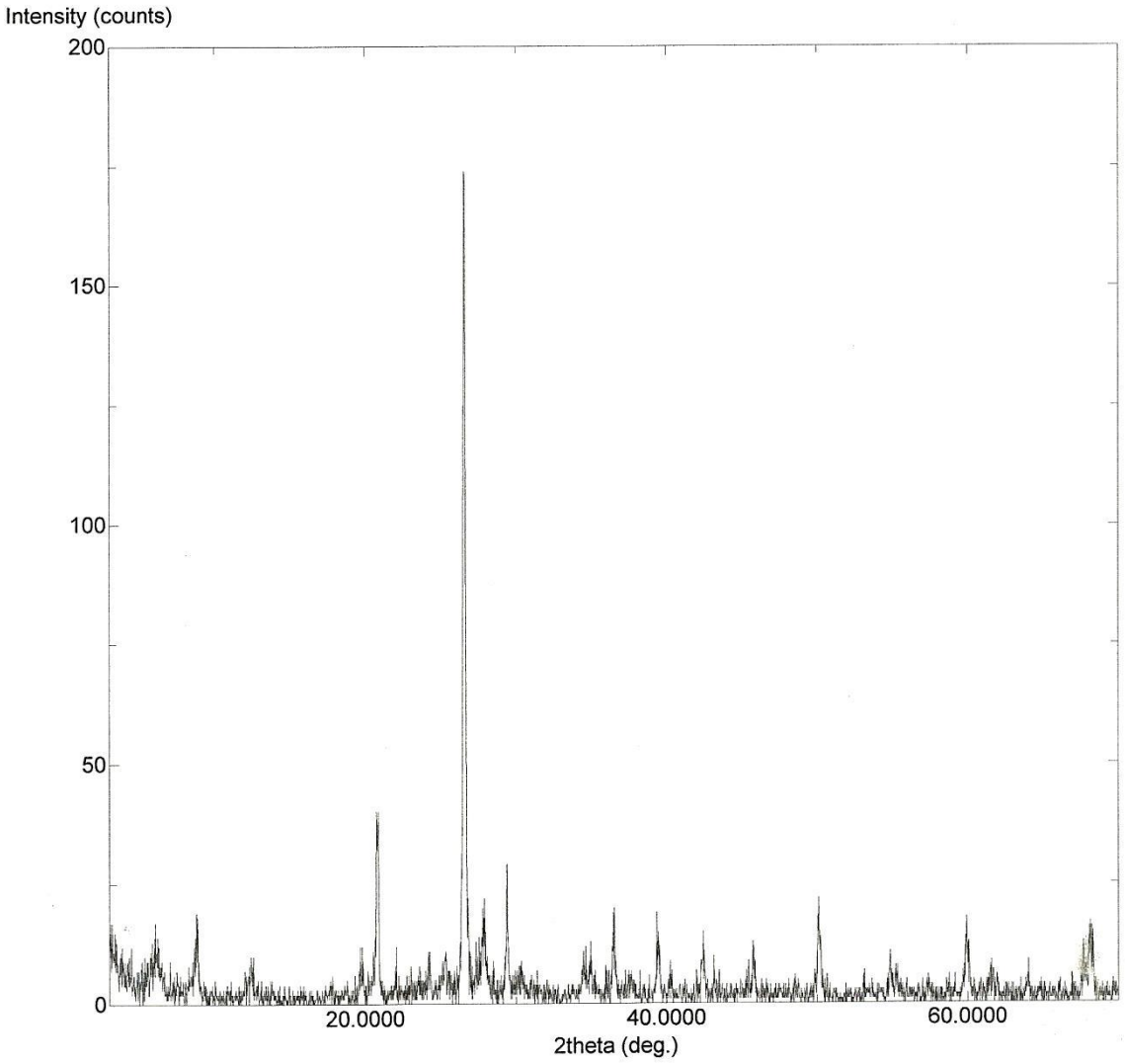

Figure A.58 C-B 3-4

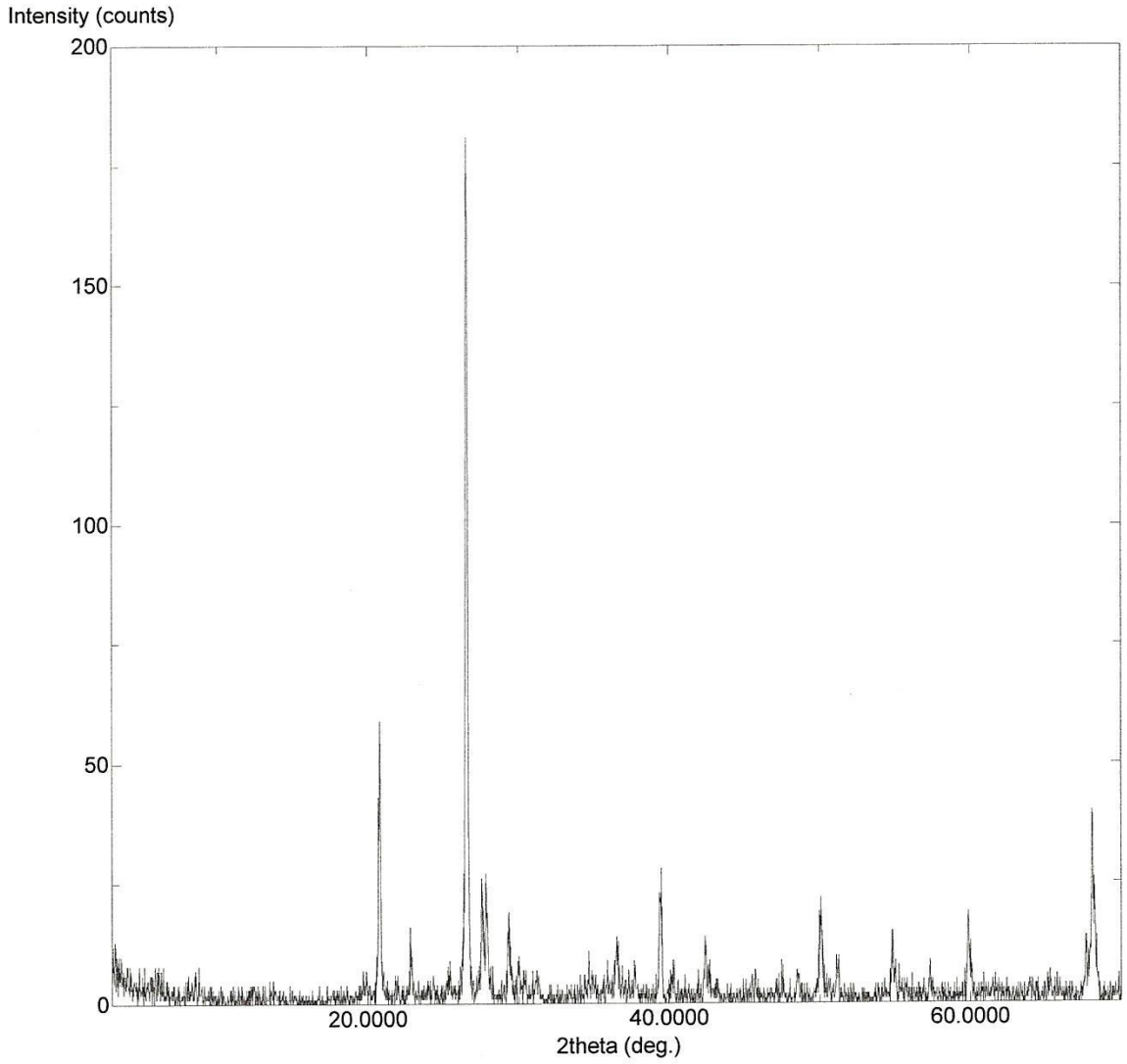

Figure A.59 WFS 1-1

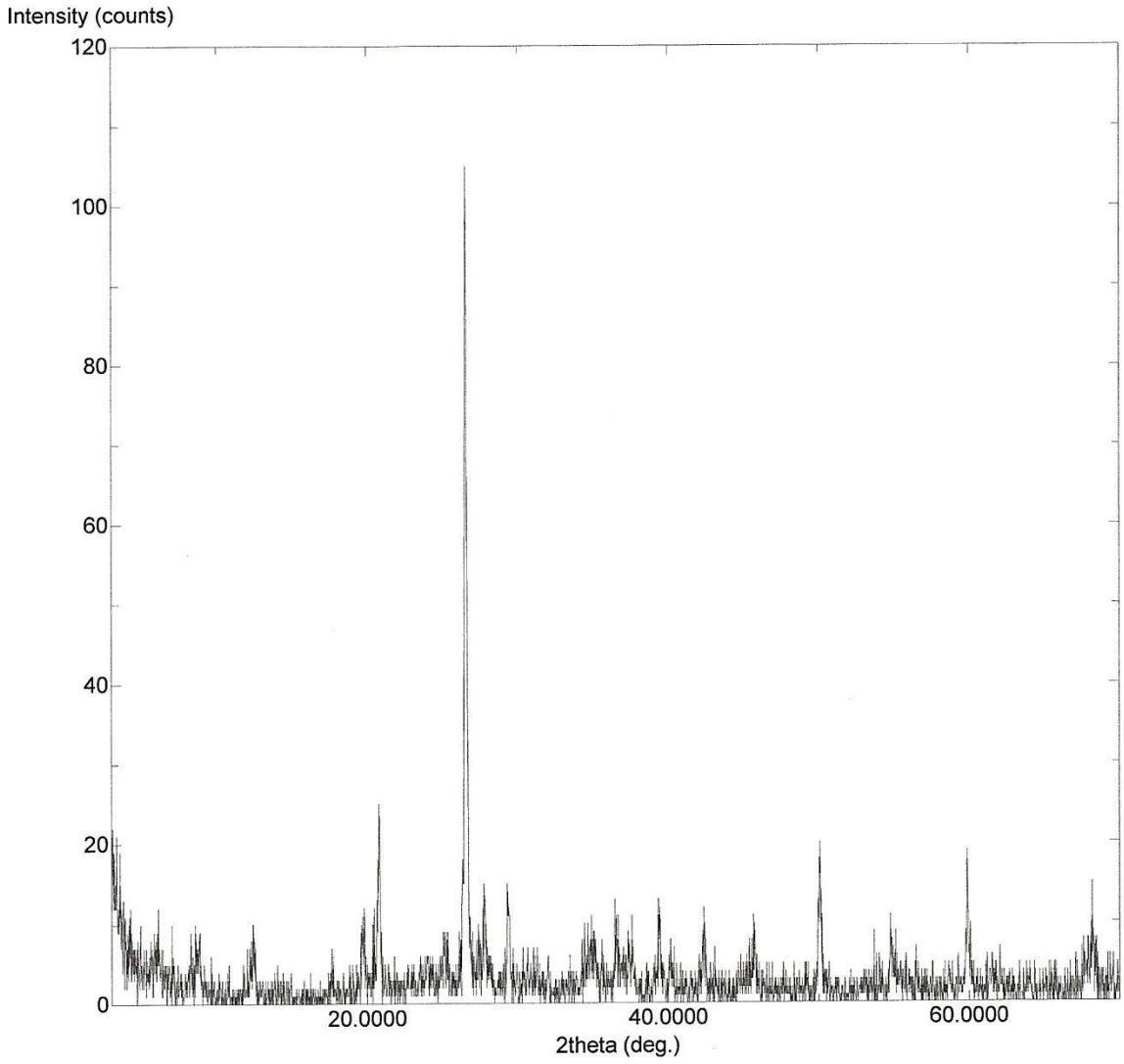

Figure A.60 K-C 1-1

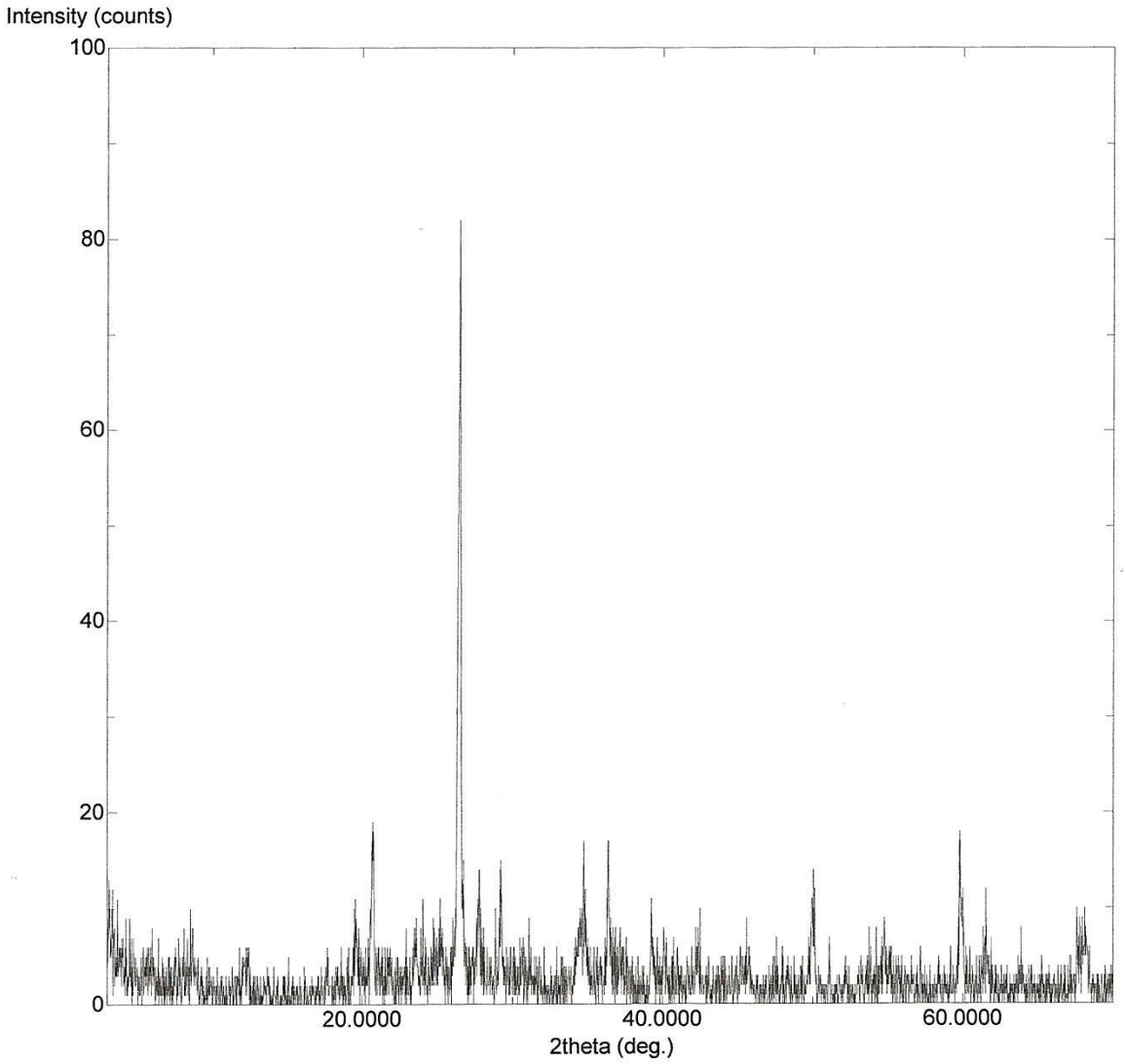

Figure A.61 K-C 2-1

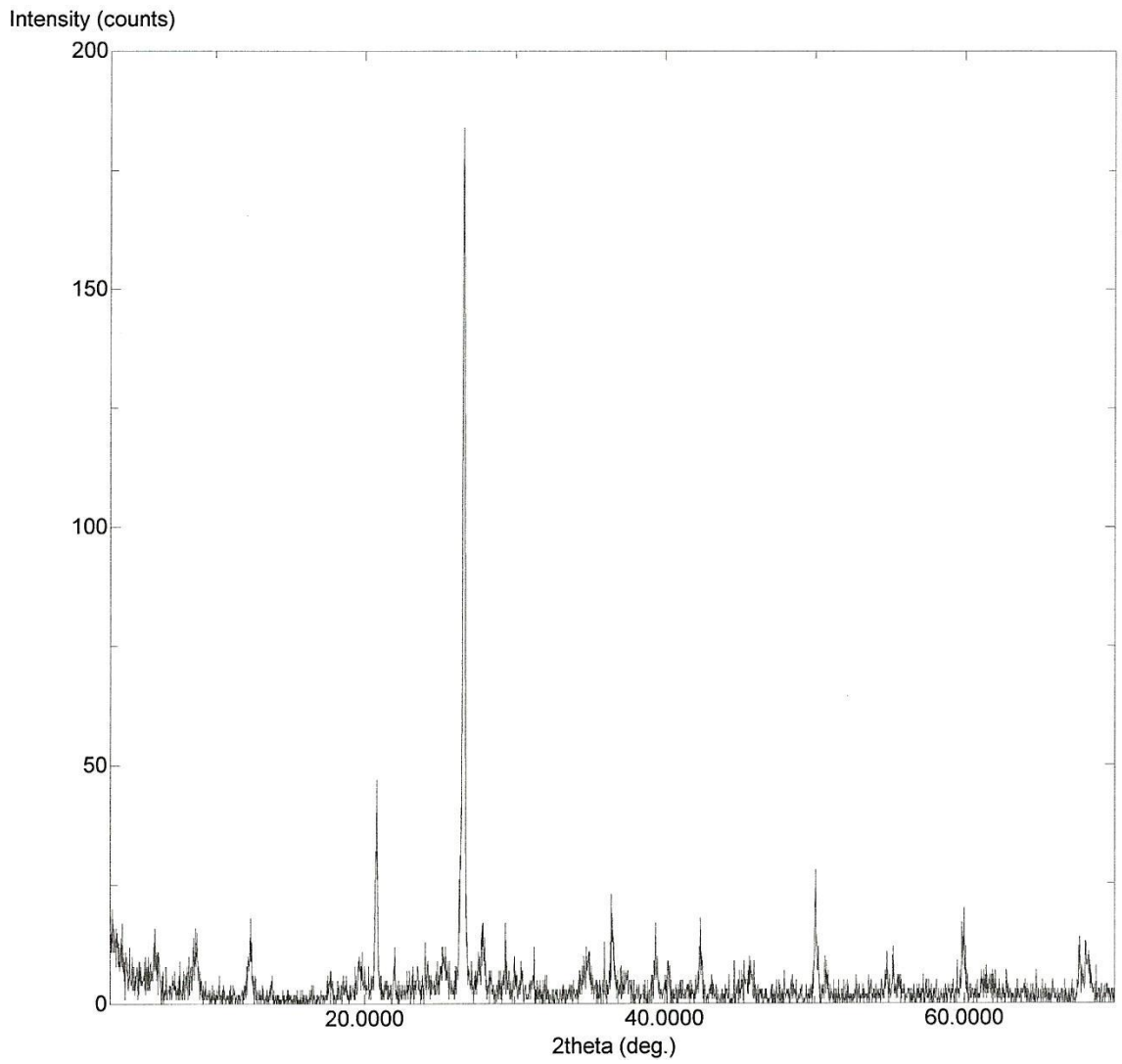

Figure A.62 K-C 3-1

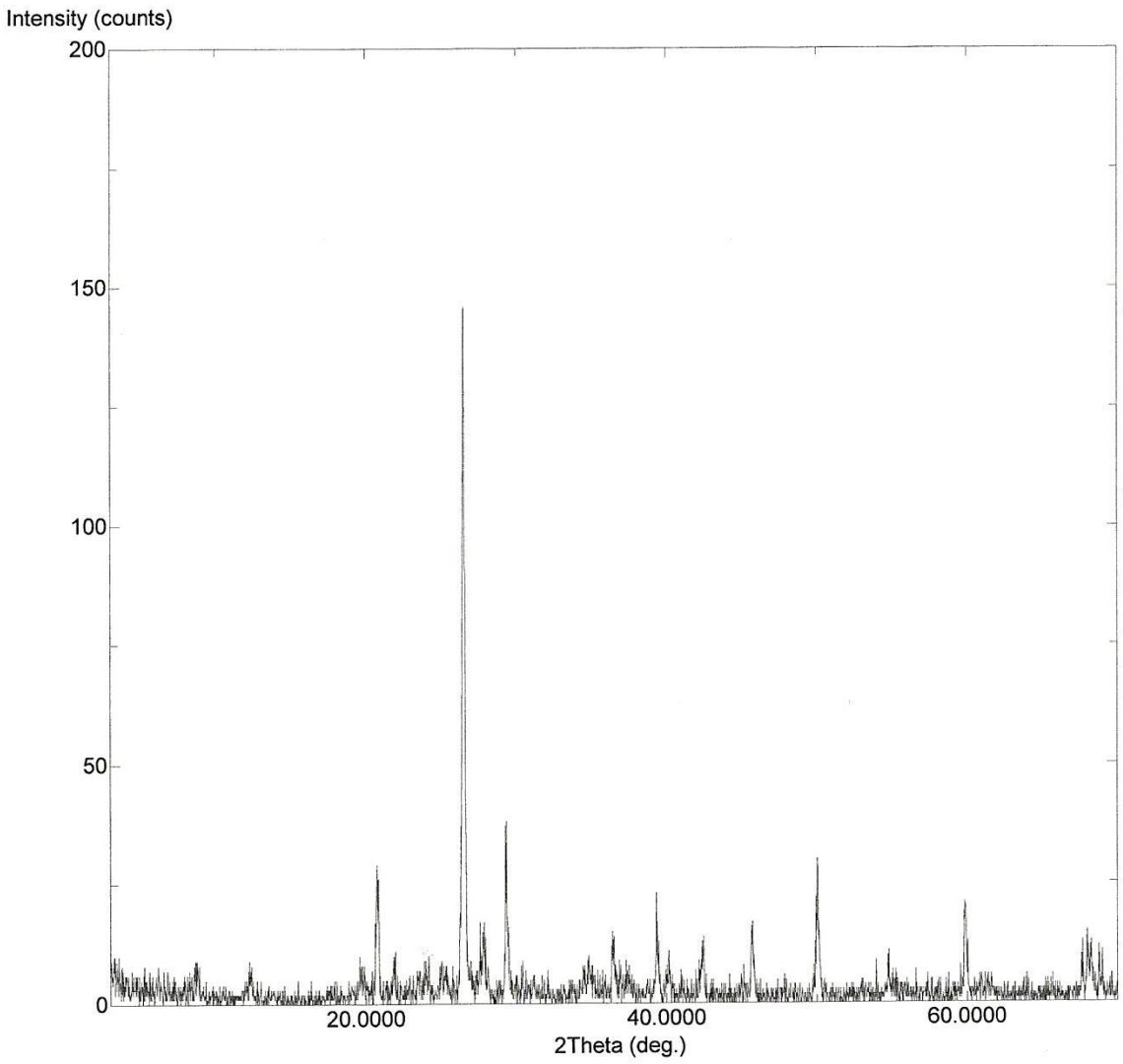

Figure A.63 K-C 3-2

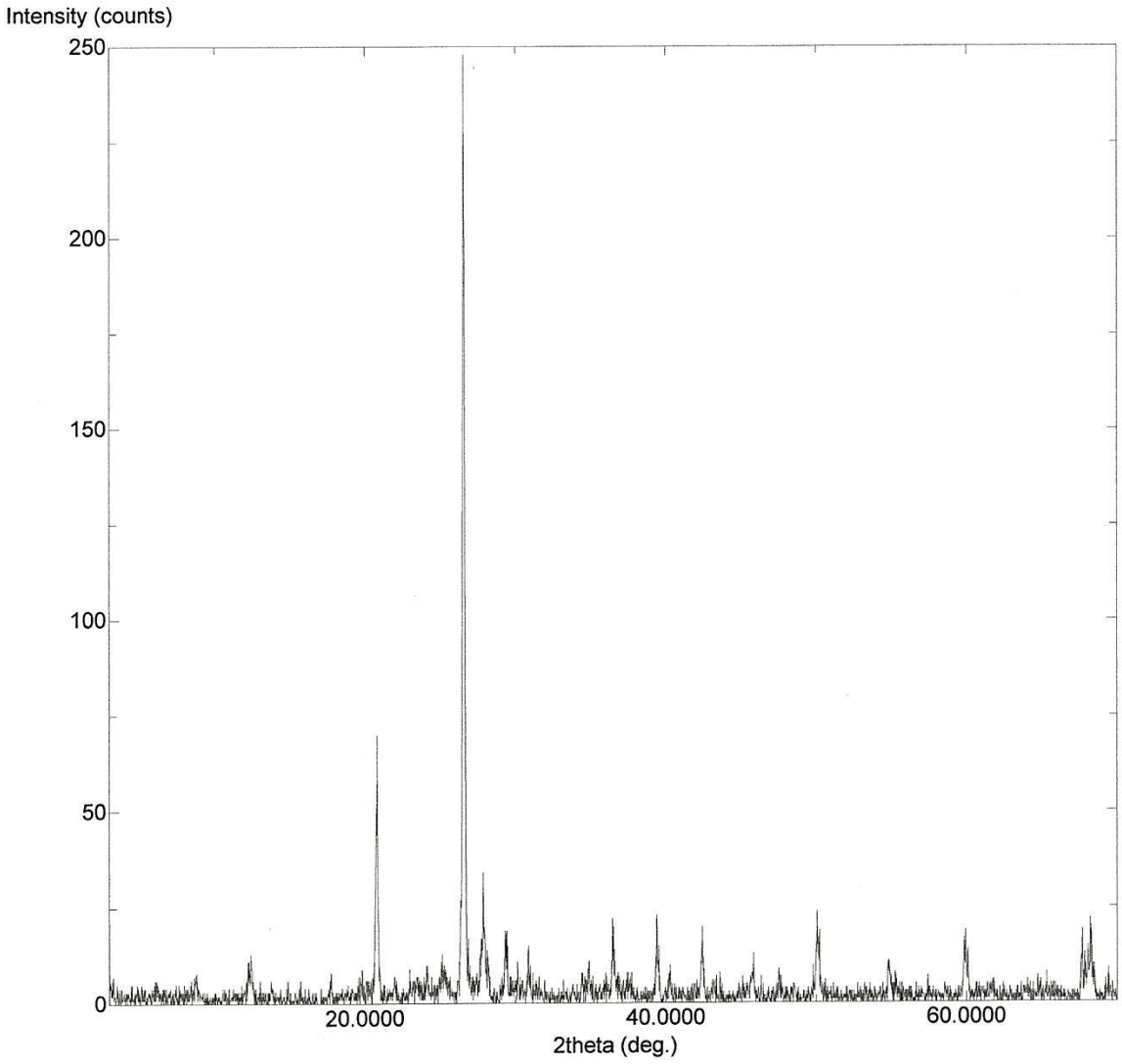

Figure A.64 K-C 3-3

APPENDIX B

DATA APPENDIX

Sample #	Raw Hydrated Sample in Crucible	Post-Separation Weight (Post-SW)	H_2O in Sample	Weight % of H_2O in Sample	Ashing	Ashing Weight % of Post-SW	Sample after LOI at 550 °C	Weight LOI at 550 °C	LOI_{550} Weight %	Sample after LOI at 950 °C	Weight LOI at 950 °C	LOI_{950} Weight %
H-C 1-1	13.68	13.51	0.17	1.24	7.90	58.48	7.60	0.30	3.80	7.53	0.07	0.89
H-C 1-4	21.29	18.00	3.29	15.45	11.28	62.67	11.13	0.15	1.33	10.47	0.66	5.85
H-C 1-12	12.34	10.06	2.28	18.48	4.76	47.32	4.60	0.16	3.36	4.38	0.22	4.62
Sch-C 1-1	11.61	10.42	1.19	10.25	5.52	52.98	5.39	0.13	2.36	5.10	0.29	5.25
Sch-C 3-1	15.84	12.20	3.64	22.98	5.85	47.95	5.63	0.22	3.76	5.54	0.09	1.54

Figure B.1 Shows the results of methods previously described of samples comprised of the light grey clay unit.

Sample #	Raw Hydrated Sample in Crucible	Post-Separation Weight (Post-SW)	H_2O in Sample	Weight % of H_2O in Sample	Ashing	Ashing Weight % of Post-SW	Sample after LOI at 550 °C	Weight LOI at 550 °C	LOI_{550} Weight %	Sample after LOI at 950 °C	Weight LOI at 950 °C	LOI_{950} Weight %
M-C 1-2	13.51	13.51	0.00	0.00	7.31	54.11	7.22	0.09	1.23	7.17	0.05	0.68
M-C 2-2	21.32	19.76	1.56	7.32	12.47	63.11	12.29	0.18	1.44	12.23	0.06	0.48
M-C 2-3	5.33	7.18	-1.85	-34.71	3.86	53.76	3.74	0.12	3.11	3.67	0.07	1.81
C-B 1-3	16.68	12.19	4.49	26.92	8.89	72.93	8.67	0.22	2.47	8.20	0.47	5.29
C-B 1-4	26.69	23.80	2.89	10.83	14.82	62.27	14.58	0.24	1.62	14.19	0.39	2.63
C-B 2-1	10.65	11.68	-1.03	-9.67	6.31	54.02	6.17	0.14	2.22	6.02	0.15	2.38
C-B 3-1	13.79	13.75	0.04	0.29	7.64	55.56	7.51	0.13	1.70	7.25	0.26	3.40
C-B 3-2	14.23	12.60	1.63	11.45	6.49	51.51	6.36	0.13	2.00	6.11	0.25	3.85
H-C 1-14	9.56	10.94	-1.38	-14.44	5.10	46.62	4.95	0.15	2.94	4.81	0.14	2.75
G-C 2-2	12.93	11.74	1.19	9.20	6.44	54.86	6.26	0.18	2.80	6.07	0.19	2.95

Figure B.2 Shows the results of methods previously described of samples comprised of the allogenic glacial outwash unit.

Sample #	Raw Hydrated Sample in Crucible	Separation Weight (Post-SW)	H_2O in Sample	Weight % of H_2O in Sample	Ashing	Ashing Weight % of Post-SW	Sample after LOI at 550 °C	Weight LOI at 550 °C	LOI_{550} Weight %	Sample after LOI at 950 °C	Weight LOI at 950 °C	LOI_{950} Weight %
S-B 1-2	19.75	15.05	4.70	23.80	6.65	44.19	6.51	0.14	2.11	6.27	0.24	3.61
M-C 1-1	26.05	21.32	4.73	18.16	9.43	44.23	9.35	0.08	0.85	8.75	0.60	6.36
M-C 2-1	15.27	15.58	-0.31	-2.03	11.57	74.26	11.34	0.23	1.99	11.26	0.08	0.69
C-B 1-1	16.78	13.91	2.87	17.10	7.19	51.69	7.04	0.15	2.09	6.68	0.36	5.01
C-B 1-2	14.35	12.44	1.91	13.31	8.43	67.77	8.31	0.12	1.42	7.90	0.41	4.86
C-B 3-3	19.33	16.20	3.13	16.19	9.05	55.86	8.78	0.27	2.98	8.47	0.31	3.43
C-B 3-4	18.30	14.16	4.14	22.62	5.86	41.38	5.77	0.09	1.54	5.58	0.19	3.24
H-C 1-0	9.39	11.14	-1.75	-18.64	5.36	48.11	4.93	0.43	8.02	4.81	0.12	2.24
H-C 1-3	21.92	17.46	4.46	20.35	10.04	57.50	9.81	0.23	2.29	9.30	0.51	5.08
H-C 1-10	21.52	15.49	6.03	28.02	8.78	56.68	8.46	0.32	3.64	8.38	0.08	0.91
H-C 1-11	19.76	17.62	2.14	10.83	10.08	57.21	9.85	0.23	2.28	9.27	0.58	5.75
G-C 2-3	14.25	15.85	-1.60	-11.23	9.97	62.90	9.81	0.16	1.60	9.10	0.71	7.12
G-C 2-4	19.31	15.21	4.10	21.23	9.76	64.17	9.56	0.20	2.05	8.85	0.71	7.27
Sch-C 1-3	13.06	10.29	2.77	21.21	6.11	59.38	4.85	1.26	20.62	3.28	1.57	25.70
Sch-C 1-4	15.21	10.85	4.36	28.67	5.64	51.98	5.51	0.13	2.30	5.26	0.25	4.43
Sch-C 2-1	11.34	9.22	2.12	18.69	4.30	46.64	4.17	0.13	3.02	4.02	0.15	3.49

Figure B.3 Shows the results of methods previously described of samples comprised of the tan ‘white’ clay unit.

Sample #	Raw Hydrated Sample in Crucible	Post-Separation Weight (Post-SW)	H_2O in Sample	Weight % of H_2O in Sample	Ashing	Ashing Weight % of Post-SW	Sample after LOI at 550 °C	Weight LOI at 550 °C	LOI_{550} Weight %	Sample after LOI at 950 °C	Weight LOI at 950 °C	LOI_{950} Weight %
WFS 1-1	17.38	15.24	2.14	12.31	9.64	63.25	9.53	0.11	1.14	9.21	0.32	3.32
K-C 1-1	21.70	19.39	2.31	10.65	12.91	66.58	12.62	0.29	2.25	12.16	0.46	3.56
K-C 2-1	20.02	15.08	4.94	24.68	8.26	54.77	8.11	0.15	1.82	7.76	0.35	4.24
K-C 3-1	16.41	15.94	0.47	2.86	9.35	58.66	9.14	0.21	2.25	8.93	0.21	2.25
K-C 3-2	10.59	11.03	-0.44	-4.15	5.05	45.78	4.93	0.12	2.38	4.81	0.12	2.38
K-C 3-3	13.15	12.57	0.58	4.41	7.25	57.68	7.15	0.10	1.38	6.85	0.30	4.14

Figure B.4 Shows the results of methods previously described of samples comprised of the control sediments.

Sample #	Raw Hydrated Sample in Crucible	Post-Separation Weight (Post-SW)	H_2O in Sample	Weight % of H_2O in Sample	Ashing	Ashing Weight % of Post-SW	Sample after LOI at 550 °C	Weight LOI at 550 °C	LOI_{550} Weight %	Sample after LOI at 950 °C	Weight LOI at 950 °C	LOI_{950} Weight %
S-B 1-0	13.25	5.44	7.81	58.94	3.96	72.79	3.70	0.26	6.57	3.67	0.03	0.76
S-B 1-1	17.48	10.71	6.77	38.73	6.46	60.32	6.28	0.18	2.79	6.01	0.27	4.18
S-B 1-3	15.54	11.20	4.34	27.93	8.12	72.50	7.85	0.27	3.33	7.54	0.31	3.82
B-C 1-1	14.29	14.15	0.14	0.98	9.09	64.24	8.91	0.18	1.98	8.84	0.07	0.77
B-C 1-2	13.11	12.15	0.96	7.32	7.61	62.63	7.45	0.16	2.10	7.10	0.35	4.60
B-C 1-3	12.42	13.40	-0.98	-7.89	8.03	59.93	7.89	0.14	1.74	7.66	0.23	2.86
B-C 1-4	18.61	16.51	2.10	11.28	11.41	69.11	11.18	0.23	2.02	11.09	0.09	0.79
B-C 1-5	18.62	16.38	2.24	12.03	7.55	46.09	7.41	0.14	1.85	7.37	0.04	0.53
B-C 1-6	19.72	16.79	2.93	14.86	9.98	59.44	9.79	0.19	1.90	9.73	0.06	0.60
M-C 1-3	17.89	15.71	2.18	12.19	10.15	64.61	10.02	0.13	1.28	9.95	0.07	0.69
C-B 1-5	16.26	11.32	4.94	30.38	5.45	48.14	5.33	0.12	2.20	5.26	0.07	1.28
H-C 1-2	14.75	10.33	4.42	29.97	5.02	48.60	4.86	0.16	3.19	4.63	0.23	4.58
H-C 1-5	23.75	21.03	2.72	11.45	10.14	48.22	10.00	0.14	1.38	9.42	0.58	5.72
H-C 1-6	21.93	14.78	7.15	32.60	7.67	51.89	7.52	0.15	1.96	7.11	0.41	5.35
H-C 1-7	14.12	13.29	0.83	5.88	6.86	51.62	6.66	0.20	2.92	6.49	0.17	2.48
H-C 1-8	11.02	12.94	-1.92	-17.42	7.11	54.95	7.06	0.05	0.70	6.59	0.47	6.61
H-C 1-9	11.35	12.16	-0.81	-7.14	7.91	65.05	7.65	0.26	3.29	7.43	0.22	2.78
H-C 1-13	16.02	14.27	1.75	10.92	7.89	55.29	7.77	0.12	1.52	7.31	0.46	5.83
H-C 1-15	16.62	15.01	1.61	9.69	7.91	52.70	7.80	0.11	1.39	7.29	0.51	6.45
G-C 1-1	14.56	14.44	0.12	0.82	8.60	59.56	8.40	0.20	2.33	8.18	0.22	2.56
G-C 1-2	10.55	9.95	0.60	5.69	4.89	49.15	4.74	0.15	3.07	4.58	0.16	3.27
G-C 1-3	21.00	17.49	3.51	16.71	10.47	59.86	10.24	0.23	2.20	10.04	0.20	1.91
G-C 2-1	8.18	8.96	-0.78	-9.54	4.21	46.99	4.05	0.16	3.80	3.98	0.07	1.66
G-C 3-1	15.24	14.01	1.23	8.07	7.76	55.39	7.62	0.14	1.80	7.39	0.23	2.96
G-C 3-2	18.30	13.24	5.06	27.65	7.52	56.80	7.09	0.43	5.72	6.90	0.19	2.53
Sch-C 1-2	15.27	12.91	2.36	15.46	7.27	56.31	7.19	0.08	1.10	6.83	0.36	4.95

Figure B.5 Shows the results of methods previously described, of samples comprised of the dark grey/dark brown clay unit.

Sample #	Solvent	Solvent Weight %	Post-Dissolution of Carbonates	Weight of Dissolved Carbonates	LOD_{NaA} Weight %
S-B 1-0	1.09	20.04	0.98	0.11	10.09
S-B 1-1	2.93	27.36	2.57	0.36	12.29
S-B 1-3	2.21	19.73	1.83	0.38	17.19
B-C 1-1	3.31	23.39	3.12	0.19	5.74
B-C 1-2	2.29	18.85	2.07	0.22	9.61
B-C 1-3	4.11	30.67	3.81	0.30	7.30
B-C 1-4	3.57	21.62	3.58	-0.01	-0.28
B-C 1-5	7.09	43.28	7.07	0.02	0.28
B-C 1-6	4.45	26.50	4.37	0.08	1.80
M-C 1-3	4.11	26.16	4.03	0.08	1.95
C-B 1-5	4.47	39.49	4.39	0.08	1.79
H-C 1-2	4.02	38.92	3.67	0.35	8.71
H-C 1-5	8.64	41.08	7.63	1.01	11.69
H-C 1-6	5.79	39.17	5.04	0.75	12.95
H-C 1-7	4.40	33.11	4.20	0.20	4.55
H-C 1-8	4.40	34.00	3.63	0.77	17.50
H-C 1-9	2.43	19.98	2.14	0.29	11.93
H-C 1-13	5.10	35.74	4.40	0.70	13.73
H-C 1-15	5.73	38.17	4.94	0.79	13.79
G-C 1-1	4.62	31.99	4.46	0.16	3.46
G-C 1-2	3.65	36.68	3.38	0.27	7.40
G-C 1-3	5.51	31.50	5.30	0.21	3.81
G-C 2-1	3.51	39.17	3.41	0.10	2.85
G-C 2-2	4.18	35.60	4.02	0.16	3.83
G-C 3-1	4.73	33.76	4.64	0.09	1.90
G-C 3-2	4.38	33.08	4.09	0.29	6.62
Sch-C 1-2	4.58	35.48	4.01	0.57	12.45

Figure B.6 Shows the results of methods previously described of samples comprised of the dark grey/dark brown clay unit.

Sample #	Solvent	Solvent Weight %	Post-Dissolution of Carbonates	Weight of Dissolved Carbonates	LOD_{NaA} Weight %
H-C 1-1	4.48	33.16	4.45	0.03	0.67
H-C 1-4	5.23	29.06	4.65	0.58	11.09
H-C 1-12	4.19	41.65	3.89	0.30	7.16
Sch-C 1-1	3.56	34.17	3.04	0.52	14.61
Sch-C 3-1	4.14	33.93	3.65	0.49	11.84

Figure B.7 Shows the results of methods previously described of samples comprised of the light grey clay unit.

Sample #	Solvent	Solvent Weight %	Post-Dissolution of Carbonates	Weight of Dissolved Carbonates	LOD_{NaA} Weight %
M-C 1-2	4.98	36.86	4.90	0.08	1.61
M-C 2-2	5.62	28.44	5.55	0.07	1.25
M-C 2-3	2.05	28.55	1.96	0.09	4.39
C-B 1-3	2.03	16.65	1.74	0.29	14.29
C-B 1-4	6.23	26.18	5.89	0.34	5.46
C-B 2-1	4.25	36.39	4.07	0.18	4.24
C-B 3-1	4.62	33.60	4.46	0.16	3.46
C-B 3-2	4.86	38.57	4.46	0.40	8.23
H-C 1-14	4.69	42.87	4.47	0.22	4.69
G-C 2-2	4.18	35.60	4.02	0.16	3.83

Figure B.8 Shows the results of methods previously described of samples comprised of the allogenic glacial outwash unit.

Sample #	Solvent	Solvent Weight %	Post-Dissolution of Carbonates	Weight of Dissolved Carbonates	LOD_{NaA} Weight %
S-B 1-2	4.93	32.76	4.86	0.07	1.42
M-C 1-1	8.29	38.88	7.78	0.51	6.15
M-C 2-1	3.14	20.15	3.11	0.03	0.96
C-B 1-1	5.11	36.74	4.54	0.57	11.15
C-B 1-2	2.68	21.54	2.37	0.31	11.57
C-B 3-3	5.94	36.67	5.66	0.28	4.71
C-B 3-4	4.66	32.91	4.44	0.22	4.72
H-C 1-0	4.46	40.04	4.43	0.03	0.67
H-C 1-3	5.69	32.59	5.04	0.65	11.42
H-C 1-10	5.74	37.06	5.64	0.10	1.74
H-C 1-11	6.06	34.39	5.22	0.84	13.86
G-C 2-3	4.58	28.90	3.79	0.79	17.25
G-C 2-4	4.38	28.80	3.66	0.72	16.44
Sch-C 1-3	3.05	29.64	2.75	0.30	9.84
Sch-C 1-4	3.61	33.27	3.28	0.33	9.14
Sch-C 2-1	3.54	38.39	3.31	0.23	6.50

Figure B.9 Shows the results of methods previously described of samples comprised of the tan ‘white’ clay unit.

APPENDIX C

BOX PLOT DIAGRAM APPENDIX

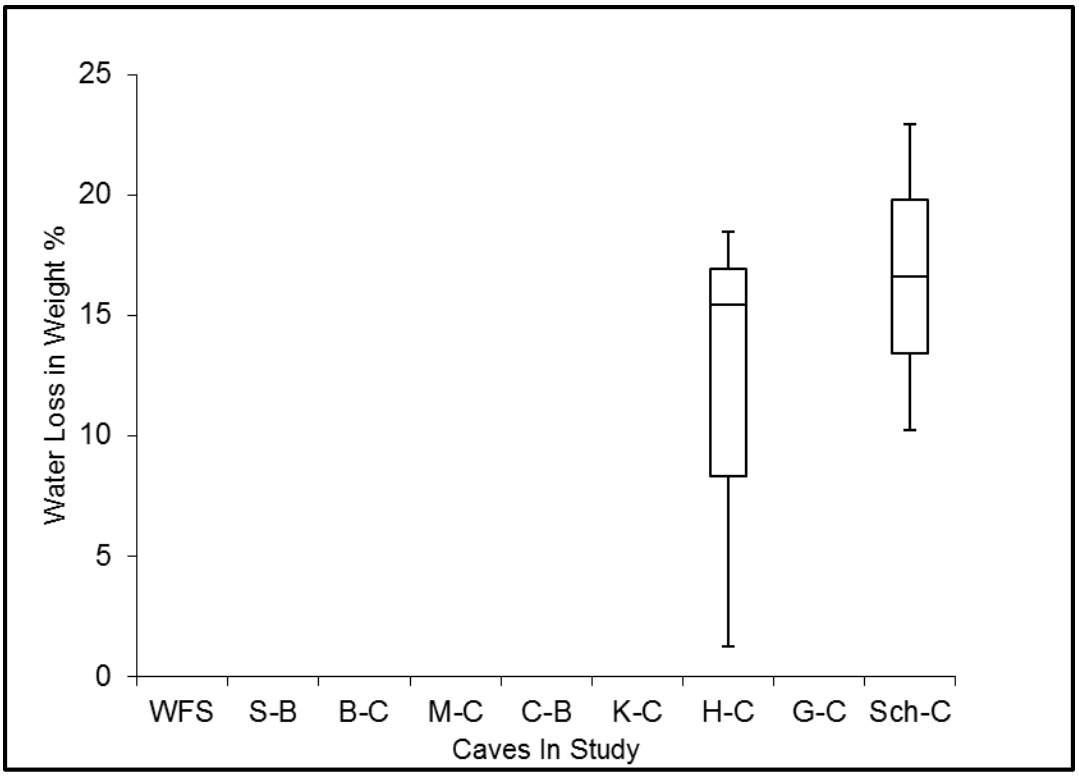

Figure C.1 A box plot diagram comparing the amount of water as a weight percent lost by samples, containing the light grey clay unit, resulting from being heated to 105 °C.

Note the light grey unit was only observed and collected in Howe Caverns and Schoharie Caverns.

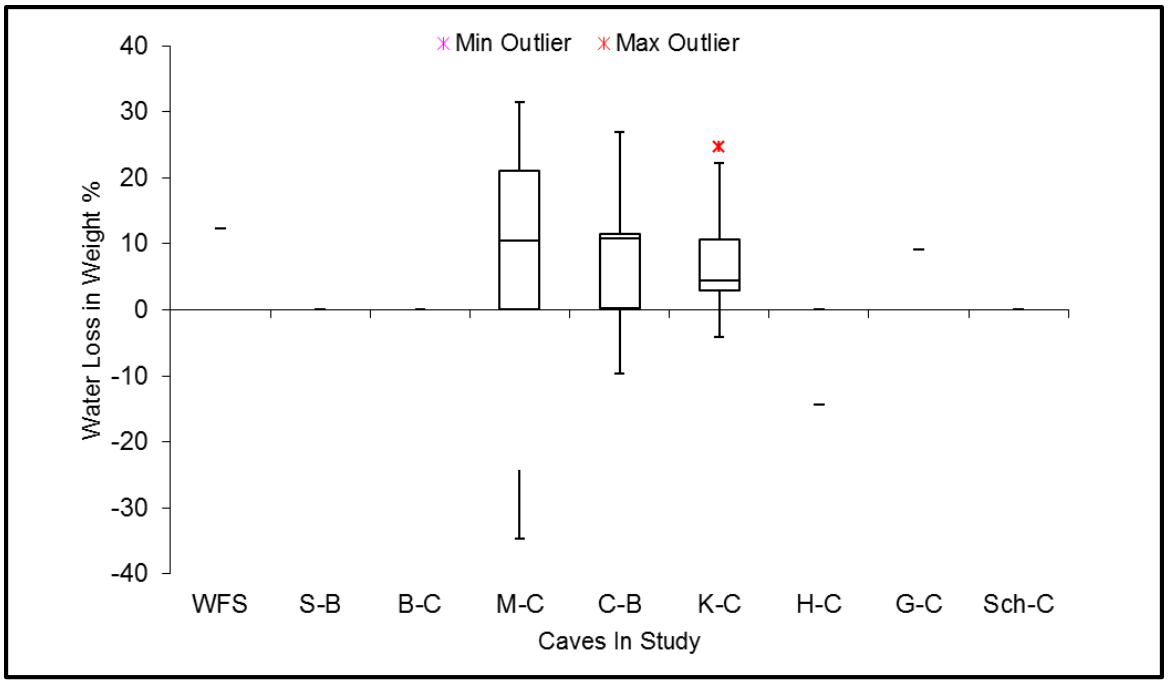

Figure C.2 A box plot diagram comparing the amount of water as a weight percent lost by samples, containing the allogenic glacial outwash unit, resulting from being heated to 105 °C.

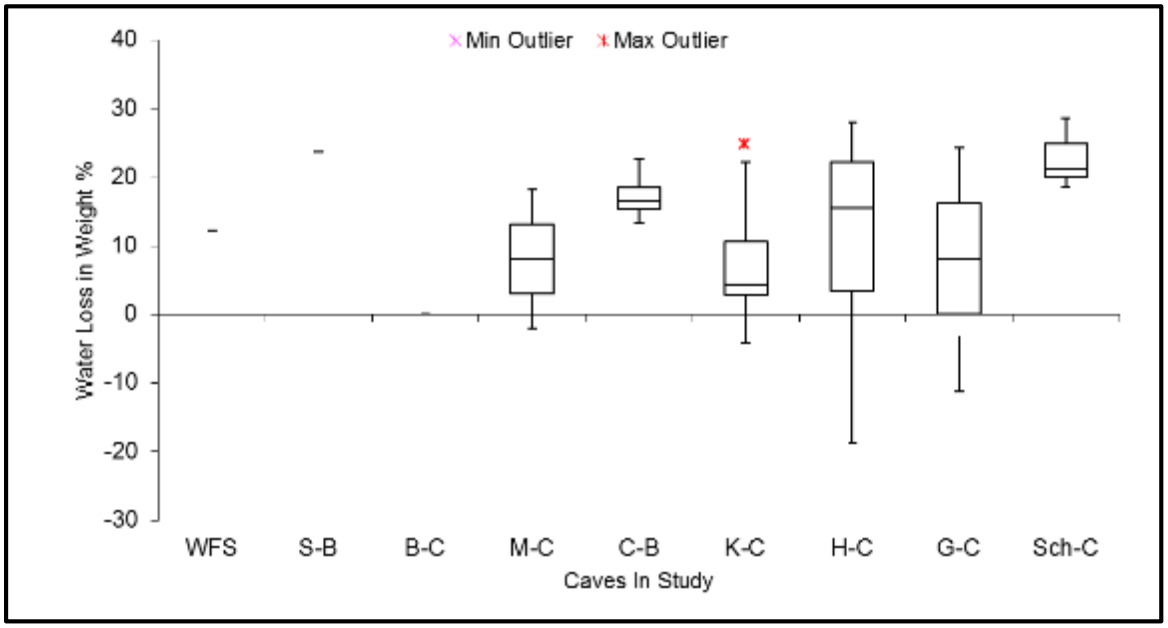

Figure C.3 A box plot diagram comparing the amount of water as a weight percent lost by samples, containing the tan 'white' clay unit, resulting from being heated to 105 °C.

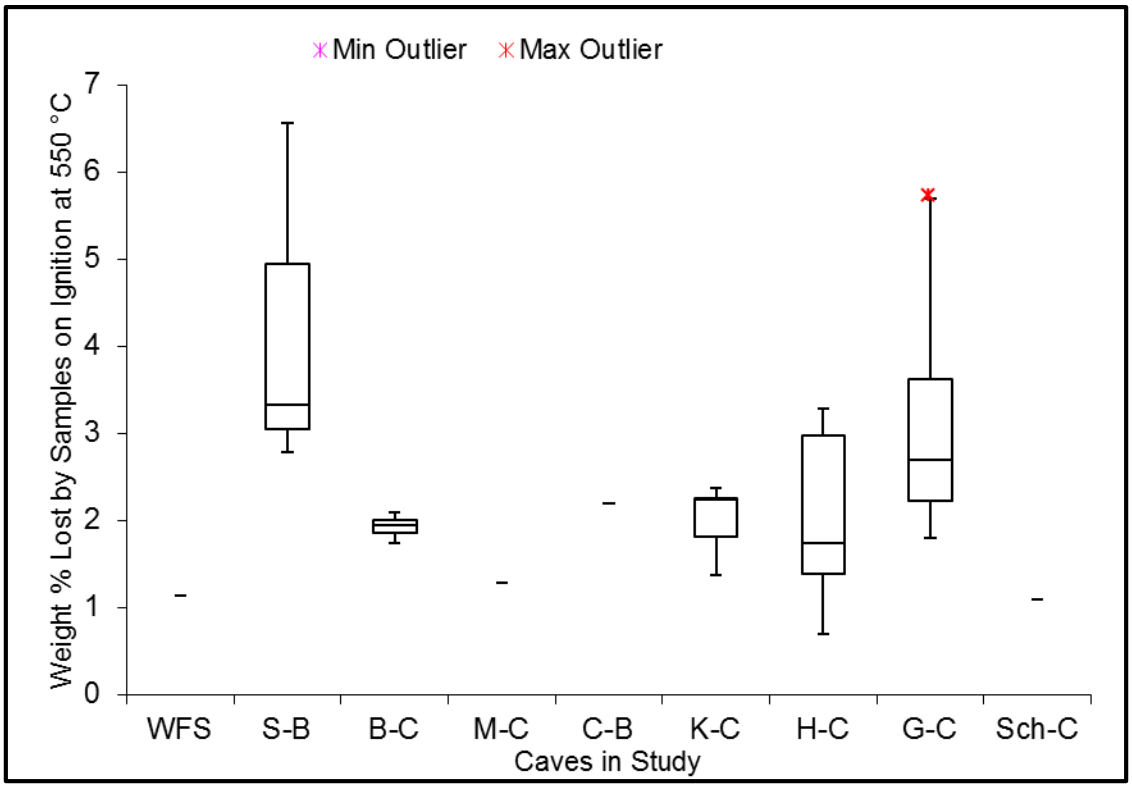

Figure C.4 Appendix 3.2a A box plot diagram comparing the amount of weight lost by samples, containing the dark grey/dark brown clay unit, by ignition at 550 °C.

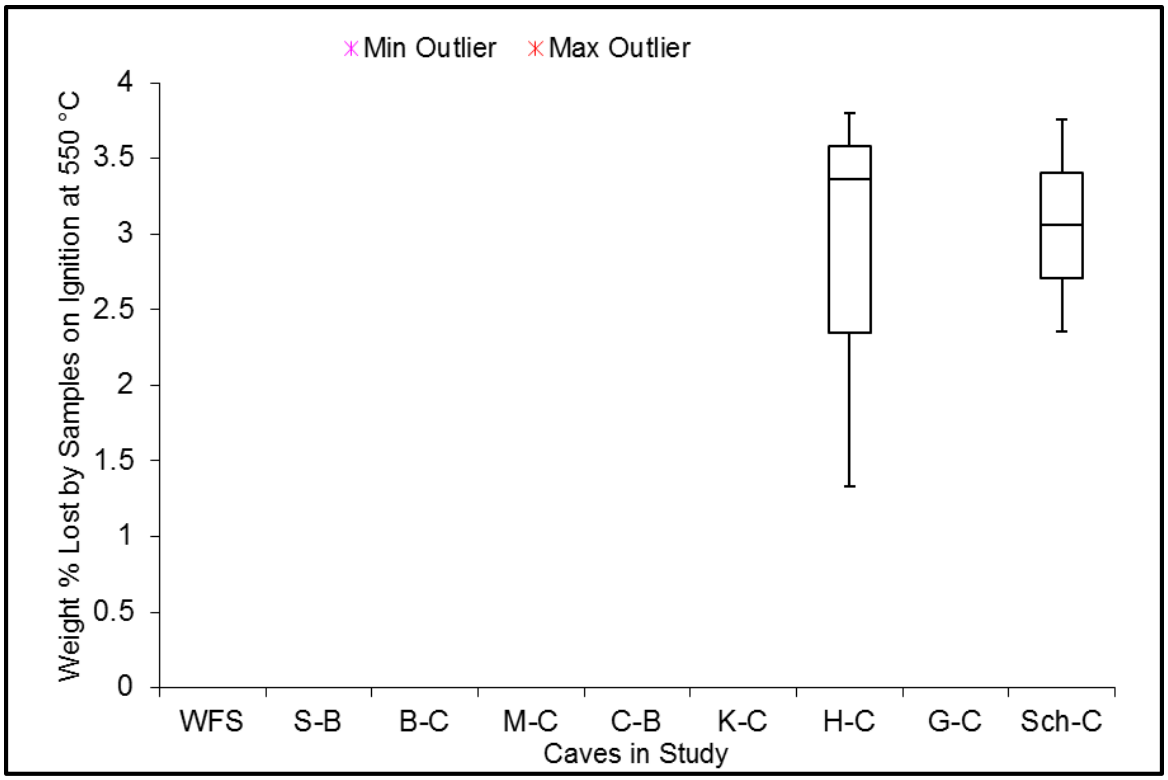

Figure C.5 A box plot diagram comparing the amount of weight lost by samples, containing the light grey clay unit, by ignition at 550 °C.

Note the light grey clay unit was only observed and collected in Howe Caverns and Schoharie Caverns.

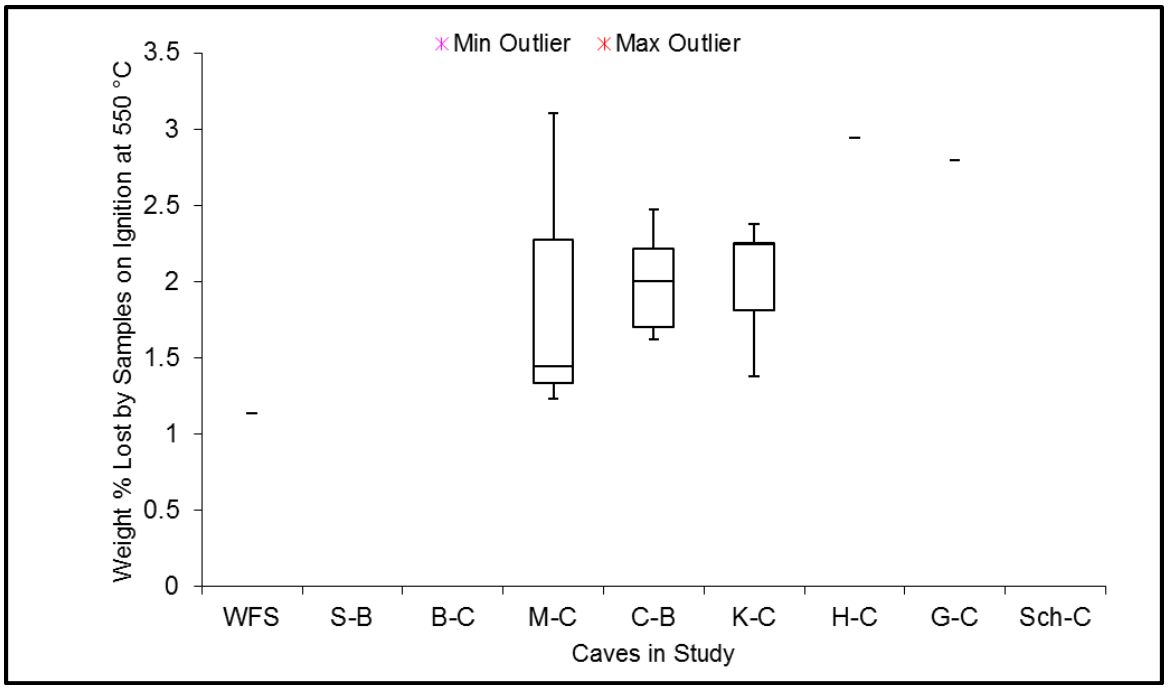

Figure C.6 A box plot diagram comparing the amount of weight lost by samples, containing the allogenic glacial outwash unit, by ignition at 550 °C.

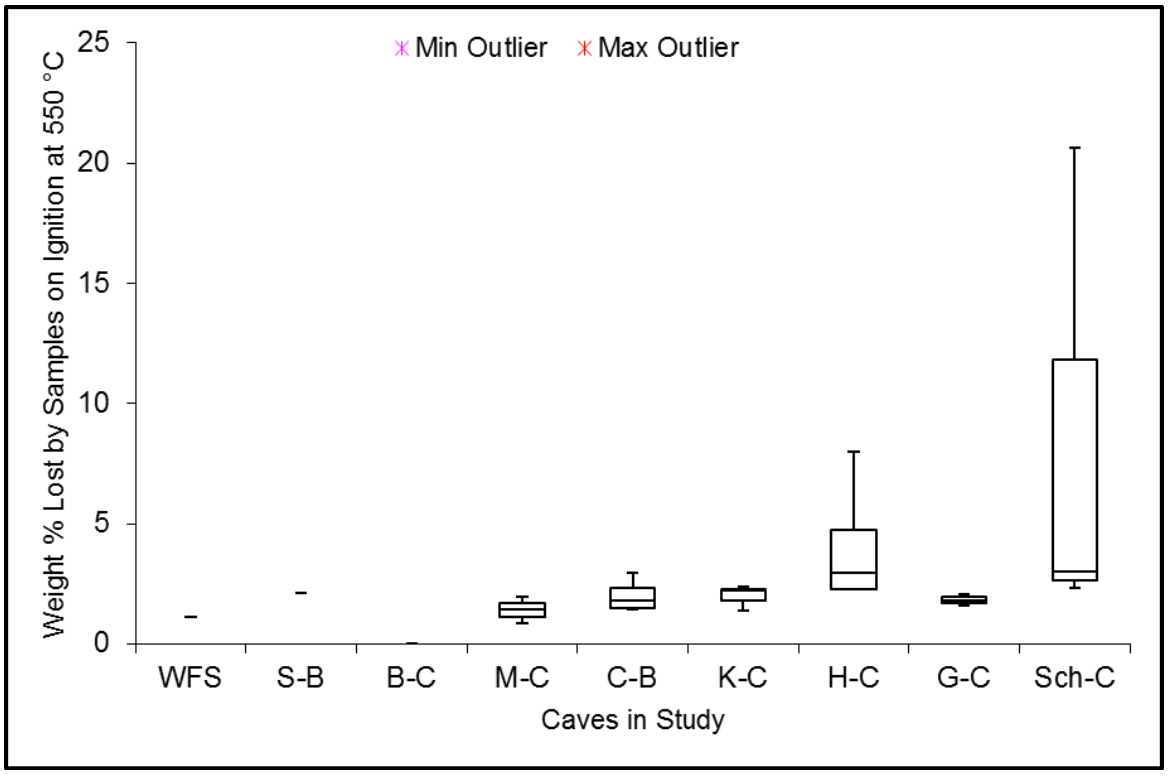

Figure C.7 A box plot diagram comparing the amount of weight lost by samples, containing the tan 'white' clay unit, by ignition at 550 °C.

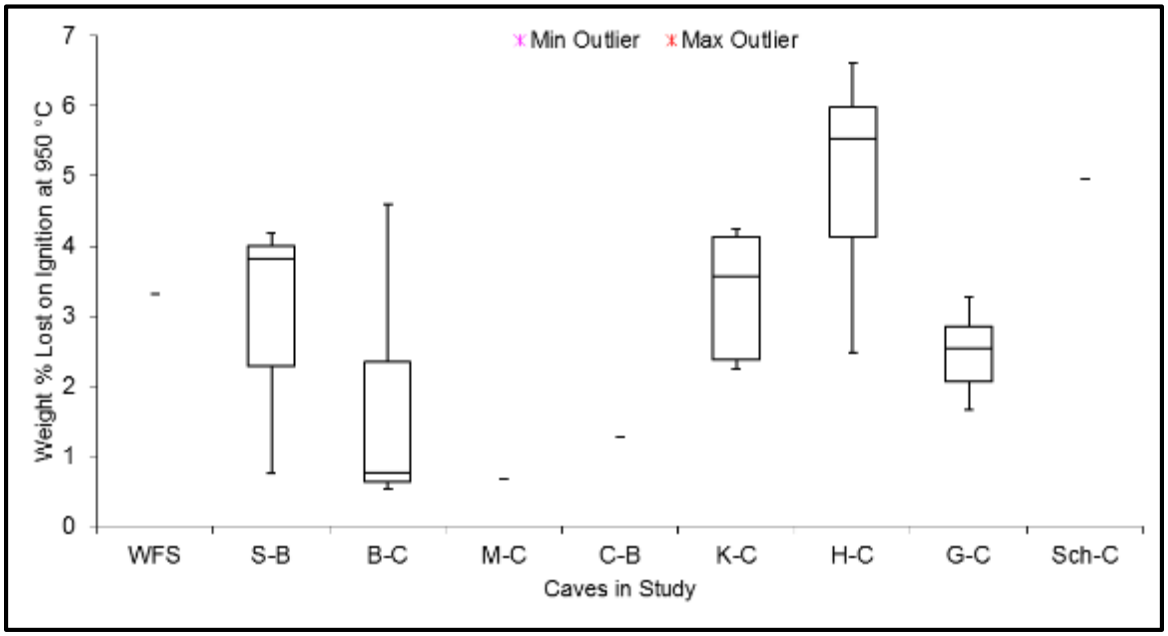

Figure C.8 A box plot diagram comparing the amount of weight lost by samples, containing the dark grey/dark brown clay unit, by ignition at 950 °C.

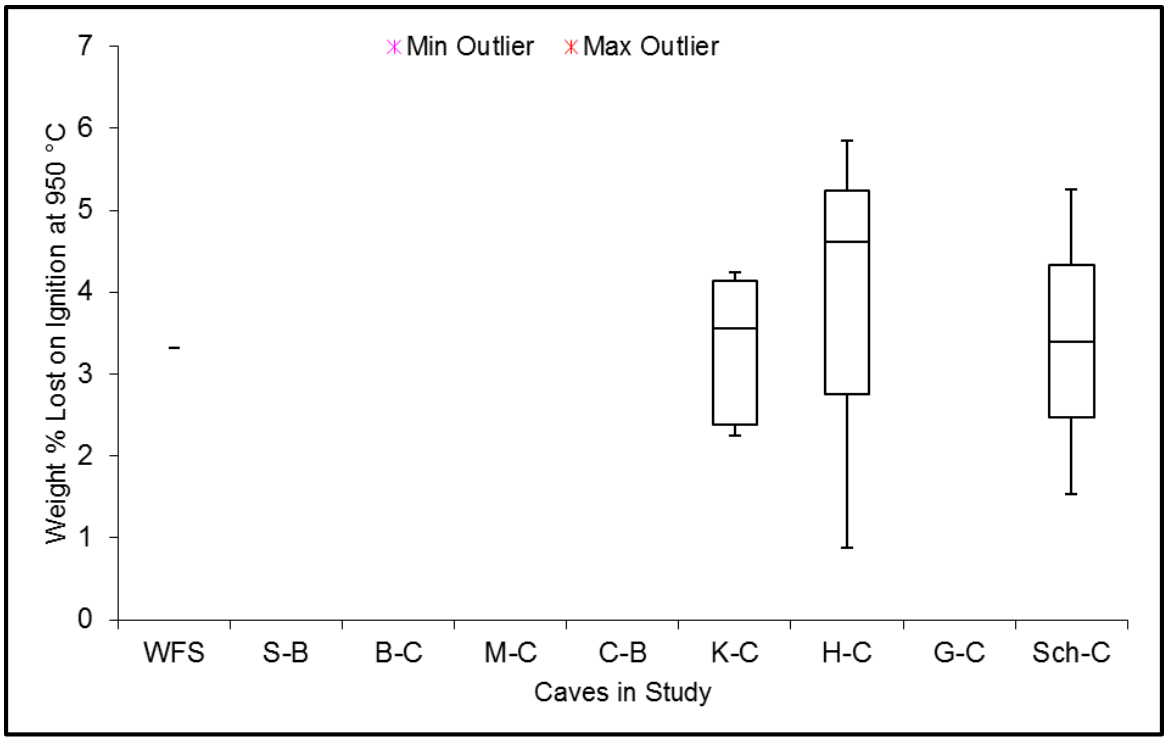

Figure C.9 A box plot diagram comparing the amount of weight lost by samples, containing the light grey clay unit, by ignition at 950 °C.

Note the light grey clay unit was only observed and collected in Howe Caverns and Schoharie Caverns.

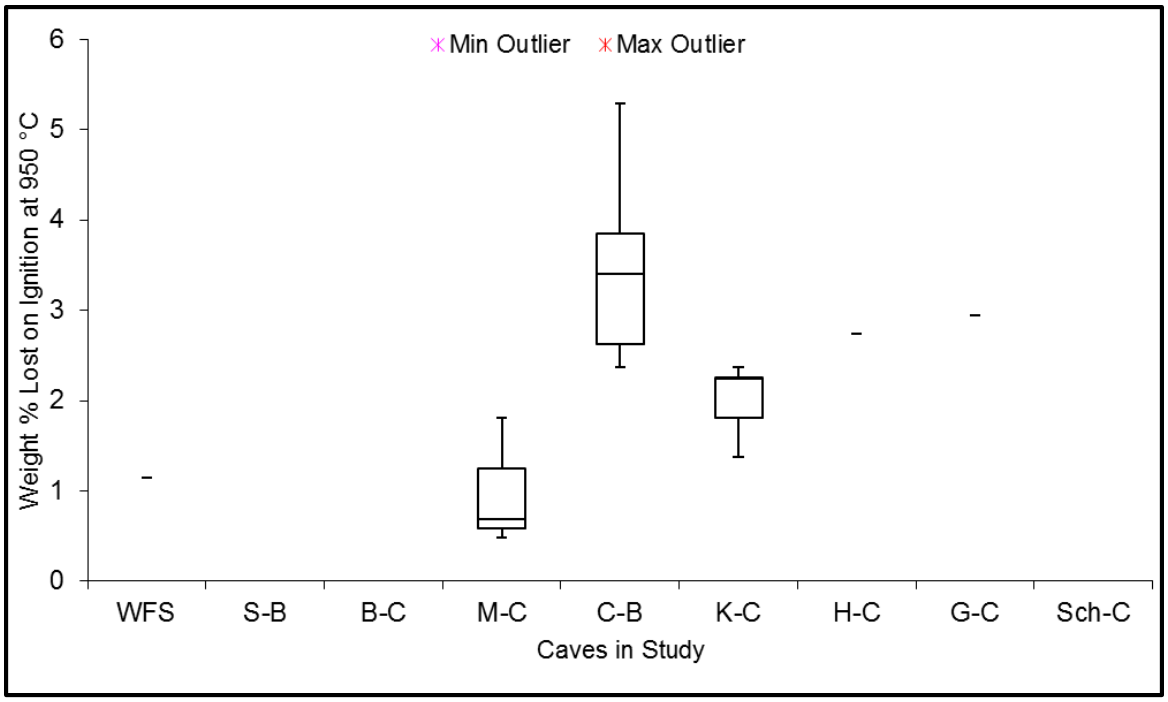

Figure C.10 A box plot diagram comparing the amount of weight lost by samples, containing the allogenic glacial outwash unit, by ignition at 950 °C.

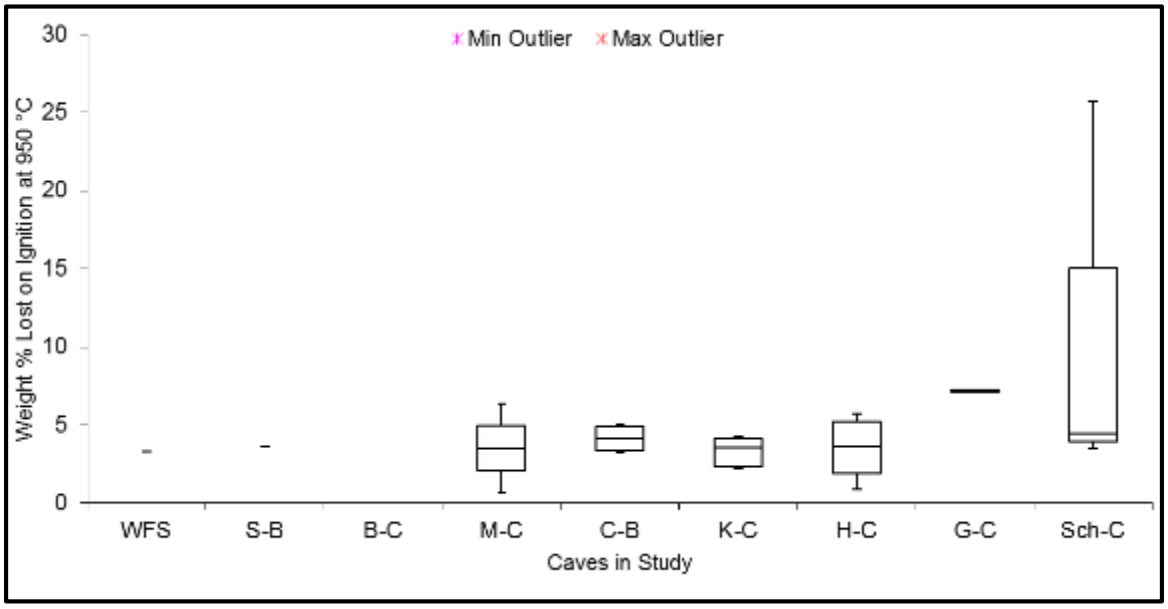

Figure C.11 A box plot diagram comparing the amount of weight lost by samples, containing the tan 'white' clay unit, by ignition at 950 °C.

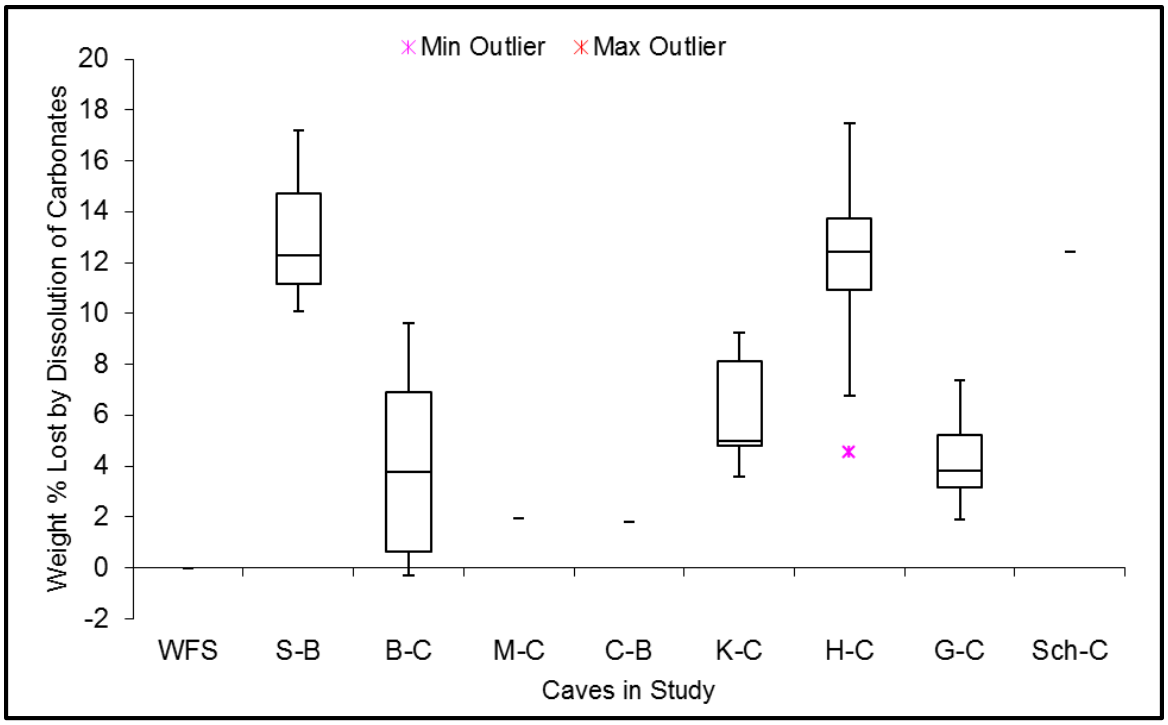

Figure C.12 A box plot diagram comparing the amount of weight lost by samples, containing the dark grey/dark brown clay unit, by dissolution of carbonates present.

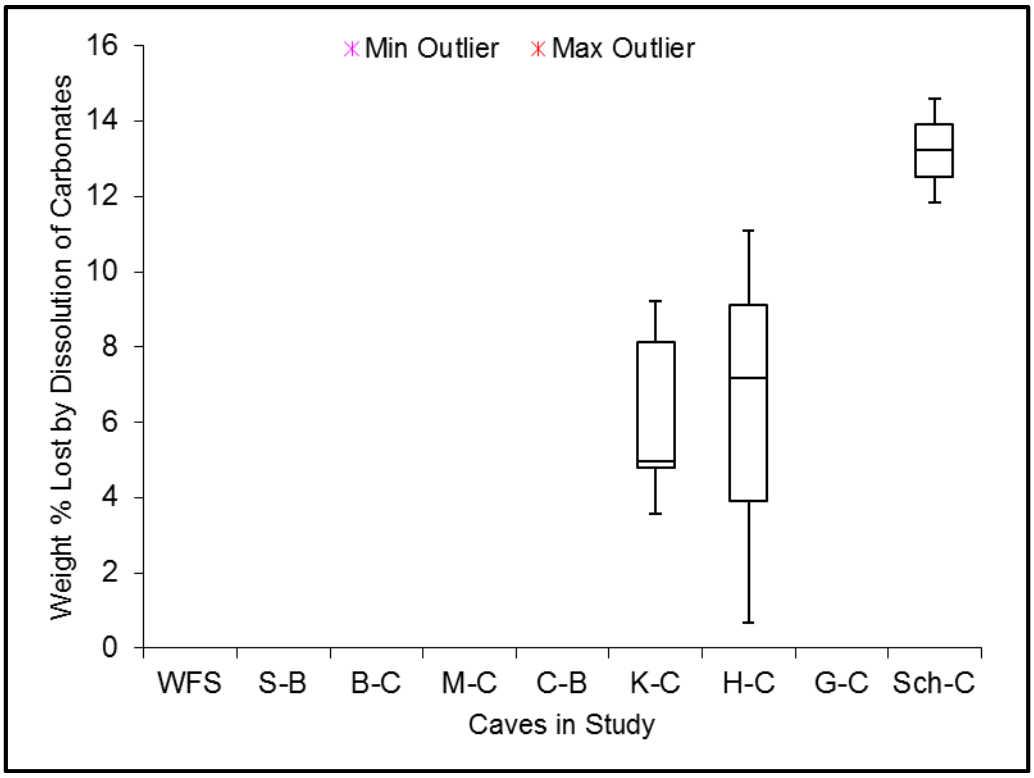

Figure C.13 A box plot diagram comparing the amount of weight lost by samples, containing the light grey clay unit, by dissolution of carbonates present.

Note the light grey clay unit was only observed and collected in Howe Caverns and Schoharie Caverns.

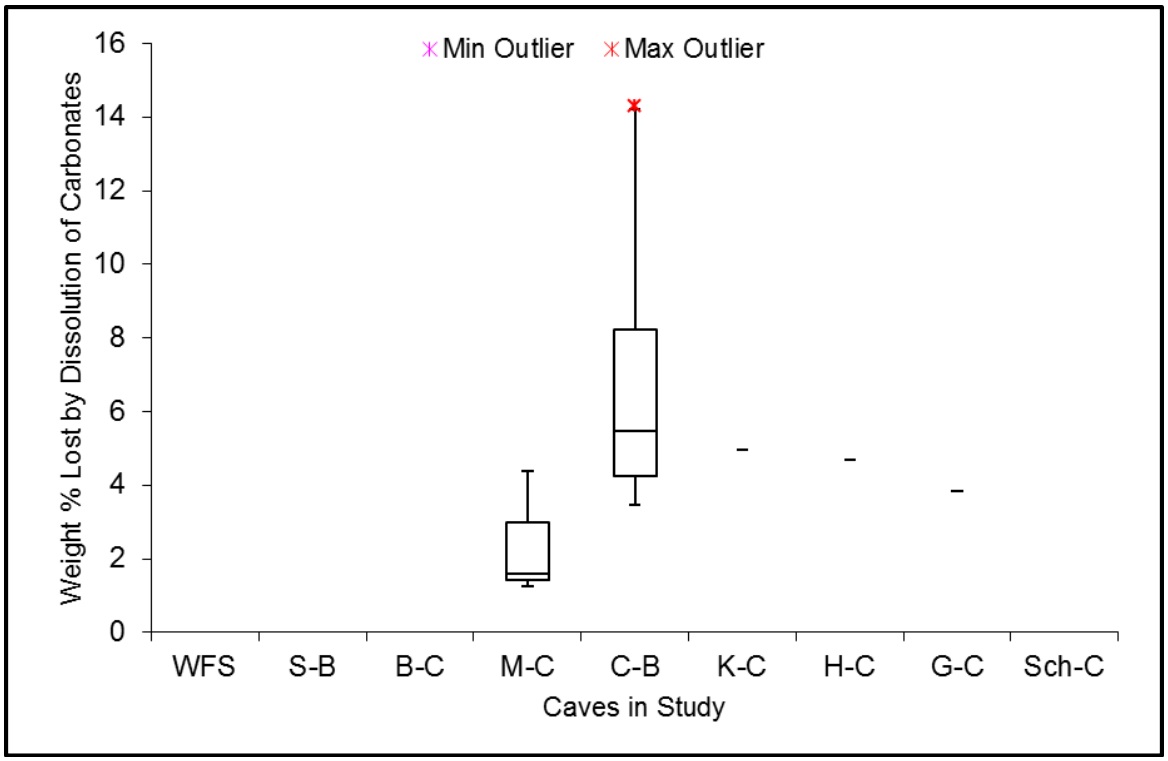

Figure C.14 A box plot diagram comparing the amount of weight lost by samples, containing the allogenic glacial outwash unit, by dissolution of carbonates present.

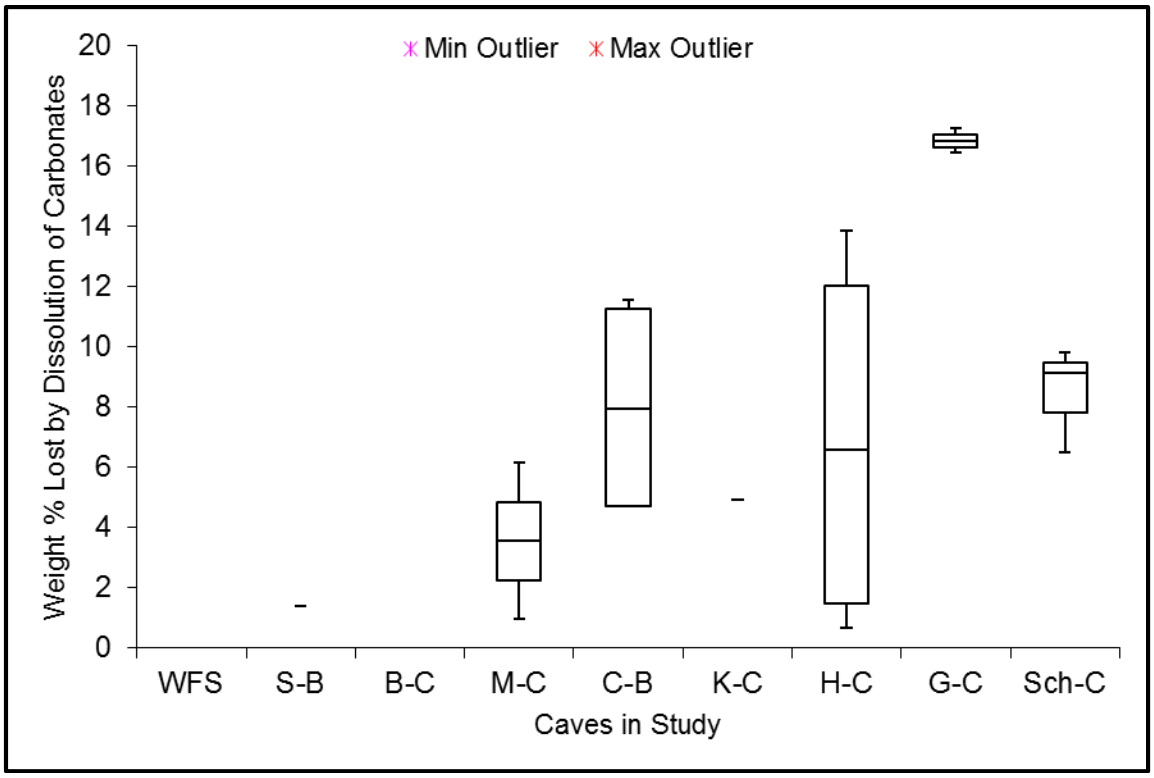

Figure C.15 A box plot diagram comparing the amount of weight lost by samples, containing the tan 'white' clay unit, by dissolution of carbonates present.